# *Reconstructing Loch Lomond Stadial Glaciers and Climate in the south-west English Lake District*

VICTORIA HELEN BROWN

# RECONSTRUCTING LOCH LOMOND STADIAL GLACIERS AND CLIMATE IN THE SOUTH-WEST ENGLISH LAKE DISTRICT

**VICTORIA HELEN BROWN**

**A thesis submitted for the degree of Master of Science**

**Department of Geography**
**University of Durham**

**January 2009**

# Declaration of Copyright

I confirm that no part of the material presented in this thesis has previously been submitted by me or any other person for a degree in this or any other university. In all cases, where it is relevant, material from the work of others has been acknowledged.



Victoria Helen Brown

Department of Geography
University of Durham
January 2009

*For Ann and John*
*My Parents*

**ABSTRACT**

The most recent glaciation of the English Lake District occurred during the Loch Lomond Stadial (Younger Dryas) when full glacial conditions returned to the British Isles. The largest ice mass formed over the Western Scottish Highlands with smaller ice masses developing throughout the British uplands.

In the Lake District, our understanding of the extent and timing of the Loch Lomond Stadial glaciation is patchy and poorly constrained by geochronology. Sissons (1980) proposed the development of 64 independent alpine-style ice masses in the district during the Loch Lomond Stadial. The location and geometry of these ice masses showed some agreement to the earlier, but coarser scale, map of ice masses produced Manley (1959) for the same period, however some significant differences were also apparent. More recently, McDougall (1998: 2001) has proposed the development of plateau icefields in the Lake District centred over High Raise, Grey Knotts/Dale Head, Brandreth and Kirk Fell. This much more extensive style of glaciation involved 40-50 m of cold based non-erosive ice occupying the plateau summits and feeding down into warm-based geomorphologically active outlet glaciers in the valleys. Further Loch Lomond Stadial sites have also been identified in the Lake District by Wilson (2002: 2004) and Wilson and Clark (1998: 1999).

The geomorphology of the south-west Lake District is identified and presented here and glaciers are then reconstructed based upon this evidence. Palaeoclimatic inferences made based upon the reconstructed glacial extent vary greatly depending on the style of glaciation that occurred during Stadial (alpine or plateau icefield). Of particular note, plateau icefields have the potential to significantly raise the equilibrium line altitude (ELA) across a region. This lowers the temperature at the ELA and therefore increases the reconstructed palaeoprecipitation at the ELA. In order to test the viability of the reconstructed glaciers in the Lake District, a 2D velocity-mass balance model is applied to the glaciers (adapted from Carr and Coleman,2007). This model assumes that where a glacier is glaciologically viable under the parameters used to drive the model, the basal velocity ($U_b$) accounts for < 90 % of the surface velocity in the centre of the channel ($U_s$).

Further mass contributions to the glaciers via mechanisms such as snowblow are quantified using a revised definition of potential snowblow areas. The significance of these areas is then assessed with respect to the ELA of the glaciers. Digitisations of the work of Sissons (1980), McDougall (1998), Wilson and Clark (1998: 1999) in the Lake District are then presented and compiled with the work of the current author to illustrate the extent of the Loch Lomond Stadial throughout the whole district.

**CONTENTS** **Page**

**LIST OF FIGURES**

**LIST OF TABLES**

**AKNOWLEDGEMENTS**

First of all, it has been a privilege to work with my supervisors, Ian Evans and Dave Evans. Ian in particular has given up a large amount of time to support this project, including coming with me on fieldwork, for which I am very grateful. A few days in the field with Ian made me realise just how much I still have to learn (lots!). Within the department, Dave Roberts deserves particular mention, not only for the valuable discussions but also for allowing me to use his core from Mosedale.

The laboratory/technical staff in the Geography Department were also incredibly helpful, particularly in supplying me with fieldwork equipment when I decided at the last minute to head off to the Lakes for the weekend.

The aerial photography used in this project was kindly supplied by the Lake District National Park Authority. I am particularly grateful to Martin Sleath for providing me with copies of the photographs and for meeting with me to discuss my work.

Discussions with Colin Ballantyne at the University of St Andrew's were inspiring and he kindly provided me with some, as-yet, unpublished cosmogenic dates for reference in this project. Doug Benn also provided a copy of the Osmaston (2005) spreadsheet for which I am very grateful.

To all those who have come on fieldwork with me; Cat, Hels, Andy, Kate, Jonah, Mum and Dad (and Bell), thank you. To the Mildert lot past and present: Margo, Emma, Will, Cat, Dave, Adam, thank you for being fantastic friends and making life outside of geography so special. A couple of Mildertians deserve special thanks. Tom: thank you for your patience, help with the numbers and for never doubting that I would get there in the end. Gary: (the best tea maker in the world): thank you for the never-ending supply of Yorkshires finest, custard creams and for knowing just what to say when things were not going to plan. Finally, thanks to Mum and Dad for your love and support from start to finish!!

# Chapter 1

# INTRODUCTION

# 1: INTRODUCTION

## 1.0: Introduction

Deglaciation and the associated climatic amelioration following the Last Glacial Maximum (LGM) at ~ 21 ka BP was, according to Alley and Clark (1999), triggered by an orbitally induced increase in northern hemisphere summer insolation. Several millennial scale warming and cooling events have punctuated the last deglaciation with climatic changes most widespread and rapid around the North Atlantic. Such events can be linked to changes in the delivery of freshwater to the North Atlantic as a result of internal ice sheet reorganisation. The Younger Dryas, or Loch Lomond Stadial in Britain, is the most well documented of these events which saw an abrupt return to full glacial conditions during deglaciation (Fawcett et al., 1997). During this period, 12,860 – 11,690 ka BP, North Atlantic sea surface temperatures dropped, salinities decreased and the Laurentide ice sheet advanced (Bond et al., 1993) (see figure 1.1 below).


**Figure 1.1: Temperature variations indicated by the GISP2 ice core from the LGM to 8 ka BP. The Younger Dryas cooling is shaded in grey. Note the gradual cooling during the Younger Dryas and the abrupt warming at the beginning of the Holocene. Taken from Rowan (2007).**

During this climatic downturn, the Lake District is assumed to have been characterised by an alpine style of glaciation by Sissons (1980). 64 independent cirque/valley glaciers were reconstructed in the district by Sissons (1980). The largest of these glaciers were located in an east-west transect across the central fells with smaller glaciers found in the north-western and northern fells. Prior to the work of Sissons (1980), Manley (1959) was the first to reconstruct the extent of glaciers in the Lake District despite it being recognised for over a century that glaciers occupied the region during the Loch Lomond Stadial (LLS). The maps of Manley (1959) and Sissons (1980) show clear similarities in the central fells however Sissons (1980) indicates a more extensive glaciation particularly in the western fells. The coarse scale of the map

produced by Manley (1959) also makes it hard to distinguish the exact location of glacier limits and the map does also not include any field data. Further LLS sites have since been recognised in the Lake District. Most notably, the work of Wilson and Clark (1998: 1999) reconstructs 3 glaciers near Haweswater and 3 in the Skiddaw/Blencathra range in the northern Lake District. Much other work unfortunately does not present a glacier reconstruction but instead provides a discussion of the geomorphology of individual sites such as Upper Eskdale and Stockdale Head (Wilson, 1977: 2004a: 2005, and Clark, 1990). In Upper Eskdale, Wilson (2004) has found geomorphological evidence for a valley glacier but does not reconstruct a glacier due to uncertainty surrounding the age of the moraines. Similarly, several authors have suggested that some of the moraines used by Sissons (1980) to delimit ice masses may infact be protalus ramparts resulting from the presence of snow-patches, para- and post-glacial slope failure deposits or true moraines formed by the Late Devensian ice sheet (Wilson and Smith, 2006: Wilson, 2005: Wilson et al., 2004: Wilson, 2004a: Wilson, 2004b).

More recently, McDougall (1998: 2001) has proposed a far more extensive style of glaciation in the Lake District during the Loch Lomond Stadial. McDougall (1998: 2001) suggests that plateau icefields occupied the district with icefields centred on High Raise in the central fells and Grey Knotts and Dale Head further to the north-west. This work examines the influence of the broad, rounded summits, particularly found in the central fells, on the style of glaciation that occurred during the Stadial based on the subtle geomorphology found on the plateau summits. The plateau icefields proposed by McDougall (1998: 2001) only cover the central fells and replace 14 of the cirque/valley glaciers proposed by Sissons (1980) with ice covering the plateau summits and feeding down into 20 outlet glaciers in the valley bottoms.

Principally, these reconstructions present scenarios with substantially different ice volumes and maximum ice altitudes. The identification of plateau icefields as proposed by McDougall (1998: 2001) has crucial implications for the reconstruction and palaeoclimatic interpretation of equilibrium line altitudes (ELAs). By simply calculating an ELA based on a glacier confined to a valley, as invoked by Manley (1959) and Sissons (1980a), a substantial underestimation of the ELA is likely. As noted by Rea et al. (1999), the size of the contributing plateau area and the altitudinal difference between the plateau and the valley/s will affect the size of the error in an ELA calculation. Such ELA variations therefore require reinterpretations of the climatic parameters controlling the ELA and consequently accurate landform interpretation is initially required.

## 1.1: Aims and objectives

### 1.1.1 Aims

Within the English Lake District previous reconstructions of the Loch Lomond Stadial glaciation have therefore been patchy, non-systematic and poorly constrained by geochronology. As described above, the work of McDougall (1998: 2001) provides a contrasting style of glaciation in the district during the Loch Lomond Stadial to that proposed by earlier workers such as Sissons (1980) and Manley (1959). Furthermore McDougall (1998: 2001) does not address the style of glaciation that occurred within the south-west Lake District during this period. For these two reasons, this project aims to do the following:

- undertake systematic geomorphological mapping of the under-investigated south-west Lake District.
- consider the applicability of the different alpine vs plateau icefield models suggested in the previous work of Manley (1959), Sissons (1980), Pennington (1978: 1996), McDougall (1998: 2001) and Wilson and Clark (1998:1999).

### 1.1.2 Objectives

In order to achieve these aims the following objectives were developed:

- to map the glacier-related features in the south-west Lake District covering Upper Eskdale, the fells north of Wrynose Pass, Little Langdale and Wastwater using NextMap Britain, aerial photography and ground survey.
- to assess the effectiveness of NextMap Britain, aerial photography and ground survey for local scale mapping of Loch Lomond Stadial glacial geomorphology.
- to reconstruct proposed Loch Lomond Stadial glaciers based on this geomorphology.
- to estimate the ELAs, potential snowblow areas and ice velocities of the reconstructed glaciers.
- to assess the viability of the reconstructed glaciers using a numerical mass balance model and qualitatively in terms of their geomorphological context with respect to the proposed plateau icefield (McDougall; 1998).

## 1.2: Rationale

The reconstruction of former ice masses by the interpretation of ancient landform assemblages has long been a source of powerful proxy records. By establishing quantitative data for a variety of palaeoglaciological and palaeoclimatic variables it is possible to further understand broader global issues relating to past atmosphere – ocean – cryosphere interactions (Lukas, 2006). Current research aims to establish whether the dynamics of past

ice masses, particularly those of the Quaternary, can be modelled in comparison to modern glaciers on different spatial and temporal scales (Carr and Coleman, 2007). According to Patterson (1994), inputs to the modelling of glaciers/ice sheets are those factors which determine the extent and behaviour of glaciers, notably, climate and the physical properties of ice. We must therefore fully understand these factors before we are able to model glaciers/ice sheets effectively.

As noted by Benn and Lukas (2006), explicitly linking process to form at a variety of spatial scales can provide important insights into processes which operated in ancient environments. This concept underpins the widely used landsystems approach whereby a characteristic set of criteria are developed for a particular landsystem and later identified elsewhere. Benn and Lukas (2006) use the example of 'hummocky moraine' to illustrate the complexities associated with this method. Since some characteristics of a landscape can originate from more than one process (equifinality), it is often easy to find a modern analogue that 'fits' the ancient landscape but is not necessarily the correct one or is simply a close counterpart (Benn and Lukas, 2006). Despite the criticism that over-reliance on landscape morphology can induce error this remains a valuable source of insight into ancient landscapes and certainly provides the foundations for further investigation.

This method also allows links to be drawn between glacier dynamics and palaeoclimate. Correlations between these two variables on a more global scale, enables predictions to be made regarding the response of modern mountain glaciers to more recent climatic change. Ongoing concerns over current 'climate change' suggest that it is arguably now more vital than ever to understand fully the processes which are controlling the widespread retreat of mountain glaciers and ice sheets that we are currently witnessing (Stokes et al., 2007: Haeberli et al., 2007). Examples such as that provided by Bauder et al. (2007) for 19 glaciers in the Swiss Alps suggest overall retreat since the end of the Little Ice Age around 1850 although most notably, retreat rates have increased since 1980. Although fluctuations in ice extent have occurred over geological time, particularly throughout the Quaternary, the current retreat, popularly accounted for by the notion of human induced 'global warming', has impacts on global sea level and therefore deserves attention. It is hoped that a further understanding of glacier response to palaeoclimatic change on a variety of scales will provide the foundations for more robust models pertaining to the future of contemporary mountain glaciers.

## 1.3: The Loch Lomond Stadial (Younger Dryas)

### 1.3.1 The cause and global impact of the Younger Dryas

The gradual cooling into the Younger Dryas contrasts with the abrupt closure of the Stadial at the start of the Holocene. The most likely cause of this abrupt transition at the start of the Holocene relates to the reinitiation of North Atlantic Deep Water (NADW) formation following a shut down during the Younger Dryas. Since heat transport into the three main areas of deep water production (northern North Atlantic, the Ross Sea and the Weddell Sea) can account for up to 10°C temperature increase compared to the latitudinal mean (Rahmstorf, 2002), it is reasonable to account for the ~ 7°C warming seen at the close of the Younger Dryas with a shut down of this circulation.

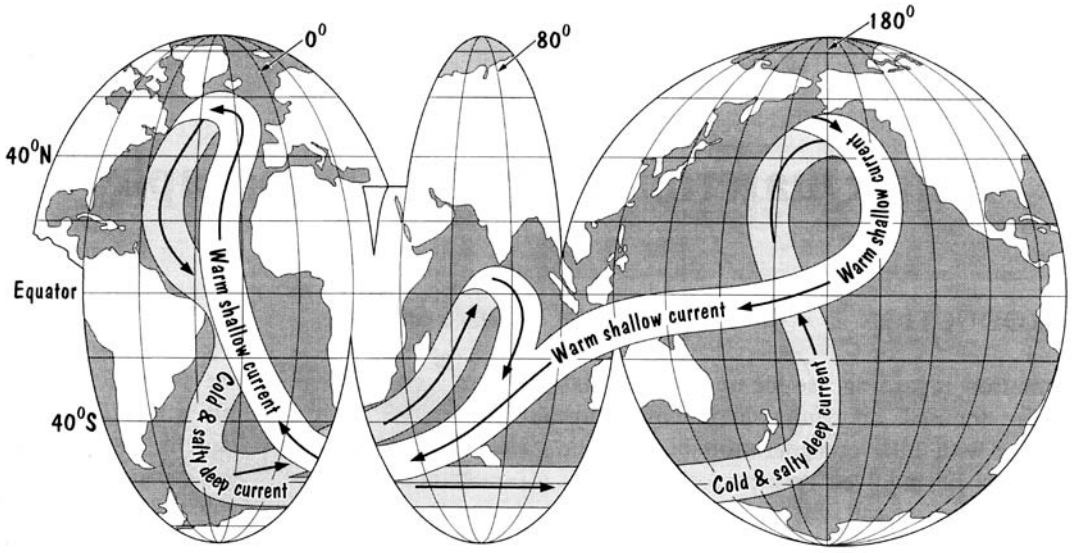


**Figure 1.2: The path of the Thermohaline circulation system or global ocean conveyor. Note the formation of cold salty NADW. Taken from Siegert (2001).**

The impacts of the Younger Dryas were seen globally however the response of the Southern Hemisphere was somewhat muted compared to that of the Northern hemisphere and particularly of the North Atlantic. An example of the localised nature of this event is found in pollen records from North America which according to Broecker and Denton (1990) show no evidence of a cooling event with the exception of those in maritime locations. Similarly no representation of the Younger Dryas is found in Antarctic dust records (Broecker and Denton, 1990). Ruddiman and McIntyre (1981) record a shift from forests to tundra flora in Northern Europe and the introduction of polar planktic foraminifera species to replace temperate species in the northern North Atlantic. This global pattern of response to the Younger Dryas cooling implies that the whole ocean – atmosphere system did not fully revert to its glacial state, instead only changes to the Atlantic's circulation occurred (Broecker and Denton, 1990).

### 1.3.2 The impact on the British Isles

The British Isles provide evidence for a sensitive response to this climatic deterioration at the end of the last glacial cycle (Broecker et al., 1988). The presence of landforms which are distinct from those associated with the Late Devensian ice sheet provide evidence for a contrasting renewed glaciation (see figure 1.3 below). During the Loch Lomond Stadial, ice advanced over terrain containing abundant glacigenic sediment which had been freshly incised and remobilised by paraglacial processes and thus provided favourable conditions for substantial depositional landform production (Evans, 2006).

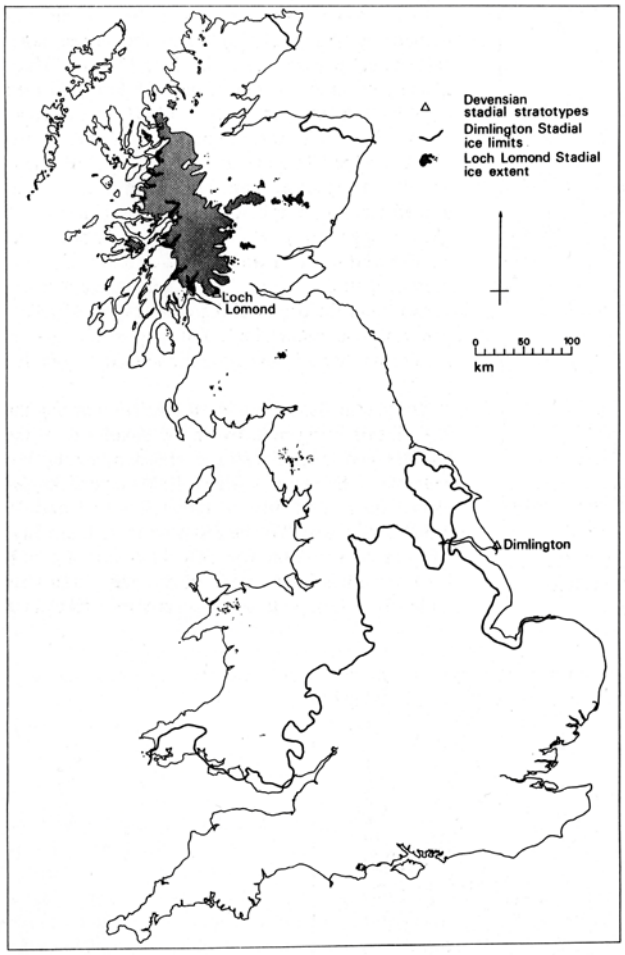


**Figure 1.3: The distribution of Loch Lomond Stadial ice masses in Great Britain and Ireland along with the location of the most southerly margin of the Late Devensian ice sheet. Taken from Gray and Coxon (1991).**

The Loch Lomond Stadial saw the development of glaciers and ice caps in the mountainous regions of the British Isles (see figure 1.3 above). Outside of the glacier limits, the terrain experienced severe periglacial conditions and supported tundra-like vegetation. The largest of these ice caps was situated over the western Scottish Highlands, reaching Torridon in the north and Loch Lomond in the south (175 km), Loch Shiel in the west and Loch Rannoch in the east

(100 km) (Gray and Coxon, 1991). At its maximum extent the asymmetric icefield also contained ~ 60 nunataks, most of which were found in the Western Mountain Zone (Thorp, 1986). The surface of the ice cap in the western Grampians reached an altitude of ~ 700 m OD while the snouts of the outlet glaciers descended to below present day sea level along the western coast. Over 200 other ice masses have been identified in the Scottish Highlands by various authors. Ice caps also existed on the Isles of Mull and Skye, in the Cairngorms and central Highlands, and the north-west Highlands. Significant clusters of valley glaciers have also been reconstructed on the Isle of Arran, on Harris and south-west Lewis in the Outer Hebrides and in the Southern Uplands. Further south, glaciers developed in more marginal regions including the Pennines, Lake District, Cheviots, Snowdonia and the Brecon Beacons. In contrast to the ice cap in the western Grampians, the largest glacier in Snowdonia was in Cwm Llydaw and was just 4 km long (Gray, 1982). Furthermore, the total area of the 35 glaciers reconstructed by Gray (1982) in Snowdonia was just 17.5 $km^2$.

# Chapter 2

# STUDY AREA

## 2.0: STUDY AREA

### 2.1 The English Lake District

Located in north–west England, the Lake District covers an area of ~ 3000 km$^2$. The Lake District is the largest national park in England contains the highest peak in England, Scafell Pike (978 m OD), along with 12 of England's largest lakes. The Lake District is characterised by mountainous topography which predominantly supports agriculture, quarrying and forestry. Current precipitation is ~ 2061 mm per annum. The mean July temperature stands at ~ 14.9°C and mean January temperature 3.1°C. To the north of the Lake District are the Solway Lowlands and to the east the Vale of Eden which is believed to have been occupied by an ice stream at some stage during the Late Devensian glaciation (see figure 2.1 below).

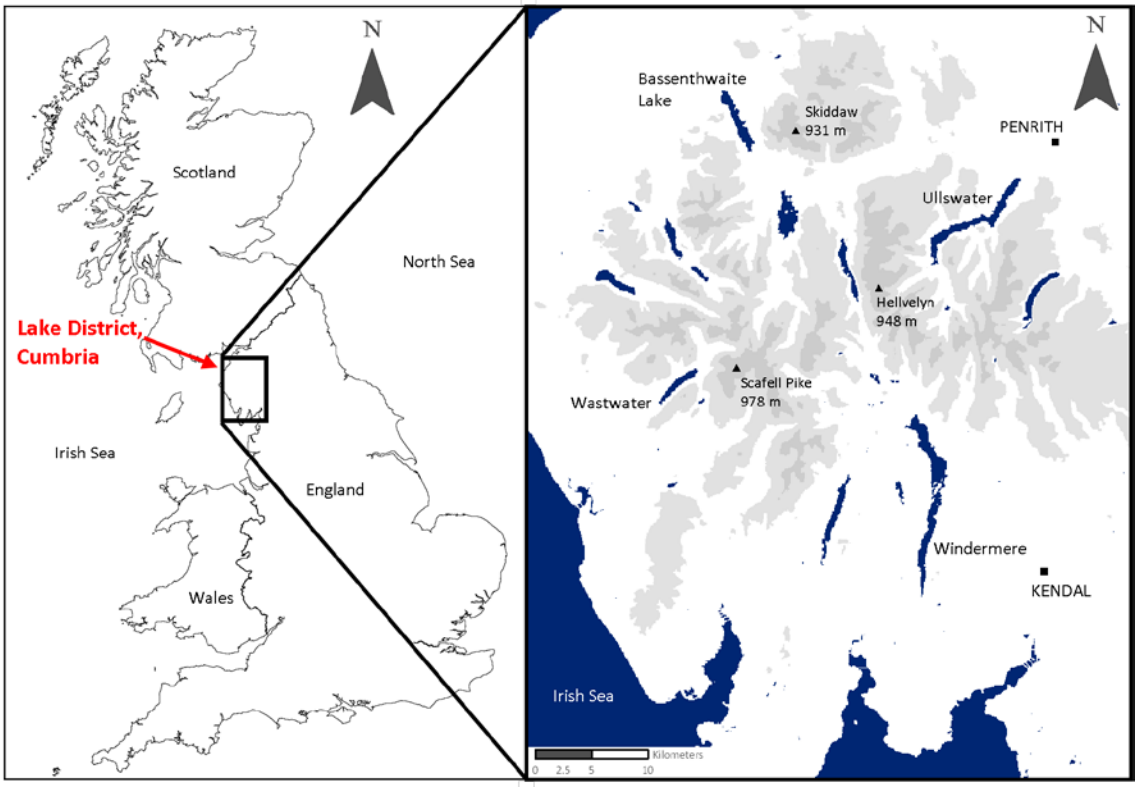


**Figure 2.1: The location of the Lake District within the British Isles and its regional topography.**

### 2.2 Regional glaciation history

The Dimlington Stadial ice sheet of the Late Devensian was the last ice sheet to cover Great Britain. Despite many years of research, in many areas only very general ice flow directions have been established. In northern England it is believed that three ice

domes formed over the north-west Yorkshire Dales, the Alston Block and the Lake District (Mitchell and Clark, 1994). These ice domes were crucial in maintaining the ice sheet throughout its cycle but made relatively minor contributions to an ice sheet that was ultimately dominated by a major ice dome centred over the Scottish Highlands. In the Lake District, ice flowed radially out from the mountain core causing Scottish ice coming from the north to be deflected eastwards across northern England and south-westwards across the Solway lowlands and into the Irish Sea basin (see figure 2.2 below). Striae orientations, the dispersal of Borrowdale Volcanic erratics, the absence of foreign erratics and landform flow signatures are testament to the complex interaction between Scottish ice and the local Lake District and Pennine ice (Mitchell, 1991).

Mitchell (1994) has since argued for the presence of a regional scale ice divide during the Dimlington Stadial across north-west England from the Derwent Fells in the central Lake District north-westwards over 50 km to Dentdale. It is suggested that this linear, topographically independent, ice divide migrated northwards through glacial/deglacial phases. This model can be used to explain the contrary flow events indicated by superimposed drumlins in the Vale of Eden and Western Pennines and also the dispersal patterns of Shap granite erratics.

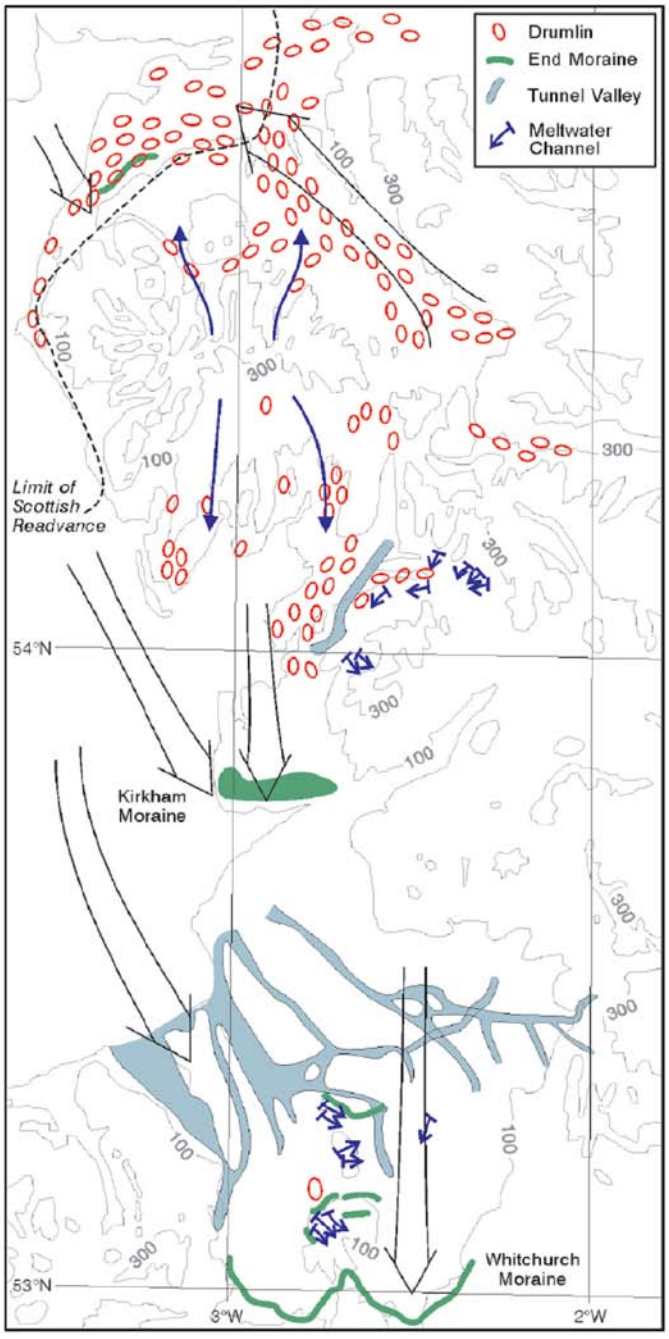


**Figure 2.2: Regional ice flow directions during the Late Devensian including the maximum extent of the Scottish Readvance ice along the western coast. Taken from Delaney (2003).**

Deglaciation following the peak of the Dimlington Stadial at ~ 22 ka BP (Boulton et al., 1977) resulted in the deposition of widespread glaciofluvial sands and gravels as kames, eskers, proglacial sandur, deltaic sands and gravels, and glaciolacustrine deposits (Busby and Merritt, 1999). These landforms all provide evidence of climatic oscillations during deglaciation comparable to those shown in the GRIP and GISP2 ice cores, which induced a series of glacial readvances. Questions remain however surrounding the impact of these climatic down turns on an already decaying the ice sheet margin in Britain. According to Merritt and Auton (2000), who provide a

lithostratigraphic history of west Cumbria, two post-Dimlington Stadial readvances can be identified Cumbria.

In response to Heinrich Event 1 in the North Atlantic, the Gosforth Oscillation is believed to have occurred in the British Isles between ~ 17.6 and 16.8 cal. ka BP (Thomas, 1985: Pennington, 1978: Merritt and Auton, 2000: Delaney, 2003). During this period, Merritt and Auton (2000) propose that two extensive coeval valley glaciers occupied Wasdale and Eskdale. Pennington (1978) however provides $^{14}C$ dates which indicate that the Windermere basin and consequently, the catchment of the Brathay-Rothsay rivers, remained ice free during the period ~ 17.4-16.8 cal. ka BP. Pennington (1978) is therefore unable to find any biostratigraphic evidence to support the idea that these moraines were produced during ice sheet decay pre-Windermere Interstadial. The Scottish Readvance is the second of the two glacial phases mentioned above and involved the encroachment of Scottish ice streaming to the south and south-east around Cumbria ~ 14 ka BP (Busby and Merritt, 1999). Consequently, based on the scale and well defined nature of the moraines, McDougall (1998) suggests that the Scottish Readvance is the only event other than the LLS that had the potential to create moraines such as these.

Following these two readvances, the final phase of glaciation in the Lake District occurred during the Loch Lomond Stadial (Younger Dryas). As previously described, the extent and style of glaciation in the region during this period is debated with recent work suggesting a contrasting plateau icefield arrangement to replace the alpine glaciation first suggested in the central fells.

## 2.3 Geological history

Considerable geological diversity is found within the Lake District. In the north the Skiddaw Group have been moulded into conically shaped hills (see figure 2.3 below). These contrast with the more rugged appearance of the Borrowdale Volcanic Group which stretches from Ullswater in the east to Wasdale in the west. The more subdued hills of the southern district form the Windermere Supergroup, a series of Silurian sedimentary rocks (Shipp, 1982). Together these rocks form a small dome of WSW – ENE trending Lower Palaeozoic rocks protruding as an inlier into the surrounding

Carboniferous and Permo–Triassic formations. The region has undergone three main episodes of mountain building: the Caledonian, Variscan and Alpine orogenies, along with extended periods of faulting. These massive structural movements have caused rocks which were once horizontally above or below each other or formed millions of years apart to now be side–by–side (Prosser, 1977). It is the period extending from the Early Ordovician to the end of the Silurian during which time a Late–Proterozoic–Lower–Palaeozoic ocean (the Iapetus Ocean) was destroyed that was most eventful in Lakeland geological history. The closure of the Iapetus Ocean culminated in the continental collision of the Caledonian Orogeny, the most significant of the three orogenic events.

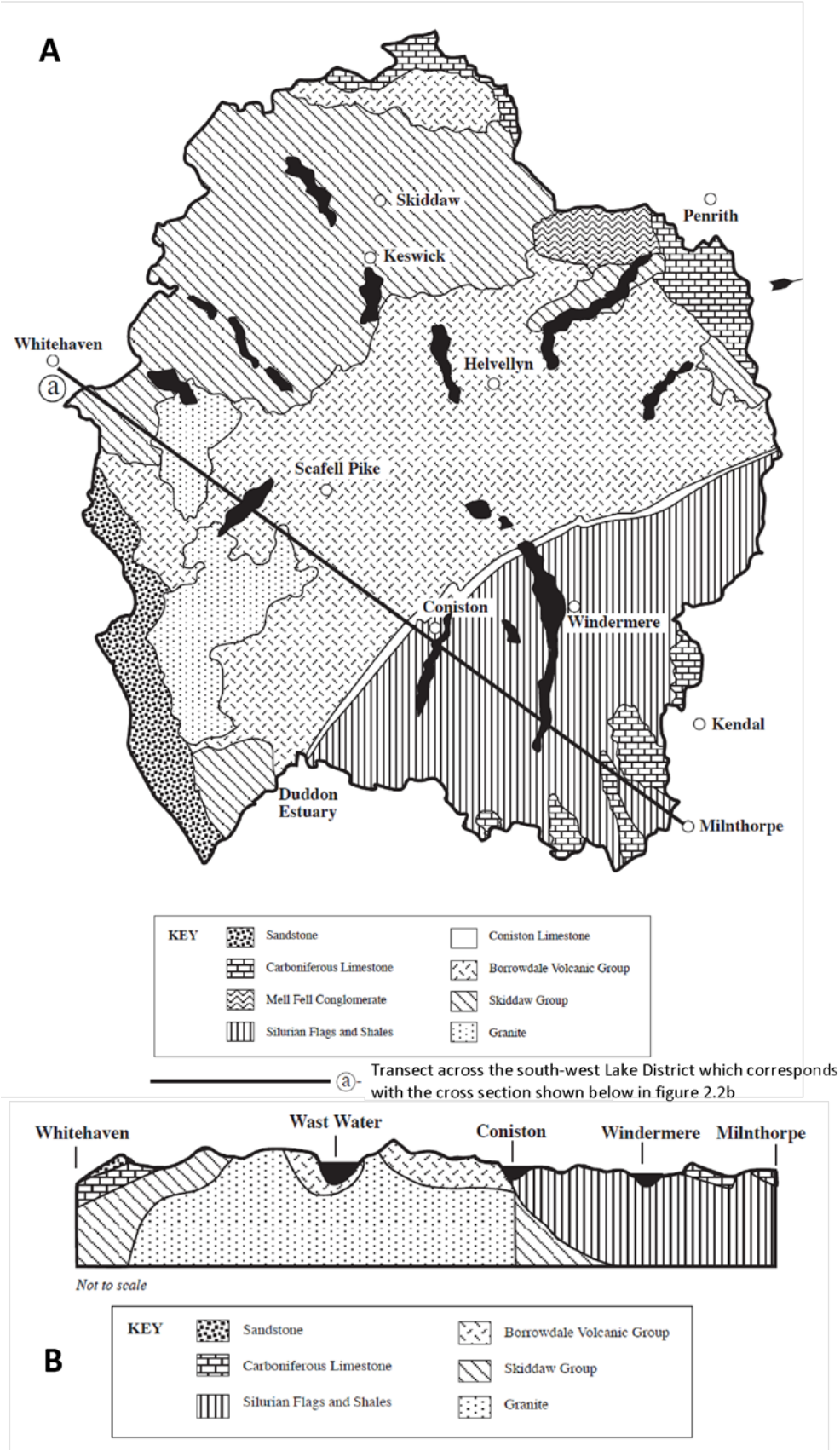


**Figure 2.3: The regional geology of the Lake District. A: overview of the regional geology. B: the sub-surface geology along a transect across the south-west Lake District as indicated on 2.2A. Adapted from LDNPA (2003).**

### 2.3.1 The Skiddaw Group

The Skiddaw Group contains the oldest rocks in the Lake District which, at ~ 3000 m thick, form almost one third of the mountain core. The group is largely composed of greywackes, siltstones, mudstones and sandstones deposited by turbidity currents on the continental slope of the Iapetus Ocean. Fossils are rare within the group but the most common is the grapolite (Prosser, 1977). The structure of these rocks is now very complex. They have undergone multiple phases of folding along with thermal metamorphism and mineralization. Moore (1992) has interpreted this intense folding as evidence for fore–arc sedimentation. These fine grained clastic sedimentary rocks display major north–east trending faults which split the Skiddaw Group into distinct zones. These highly cleaved, now laminar shales outcrop in a wide belt in the northern and western fells with their most southerly exposure found at Black Combe in the south–west Lake District (Smith, 1992).

### 2.3.2 Ordovician Volcanic Rocks

As the closure of the Iapetus Ocean continued and the American and European tectonic plates moved closer, subduction began. This initiated Island Arc volcanic activity around 470 Ma BP (Prosser, 1977).

The Ordovician volcanic group emerged from two phases of volcanic activity. The first of these formed the Eycott Volcanic Group; a series of basaltic and basaltic–andesitic lavas which appear to have formed synchronously with the upper parts of the Skiddaw Group (Shipp, 1982). It is the Borrowdale Volcanic Group however, which succeeds the Eycott Group that is most relevant here. The Borrowdale Volcanic Group (BVG) makes up the central belt of the Lake District and stretches from Dingle in south–west Ireland to the north Pennines of England to form a chain of Caledonian magmatism. They were erupted during a 10 Ma period in the Mid–Ordovician and are some 6000 m thick. The first phase of formation was dominated by lava flows with only occasional explosive volcanic eruptions. These andesitic lava flows produced localised low relief accumulations. In contrast, the onset of the second phase of volcanic activity witnessed an abrupt shift to continuous explosive activity (Moseley, 1978). These eruptions released silica–rich andesitic, dacitic and rhyolitic magmas high into the atmosphere. Such magmas then returned to the ground as air–fall tuff with some

becoming involved in the formation of ignimbrites which now appear to dominate the upper Borrowdale succession (Smith, 1992).

Since the Ordovician, the BVG has undergone severe changes. Most notably, the lavas, ashes and breccias have undergone volcanic collapse, vertical and horizontal fault movement, and differential erosion (both glacial and otherwise) producing the varied topography of the region. Much contrast is found between the 'alpine–like' terrain of the Scafell massif and the more 'plateau–like' relief of High Raise further to the east (Prosser, 1977). All field sites considered in this work are underlain by andesitic and rhyolitic lavas of the BVG.

### 2.3.3 Windermere Supergroup

The southern section of the Lake District is underlain by sedimentary rocks of Late–Ordovician to Late Silurian age. These rocks overlay the volcanic rocks from the Duddon Estuary to the Howgill Fells (Smith, 1992). The younger Windermere Supergroup consists of a thin deposit of lime–rich fossiliferous mudstones, shales, gritstones and flagstones which have been tilted and folded by crustal movements (Shipp, 1982: Prosser, 1977). These rocks, which are the result of continuous deposition in a marine environment, account for the more subdued topography of the southern district.

## 2.4: Selection of specific study locations

Based on the work that has previously been carried out in the Lake District, six sites have been chosen for study in this project (see figure 2.4 below). Firstly, the chosen sites are all located within the south-west Lake District as a result of the work of McDougall (1998: 2001) which reconstructs a plateau icefield in the central fells but does not consider the ice extent or the possibility of a plateau icefield in the south-west Lake District. For the purposes of this research the south-west Lake District is defined as the quadrant of the district covering from Ennerdale in the north round to Wrynose Pass in the east. Of particular interest are those sites in the south-west Lake District which had the potential to support outlet glaciers of the plateau icefield proposed by McDougall (1998: 2001). Such sites included Upper Eskdale, Red Tarn/Wrynose Bottom and Lingmell Beck. For reference, figure 2.5 shows the location

of the chosen field sites along with the location of any specific areas of interested noted in subsequent chapters of the thesis.

Two of the chosen sites have also been chosen as a result of the work of Wilson (2002: 2004). In Upper Eskdale, Wilson (2002) provides a comprehensive description of moraines at the southern end of the valley but does not reconstruct the Loch Lomond Stadial glacier in the valley. At Widdygill Foot Wilson (2004) has identified and described moraines which he believes to be of Loch Lomond Stadial origin at a site that was not previously considered to have supported a glacier during the Stadial by Sissons (1980), Pennington (1978) or McDougall (1998: 2001).

The other chosen sites, Mosedale and Lingmell Gill, were both suggested by Sissons (1980) to have supported a Loch Lomond Stadial glacier. In light of the work of McDougall (1998: 2001) and Carr and Coleman (2007) however, it was decided that a reassessment of the potential of these sites to support a glacier during the Stadial was necessary. Details of the chosen sites can be found below:

1. **Mosedale:** an east-south-east facing valley at the northern end of Wastwater. The site is surrounded by the peaks of Red Pike (826 m OD) to the south, and Pillar (892 m OD) to the north, and is the furthest west of the chosen sites. On the opposite side of the Mosedale valley to Red Pike is Kirk Fell (787 m OD) which McDougall (1998: 2001) suggests supported a plateau icefield during the Loch Lomond Stadial.
2. **Lingmell Beck:** a north-north-east facing valley on the northern side of the Scafell range. The valley is also located at the northern end of Wastwater. The complex long profile of this valley is dominated by the deep bedrock gully of Piers Gill. According to McDougall (1998: 2001) the glacier occupying this site during the Stadial was connected to the plateau icefields centred on the central fells of the Lake District.
3. **Lingmell Gill:** a small west-north-west facing valley directly to the south of Lingmell Beck on the western side of the Scafell range. Directly to the south of Lingmell Gill is Sca Fell (964 m OD).

4. **Upper Eskdale:** a large glacial valley facing directly south. The upper half of the valley can be split into two smaller valleys. The western upper valley contains the River Esk and runs along the eastern side of the Scafell range. The eastern valley contains Lingcove Beck which sources below Bow Fell (902 m OD) and Esk Pike (885 m OD) to the north. The lower half of Upper Eskdale contains just a single valley with heavily scree covered slopes and a series of large moraines at the southern end of the valley.
5. **Red Tarn/Wrynose Bottom:** a south-east facing valley on the western side of Wrynose Pass. Sissons (1980) suggests that the glacier occupying this valley was connected to a glacier in Oxendale to the north across an ice divide. The upper part of the valley contains Red Tarn and then descends to join the large glacial trough of Wrynose Bottom.
6. **Widdygill Foot:** an east facing valley on the eastern side of Wrynose Pass at the source of the River Brathay. Widdygill Foot lies furthest to the east of the all the chosen sites and lies to the south-east of Pike of Blisco (705 m OD).

In order for the plateau icefield hypothesis to be tested, a further two locations were also considered in this project and are discussed in the context of the literature in chapter 7:

7. **Mickleden:** a south-east facing valley at the western end of the large glacial trough of Langdale.
8. **Oxendale:** an east-north-east facing valley to the north of Red Tarn. Oxendale also lies at the western end of the Langdale trough.

Sissons (1980) proposed valley glaciers in both Mickleden and Oxendale however McDougall (1998: 2001) later suggests that the ice in these valleys during the Loch Lomond Stadial was part of a plateau icefield centred over High Raise further north. It is the authors intention that this study will address the knowledge gap currently present with respect to the south-west Lake District.

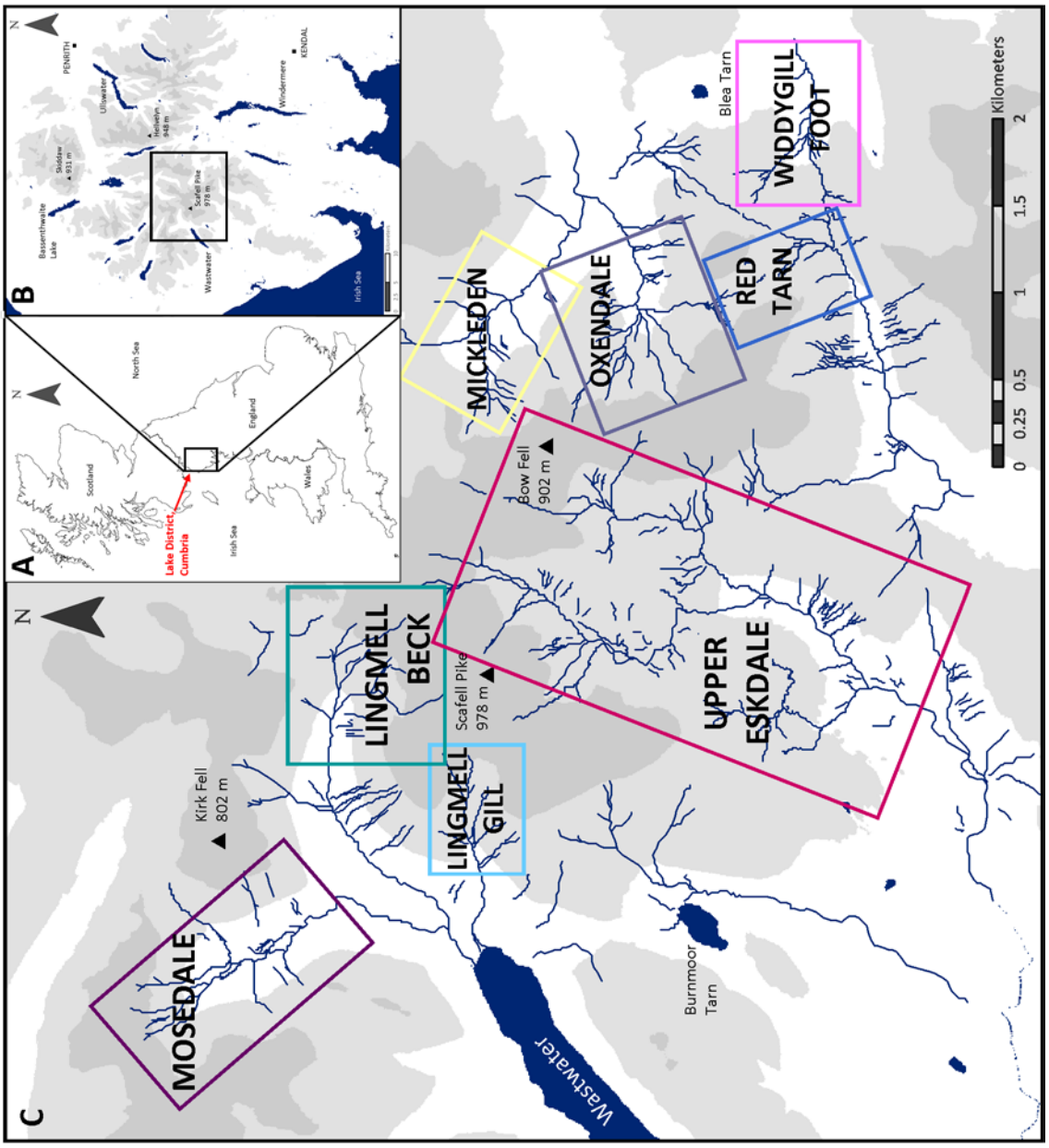


**Figure 2.4: The location of the field areas within the Lake District as described above.**

**Figure 2.5: The location of key areas in the south-west Lake District which are noted throughout the thesis.**

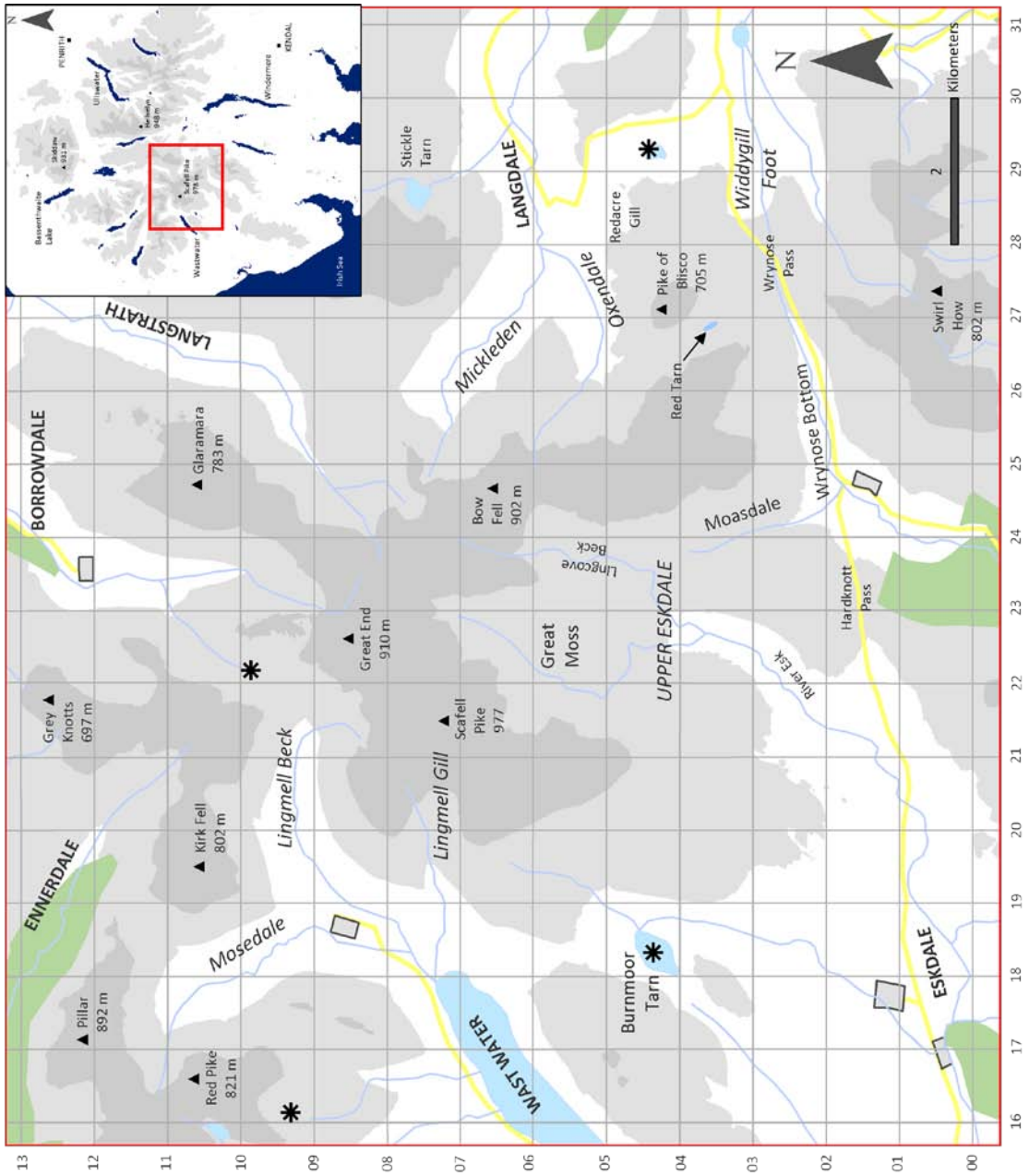

# Chapter 3

# METHODS PART 1: GLACIOLOGICAL RECONSTRUCTION

# 3: METHODS

## 3.0 Introduction

Mountain glaciers are relatively small, discrete features within a glaciated landscape which may eminate from a much larger ice mass feeding down from a higher altitude, or may be isolated within in their own mountainous niche environment; often with their accumulation areas occupying cirques. Mountain glaciers are therefore highly sensitive indicators of climatic change so by coupling the known characteristics and dynamics of mountain glaciers to traditional theories of glacial geomorphology it is possible to link glaciological processes to the form of even the most subtle geomorphology seen now as the remnants of palaeo-glaciers (Stokes, 2000).

Ideally, numerical absolute dating of sites would be widespread and would unquestionably identify sites occupied by ice during the LLS and those which were not. In the absence of widespread dating, it has been argued that distinct glacial events or stages have left behind a characteristic set of landforms on a local to regional scale (Lukas, 2006). As a result, geomorphological mapping and the associated glaciological reconstructions have been common place throughout the 20$^{th}$ century for sites around the British Isles. With the advent of more complex glaciological models it is now possible to test the viability of glaciers reconstructed on the basis of geomorphology along in terms of their relative surface and basal velocities. Furthermore, the increased availability of digital elevation models has encouraged a much more quantitative approach to geomorphological mapping and glaciological reconstructions. Such tools enable variables such as the ELA and snowblow factor to be calculated much more accurately.

## 3.1 Geomorphological mapping

As noted by Demek and Embleton (1978), geomorphological mapping is the main research method of geomorphology in numerous countries. This type of mapping relies on some form of landform classification e.g. the grouping or ordering of landforms by age, dimensions or origin, and is therefore built upon the assumption that all landforms have a characteristic shape (morphology) that can be used as a means of identification (Hubbard and Glasser, 2005). Such mapping can be carried out in the field however, more recently, the use of photogrammetric techniques and the availability of range of remotely sensed satalite and airborne imagery has revolutionised approaches to geomorphological mapping.

### 3.1.1 Landform identification and classification

Applied globally, morphostratigraphy utilises the spatial relationship between individual landforms to assign them to particular glacial episodes or stages (Colhoun, 1988; Lehmkuhl, 1998; Lemmen and England, 1992; Lukas, 2006). In order to apply the principles of morphostratigraphy successfully to glaciological reconstructions a series of criteria are required for the identification of specific glacial episodes such as the LLS in the British Isles. The morphostratigraphic criteria used in this project are shown in table 3.1.

As outlined in table 3.1 a number of different lines of evidence have been used in the glaciological reconstructions presented in this thesis in order to prevent erroneous reconstruction. The evidence used includes moraines, slope movement features, river terraces, periglacial trimlines and the vertical limits on sediment covered slopes. The presence of glaciofluvial landforms was also considered during the mapping process, however, such landforms were not present in the area mapped. In addition, river terraces were sparse in the area mapped and often did not follow the expected arrangement of one terrace inside the proposed LLS limit and multiple terraces outside of the limit. Instead, just one terrace was found both inside and outside of the proposed limit. This trend was traced down valley several kilometres. As a result it can only be assumed that river terraces are not apparent in the south-west Lake District possibility as a result of the being covered by the active, heavily scree covered slopes present throughout the region.

Throughout the project, moraines were identified by initial inspection of their basal breaks of slope and crest lines. On the NextMap relief shaded DEM, lateral and end moraine crestlines were visible as sharp continuous boundaries between light and dark shaded areas. With reference to lateral moraines, these were identified as generally linear forms trending along a valley side and increasing in elevation further up valley. End moraines were expected to have a similar form but with a more curved crest line curving up valley to form an arcuate ridge around the down-slope limit of the reconstructed glacier. In some cases these moraines also displayed steep proximal and shallow distal slopes. In contrast, hummocky moraine was identified as a series of ridges and mounds displaying a lesser degree of linearity and arranged in a more ‘chaotic’ manner (Benn, 1992).

As it was not possible to map trimlines from aerial photography, it was intended that the identification of such features would be done in the field however it soon became apparent that trimlines are not present throughout much of the south-west Lake District. Similarly, the presence of still active scree slopes/slope movements in the Lake District, make depositional

evidence of ice margin locations (including the uppermost limit) sparse. In the absence of trimlines and depositional evidence, the upper limit of the glacier was drawn based on the assumption that glaciers fill their accumulation areas (cirques/valley heads) to an elevation ~ 30 m below the top of the headwall (Wilson and Clark, 1998).

| Landform/landform assemblage | Inside LLS limits | Outside LLS limits | References |
|---|---|---|---|
| Lateral/end/hummocky moraine/s | Clear end moraines with sharp breaks of slope, bouldery moraines and moraines which are closely spaced. Hummocky moraine. | Subdued moraines with more rounded breaks of slope. Isolated moraine ridges which are spread further appart. | Sissons, 1974: 1976: 1979: 1980; Ballantyne, 1988: 1989: 2002: 2007; Ballantyne et al., 1998; Benn, 1992; Bennett, 1999; Gray, 1982: 1991; Lukas and Benn, 2007; Lukas, 2006. |
| Slope movement features | Small debris cones, localised 'immature' talus slopes. 'Freshly' glacially polished bedrock. | Large debris fans/accumulations which cover extensive areas of the slope face. | Ballantyne and Wain-Hobson, 1980; Ballantyne, 1989: 2007: 2002; Ballantyne and Hall, 2008; Sissons, 1974; Benn and Ballantyne, 2005; Ballantyne and Benn, 1994; Lukas, 2006. |
| Fluvially cut breaks of slope (river terraces) | One river terrace. | Multiple distinct river terraces. | Not previously used in glacier reconstuction. |
| Vertical limits on bedrock (periglacial trimlines) | Ice moulded and plucked bedrock. | Heavily jointed rock, blockfields, *in situ regolith*. | Ballantyne, 1986: 1989: 1997: 1998: 2002; Thorp, 1986; Benn and Ballantyne, 2005; Rae et al., 2004; McCarroll and Ballantyne, 2000; Lamb and Ballantyne, 1998; Lukas, 2006. |
| Glaciofluvial landforms (eskers etc.) | Smaller terraces. | Large kames, eskers and kettled outwash. | Sissons, 1974: 1976. |
| Vertical limits on sediment-covered slopes | Upslope and lateral termination of thick sediment cover, limits of glacially transported boulders and lateral moraines. | Large solifluction lobes and scree. | Thorp, 1986; Benn and Ballantyne, 2005; Gray and Brooks, 1972; Ballantyne, 1989: 2002; Lukas, 2006. |

**Table 3.1: The morphostratigraphic criteria used to the identify the location of LLS glaciers in the south-west Lake District. Modified from Lukas (2006).**

### 3.1.2 Use of aerial photography and NextMap (IfSAR) data

Reconstructions of Loch Lomond Stadial glaciers at their maximum extent and at various stages throughout deglaciation were initially carried out using aerial photography. Black and white aerial photographs at a variety of scales between 1:7,000 and 1:25,000 were used to identify moraine ridges and hummocks, flutes, kame and kettle topography, debris flows and fans, river terraces and post-glacial slope movement. All 1:25,000 photography was sourced from the Lake District National Park Authority and was flown by Ordnance Survey in 1972. These photos were complemented with more recent colour Google Earth imagery constructed from 2004 Infoterra aerial photography.

It was believed important to also consider landforms of post-glacial origin in order to confirm the terminal landforms as being of glacial origin. Evidence for the upslope glacier limit was also considered by looking for trimlines which marked the transition from ice-moulded to frost–weathered bedrock. In accordance with McDougall (1998: 2001), lateral moraines were deemed particularly important, not only in identifying lateral ice margins but also in the identification of palaeo-plateau icefields. In some areas, lateral moraines have been found to continue upslope to plateau areas, one example being High Raise in the central Lake District. This evidence suggests that such areas were sources of ice during the Loch Lomond Stadial and thus confirms that plateau icefields were present.

Areas of 'hummocky' moraine also required careful attention. The application of aerial photography was particularly valuable in this case as it facilitated the identification of any linearity between and within the landforms, which is often not clear from the ground. The contested genesis of 'hummocky' moraine makes this an important consideration. Both ice-marginal and subglacial origins of 'hummocky' moraine are proposed in the literature, and are believed to reflect differing styles of deglaciation (i.e. stagnation or active retreat). Crucially this has implications for the way in which glaciers responded to palaeo-climatic changes.

### 3.1.3 Field Mapping

Once areas had been mapped using aerial photography they were checked in the field. Landforms were recorded on 1:5,000 maps before being compared with those produced from airborne imagery. Although fieldwork was time consuming, time in the field was minimised by firstly using aerial photography to map the areas and then checking these maps in the field rather than vice versa. This approach allowed for a more comprehensive coverage of the field areas than would have been possible from aerial photography alone. This was particularly the case in areas where shadows on the photography caused some areas of landforms to be

'blacked out' or where the quality of the photographs had been reduced as a result of scanning. Fieldwork also allowed photographs of each site to be taken.

When in the field, it was necessary to check the landforms mapped from the DEM and the aerial photography with what was actually present on the ground. Firstly, the geomorphology mapped using the DEM and aerial photographs was compared to the Ordnance Survey 1:5,000 contours and each contour accounted for in terms of the landscape morphology as it was seen in the field. This was particularly important in areas where the data provided by the DEM and aerial photography was poor e.g. in areas of shadow on the photography or areas of steep ground where data was missing from the DEM. In such areas, the remotely sensed data failed so field mapping was the only way to record the geomorphology.

It was also necessary to check that each landform mapped remotely had been classified correctly i.e. a moraine mapped remotely still showed the characteristics used to distinguish a moraine in the field. Of particular note were the problems associated with some 'lateral moraines' which ran horizontally along the sides of Kirk Fell. Although these appeared on the aerial photography and DEM as clear lateral moraines, when in the field it became apparent that they were infact not glacial at all but were the result of much more recent slope instabilities/slumping.

Some small but significant changes in the landscape since the aerial photography was taken were also noted. Such changes, which included river bank slumps etc, were often indetectable on the DEM as they were beyond its resolution so field mapping was the only way to ensure that the geomorphological maps produce were true representations of the present day geomorphology.

### 3.1.4 Mapping using Erdas Imagine

The majority of the geomorphological mapping for this project was done in Erdas Imagine: a raster graphics editor and remote sensing application, running in Windows. NextMap IfSAR data of the chosen field sites was first mosaiced using the 'data prep' application in Erdas Imagine; a process that was found to be much more efficiently done in Erdas Imagine than in ArcGIS.

Having mosaiced the photographs, a series of vector layers in which to map were then created and labelled appropriately. In total, 12 vector layers were created to map the following landforms: moraines, debris flows and fans, rivers, river terraces, flutes, postglacial slope

movement, ice sheet lateral moraines, protalus rampart deposits, kettle holes and cirque headwalls. Vector layers were overlain onto the NextMap Digital Surface Model (DSM) and geomorphological information gained from both aerial photography and ground survey was transferred onto the DSM. This allowed for the creation of an accurately georeferenced map and the compilation of geomorphological information from 3 independent sources (NextMap, aerial photography and ground survey).

It was decided that mapping the crest lines of landforms would produce the most informative mapping, particularly in areas where deciphering inter- and intra-landform linearity was crucial. It was also important to ensure that the mapping was clear in order to accurately establish definitive glacier limits. As noted by Carr and Coleman (2007), the foundations of accurate glacier reconstructions are found within the initial interpretations of geomorphology. An approach which restricted interpretive error was therefore necessary and drawing of crest lines was seen as one way of achieving this.

## 3.2 Glacier reconstruction

The reconstruction of LLS glaciers can encompass a range of qualitative and quantitative techniques. These include; geomorphological mapping, the identification of the ice extent and surface morphology using hand-drawn ice surface contours, the calculation of ELAs, theoretical 2-dimensional modelling of glacier mass balance based on manual reconstructions, or, more complex 3-dimensional modelling which graphically reconstructs ice masses based on the input of a series of numerical variables. Here, the mass balance modelling carried out takes a geomorphological approach. As stated by Benn and Evans (1998), one of the most fundamental characteristics of glaciers and ice sheets is their ability to flow and move. These features of glaciers result in the production of landforms upon which many palaeo-glaciological reconstructions are based. A fundamental aim of modelling glacier mass balance and velocity is to quantitatively establish the link between glaciers and climate. In doing so, it is also possible to formulate a series of process-form relationships which link internal glaciological process to the genesis of the landforms which are seen in the landscape today as remenants of palaeo-glaciers. In turn such relationships can feed back into glaciological models by taking the geomorphological approach used here to test the viability of glaciers in the absence of more reliable absolute dating.

### 3.2.1 Reconstruction of ice extent and surface morphology

The extent of the LLS ice masses in the south-west Lake District were drawn based on the geomorphology. Based on the morphostratigraphic criteria outlined in table 3.1, the ice limit

was placed along the crestline of the moraines deemed most likely to represent the maximum extent of LLS ice. Moraines were used in this way to identify the downslope and lateral extent of the ice while the upslope ice extent was placed 30 m below the top of the cirque/valley headwall.

The surface morphology of the ice mass was then established by drawing a series of ice surface contours. Ice surface contours were drawn at 50 m intervals perpendicular to the orientation of ice flow indicated by the geomorphology. In the accumulation area convergent flow away from the ice margins and towards the ELA is indicated by contours which curve up glacier. In contrast the contours in the ablation area were drawn to suggest divergent ice flow towards the ice margin. In addition, the ice surface contours subtly take into account the morphology of the glacier's bed, most notably, in some cases, the ice surface contours become much more linear and closely spaced where the bed becomes much steeper close to the ELA.

### 3.2.2 The calculation of the Equilibrium Line Altitude (ELA)

The calculation of a glacier's ELA has long been used as a basis for palaeoclimatic inferences and is the theoretical altitude on a glacier at which accumulation and ablation are exactly balanced over the period of one year (Mitchell, 1996: Benn and Lehmkuhl, 2000). The close relationship between climate and the ELA means that the ELA can often provide an important indication of a glacier's response to climate change. Furthermore if a temperature proxy, for example based on palynological records is used, simple calculations of the temperature at the ELA and the annual precipitation required at the ELA to maintain a steady state glacier are possible. ELA reconstructions therefore provide the foundations for further quantification of numerous palaeoclimatic and palaeoglaciological variables. It is therefore vitally important that ELA calculations are provided by a sound methodology which incorporates a variety of glaciological variables such as glacier type, catchment topography, hypsometry and environmental conditions. Numerous methods of ELA calculation have been employed and will be reviewed here.

Arguably the least accurate method of ELA estimation are those values based upon lateral moraine elevations or cirque floor elevations. The use of lateral moraines as ELA indicators assumes that lateral moraines are only able to form below the ELA in the ablation area of a glacier. Lateral moraines are able to develop where ice flows outwards towards the margins of a glacier. In the accumulation zone ice flows inwards while in the ablation zone ice flows radially outwards towards the ice margins. Since the ELA is the altitude at which net balance is equal to zero the ELA theoretically marks the divide between the accumulation and ablation

zone. Thus, below the ELA lateral moraines are expected and the upper limit of these moraines lies at approximately the same altitude as the ELA. Problems however arise with this method when lateral moraines are not present or when lateral moraines have formed as a result of small glacier readvances during periods of overall glacier recession. It is often the case that lateral moraines are not present in high-relief or high-altitude catchments (Benn and Lehmkuhl, 2000).

Similar problems occur with the use of cirque floor altitude as a means of ELA estimation. In many cases cirques are not present in the vicinity of the glacier and consequently this method cannot be employed. Unlikely glacial deposits which can be confidently dated using a chosen absolute dating technique it is arguably more complex to assign a cirque to a particular glacial phase. It is assumed that cirque development is an indirect long term response to regional climate, through the formation of glaciers on favourably located slopes. Cirque formation in the Lake District occurred prior to the Loch Lomond Stadial and consequently glaciers during the stadial exploited the already present cirques which provided a localised environment ideally suited to glacier nourishment. A potential correlation between glacier location, cirque location and aspect is therefore recognised. ELA estimations based on cirque floor elevations can therefore also not be reliably assigned to a particular glacial phase and in many cases their formation pre-dates the particular time period being investigated (Benn et al., 2005). Crucially, both of the methods above do not take into account many of the key variables which ultimately dictate the ELA. Consequently these methods have not been used to determine the final mean value of the ELA for any of the glaciers considered in this research.

The terminus-to-head altitude ratio method (THAR) assumes that the THAR is equal to the ratio of the altitude difference between the terminus and the ELA divided by the total altitudinal ratio of the glacier. An ELA is therefore estimated as follows:

$$\text{ELA} = A_t + \text{THAR}(A_h - A_t)$$

(equation 1)

where $A_t$ is the altitude of the terminus and $A_h$ the altitude of the head (the maximum altitude). This method relies on the correct value for THAR being used and this often varies between glaciers both within and across regions. Furthermore this method does not take into account glacier hypsometry or mass balance and thus Benn and Lehmkuhl (2000) describe this method as a 'very crude' estimation of an ELA. In the absence of trimlines difficulties can also arise in accurately defining the maximum altitude of a glacier: a problem that was frequently

encountered in the Lake District. For the purposes of this research it was therefore assumed that the maximum altitude of the glacier was located approximately 30 m below the altitude of the headwall as suggested by Wilson and Clark (1998). This method also works most successfully on glaciers with 'simple' linear long axis'. Where glaciers display much more complex hypsometry the method should be applied with extreme caution.

To improve on the crude ELA estimation provided by the THAR method, the Accumulation-area ratio (AAR) method was implemented. Unlike the methods described above the AAR method takes into account the area occupied by the accumulation and ablation areas by assuming that the accumulation area occupies some fixed proportion of the glacier's surface area. On modern mid- to high-latitude glaciers, such as those in the maritime climate of north-western North America, Porter (1975) suggests that AAR values fall between 0.5 and 0.8 (i.e. 50-80 % of the glacier's surface area). Observations from glaciers in central Asia by Grosval'd and Kotlyakov (1969) also generally fall between 0.5 and 0.8. A mean value of 0.6 ± 0.05 is therefore suggested by Porter (1975) as suitable mean value for an AAR. Meierding (1982) however has calculated ELAs using AAR values ranging from 0.5 to 0.75 and concludes that an AAR of 0.65, which provided the lowest RMSE value in his investigation, is the most suitable AAR for the mid-latitude glaciers of northern Front Range in Colerado. Furthermore, Murray and Locke (1989) agree with these findings, and consequently, AAR values of 0.6, 0.65 and 0.7 were applied to the reconstructed Lake District glaciers, which are also in a mid-latitude locality ~ 57° N.

It follows that steeper ablation gradients result in higher steady state AARs. As a result, AARs can be highly variable in mountainous regions where the altitudinal ranges of glaciers are greater. This method can be problematic however as it does not take into account glacier mass balance or hypsometry. Changes in climatic regime, debris cover, topographic shading, avalanching, snowblow and glacier hypsometry can also cause the AAR of glaciers to vary. Benn and Gemmell (1997) express concern over the assumption that AARs are regionally uniform and suggest that this is only reasonable in so much as AARs are influenced by regional climate. It is therefore recommended that ELAs are calculated using a variety of AARs and then these results compared to direct observations in order to determine the most appropriate AAR for that glacier or region.

The area-weighted mean altitude (AWMA) method has been used by Sissons (1976: 1980) and Sissons and Sutherland (1976) and assumes that accumulation and ablation are linearly related

to altitude over the whole altitudinal range of the glacier. The AWMA method for ELA calculation is represented as follows:

$$\text{ELA} = \frac{\sum_{i=0}^{n} A_i h_i}{\sum_{i=0}^{n} A_i}$$

(equation 2)

where $A_i$ is the surface area of the glacier between each contour interval $i$ ($m^2$), $h_i$ is the altitude of the mid-point of the contour interval $i$, and $n$+1 is the number of contour intervals.

Criticism of this method is primarily focused around its assumption that both the accumulation and ablation gradients are linear and equal. Hypothetical values for non-linear gradients were input into calculations of AWMA and although this produced a change in the ELA, Sissons and Sutherland (1976) suggest that this change is minimal and that the main control on the ELA is glacier hypsometry which this method accounts for.

In order to improve on the AWMA method outlined above, Furbish and Andrews (1984) produced a more rigorous method which takes into account both glacier mass-balance and glacier hypsometry. This method is known as the 'Balance Ratio' method. The method assumes that the accumulation and ablation gradients are both linear, however they are numerically different as a result of the different climatic variables controlling the accumulation and ablation areas. Typically, the ablation gradient ($b_{nb}$) is steeper than the accumulation gradient ($b_{nc}$) and the ratio between the two gradients provides the balance ratio (BR) as follows: BR = $b_{nb}/b_{nc}$. As with the previous methods described, this method assumes the following:

$$d_b . A_b = d_c . A_c$$

(equation 3)

where $d_b$ is the average net annual ablation in the ablation area, $d_c$ is the average net annual accumulation in the accumulation area, $A_b$ is the area of the ablation area and $A_c$ is the area of the ablation area.

For equilibrium conditions, the ELA of a glacier is determined on a trial and error basis using equation 4 below.

$$b_{nb} / b_{nc} = z_c . A_c / z_b . A_b$$

(equation 4)

where $z_c$ is the area-weighted mean altitude of the accumulation area, $z_b$ is the area-weighted mean altitude of the ablation area, $b_{nb}$ is the mass-balance gradient in the ablation area and $b_{nc}$ is the mass-balance gradient in the accumulation area.

A suitable balance ratio which is climatically representative of the study area is then defined and the ELA is determined on a trial and error basis using a hypsometric curve for the glacier. The curve can be used to determine values for $z_c$, $z_b$, $A_c$ and $A_b$ by choosing trial values for the ELA. The values for $z_c$, $z_b$, $A_c$ and $A_b$ are then input into equation 4 and this process is repeated until the desired value for $b_{nb}/b_{nc}$ is achieved (Benn and Gemmell, 1997). A spreadsheet produced by Benn and Gemmell (1997) provides a faster way of applying the method outlined by Furbish and Andrews (1984).

As previously stated, this method assumes different but linear mass-balance gradients for the accumulation and ablation zones and as a result is based on a summary of the mass-balance curve for the glacier as a whole. It also provides an improvement on previous methods which either assume a constant mass-balance gradient throughout the whole glacier or do not consider mass-balance at all. As shown in table 4.1 ELAs were calculated using this method for balance ratios (BR) of 2.0, 1.81, 1.6, 1.54 and 1.43. These values (x) indicate that the vertical change in mass balance is x times larger in the ablation area than in the accumulation area as a result of factors such as altitude or ice albedo. Typically, glaciers with high balance ratios have small ablation areas compared to the area of the glacier since only a small ablation area is required to balance the input of snow in the accumulation area. This is common on tropical glaciers. Conversely, glaciers with lower balance ratios have larger ablation areas as a proportion of the total glacier area, a situation which is more typical of polar glaciers (Benn and Evans, 1998).

### 3.2.3 The influence of snowblow on glacier development/maintenance

Local factors which relate to the specific topography and microclimate of an individual glacier can often dictate whether or not a glacier will develop. One such factor is the potential for snowblow from the ground surrounding a glacier. This has been shown by several authors to

be significant in determining glacier distribution and also the ELA (Manley, 1959: Sissons, 1980a: Sissons and Sutherland, 1976: Leonard, 1989: Mitchell, 1996: Sutherland, 1984: Benn and Ballantyne, 2005).

The production of a transparent definition of areas which have the potential to contribute mass to a glacier through snowblow is firstly required. Manley (1959) touched on the idea of 'snowblow areas' however the first definition was provided by Sissons and Sutherland (1976) who considered all ground lying above the ELA and sloping towards the glacier surface as having the potential to contribute mass to a glacier via snowblow. This definition was further modified by Robertson (1988) to include uphill snow movement and later by Mitchell (1996) to include nearby plateau surfaces. Mitchell (1996) defined snowblow areas as 'ground lying above the altitude of the equilibrium line and laterally continuous to the former glacier' (Mitchell, 1996, p. 242).

Some further clarification of the definition provided by Mitchell (1996) is required in order to minimise the variability associated with human opinion when quantifying snowblow areas. Benn and Ballantyne (2005) provide a more quantitative definition of snowblow area as follows: 'terrain located within a southwestern quadrant (180-270°) upslope and windward of ice surfaces, including plateaux, all glacier facing slopes and all other plateau-edge slopes with gradients less than 5° irrespective of orientation' (Benn and Ballantyne, 2005, p. 588).

By the authors own admission the definition provided by Benn and Ballantyne (2005) is conservative as it assumes that only terrain within the southwest quadrant may be significant and includes a limiting gradient of 5°. The current author suggests that it is more realistic to include surfaces with gradients of less than 10° irrespective of orientation.

For clarity it is suggested that areas with the potential to contribute mass to a glacier via the input of snow should fulfil each of the following criteria:

1. *surfaces sloping towards the glacier, forming part of a plateau surface or sloping away from the glacier with a slope of ≤10°.*
2. *surfaces laterally contiguous to the glacier.*
3. *surfaces above the equilibrium line altitude.*
4. *surfaces which can be connected to the glacier surface via a straight line.*

In order to accurately identify potential snowblow areas based on the above definition an IfSAR DEM was classified according to slope angle, elevation and aspect and the snowblow areas digitised. The snowblow area was also split into quadrants in order to assess the contribution of winds from different directions to snowblow. The quadrants were then further split into 15° sectors and the area within each sector was calculated.

As noted above snowblow area was split into 90° quadrants from north; NW, SW, SE and NE. Further southern (135-225°) and western quadrants (225-315°) were also developed to assess the contribution of the south-southwesterly winds believed to have been dominant during the Loch Lomond Stadial to snowblow.

In order to assess the potential of each of these quadrants to supply mass to the glacier by snowblow, snowblow factors were calculated by following the procedure outlined by Sissons (1980). This method is summarised in equation 5 below.

$$SF = \sqrt{\frac{A_{snowblow}}{A_{glacier}}}$$

(equation 5)

where *SF* is the snowblow factor of a given quadrant, sector or glacier, $A_{glacier}$ is the area of the glacier surface and $A_{snowblow}$ is the snowblow area being considered. It is necessary to take the square root of glacier area/snowblow area since large potential snowblow areas with elongate shapes will not all have an equal opportunity to contribute mass to the glacier. Because of the size of these areas the terrain further away from the glacier will be less likely to contribute snow to the glacier (Sissons, 1980: Mitchell, 1996).

### 3.2.3 Glacier dynamics

In order to test the viability of the reconstructed glaciers, it is necessary to apply a quantitative model. It is hoped that the application of such models will reduce the element of qualitative speculation associated with glaciological reconstruction. The applied model, which largely follows the methodology outlined by Carr and Coleman (2007) is based around independent palaeo-temperature data. Coope and Joachim (1980) provide a palaeo-environmental framework for St Bees Head from coleoptera and assume an environmental lapse rate of 0.0065°C/m. As noted by Hindmarsh (1989) glacier flow is directly influenced by the mass-balance dynamics of a glacier, more than the reverse (Carr and Coleman, 2007). Carr and

Coleman (2007) therefore argue that steady state 'balance' dynamics can be reconstructed from information pertaining to the mass-balance of a glacier.

This methodology can also be applied to landforms for which the genesis is uncertain in order to determine whether or not they were formed by viable active glaciers. The misidentification of geomorphological features can lead to features which originated in periglacial environments such as rock glaciers or protalus ramparts or those of paraglacial origin such as slope failures being misidentified as moraines. On a regional scale this can lead to inaccurate glacial reconstructions.

Previous methods of glaciological reconstruction have been criticised by Carr and Coleman (2007). The assumption that basal motion at the ELA is zero by Murray and Locke (1989), for example, allows them to apply continuity theory to reconstruct ice velocities down-glacier of the ELA. This assumption however is tentative since monitoring of contemporary ice masses recommends that basal motion may account for up to 90 % of total glacier motion at the ELA in cirque and valley glaciers (Andrews, 1975: Carr and Coleman, 2007).

It is evident from the literature that the most problematic part of glaciological reconstruction relates to the computation of basal motion and the relative contribution of its two key components: basal sliding and subglacial deformation. Models often fail to consider the contribution of subglacial deformation (Oerlemans, 1997) and thus it is clear that a more transparent approach to glaciological modelling is required.

- **Derivation of temperature and accumulation at the ELA.**

Using the environmental lapse rate provided by Coope and Joachim (1980), equation 6 below can be used to derive the temperature at the ELA of a glacier.

$$T_{ELA} = T_3 + 0.0065(A_{ELA} - A_{proxy})$$

(equation 6)

where $T_{ELA}$ indicates the temperature at the ELA, $T_3$ is the 3-month mean summer temperature (June-August, in °C), $A_{ELA}$ is the altitude of the ELA and $A_{proxy}$ is the altitude of the proxy site. $T_3$, a temperature proxy based on Coleoptera assemblages at St Bees Head, can be calculated from July mean temperatures ($T_j$) using equation 7 provided by Benn and Ballantyne (2005). Equation 7 was derived following the analysis of meteorological data from stations in Scotland and Scandanavia by Benn and Ballantyne (2005).

$$T_3 = 0.97T_j$$

(equation 7)

where $T_j$ is the mean July temperature in °C. In order to calculate the winter accumulation plus summer precipitation in mm $a^{-1}$ w.e. ($P_a$) at the ELA, Ohmura et al. (1992) find that the best-fit polynomial regression curve of $T_3$ against $P_a$ can be shown as follows:

$$P_a = a + bT_3 + cT_3^{\,2}$$

(equation 8)

where a = 645, b = 296 and c = 9. The standard error provided by this estimate is ± 200 mm $yr^{-1}$ w.e.. $P_a$ therefore represents the total accumulation required at the ELA in order to maintain a steady-state equilibrium and includes direct precipitation along with inputs from snowblow and avalanching; however these individual components are not quantified here. It has been observed by Ohmura et al. (1992) that winter mass balance (accumulation) correlates well with annual precipitation ($P_a$). $P_a$ can therefore be assumed to equate to the winter balance ($B_w$).

- **Derivation of the ablation gradient and net ablation**

Ablation is the result of heat supplied to the surface of snow or ice. Heat transfer from the air is a function of temperature and therefore also a function of altitude (Schytt, 1967). An indication of the influence of this heat transfer is provided by an ablation gradient which can be defined as the change in ablation consequent on a change in altitude. Ablation gradients are therefore expected to be steep (>5 mm/m) on tropical and mid-latitude glaciers and shallow (<3 mm/m) in cold polar regions (Carr and Coleman, 2007: Schytt, 1967). Steep ablation gradients are therefore taken to require rapid ice flow which replenishes the high ablation occurring in the ablation zone and particularly at the terminus. Conversely, shallow ablation gradients require slower ice flow since less mass is required to replenish that being lost through ablation. Carr and Coleman (2007) suggest that a positive correlation exists between the ablation gradient (mm $m^{-1}$) and the mass loss at the ELA (m) of a glacier using data sourced from Andrews (1972) which provides an $r^2$ value of 0.83.

As noted by Carr and Coleman (2007), if mass loss at the ELA is equivalent to $P_a$ then the ablation gradient can be used to derive a reconstructed glacier mass-balance. Andrews (1972)

has derived the following non-linear relation between the ablation gradient ($a_z$) and the total accumulation required at the ELA to maintain a glacier in steady-state equilibrium ($P_a$):

$$a_z = 7.809\times10^{-7} P_a^{\,2} - 5.681\times10^{-4} P_a + 3.3342$$

(equation 9)

where $P_a$ remains in mm $a^{-1}$ and $a_z$ is in mm $m^{-1}$ $a^{-1}$. Equations 6, 8 and 9 can then be combined to eliminate $P_a$ and $T$ , giving $a_z$ as a quartic function of the ELA altitude (for convenience here taken as $h$, not $A_{ELA}$) as follows:

$$a_z(i) = Ah^4 - Bh^3 + Ch^2 - Dh + E$$

(equation 10)

where A, B, C, D and E represent positive coefficients obtained from the coefficients of equations 6, 8 and 9 ($T_{ELA}$, $P_a$ and $a_z$ respectively). The actual net ablation, $a$, is obtained by integrating the ablation gradient (equation 10) with respect to the altitude of the ELA, $i$, based on the boundary condition that the net ablation at the ELA, $i_e$, equals net accumulation and thus zero. Hence,

$$\begin{aligned} a(h) &= \int_{h_e}^{h} a_z(h')\,dh' \\ &= \frac{1}{5}A\left(h^5 - {h_e}^5\right) - \frac{1}{4}B\left(h^4 - {h_e}^4\right) + \frac{1}{3}C\left(h^3 - {h_e}^3\right) \\ &\quad - \frac{1}{2}D\left(h^2 - {h_e}^2\right) + E\left(h - h_e\right) \quad \text{mm a}^{-1} \end{aligned}$$

(equation 11)

The total ablation, $b$, in a given height interval, e.g. from a lower height $h_l$ to an upper height $h_u$, can be found by integrating equation 11 multiplied by the glacier width as a function of the height, $G(h)$;

$$b(h_u, h_l) = 1\times1\ \ 0^3 \int_{h_l}^{h_u} a(h)\,G(h)\,dh \quad \text{m}^3\ \text{a}^{-1}$$

(equation 12)

where the factor of 1x $10^{-3}$ ensures that units of $m^3$ $a^{-1}$ w.e. are produced. Since the function $G(h)$ is not known analytically, it is necessary to approximate the integral over the 50 m ice

surface contour intervals. If $S$ represents the total surface area in $m^2$ between the 50 m contours of $h_l$ and $h_u$, then net ablation can be derived as follows;

$$b(h_u, h_l) \approx 1\times10^{-3} \frac{S}{h_u - h_l} \int_{h_l}^{h_u} a(h)\, dh$$

$$= \frac{S}{h_u - h_l} \begin{pmatrix} C_6\left(h_u^{\,6} - h_l^{\,6}\right) - C_5\left(h_u^{\,5} - h_l^{\,5}\right) + C_4\left(h_u^{\,4} - h_l^{\,4}\right) \\ - C_3\left(h_u^{\,3} - h_l^{\,3}\right) + C_2\left(h_u^{\,2} - h_l^{\,2}\right) - C_1\left(h_u - h_l\right) \end{pmatrix} \quad \mathrm{m^3\ a^{-1}}$$

(equation 13)

Table 3.2 below provides the values for the coefficients $C_n$ used in equation 13 above.

| Coefficient | Value |
|---|---|
| $C_6 = A/30 \times 10^{-3}$ | $3.764\times10^{-18}$ $\mathrm{m^{-4}\ a^{-1}}$ |
| $C_5 = B/20 \times 10^{-3}$ | $8.577\times10^{-14}$ $\mathrm{m^{-3}\ a^{-1}}$ |
| $C_4 = C/12 \times 10^{-3}$ | $7.080\times10^{-10}$ $\mathrm{m^{-2}\ a^{-1}}$ |
| $C_3 = D/6 \times 10^{-3}$ | $2.506\times10^{-6}$ $\mathrm{m^{-1}\ a^{-1}}$ |
| $C_2 = E/2 \times 10^{-3}$ | $5.954\times10^{-3}$ $\mathrm{a^{-1}}$ |
| $C_1$ | $2.258\times10^{-16}h_e^{\,5} - 4.289\times10^{-13}h_e^{\,4} + 2.832\times10^{-9}h_e^{\,3} - 7.520\times10^{-6}h_e^{\,2} + 1.191\times10^{-2}h_e$ $\mathrm{m\ a^{-1}}$ |

**Table 3.2: Coefficient $C_n$ values for use in equation 13.**

Since the glacier is assumed to be in steady-state equilibrium, the calculated net ablation can also be taken as the net accumulation.

- **Derivation of mass-flux and ice velocities**

The net ablation calculated from equation 13 in $m^3\ a^{-1}$ w.e. can be simply converted to a volume of ice by dividing by the density of ice (assumed throughout to be 910 kg $m^{-3}$).

The calculation of the cross sectional area of the ELA ($m^3$) allows an average surface velocity in m $a^{-1}$ ($U_s$) to be calculated by dividing mass flux by cross sectional area. It is then necessary to calculate the contribution of the components of this velocity which are essentially internal ice

deformation ($V_m$) and basal sliding ($U_b$) (Paterson, 1994). Internal ice deformation ($V_m$) can be calculated by subtracting $U_b$ from $U_s$ (see figure 3.1).

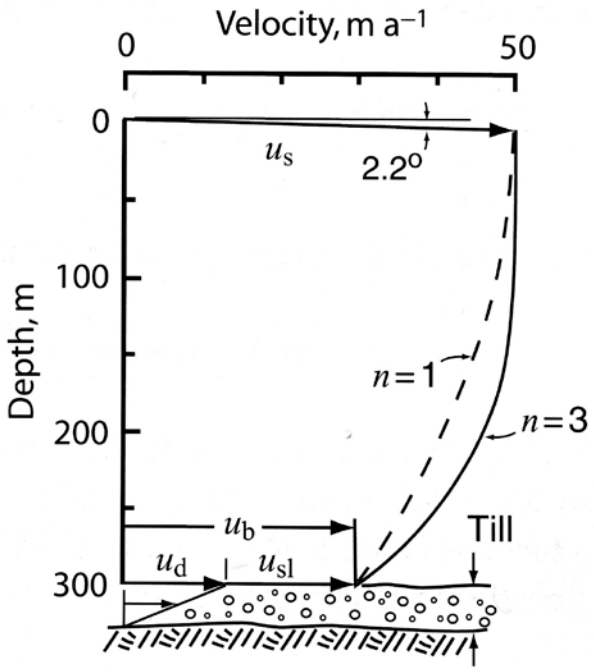


**Figure 3.1: The velocity profile of a glacier where $U_s$ indicates the mean surface velocity, $U_b$ the velocity contribution of basal motion by sliding and $V_m$ the contribution of ice deformation to overall velocity. Adapted from Hooke (2005).**

In order to derive the maximum surface velocity of ice deformation, $V_c$, it is first necessary to calculate basal shear stress which can be computed by;

$$\tau_b = (\rho g H F \sin\alpha)/100{,}000$$

(equation 14)

where $\tau_b$ is the basal shear stress (bars), ρ is the density of ice taken as 910 kg/m$^3$, g is the acceleration due to gravity (9.81 m/s$^2$), H is the ice thickness at the centre point of the ELA (m), F is the glacier's 'shape factor' (derived from equation 15 below) and ά is the ice surface slope at the ELA in degrees.

$$F = \frac{j}{km}$$

(equation 15)

*j* is the cross sectional area of the bed across the ELA, *k* is the centre line ice thickness at the ELA and *m* is the perimeter of the bed at the ELA. The calculated value for $\tau_b$ can then be used

within equation 16 which is an adapted flow law for glacier ice to compute the maximum surface velocity of ice deformation;

$$V_c = \frac{(2Q\tau_b{}^n H)}{(n+1)}$$

(equation 16)

where $V_c$ is the ice centre line deformation (m $a^{-1}$), Q is a temperature dependant constant of flow law (here taken as 0.167 $bar^{-3}$ $yr^{-1}$) and *n* is an exponential constant of flow law (here taken as 3) (Glen, 1954: Nye, 1952: Carr and Coleman, 2007). The average rate of ice deformation at the ELA (m $a^{-1}$) is then subtracted from the mean balance velocity (m $a^{-1}$) to give the required basal motion (m $a^{-1}$). This value is then taken as a percentage of the mean balance velocity (m $a^{-1}$) to give the proportional contribution of basal motion to glacier velocity (%).

## 3.3 Sedimentological evidence: Coring

Coring was carried out in order to determine the down-valley limit of ice during the Loch Lomond Stadial (LLS). The sedimentological sequences found both inside and outside of the LLS ice limits are assumed to have distinct stratigraphic differences. Classically, sequences found outside of the LLS were expected to reveal a tripartite sequence consisting of LGM/Late Devensian ice sheet, Windermere Interstadial, LLS and Holocene sediments. In contrast, sequences taken from within the LLS limits were expected to lack a clear LLS signal and instead, simply show a gradual transition from a lower unit to an upper Holocene unit. This technique therefore provided a means of relatively dating the proposed LLS limits.

### 3.3.1 Site Selection

Cores were collected from two sites in the south–west Lake District: Mosedale and Upper Eskdale. A Russian corer was used in order to prevent sediments being lost as the core was removed from the ground. Sites were identified both inside and outside of the proposed glacier limits in order to relatively date the end moraines of the Loch Lomond Stadial glaciers and thus confirm or reject these as the maximum extent of the glaciers. The locations of the coring sites are indicated on figures 4.1a/b and 5.1a/b where they can be view in the context of the local geomorphology.

Cores were pushed into the ground by hand to a maximum depth of 3.10 m. Exact coring sites within the five study areas were identified based on a number of factors including the

proximity to post-glacial/Holocene sediment influx including any rivers or streams, site wetness, the surface profile of the site and its accessibility. Ideally, sites with flat surface profiles, away from fluvial influences with a reasonably high degree of wetness and relatively easy access were preferable.

### 3.3.2 Coring method

The Russian corer was inserted vertically into the ground to the maximum depth that could be reached. On several occasions the depth of the cores was limited by rocks within the sediment (frequently part of extensive boulder/gravel layers deposited by nearby rivers) or by highly consolidated sediment which the corer could not penetrate. The corer was then rotated clockwise by 360° in order to shut the gate on the corer to entrain the sediment. Once exposed cores were stored in sealed plastic tubing in a fridge before being analysed.

## 3.4 Summary

- Geomorphological mapping was carried in the field, from aerial photography and from NextMap using a series of morphostratigraphic criteria.
- Geomorphology was first mapped from NextMap and aerial photography and the initial maps were then checked in the field.
- When sound geomorphological maps had been drawn, ice margins were drawn according to the geomorphological differences expected inside and outside of the LLS limits according to the morphostratigraphic criteria set out before the onset of mapping.
- Ice surface contours were drawn perpendicular to the ice flow orientation suggested by the geomorphology.
- The viability of the reconstructed glaciers was tested using a simple mass balance model. The model compares surface and basal glacier velocities and assumes that a glacier in which the basal velocity exceeds 90 % of the surface velocity is not glaciologically viable.
- The potential contribution of snowblow to each of the glaciers was calculated and is represented in the thesis by the snowblow factor.
- Coring was carried out at selected sites using a Russian corer and analysed for particle size using a laser granulometer.

Chapter 4

# METHODS PART 2: GEOMORPHOLOGICAL MAPPING: A REVIEW OF DATA SOURCES AND METHODS OF ORTHORECTIFICATION

# 4: METHODS

## 4.0 Introduction

This project lends itself to several methodological approaches involving various different data sources and types. Mapping was carried out in the field, from aerial photography and from IfSAR NextMap data. All aerial photography was kindly supplied by the Lake District National Park Authority from the Ordnance Survey 1972 flight series. ArcGIS and Erdas Imagine were used to produce the final maps and each program provided unique advantages and disadvantages. Problems encountered at the various stages of research are discussed along with alternative options. The use of NextMap IfSAR data will also be discussed with specific reference to this project, and compared to its use in a larger scale project. Problems that have arisen largely relate to the resolution of the IfSAR data and for this reason a comparison between IfSAR and LiDAR data is provided.

## 4.1 IfSAR data in comparison to other remotely sensed data

Operating commercially since January 1997, Intermap's single-pass across-track interferometric synthetic aperture radar (IfSAR) STAR-3i is the source of data for NextMap. The STAR-3i has an X-band SAR interferometer with a frequency of 9.5675 GHz onboard a LearJet 36. An onboard differential Global Positioning System (GPS) combined with a laser-based inertial navigation system ensure the accurate positioning and orientation of the radar. The flying altitude at which the data is collected contributes to the accuracy of the data, with lower flying altitudes producing the most accurate data as a result of a lower signal to noise ratio and shorter lever arm errors. STAR-3i flights generally occur between altitudes of 6000-7000 m (Dowman et al., 2003).

In addition to the NextMap DSM, a Digital Terrain Model was also used. A DSM displays the first ground surface that the X-band IfSAR strikes and therefore includes terrain features, buildings, power lines and vegetation cover. In contrast, DTMs represent the elevation of the bare earth and water without the inclusion of vegetation cover, buildings etc (as shown in figure 4.1). The accuracy of DTMs is however heavily dependant on the algorithms used to remove surface features.

NextMap currently provides a highly cost effective and comprehensive elevation data coverage of the United Kingdom with a spatial resolution of 5 x 5 m and vertical accuracy of 0.5-1 m. Admittedly, data sets such as LiDAR do offer a higher resolution often with a 2 x 2 m spatial resolution and a vertical accuracy of 0.15 m. This difference in accuracy can be accounted for by the higher flight height of IfSAR data (~6500 m) compared to that of LiDAR data (~800 m).

Currently, however, there is only 60,000 $km^2$ of LiDAR coverage in the United Kingdom and this does not include the south-west Lake District required for this project.

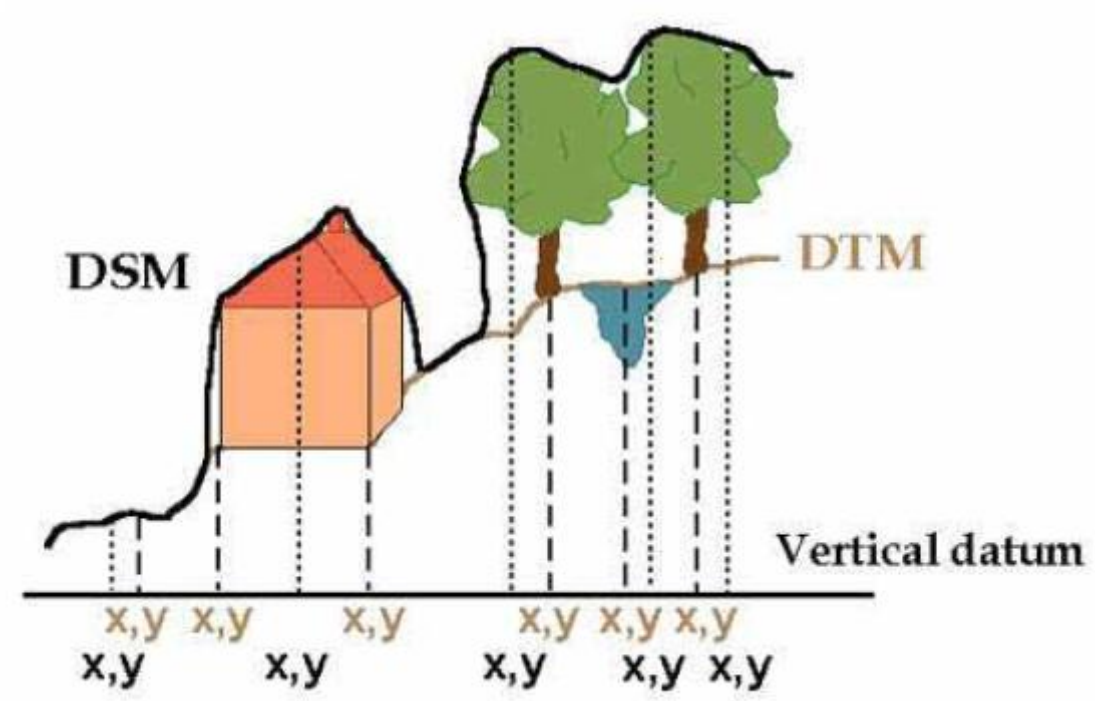


**Figure 4.1: Illustration of a DSM and DTM taken from Dowman et al. (2003). The DSM records the elevation of the first surface that the X-band IfSAR strikes so includes trees, buildings etc while the DTM is the product of such features being removed from the DSM to effectively show the elevation of the bare earth.**

The Ordnance Survey Landform PROFILE™ data available through Edina Digimap (provided by the University of Edinburgh) is a contour based data set compiled by stereo-interpretation of aerial photographs over a number of years. This is the highest resolution data set available from Edina. For comparison, OS Landform PROFILE™ data has a spatial resolution of 10 x 10 m and a vertical accuracy of ±5 m compared to the 5 x 5 m spatial resolution provided by NextMap (Chiverrell et al., 2008). Problems associated with the OS Landform PROFILE™ data include an absence of contours around anthropogenic features and the smoothing of contours during digitisation and cartographic presentation. It is clear, therefore, that NextMap IfSAR data far surpasses the capabilities of OS Landform PROFILE™ data and consequently OS Landform PROFILE™ data is not used in this project.

The elevation measured by a single pixel, however, is the result of a combined signal of scatterers. For example, when the X-band of the radar strikes a surface feature it may penetrate into the feature beyond the expected visible surface. This is the case when an X-

band strikes an area of woodland but is far less significant in the case of buildings or roads etc. Consequently in areas of woodland or vegetation the resulting pixel may not be a true representation of a feature's height but instead a combination of a number of different scatterings such that more height measurement noise is produced. Such errors should therefore be considered carefully when applying NextMap data, particularly in areas of vegetation cover.

Smith et al. (2006) also provide an evaluation of several sources of remotely sensed data: LiDAR, Shuttle Radar Topography Mission C-Band (SRTM), Landmap, OS Panorama, OS Profile, NEXTMap and Landsat Thematic Mapper. In order to assess their viability for use in geomorphological mapping Smith et al (2006) compared each of the data sets with 1:10,560-scale field geomorphological mapping. With data sets such as SRTM, OS Panorama, OS Profile, Landmap and Landsat Smith et al (2006) conclude that the spatial resolution of the data inhibits its use in geomorphological mapping. As previously stated, this is particularly the case when mapping geomorphology pertaining to the Loch Lomond Stadial which is often much smaller and subtle than the geomorphology associated with the Dimlington Stadial ice sheet. In one particular area mapped by Smith et al (2006) for example, 322 drumlins were mapped in the field. Of these, 189 drumlins were identified by NextMap, 50 by OS Profile and just 38 by OS Panorama. Furthermore, with respect to the positional accuracy of each of the mapped landforms, the work of Smith et al (2006) indicates that 36% of the landforms identified by NextMap were coincident with those mapped in the field (i.e. they were within ~ 200 m of the field mapped landforms and did not deviate in orientation by more than 15˚). This compares with just 14% of landforms from the OS profile data and 6% from the OS Panorama data. This clearly demonstrates the impact of the much higher resolution of the NextMap data set compared to the OS Panorama and OS Profile data sets.

LiDAR data has also been compared to the field mapping and has been found to provide a very close approximation of relief configuration due to its 2 m spatial resolution and a vertical accuracy of ±25 cm: much better than that of NextMap (Smith et al. 2006). As a result of this Smith et al (2006) suggest that there is case for using LiDAR as a base map for the highest resolution geomorphological mapping. With reference to the other sources of remotely sensed data named above Smith et al (2006) suggest that NextMap is the only data set to perform adequately in terms of the number of landforms identified, the similarity of the orientation of the landforms mapped and the positional accuracy of the mapping compared to the field mapping. The only exception to this is in areas of forestry where the NextMap data struggles as discussed above.

Dowman et al. (2003) also provide a comprehensive comparison of NextMap data with other airborne data acquisitions including photography and LiDAR (summarised in table 4.1). Dowman et al. (2003) conclude that overall, NextMap elevation data shows good agreement with LiDAR (Light Detection and Ranging) data. LiDAR uses much shorter wavelengths of the electromagnetic spectrum than RADAR and measures the journey time of a laser beam leaving an instrument to the time of its reflectance. This can then be converted to distance using the known value of the speed of light, and the resulting values are compiled into a DEM.

| | **NextMap DSM** | | **NextMap DTM** | |
|---|---|---|---|---|
| | mean difference (m) | RMSE (m) | mean difference (m) | RMSE (m) |
| LiDAR | -0.61 | ±0.77 | -0.22 | ±1.01 |
| Aerial Photography | -0.001 | ±0.17 | | |

**Table 4.1: A comparison of NextMap DSM and DTM data with Aerial Photogrametry and LiDAR data. The test area is near the River Severn and has a maximum relief of just over 60 m. Data taken from Dowman et al. (2003).**

Table 4.1 shows that the best agreement is found between the NextMap DSM data and aerial photography. This data covers part of the River Severn floodplain which, with a relatively low degree of land cover change and elevation variation, is effectively equivalent to bare earth. This suggests that in areas where land cover variability is minimal, NextMap is able to provide an accurate representation of the ground surface. Slightly less agreeable results are found when comparing the NextMap DSM with LiDAR DSM; however these are still thought to be in good agreement with both a mean difference and RMSE of less than 1 m. The comparison between the NextMap DTM and LiDAR DTM however produces less convincing results. Although a mean difference of -0.22 m appears consistent with results from the DSM comparison and the aerial photography, the RMSE value of ±1.01 highlights the problems associated with DTM production (Florinsky, 2002).

In summary, NextMap provides an accurate representation of the earth's surface, however caution is required in areas where a wide variety of land covers are found; this is particularly the case in woodland areas or areas with high vegetation density. In cases where land surface elevation is required for areas below woodland, for example, a DTM should be cautiously applied to the problem since it has been shown that errors are primarily inherent from two

sources. Firstly, the IfSAR STAR-3i system is able to penetrate beyond the apparent surface of a particular land cover or feature. This is most prevalent in areas of high vegetation density with such inaccuracies being later incorporated into a DTM should one be produced. In built up areas however, where features are of a lower density and land cover provides a higher degree of reflectance, NextMap provides more reliable elevation data even when changes in land cover are involved. Despite these problems it should be highlighted that NextMap is still able to provide much more satisfactory elevation data over a variety of different land covers than, for example, Ordnance Survey Landform PROFILE™ data sourced from Edina Digimap. Secondly, the creation of DTMs from surface elevation data is also a source for error and DTM accuracy is often dependant upon the algorithms applied to 'smooth' the initial elevation data.

### 4.2 The reliability of NextMap IfSAR data

Having decided that NextMap IfSAR data would be the most appropriate data set for use in this project, two problems specific to this project were encountered and should be highlighted. Firstly, the above assessment of IfSAR data is based on its application to a relatively flat area of the United Kingdom. In contrast, the areas involved in this project in the south-west Lake District include areas of high mountainous terrain. According to Smith et al. (2006) the NextMap IfSAR data, and indeed LiDAR data, is most accurate in flat, rural, unforested areas quite different from many areas of the south-west Lake District.

The second more problematic disadvantage of NextMap relates to NextMap's spatial resolution compared to the size of LLS geomorphology. This problem largely relates to the scale of this project and can be illustrated by using the example of a field of drumlins as a comparison (see figure 4.2a). The dimensions of each drumlin means that they are recognised as changes in elevation since they frequently have relief greater than the 5 m vertical resolution provided by the NextMap DSM. For this reason, NextMap is appropriate for mapping areas such as the Vale of Eden where extensive Drumlin fields record the track of a former Late Devensian ice stream (see figure 4.2). The advantages of using NextMap in the Lake District however out-weight the disadvantages particularly with the dominant landuse in the Lake District being non-forested upland which is free of settlements in the study areas.

In the section that follows, the illumination variables specified for each of the images have been chosen according to the orientation of the landforms in the image. In order to illustrate the point that while drumlins can be easily identified on the NextMap the much smaller Loch Lomond Stadial moraines found in valleys such as Hayeswater cannot, the azimuth was set perpendicular to the general orientation of the landforms as this best highlighted the crest

lines of the features. Furthermore, the elevation of the illumination was specified at 45˚ as this is the mid-point between an overhead sun and a sun theoretically at ground level (and hence between a totally blacked out image and a totally white image) and therefore provides the best light in which to view geomorphology.

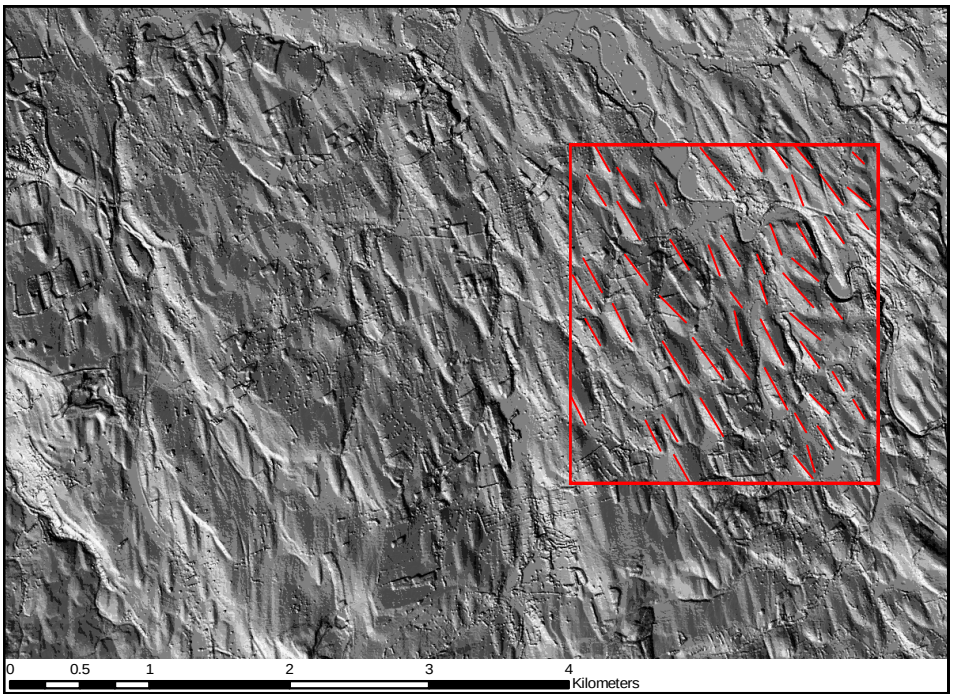


**Figure 4.2: A section of NextMap DSM showing part of the Vale of Eden. illumination variables: azimuth = 225°, elevation = 45°. Scale: 1:50,000. Drumlin crest lines are mapped onto one area of the DSM and are shown in red. Crest lines were easy to distinguish due to the size of the drumlins since they frequently exceed the 5 m vertical resolution of the NextMap DEMs.**

It is clear from figure 4.2 that drumlin crests can be easily identified. In contrast, figure 4.3a shows an area of 'hummocky' moraine surrounding Hayswater in the eastern Lake District. Despite these moraines appearing dramatic on the ground and in photographs (figure 4.3b) they are unclear on the NextMap DSM (figure 4.3a). Both figures 4.2 and 4.3 have an azimuth of 225° and an illumination elevation of 45°. To further illustrate this point, figure 4.4 shows the NextMap DSM, for Hayeswater at a scale of 1:15,000. Again the clear identification of the Hayswater moraines remains problematic despite the increased scale, primarily because the image becomes heavily pixelated. To rule out the possibility that this could be a result of an unfavourable azimuth and elevation, figures 4.5a and b show the same area of Hayeswater as figure 4.4 but with a solar elevation of 45° and an azimuth of 350° (i.e. illuminating the valley from the north rather than the west). Figure 4.5b shows the same area as figure 4.5a but has an increased scale of 1:4,000 demonstrating the problems with image resolution when scale is

increased. The blue boxes on figure 4.5a and b highlight the same area of the most prominent moraine in the image. Figures 4.5a and b again demonstrate that the identification of geomorphological features is, in this case, is not dependant on the position of the sun relative to the feature but simply a problem with the resolution of the DEM. It can thus be concluded that without the support of aerial photography (preferably covering several decades and at a variety of scales) and field mapping, NextMap DEMs may be deemed unsuitable in areas where the geomorphology displays particularly small-scale relief.

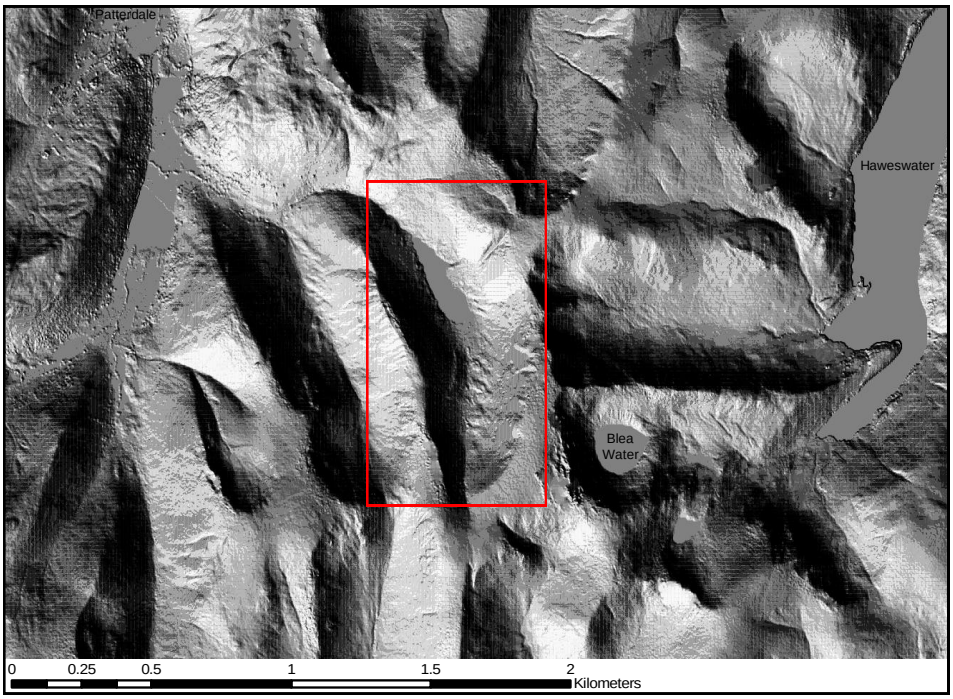


**Figure 4.3a: An area of 'hummocky' moraine surrounding Hayeswater in the High Street range of the eastern Lake District. The image shows Haweswater in the east and Patterdale in the west. The Hayswater valley is marked by a red box. Image taken from the NextMap DSM. Illumination variables: azimuth = 225°, elevation = 45°. Note the scale of this image (1:25,000) is twice that of figure 4.2. Some 'hummocky' ground is visible at the southern end of Hayeswater but these features cannot be mapped at this scale.**

i. Moraines on the eastern side of Hayswater show linearity almost perpendicular to the long axis of the lake but are barely visible in figure 3.3a above.

ii. Moraines on the western side of Hayswater looking north along the lake shoreline. Moraines have a 'hummocky' appearance and substantial height although only some exceed the 5 m vertical resolution of the NextMap DEM.

**Figure 4.3b: Photographs of the moraines surrounding Hayeswater, the same valley highlighted in figure 4.3a.**

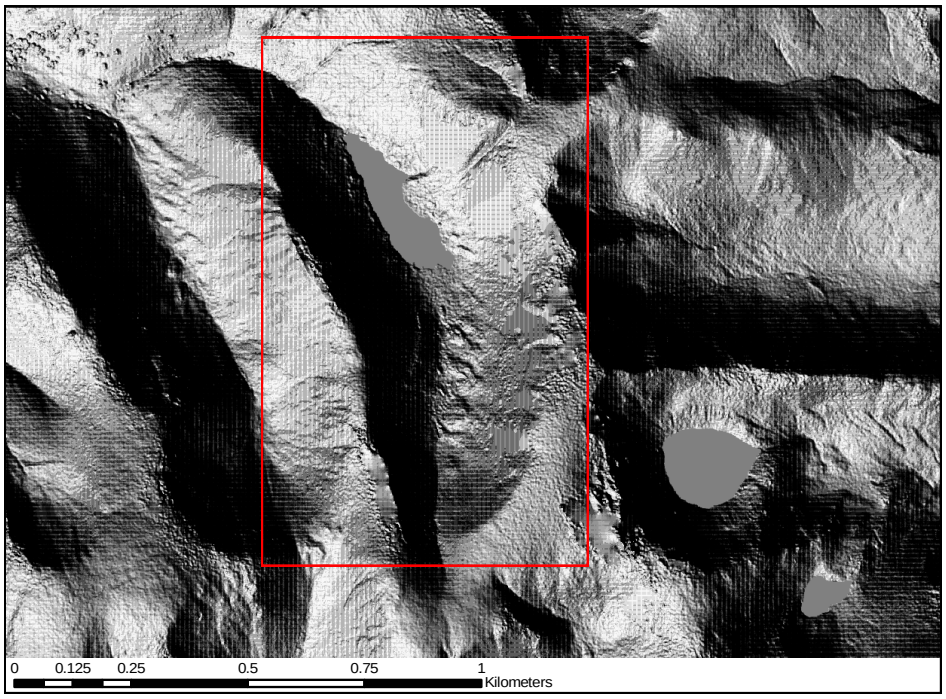


**Figure 4.4: A section of NextMap DSM covering the Hayeswater valley in the High Street range of the eastern Lake District. 'Hummocky' moraine surrounds Hayswater but is unclear from this image. Illumination variables: azimuth = 225°, elevation = 45°. The scale of the map has been increased to 1:15,000. The red box again highlights the Hayeswater valley. At this scale pixels are becoming visible indicating that the image is approaching the resolution capacity of the DEM. Some moraines are visible such as those shown in figure 4.3bi but many are not represented by the DEM due to its resolution.**

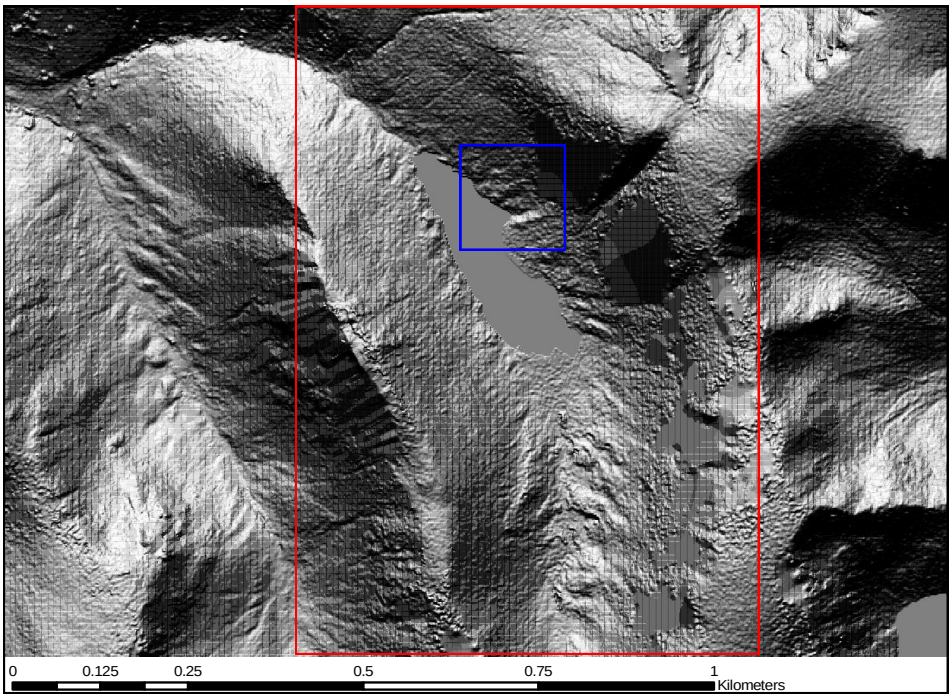


**Figure 4.5a: A section of NextMap DSM covering the Hayeswater valley in the High Street range of the eastern Lake District. The red box again highlights the Hayswater valley where areas of 'hummocky' moraine surround the lake. Image taken from the NextMap DSM. Illumination variables: azimuth = 350°, elevation = 45°. The scale of the image has been increased to 1:10,000 resulting in the image becoming more pixelated. In some cases a perpendicular shift of the azimuth can result in features becoming visible due to a more favourable angle of illumination. Since many moraines are still not visible in figure 4.5a this is not the case so instead problems with the visibility of the moraine must relate to the resolution of the DEM. The blue box indicates the area of moraine shown in figure 4.5b.**

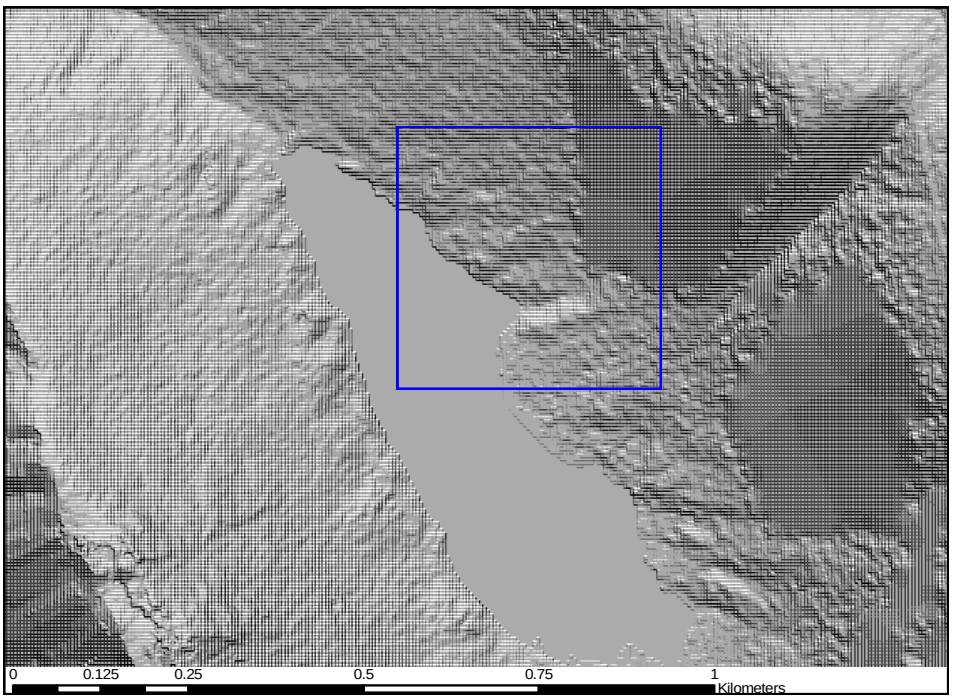


**Figure 4.5b: A section of NextMap DSM covering part of the Hayeswater valley in the High Street range of the eastern Lake District. The blue box indicates the same area as the blue box in figure 4.5a where moraines are most visible. Image taken from NextMap DSM. Illumination variables: azimuth = 350°, elevation = 55°. The scale of the image has been increased to 1:4000 and more pixels are now visible.**

### 4.3 The influence of the illumination tool on DEM interpretation

The main advantage of using Erdas to map was that a 'relief shaded' option was available for the raster layer (the DSM or DTM from NextMap). The visualisation of field sites using the 'relief shading' tool provides a simple and effective way of enhancing lineaments and other glacial landforms using low angle, oblique, illumination (Hiller and Smith, 2008: Smith et al., 2006).

Optimum conditions for feature identification involve illumination orthogonal to the principal lineament orientation of a feature (Hiller and Smith, 2008). By using the 'relief shading' tool, a set of diagnostic characteristics were developed for each vector layer/landform type. For example, assuming a fixed azimuth, the gradient or the magnitude of down slope dip (the first derivative of elevation) can be relatively large for many glacial landforms including lineaments, lateral moraines or on a smaller scale flutes and 'hummocks'. The result of this gradient change is the characteristic relief shading which emphasises steep sided features with characteristic widths/scales relative to the underlying topography. The degree of curvature displayed by a feature can also be diagnostic. Aside from horizontal sinuosity, the degree of

curvature orthogonally across the features profile can provide a distinctive 'relief shading'. Typically, curvature is high at breaks of slope (i.e. at the top and bottom of features) but low on the top of features and at mid-slope locations. The resulting 'relief shading' will therefore principally show changes in shading colour where curvature is highest, i.e. at the tops and bottoms of features where major breaks of slope occur. The application of 'relief shading' therefore highlights crest lines well and to a lesser degree the initial break of slope found at the base of larger features such as moraines, lineaments and drumlins.

Problems however are frequently associated with the relief shading tool. One particular problem is the degree to which the tool distorts results by the introduction of human dependent variables (azimuth and elevation). Knowingly or unknowingly, it is therefore easily possible for mapping to be biased by the individual using the function. The result can often be landforms which show linearity contrary to the 'actual' angle/direction of linearity shown in the field. An illustration of this problem is shown in figure 4.6 below where linearity found inside Sissons (1980) Loch Lomond Stadial ice limit in Mosedale can be mapped at perpendicular angles depending on the illumination variables. It was decided that the most effective way of eliminating this problem was to check all mapping in the field and with aerial photography.

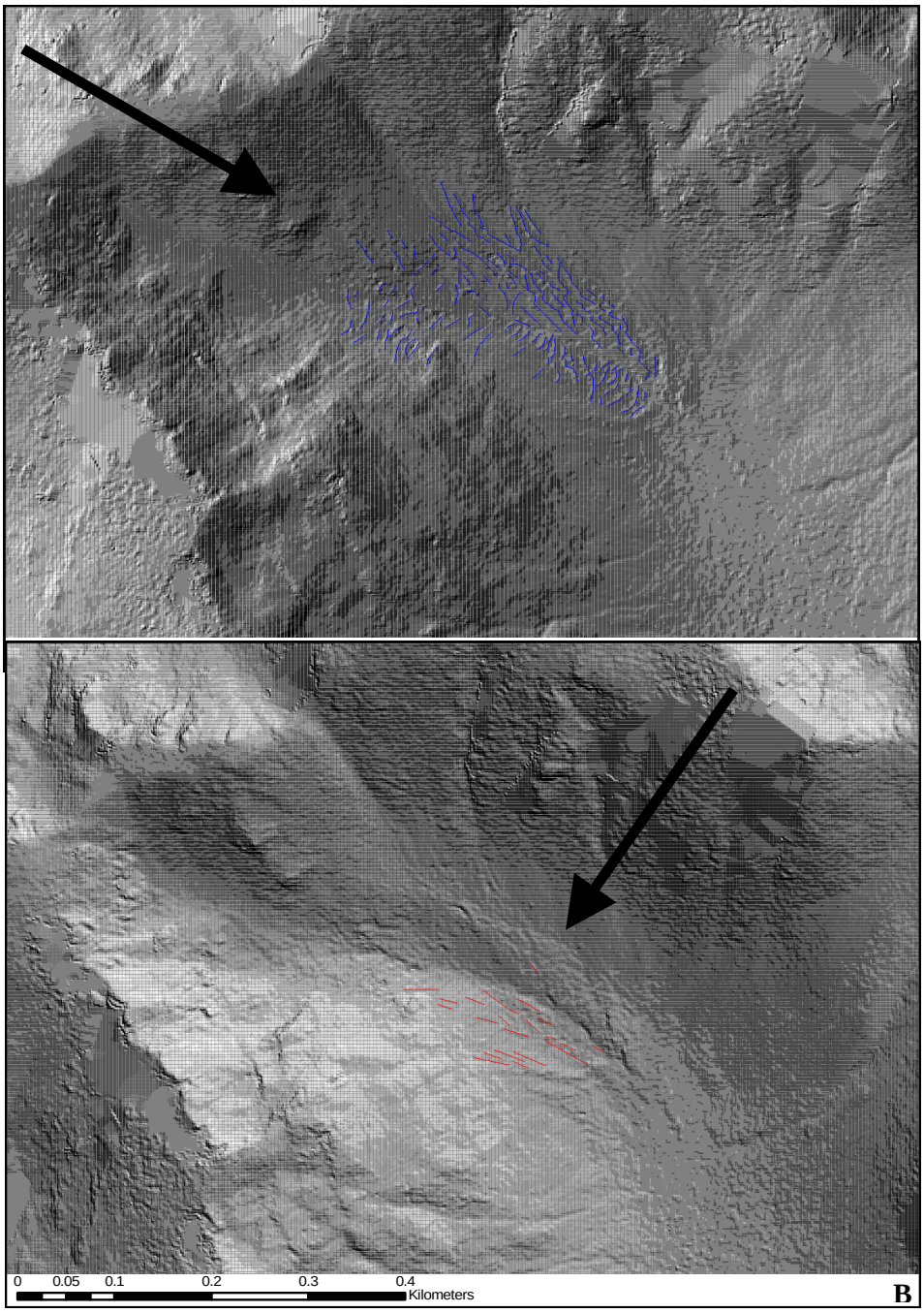


**Figure 4.6a and b: A comparison between mapping using different sun angles. Mapping in the same area behind the Loch Lomond Stadial moraines in Mosedale near Wastwater reveals linearity in perpendicular directions. Figure 4.6a: illumination variables: azimuth = 300°, elevation = 45°. Image scale 1:7000. Figure 4.6b: illumination variables: azimuth = 35°, elevation = 45°. Image scale 1:7000.**

Although the relief shading tool should be used with caution, it is a highly valuable tool which is able to pick up a high level of detail. Illumination variables are also easily changeable and thus allow for much more comprehensive mapping. Without the relief shading tool, many of the features mapped would not have been recognised.

## 4.4 Georeferencing and orthorectification of aerial photography

Multiple methods were employed when accurately georeferencing, orthorectifying and mosaicing aerial photography from the Ordnance Survey 1972 series. Supplied by the Lake District National Park, these were black and white photographs at a scale of 1:25,000.

As outlined above, problems are encountered with the resolution of NextMap DEMs when considering small scale landforms which may be vertically smaller than the 5 m resolution of the DEM. This has been found to be particularly the case with landforms pertaining to the Loch Lomond Stadial due to the small spatial extent of ice development. In order to alleviate this problem, it was necessary to use aerial photography and this could be most conveniently used when accurately georeferenced and mosaiced.

### 4.4.1 In ArcMap

A 1:25,000 Ordnance Survey map downloaded from Edina Digimap was used as the base map. The layer to be georeferenced was then selected from the drop-down menu labelled 'layer' and ground control points (GCPs) were added by matching up points on the aerial photographs with points on the OS base map. This process was repeated to produce a minimum of 10 GCPs on each photograph. In order to make the georeferencing as accurate as possible, evenly spread GCPs were chosen as close to the edge of the photographs as possible. In order to take the terrain variations into account, GCPs were also necessary at both the highest and lowest altitudes of the photograph.

The features to be used as control points were considered carefully with the most successful features found to be roads, railways, bridges and small low buildings with minimal shadowing effect. Such features were termed 'cultural features'. 'Line features' were also used but with caution; this class of feature includes fence boundaries and footpaths which may have been moved/rebuilt or represented incorrectly on the base map. 'Line features' were only used where they were clearly identifiable on the map and where well defined edges, corners or intersections were present. The final group of features was labelled 'natural features' and included trees, forest boundaries, forest clearings and river confluences. Such features are subject to frequently change either anthropogenically or naturally and consequently do not provide reliable GCPs, particularly when considering the difference in the date of production between the photographs (1972) and the OS base map (2006). Although water bodies fall into the category of 'natural features', they were often used as GCPs mainly due to convenience. It was noted however that the level of many lakes and tarns have varied since the aerial photographs were taken, so for this reason shorelines were only taken as GCPs where the

same water level could be identified on the photographs and the map. For example, particular care was taken when georeferencing photography from the Levers Water area since the level of the lake appears much higher on the more recent OS base map than on the 1972 aerial photography. As a result Levers Water was not used as a GCP.

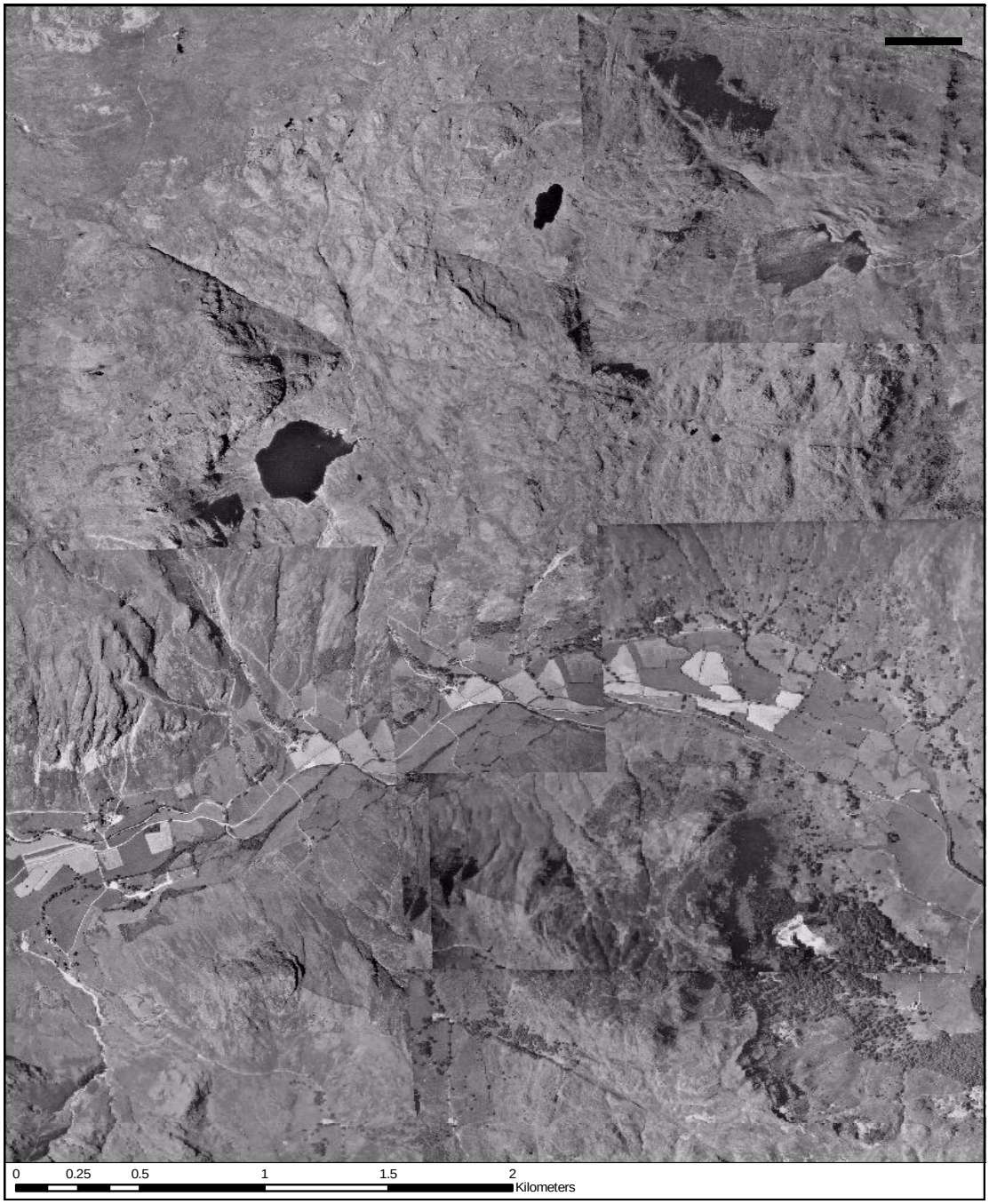


**Figure 4.7a: An example of photographs that have been georeferenced in ArcGIS for the area around Langdale. The edges of each photograph are clearly visible despite cropping to remove colour variations associated with the edges of the photographs. The match of the photographs is also poor with some fields and road junctions, for example, visible in multiple photographs.**

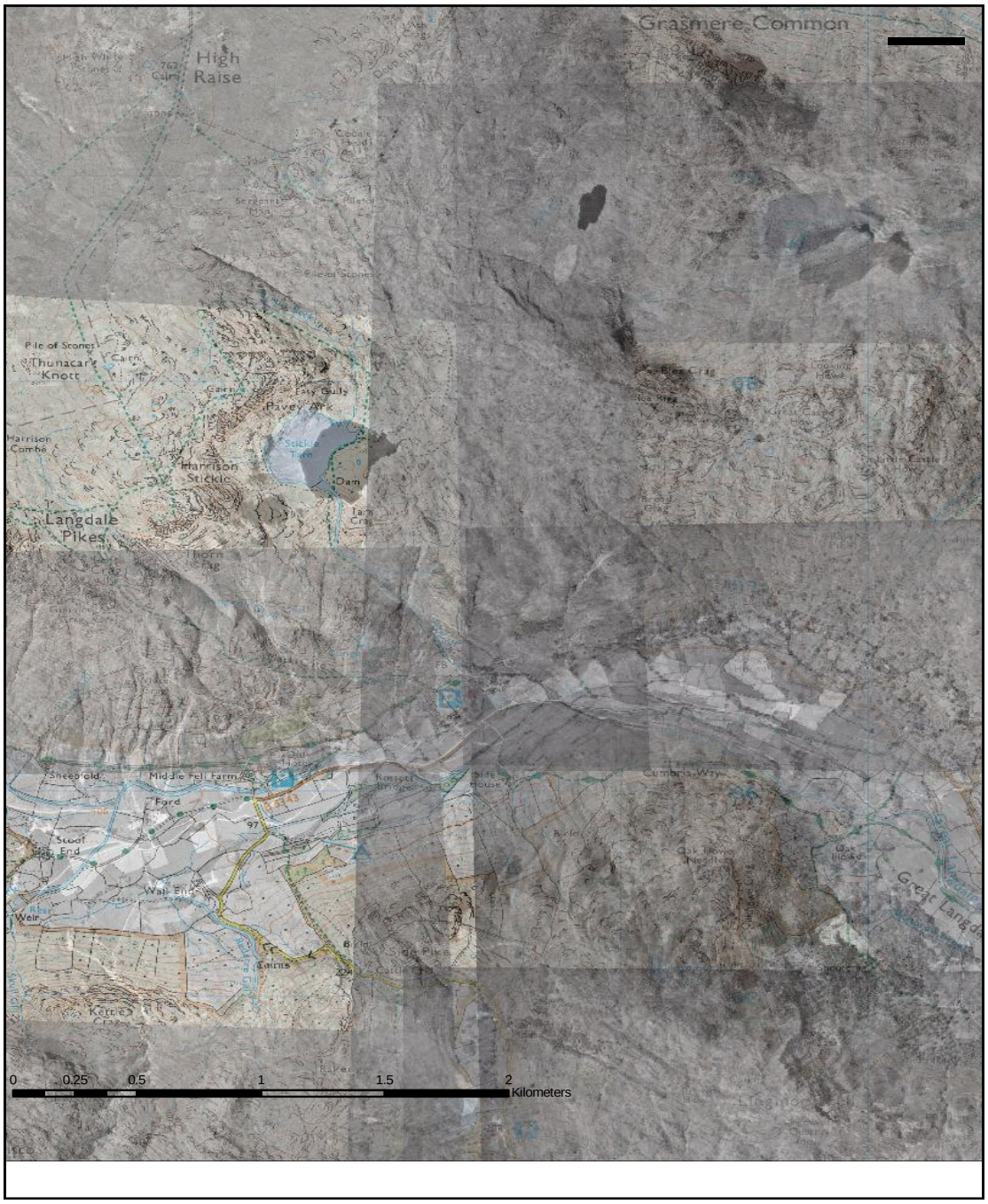


**Figure 4.7b: An example of photographs that have been georeferenced in ArcGIS. Aside from the accuracy of the georeferencing between the photographs, the georeferencing with the underlying reference image (a 1:25,000 OS map) is also poor. The location of Stickle Tarn (the largest lake in the photograph) clearly demonstrates the discrepancy between the photographs and the 1:25,000 map with the lake clearly lying further east in the photographs than on the map.**

The problems associated with georeferencing in ArcMap are clear from figure 4.7. It was found that although ArcMap was competent at georeferencing images with only a small number of GCPs on photographs where there was minimal distortion; problems were

encountered when photographs required many GCPs due to a high degree of unevenly spread distortion. For clarity, it is necessary to define the word 'distortion' which in this case is taken to mean: 'the degree to which a photograph is required to be reshaped in order to be georeferenced accurately with the base map' as shown in figure 4.8 below.

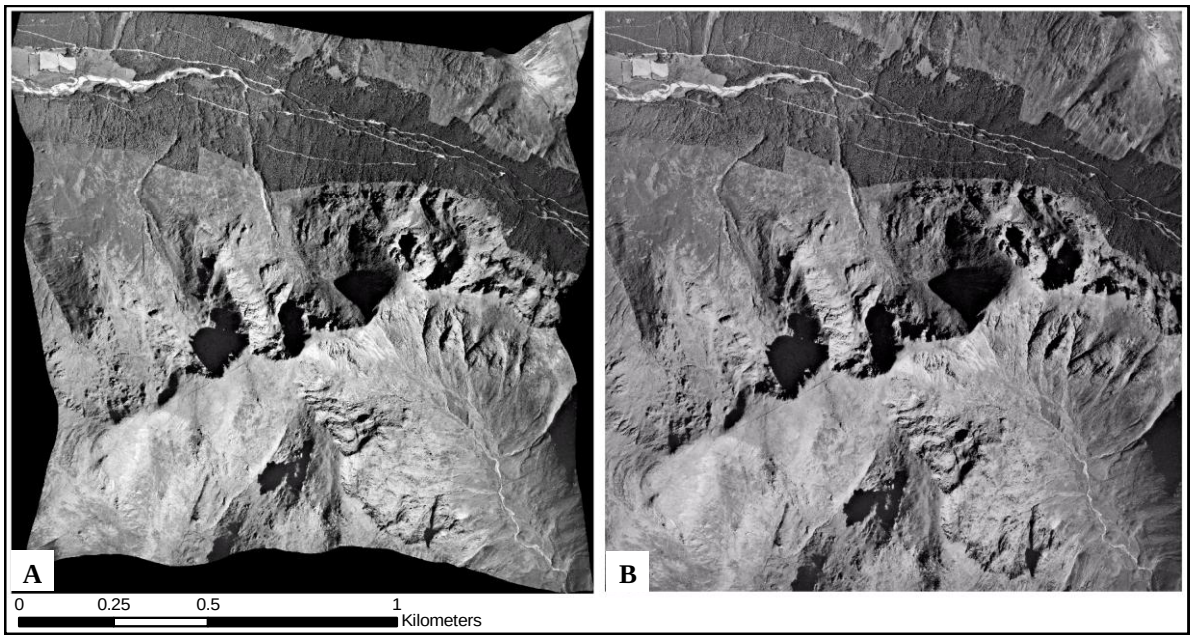


**Figure 4.8: Examples of photograph distortion in the process of orthorectification. The above photographs were rectified in Erdas Imagine. Figure 4.8a shows the rectified image with the black areas representing image displacement away from the original outer limits of the photograph. This is the result of the image being transformed from an image co-ordinate system to a ground co-ordinate system in order to remove any relief displacement. For comparison, figure 4.8b shows the original image that was orthorectified to produce figure 4.8a for comparison.**

It was found that ArcMap was unable to reshape the photographs sufficiently to make georeferencing accurate. As a consequence, it was difficult to georeference multiple photographs which not only fitted accurately with the base map but also with each other. Where photographs overlapped, problems were also encountered with colour differences. In order to alleviate this problem, all photographs were cropped so that colour variations associated with the edges of the photography were eliminated. Despite this, colour variations still remained a problem in ArcMap with the edges of every photograph clearly visible (see figure 4.7).

The main reason that ArcGIS struggles to accurately georeference aerial photography, particularly in mountainous regions, is due to the effects of relief displacement. Relief

displacement is the phenomena by which areas of higher elevation are shifted away from their actual position when recorded in a photograph (see figure 4.9 below). This occurs because the angle at which the X-band is reflected back from the earth through the camera lens is different when the land surface is elevated. In order to correct for relief displacement, it is necessary to orthorectify aerial photographs rather than just georeferencing them. Orthorectification involves the transformation of a 2 dimensional image co-ordinate system into a 3 dimensional ground co-ordinate system by the incorporation of elevation data (in the form of a DEM) into the georeferencing process. It is the inclusion of elevation data that distinguishes georeferencing from orthorectification. Theoretically, relief displacement can also occur where areas of high vegetation or other land cover occur although that is negligible in this area. The idea of relief displacement further explains why ArcGIS is able to georeference maps, (e.g. Sissons (1980)) since these maps have already been corrected for relief displacement and are projected onto the OS British Grid.

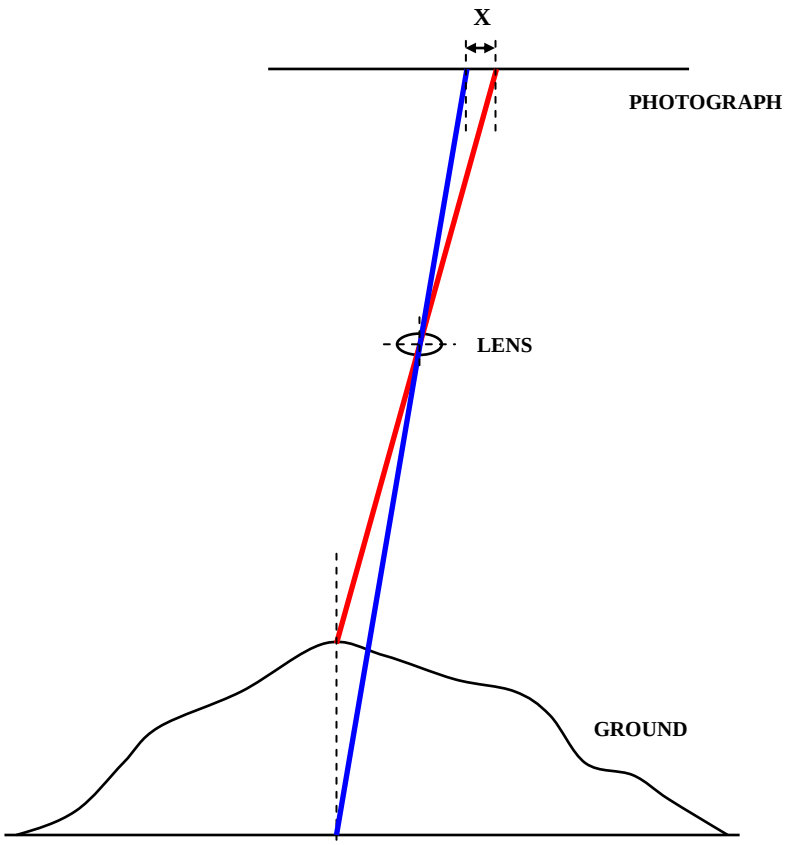


**Figure 4.9: A schematic illustration of relief displacement. Higher elevations produce photographs with a greater degree of displacement as reflectance occurs at different angles. X indicates the displacement of the X-band produced by different elevations over the same point on the ground. X is also dependant on the angle at which the photograph is taken relative to the ground surface. The greater the angle at which the X-band strikes the ground the great the relief displacement in areas of higher elevation.**

### 4.4.2 In Hugin

Hugin is a cross-platform photograph stitcher which can be freely downloaded from http://hugin.sourceforge.net/. The primary aim of using this program was to remove problems associated with colour differences between the photographs before georeferencing them in another package such as ArcGIS or Erdas Imagine.

As with ArcMap, photographs were uploaded and a minimum of 10 GCPs were added around the edge of each photograph. Since photographs were not being georeferenced in Hugin a base map was not required: instead, GCPs were identified on overlapping areas of neighbouring photographs. The number of photographs that can be uploaded at once is not limited by Hugin but by the specification of the computer being used.

The result of a test run to stitch only 2 photographs together was promising and later improved upon using the 'correction' and 'blending' tools within Hugin. Having been successful with two photographs, it was decided that photographs should be stitched together in columns, and the columns later stitched since the computer was unable to handle stitching 27 photographs simultaneously. The result of the first column to be stitched is shown in figure 4.10 and shows a good degree of colour blending. Upon close inspection some errors are present in areas where features in the photographs do not exactly match up e.g. roads, rivers etc but in comparison to ArcMap the colour:accuracy ratio appears to improve by following this method in Hugin.

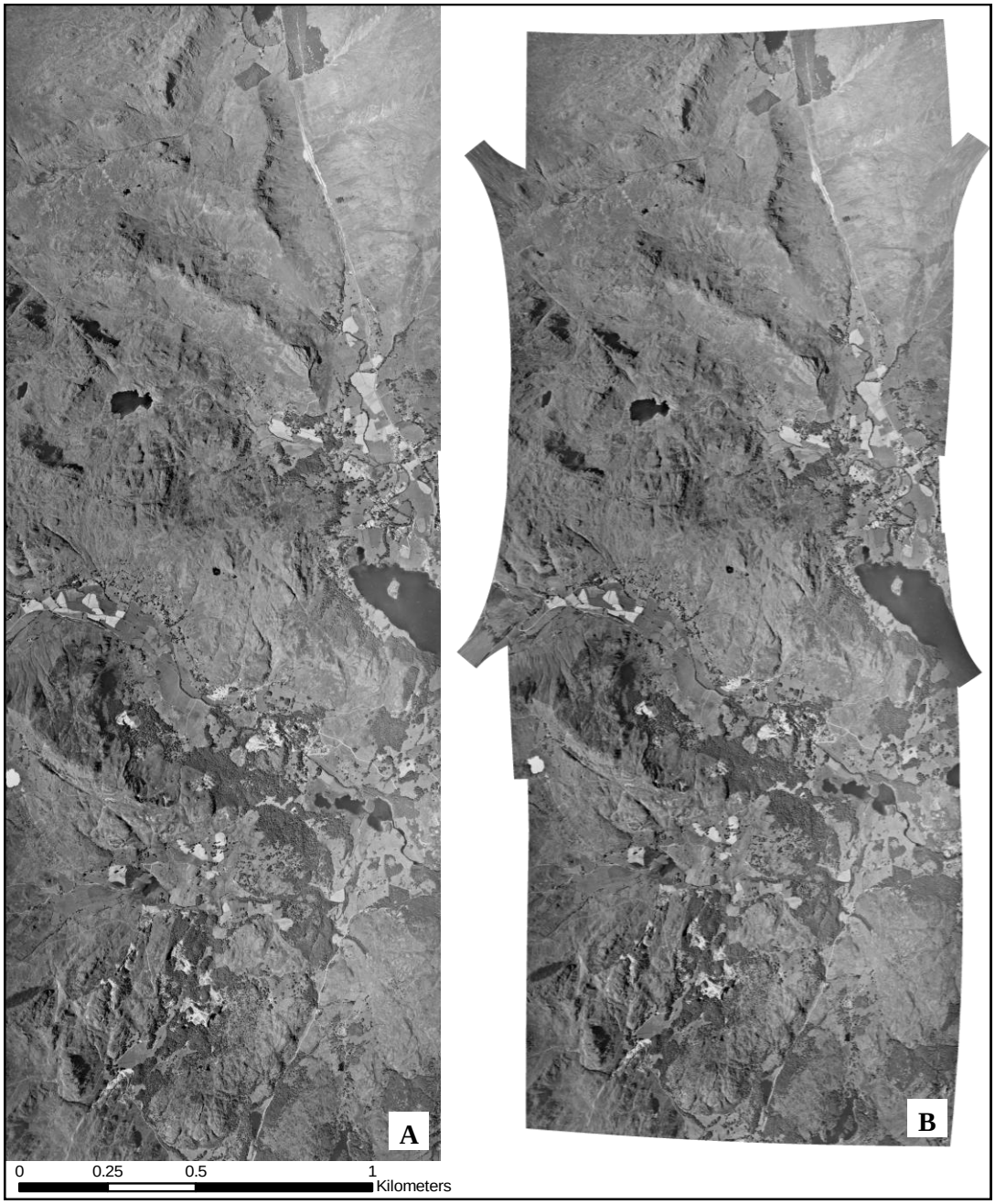


**Figure 4.10: A column of photographs stitched using Hugin showing a North to south transect from Great Tongue to Tarns How. Colour differences between the photographs are well blended and accuracy shows an improvement on that provided by ArcGIS with a similar number of photographs.**

Problems did however arise when later trying to stitch together the six columns of photographs. The three most easterly columns were attempted first and appeared promising (see figure 4.11) with good colour blending and accuracy.

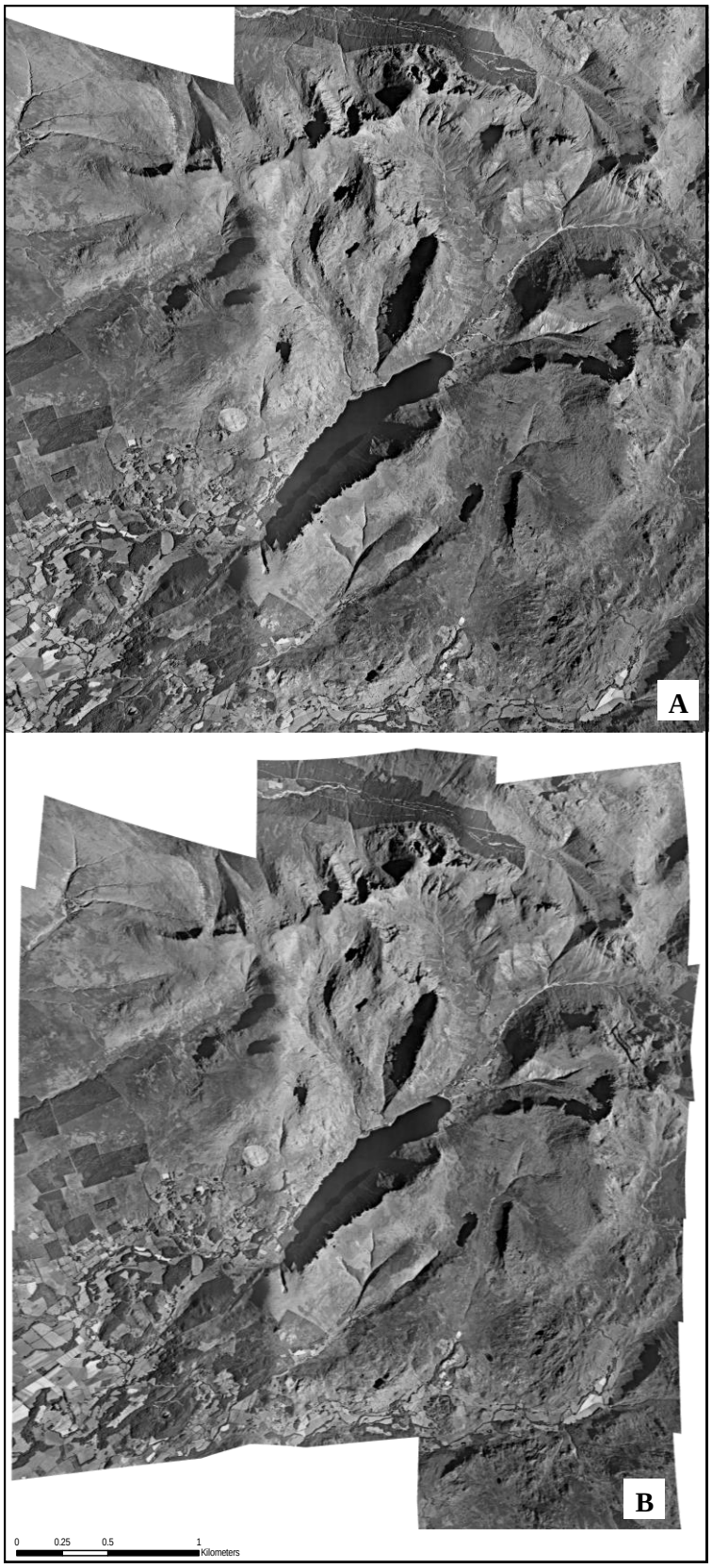


**Figure 4.11: The results of three columns of photographs being stitched together using Hugin. Photographs cover the western half of the fieldsite including Mosedale, Lingmell Beck and part of Upper Eskdale.**

However when photographs from figure 4.11 were stitched with the three columns of photographs from the western side of the photograph area the result was less pleasing. Figure 4.12 shows how the stitching of the western and eastern photographs produced a 'fisheye' type of effect across the photograph. This was particularly unsatisfactory since Upper Eskdale (in the centre of the image) is one of the key field sites focused upon in this project. There are several explanations for this problem. Firstly, if the camera used to take the photographs was set in an automatic exposure mode then the photographs may have been taken at varying exposures and aperture settings: hence the colour variation. However, having tried several different settings to prevent this effect from occurring it was decided that the degree of parallax correction required on the aerial photography was simply beyond the scope of Hugin. This, combined with the quantity of photographs involved suggested that an alternative method of mosaicing the photography was necessary.

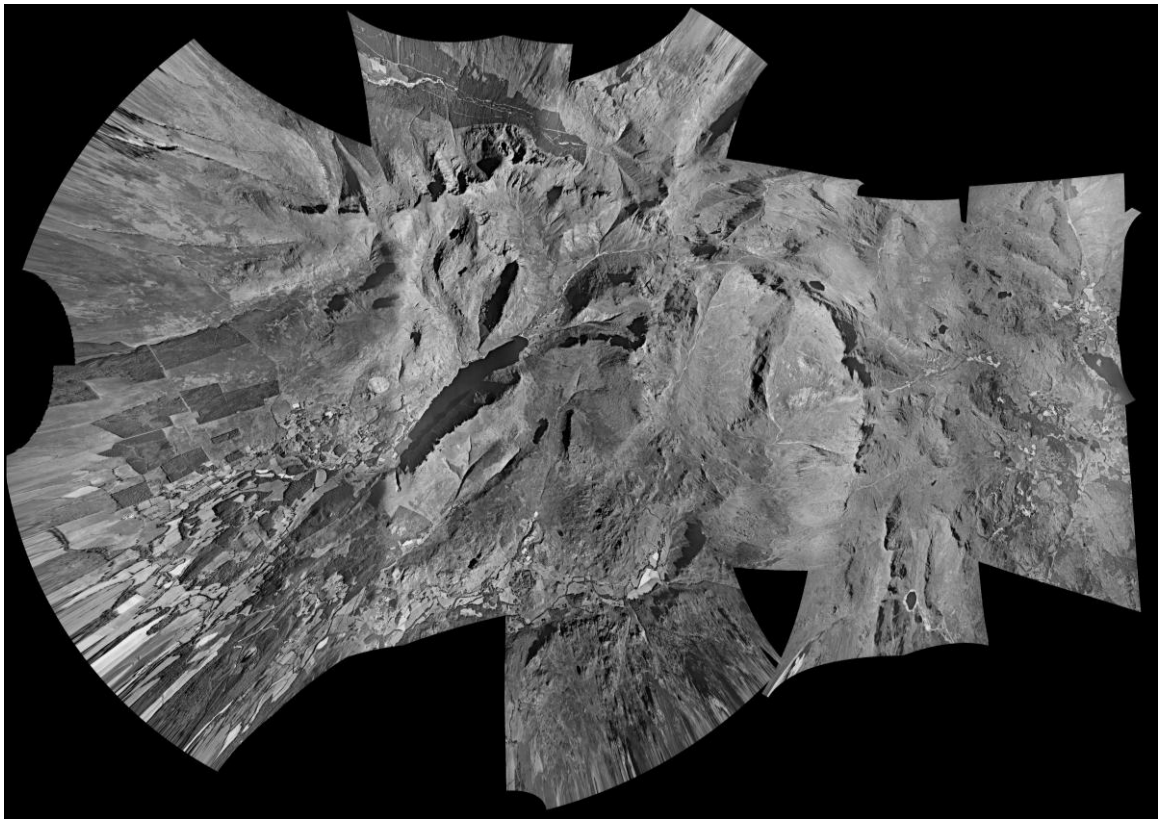

**Figure 4.12: The result of the eastern and western sides of the photograph area being stitched. A 'fisheye' type effect is seen particularly in the centre and far left of the photograph making it unsuitable for use.**

### 4.4.3 In Erdas Imagine

The final method used to mosaic the aerial photography of the south-west Lake District involved the use of IMAGINE AutoSync, a workstation within Erdas Imagine which provides automated rectification of imagery.

Resampling is the process by which values are reassigned to rectified pixels, a process that is complicated by changes in the scale of the photography resulting from the process of removing geometric distortion. Several resampling algorithms are provided by Erdas Imagine: Nearest Neighbour, Bilinear Interpolation, Cubic Convolution and Bicubic Spline. Bilinear Interpolation involves each pixel receiving the distance-weighted average value of the 4 pixels that were closest to it after being shifted. This was deemed the most appropriate method for resampling of the photography in this project since it averages the data and therefore smoothes out extreme values. As a result, this method reduces the sharp edges associated with the faster Nearest Neighbour approach (the method used in ArcGIS). Overall this method is also the most spatially accurate in assigning approximate values to locations.

In order to prevent potential matching problems between uncorrected, vertically displaced mountain regions in the raw input image (the photograph) and the British Grid projected OS base map, a sensor model was applied. This model involves a DEM (in this case the NextMap DSM) being incorporated into the georeferencing process and used as an earth model. The DEM provides additional model-solving information which can result in the location of features in the output image being more accurate when converted from a 2D image co-ordinate system to a 3D ground co-ordinate system. In the Lake District, the large amount of mountainous terrain can drastically affect the quality of the rectified output image. Variations in elevation between the input image and the 'flat' orthorectified reference image can cause vertical/relief displacement and thus errors within the rectified images. The incorporation of the DEM into this method was therefore vital and is the key element that distinguishes the methodology used in Erdas Imagine from those described previously. With this method, photographs were no longer simply georeferenced but instead orthorectified.

When all GCPs had been added to the images, the errors associated with the GCPs were calculated. It was decided that in order to minimise and cap the error on the rectified images, all RMSEs should be < 3 m and all SDs < 2 m. Any input images with values above these therefore required editing of the GCPs in order to reduce the values. The SDs of individual GCPs were then considered and GCPs with SDs > 10 m were removed one by one with the

RSME and SD values being recalculated after each removal. This process was continued until useable RMSE and SD values were calculated for the image. Figure 4.13a and b below demonstrates how low RMSE and SD values result in accurately orthorectified photography. The output image could then be viewed in the workstation viewer. This process was repeated for each of the 27 images.


**Figure 4.13a: Two rectified aerial photographs layered over a 1:25,000 OS base map with a transparency of 50%. The photographs match very well with the base map and demonstrate the high degree of accuracy associated with this method. The RMSE and SDs for these photographs were 2.697964 m (RMSE) and 1.718323 m (SD) for the top photograph and 2.508552 m (RMSE) and 1.0207309 m (SD) for the bottom photograph.**

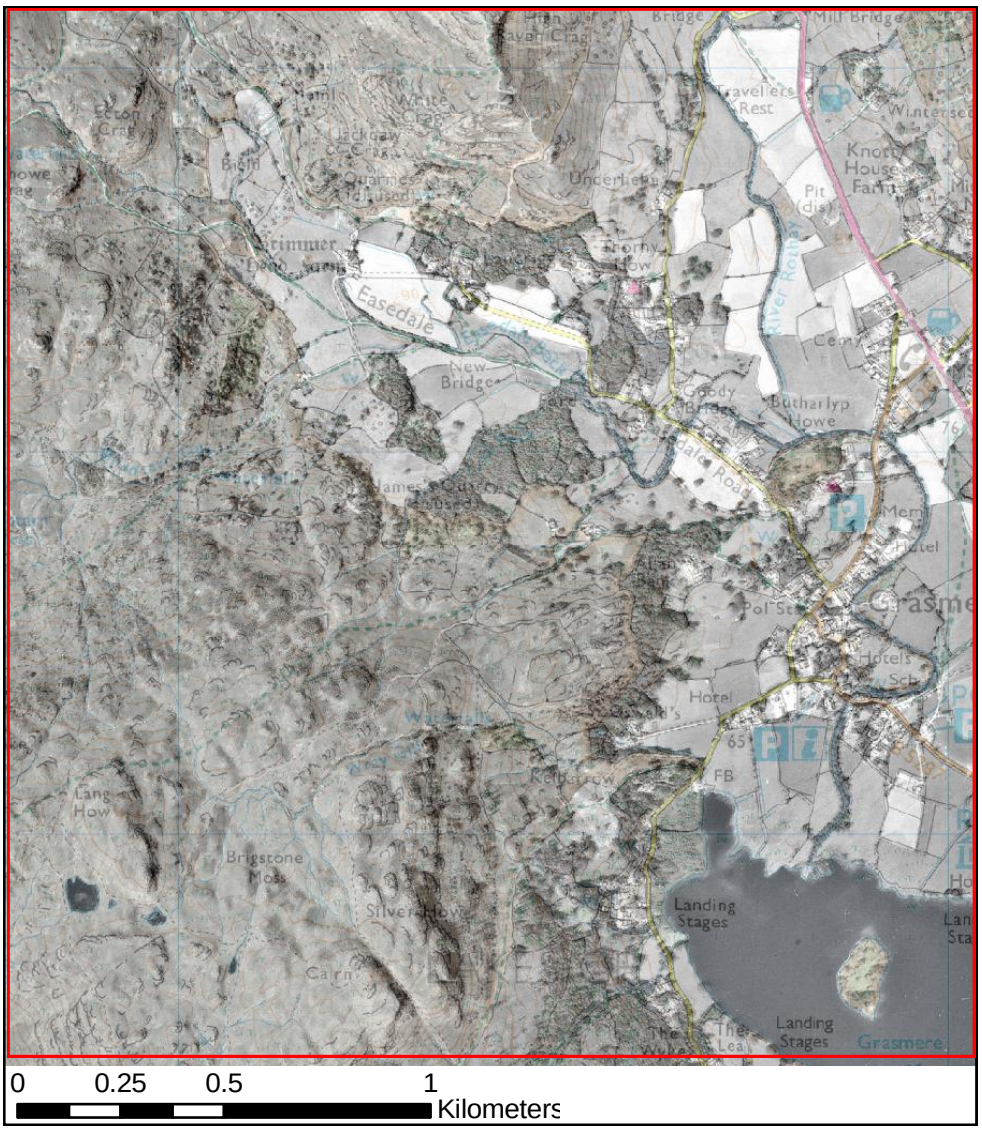


**Figure 4.13b: A section of rectified photography overlain on a 1:25,000 base map. The red box indicates the area covered by figure 4.13b on figure 4.13a. Again a good match between the photography and map is seen. Photograph transparency is set to 50%.**

The resulting, now orthorectified photographs were then mosaiced using the mosaic tool in Erdas Imagine, the methodology for which has previously been described. Figures 4.14a and b below show the final mosaic which despite the visibility of photograph edges in some areas was deemed suitable for purpose since its main use would be to view individual field sites rather than the whole area.

**Figure 4.14a: The final mosaic of the orthorectified aerial photography covering the south-west Lake District. The area covered by the photography is indicated by the red box on map A. Photograph transparency = 40%.**

**OVERSIZE FIGURE APPEARS AT END OF THESIS**

**Figure 4.14b: The orthorectified aerial photograph covering two of the selected field sites at the northern end of Wastwater: Mosedale and Lingmell Beck. This zoomed in Image means that the edges of some photographs become visible. Photograph edges are, however, barely visible compared to the georeferencing done in ArcGIS (see figure 3.7) and consequently, due to the high degree of accuracy associated with this method, the mosaic shown in figure 3.14a was accepted as the final product of the orthorectification.**

**OVERSIZE FIGURE APPEARS AT END OF THESIS**

## 4.5 Summary

- Compared to many remotely sensed data sets such as OS Profile, OS Panorama, SRTM, Landmap and Landsat, NextMap provides cost effective digital elevation data with excellent spatial coverage.
- The 5 m resolution of NextMap means that it matches well with the most reliable data sets such as LiDAR and ground survey in accuracy tests relating to geomorphological mapping.
- In small scale mapping projects however such as those pertaining to the Loch Lomond Stadial, NextMap should be used cautiously since landforms often do not exceed the 5 m resolution of the data set.
- The use of the relief shading tool in Erdas Imagine is a potential source of error in geomorphological mapping when using NextMap. Consequently, all mapping should be checked in the field or at least against aerial photography.
- A number of different software packages are capable of image orthorectification/georeferencing however Erdas Imagine has been shown to be by far the most powerful of the three packages discussed above.

## Chapter 5

# MOSEDALE, LINGMELL BECK & LINGMELL GILL

# 5: MOSEDALE, LINGMELL BECK AND LINGMELL GILL

## 5.0 INTRODUCTION

Chapters 5 and 6 provide a detailed account of the geomorphology and associated palaeoglaciological reconstruction at each of the 6 field locations identified in chapter 2. Each chapter addresses 3 locations both of which are summarised at the end of chapter 5 with an overview of the geomorphology of the whole of the south-west English Lake District presented in figure 5.30.

## 5.1 Mosedale

Mosedale is a relatively small south-east facing valley located at the northern end of Wastwater in the south-west Lake District. The valley is approximately 2.5 km at its longest point and is surrounded by some of the highest ground in the Lake District. Kirk Fell, a summit which is suggested by McDougall (1998) to have supported a plateau icefield during the Loch Lomond Stadial, sits on the eastern side of the valley and attains an altitude of 802 m OD. At the valley's most northerly point Pillar (892 m OD), and further to the west, Little Scoat Fell (841 m OD) and Red Pike (826 m OD), all facilitate the isolation of the valley from the neighbouring valleys of Ennerdale and Nether Beck. In contrast, the relatively subdued topography of the valley floor is dominated by a heavily meandering river system which sources from both Black Comb and Black Sail Pass and has clearly supported much greater discharges than at present.

This chapter will provide a qualitative assessment of the geomorphology within Mosedale, Lingmell Beck and Lingmell Gill. These inferences will then be supported by sedimentological evidence and a reconstruction of glacier dynamics to test the viability of the proposed glacial limits. The potential for mass accumulation through the blowing of snow will also be considered and the reconstruction compared to previous glacial reconstructions in the same areas.

### 5.1.1 Geomorphology in the valley of Mosedale

Unlike many valleys in the Lake District, Mosedale provides geomorphological evidence of glacier occupation throughout its entire length. At the most southerly end of the valley, large rounded moraines, some perpendicular and some parallel to the valley walls, are common. These moraines are of substantial size both in width and height and are frequently greater than 10 m high. Little consistent variation is seen between the proximal and distal slope angles of these moraines, and many of the moraines appear circular. From the ground, moraines do therefore not appear to display a consistent orientation of inter-moraine linearity

or in some cases any linearity at all. However, the mapping of crest lines using aerial photography and IfSAR data suggests that the arrangement of the moraines may be less chaotic than it first appears from ground survey. Figures 5.1a and b below show the geomorphology of Mosedale with moraines orientated at approximately 45° to the valley sides.

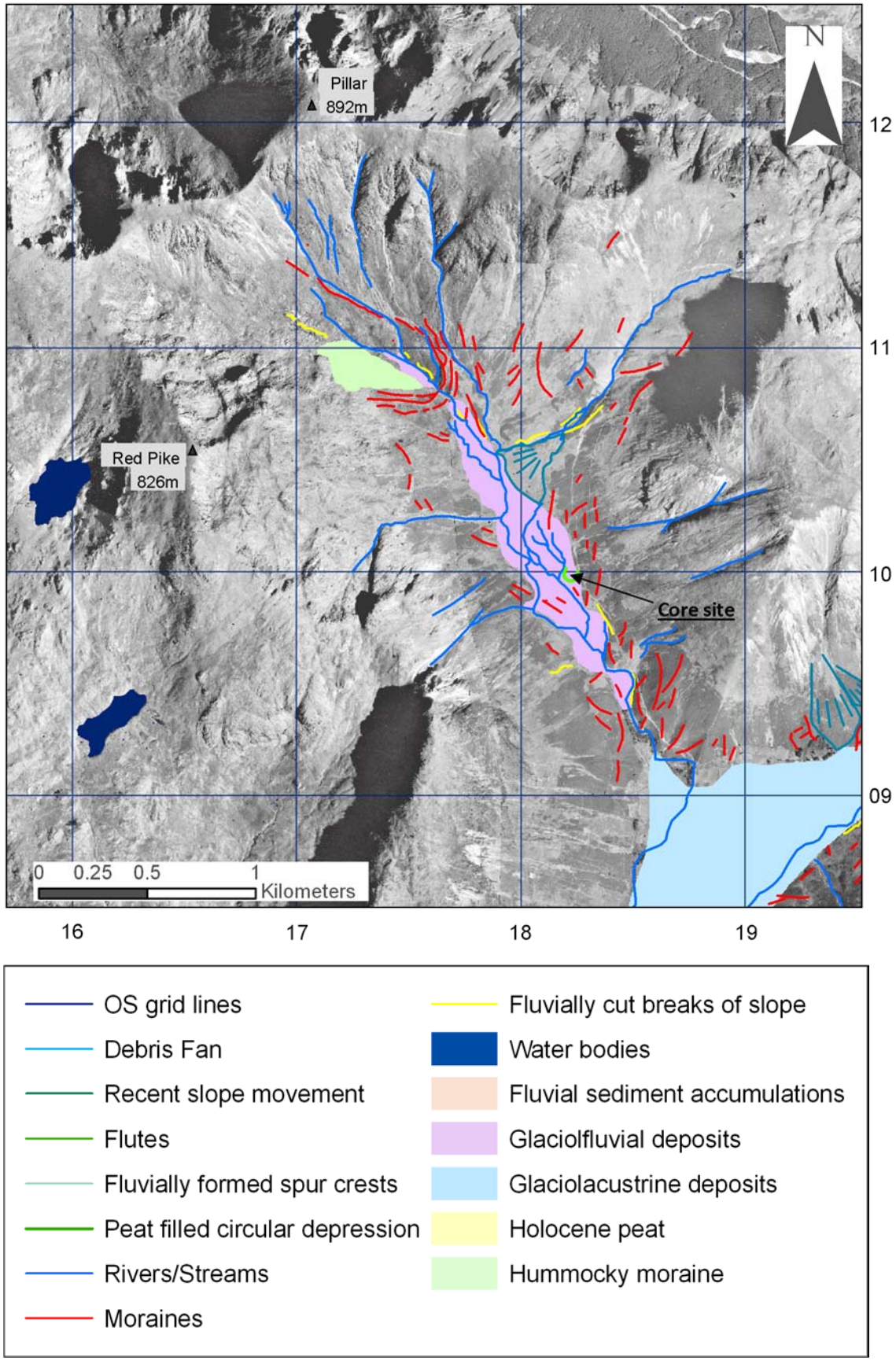


**Figure 5.1a: The geomorphology of the valley of Mosedale.**

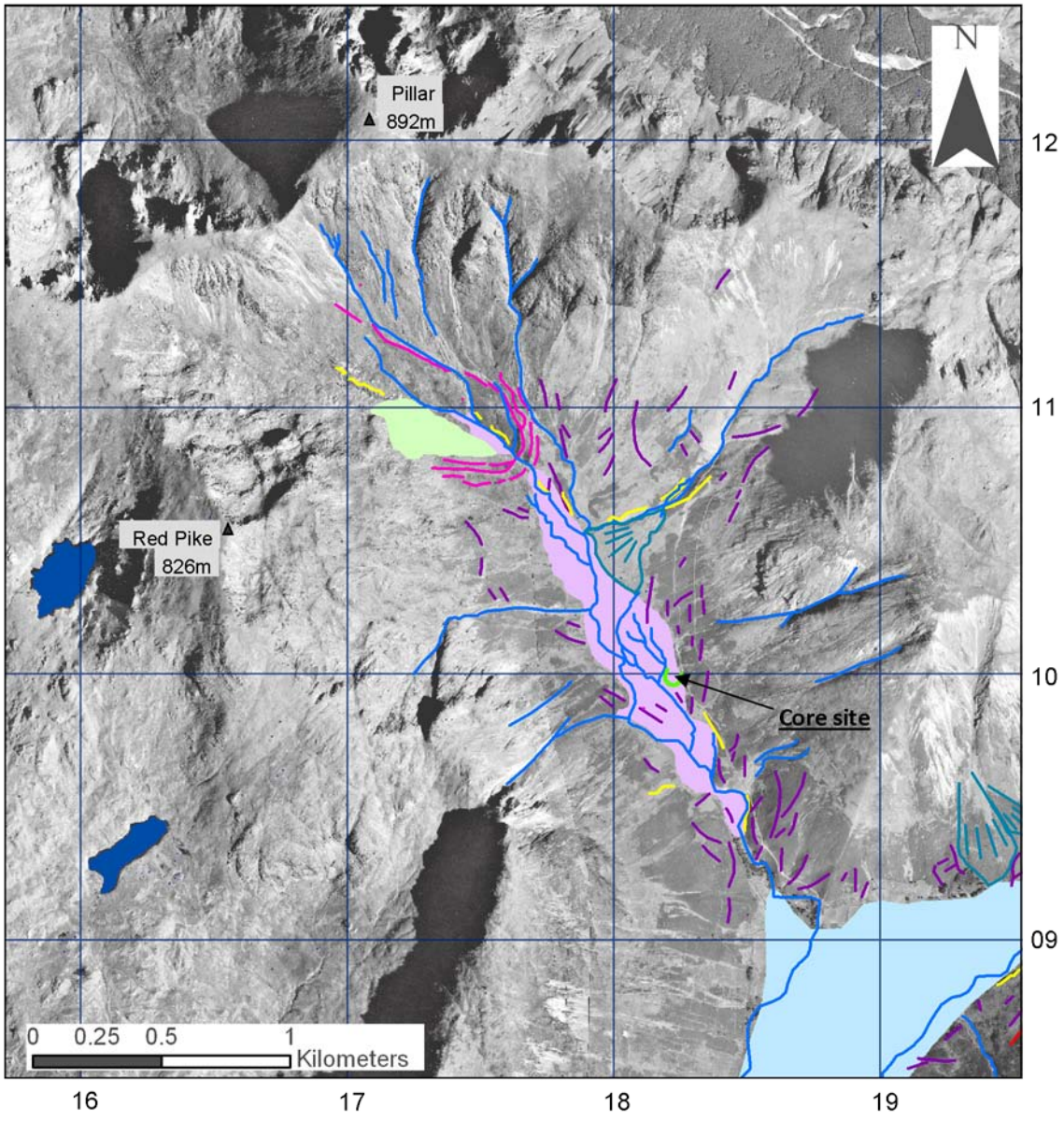


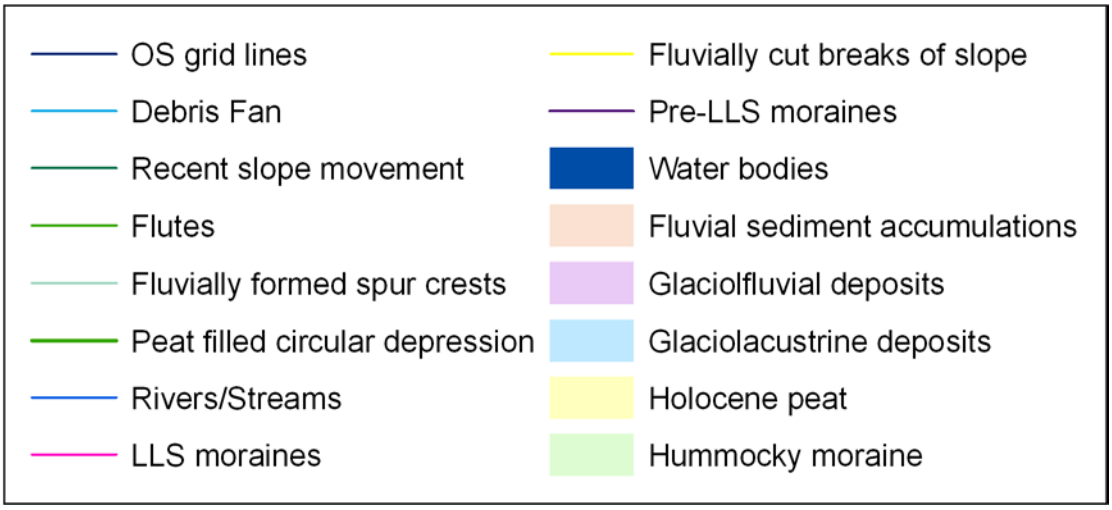


**Figure 5.1b: The geomorphology of the valley of Mosedale including the distinction between Loch Lomond Stadial and pre-Loch Lomond Stadial moraines.**

The largest of these rounded moraines can be found at the most southerly end of the valley, to the north of Wastwater, where a pair of moraines separate the valley from the flat farmland believed to be formed of glaciolacustrine deposits. These semi-arcuate moraines do not join to form a cross valley moraine. If this was at some point the case the most obvious explanation for their separation is glaciofluvial or post-glacial fluvial activity. As noted by Manley (1959), it is often the case that moraines within the Lake District are incomplete, a phenomenon which he too attributes to fluvial activity. Figure 5.2 below illustrates the dominance of these moraines, which are over 30 m high, at the southern end of Mosedale.

**Figure 5.2: Looking north-west up Mosedale from south-east of the most southerly moraines in Mosedale. Large rounded moraines at the southern end of Mosedale mark the transition from flat farmland to the south into the dramatic glacial geomorphology of the valley further north.**

Further large rounded moraines can be found covering the valley bottom further north of the moraines pictured in figure 5.2. The moraines covering the valley bottom appear to have a slightly more subdued topography although they remain prominent amongst the surrounding flat fluvial gravels. Again, these moraines are fragmented with no continuous across-valley moraines present. A series of fluvially cut breaks of slope are also present in the valley figure 5.3 below shows the moraines described above.

**Figure 5.3: Looking north-west up Mosedale with Pillar (982 m OD) being the highest visible peak. Large moraines of over 10 m height have been dissected by the actively meandering river. Crest lines are marked with a red line.**

The moraines shown in figure 5.1 are also interspersed with features resulting from post-glacial slope movement and grade into the valley sides but do not grade into lateral moraines of an elevation any greater than 257 m OD in the main valley. Moving further north up the valley these moraines become more sparse until two arcuate moraine ridges appear at the entrance to Black Comb at an elevation of 178 m OD. These moraines, which are shown in figure 5.1 as pink lines, possess sharp crest lines and form two arcuate ridges which grade into lateral moraines, particularly on the eastern side of the Black Comb valley. In comparison with moraines further south in the valley these moraines are considerably smaller both in height and width and show a much lesser degree of post-glacial modification. These smaller moraines are also much closer together than the moraines further to the south.

The qualitative assessment of moraine 'freshness' as a means of assigning an age to the formation of moraines is a method which should be approached with extreme caution. Manley (1955: 1959) was the first to introduce this idea which assigned the 'freshest' moraines assigned to the most recent glaciation of the area, the Loch Lomond Stadial. Sissons (1980) also adopted this approach in his identification of 64 independent ice masses in the Lake

District during the Loch Lomond Stadial. Wilson (2002), however, notes that the differences found between the maps of glacier masses produced for the Loch Lomond Stadial in the Lake District by Manley (1959) and Sissons (1980) are substantial, with some glaciers identified by Manley (1959) and Pennington (1978) not included on Sissons (1980) map and vice versa. This difference highlights the difficulties associated with 'freshness' of form as a means of assigning landforms to a particular glacial phase (Wilson, 2002). More recent work has emphasised that moraine morphology is a reflection of a range of glaciological and sedimentological factors, which, along with the human impact mean that the qualitative assessment of moraine morphology in terms of 'freshness' in order to assign an age may be unfounded (McDougall, 1997: Wilson, 2002). It is therefore important to find other means by which to distinguish between moraines pertaining to different time glacial episodes. The most reliable way to achieve this is to implement dating techniques such as radiocarbon and cosmogenic radio nuclide dating which provide absolute dates on glacial landforms and thus uniformity across palaeo-glaciological reconstructions. Where the use of absolute dating is not feasible it is possible to relatively date glacial landforms as has been done in this project using sediment cores.

Mosedale is one example where assigning an age to the moraines is very difficult based purely on their degree of 'freshness'. Moraines with crest lines drawn in purple on figure 5.1b do however show obvious morphological differences from those drawn in pink, however this is mainly in terms of their size rather than their 'freshness'. The moraines which form two arcuate ridges are smaller both in height and width and as previously stated show a lesser degree of post-glacial modification. This lesser degree of modification could in the context of Manley's idea of 'freshness' be taken as evidence to suggest that these moraines belong to a later glacial episode. However, it could also be attributed to the lower discharge of the river in Black Comb compared to that in the main valley. Alternatively the steep sided valley in Black Comb channels water into one central river which doesn't not have the opportunity to meander and cause further moraine dissection as has been the case in the main valley.

### 5.1.2 Sedimentological evidence in Mosedale

Since both the large more southerly moraines and the smaller arcuate moraines cannot be confidently assigned an age based on 'freshness' or morphology, it was necessary to attempt relative age dating.

Amongst the large moraines within the main valley of Mosedale one unusual feature was identified. On the eastern side of the valley a feature resembling a circular moraine was found

(here referred to as feature A). The outer ridge of feature A has distinct morphological similarities to many of the surrounding more linear moraines with a smooth crest and steep sides of comparative amplitude (see figure 5.4).

**Figure 5.4: Feature A on the east side of the main Mosedale valley; a circular peat filled depression. The crest of the feature is highlighted in green and the coring site with a black arrow (crestline of feature also shown in green on figure 5.1a/b along with coring site arrow in black). Photograph taken from Black Sail Pass looking south-west.**

The peaty, soft and saturated ground which is found in the centre of the circular feature contrasts with the much more gravely fluvial deposits found outside the feature. This suggests that feature A has remained isolated from the influence of the dynamic river system and thus it was identified as a suitable site to carry out the coring.

A Russian corer was used to retrieve a 50 cm long core with a base depth of 3.4 m below the peat surface (see figure 5.1a/b for core location in valley). Five stratigraphic units have been identified within the core which can be seen below in figure 5.5.

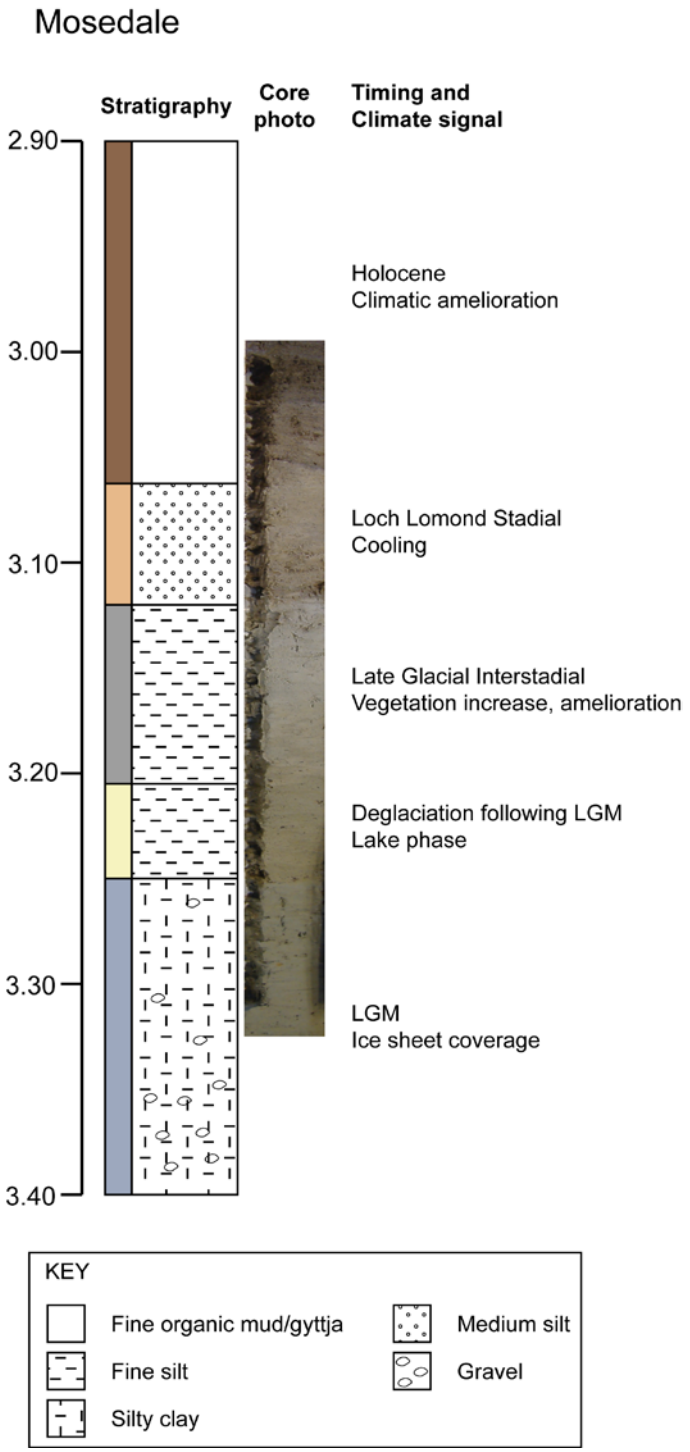


**Figure 5.5: The stratigraphy and interpretation of a sediment core recovered from the centre of feature A in Mosedale.**

The upper 16.4 cm of the core is composed of sandy silt with the highest proportion of the sediment being classified as a very coarse silt (figure 5.6). This unit also includes organic material which, crucially, is not found anywhere else within the core. The amount of organic material present in this upper unit decreases gradually with depth and consists of a peaty material with no visible solid fragments of organics. This layer is believed to represent climatic amelioration at the onset of the Holocene. The second unit between 16.4 and 22.0 cm

consists again of a sandy silt, however particle size analysis using a laser granulometer shows that this unit contains a lower percentage of sand (14.2%) compared with the uppermost unit (23.7%) (figures 5.6 and 5.7). This unit is dominated by medium silt and displays a much lighter colouring than the above upper unit. Unlike the transition between units 2 and 3 the transition between units 1 and 2 is gradual over a depth of approximately 5 cm, thus suggesting that a gradual climatic change was occurring at the time when this section of the core was deposited. This entirely minerogenic layer is therefore thought to represent the Loch Lomond Stadial with a rapid onset and slightly slower climatic amelioration into the Holocene at ~10 ka BP.

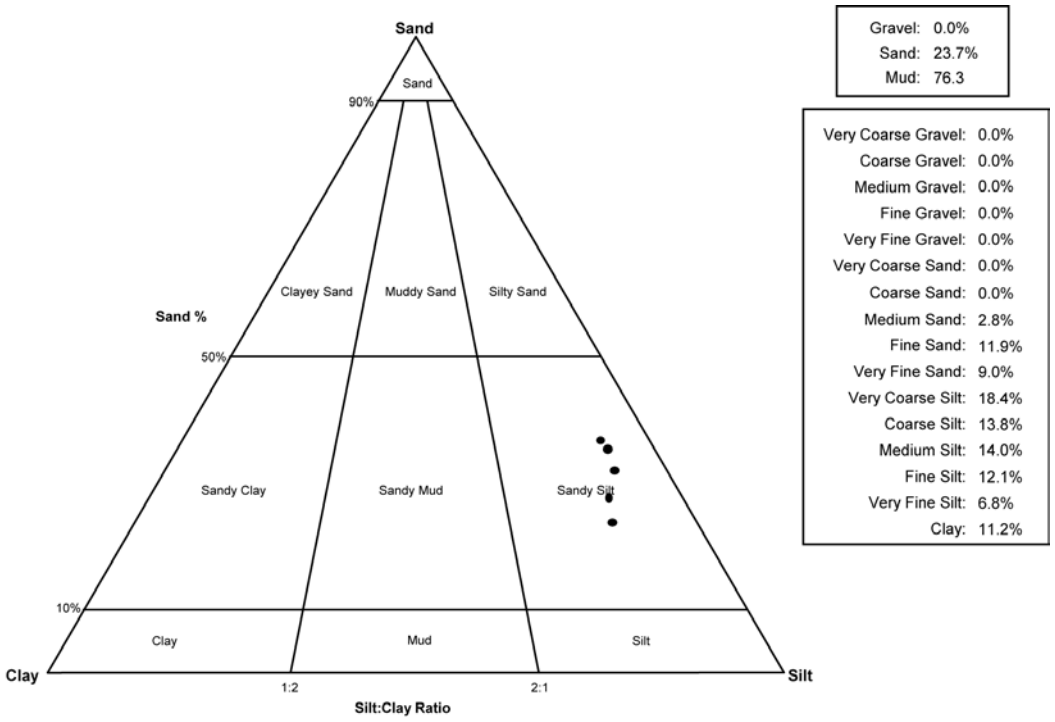


**Figure 5.6: Particle size analysis using a laser granulometer classifies 18.4% of the uppermost unit of the core from feature A as a very coarse silt. All samples measured show close agreement within the sandy silt sector of the above triplot.**

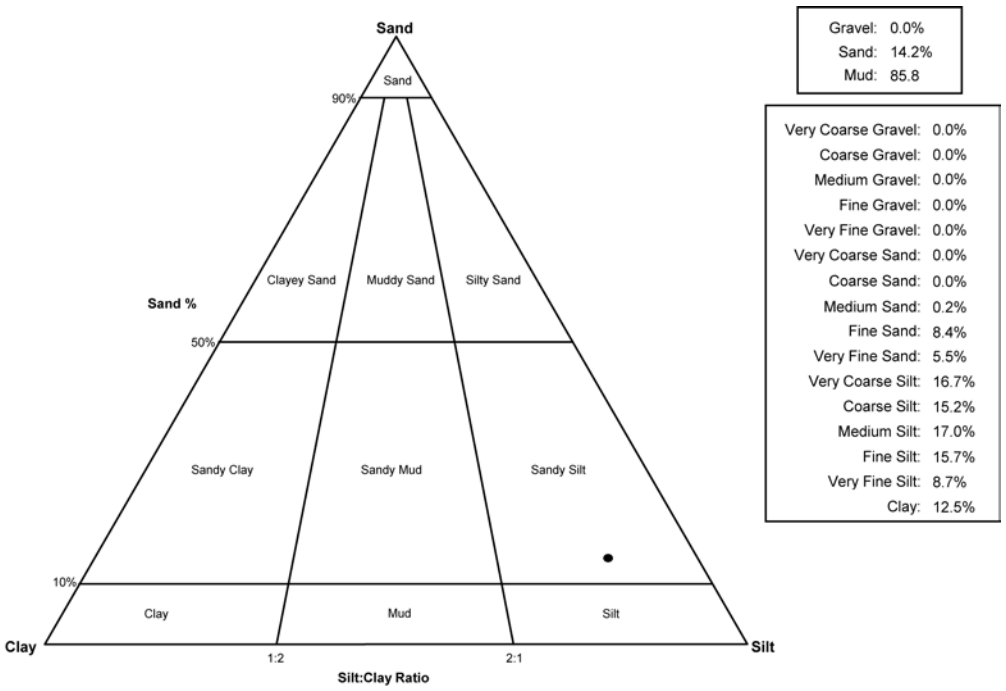


**Figure 5.7: Particle size analysis using a laser granulometer classifies 17.0% of the sample taken from unit 2 of the core from feature A as medium silt.**

A thicker unit of grey minerogenic sediment forms unit 3 and consists of just 7.3% sand and 92.7% mud (figure 5.8). Furthermore 25.9% of the layer is composed of a fine silt which again contains fine laminations. This unit is believed to represent a warming during the late glacial when vegetation was increasing in response to an ameliorating climate. As previously mentioned, a sharp transition is seen in the core between unit 2 and unit 3 thus suggesting that an abrupt climatic change occurred at the time when these sediments were being deposited.

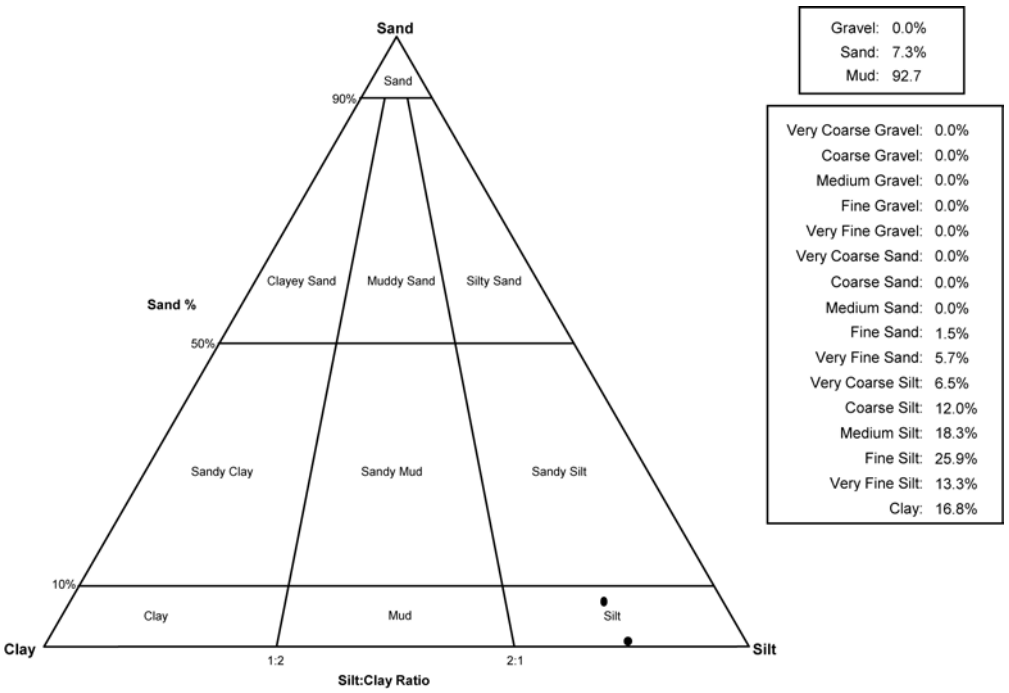


**Figure 5.8: Particle size analysis using a laser granulometer classifies 25.9% of the samples taken from unit 2 of the core from feature A as fine silt.**

The more yellow/brown sediment forming unit 4 of the core contains a higher percentage of clay (20.5%) than units 1-3 and is also noticeably more dense. Much clearer laminations within unit 4 of the core suggest that this unit may have formed in lacustrine conditions which occurred during deglaciation following the Last Glacial Maximum (LGM) of ~21 ka BP. A transitional boundary which occurs over ~8 cm of sediment is found between unit 4 and unit 3. This further suggests that the climatic amelioration represented by this section of the core occurred gradually, and produced 8 cm of sedimentation during deglaciation.

The lowest unit of the core, unit 5, is also considerably denser than units 1-3 and a clear change in sediment colour from a much more blue/grey sediment in unit 5, to a more yellow/brown sediment in unit 4, implies that there was a marked abrupt change in sedimentation source in feature A at the time when the unit 4/5 boundary was deposited. Again, this supports the suggestion that unit 4 formed during deglacial conditions following the LGM when meltwater was beginning to pond. The minerogenic sediment of unit 5, which pre-dates that of unit 4, is therefore believed to have been deposited subaerially under full glacial conditions. This unit is the only unit in the core which contains a gravel fraction. This gravel fraction is greater towards the base of the core and consists of small rock fragments not greater than 4 mm diameter. The presence of a gravel fraction is consistent with subglacial erosion under a large ice mass. The results of particle size analysis for units 4 and 5 can be seen below in figures 5.9 and 5.10 respectively.

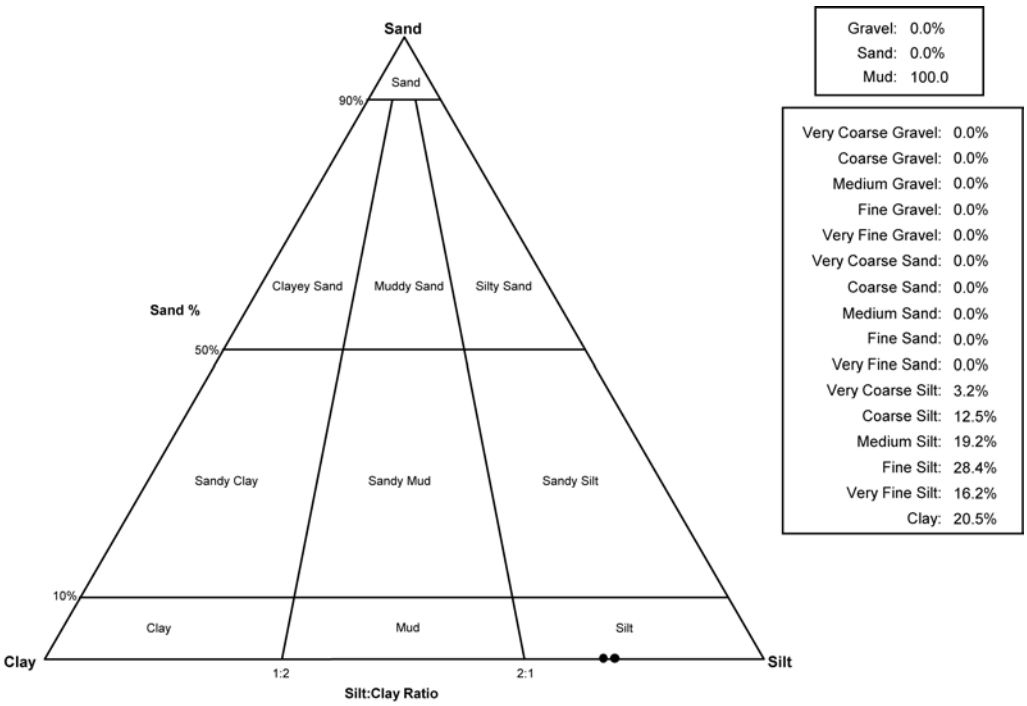


**Figure 5.9: Particle size analysis using a laser granulometer classifies 28.4% of the samples taken from unit 4 of the core from feature A as fine silt.**

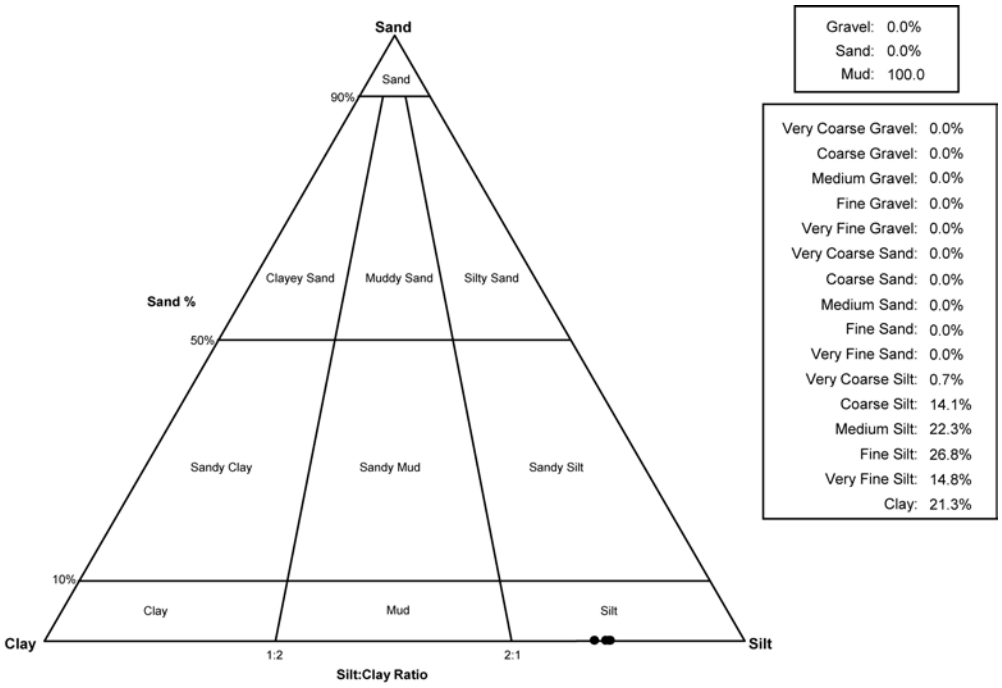


**Figure 5.10: Particle size analysis using a laser granulometer classifies 26.8% of the samples taken from unit 5 of the core from feature A as fine silt.**

The core obtained from the centre of feature A therefore displays a tripartite sequence with units representing glacial-Interstadial-stadial-interglacial conditions from full glacial conditions through to Holocene warming post-10ka BP. Since sediment accumulation has therefore occurred throughout the Loch Lomond Stadial at this site, two crucial assumptions can be made. Firstly, the limit of the Loch Lomond Stadial glacier within this valley must lay up-valley of feature A, and secondly, the formation of feature A must pre-date the Loch Lomond Stadial. Given that deglacial sediments are also found within the core it is most likely that feature A formed during the early stages of deglaciation. Clearly, it is necessary to make some assumptions in order to relatively date feature A, an improvement on this would be to apply an absolute dating technique such as radiocarbon dating to the feature/core however this was beyond the scope of this project.

The morphology of this feature and its location within the valley make it possible to explain the formation of the feature by a number of processes. Firstly, it has been suggested that this feature is a pingo formed under permafrost conditions. Such conditions are likely to have been present during the early stages of deglaciation when the sedimentological evidence above suggests that feature A may have been formed. However it seems most likely that this feature is the result of a multi-phase process. During deglaciation, it is suggested that a portion of ice became isolated on the valley bottom and was later covered with debris. The formation of feature A by isolated ice may suggest that ice stagnated for at least part of deglaciation at the close of the Dimlington Stadial. As climate warmed into the Windermere Interstadial, the slopes of Kirk Fell directly to the north will have become re-mobilised and were thus a potential source of debris. Later, as climate further ameliorated, the ice below the sediment melted out to form the feature seen at present. The gradual process of ice melt may account for the smooth slopes and circular appearance of the feature which is referred to hear after as a peat filled circular depression.

### 5.1.3 Loch Lomond Stadial glacier reconstruction in Mosedale

It has therefore been established that if Mosedale supported a glacier during the Loch Lomond Stadial the limit of this glacier must have been located north of feature A in the valley. In delimiting Loch Lomond Stadial glaciers in the Lake District, Manley (1959) suggests that the highest elevation moraines on a valley floor can be assumed to have been formed during the most recent glacial episode; the Loch Lomond Stadial.

In Mosedale, the application of this theory places the limit of the Loch Lomond Stadial glacier along the crest of the outermost arcuate moraine marked in pink on figure 5.1. This produces

a glacier with the same down-slope limit as that proposed by Sissons (1980). Given the morphological similarities between the moraines which occupy the valley floor (marked on figure 5.1 in purple) it is difficult to envisage how some of these moraines could have been affected by the processes operating at the front of a Loch Lomond Stadial glacier, yet maintain or produce such a similar morphology to the moraines further down valley which have been shown, from the stratigraphic evidence in feature A, to have been formed pre-Loch Lomond Stadial. A clear morphological change however is seen between the moraines on the valley floor and those which form the subtle arcuate ridge around Black Comb at 178 m OD (marked on figure 5.1 in pink). By linking the process which formed the moraines within Mosedale to their morphology it is inferred that the moraines occupying the valley floor were formed pre-Loch Lomond Stadial, while those surrounding Black Comb were formed at the front of a small valley glacier present during the Loch Lomond Stadial. Figure 5.11 below shows the reconstructed glacier which is proposed to have occupied Mosedale during the Loch Lomond Stadial based on the above findings.

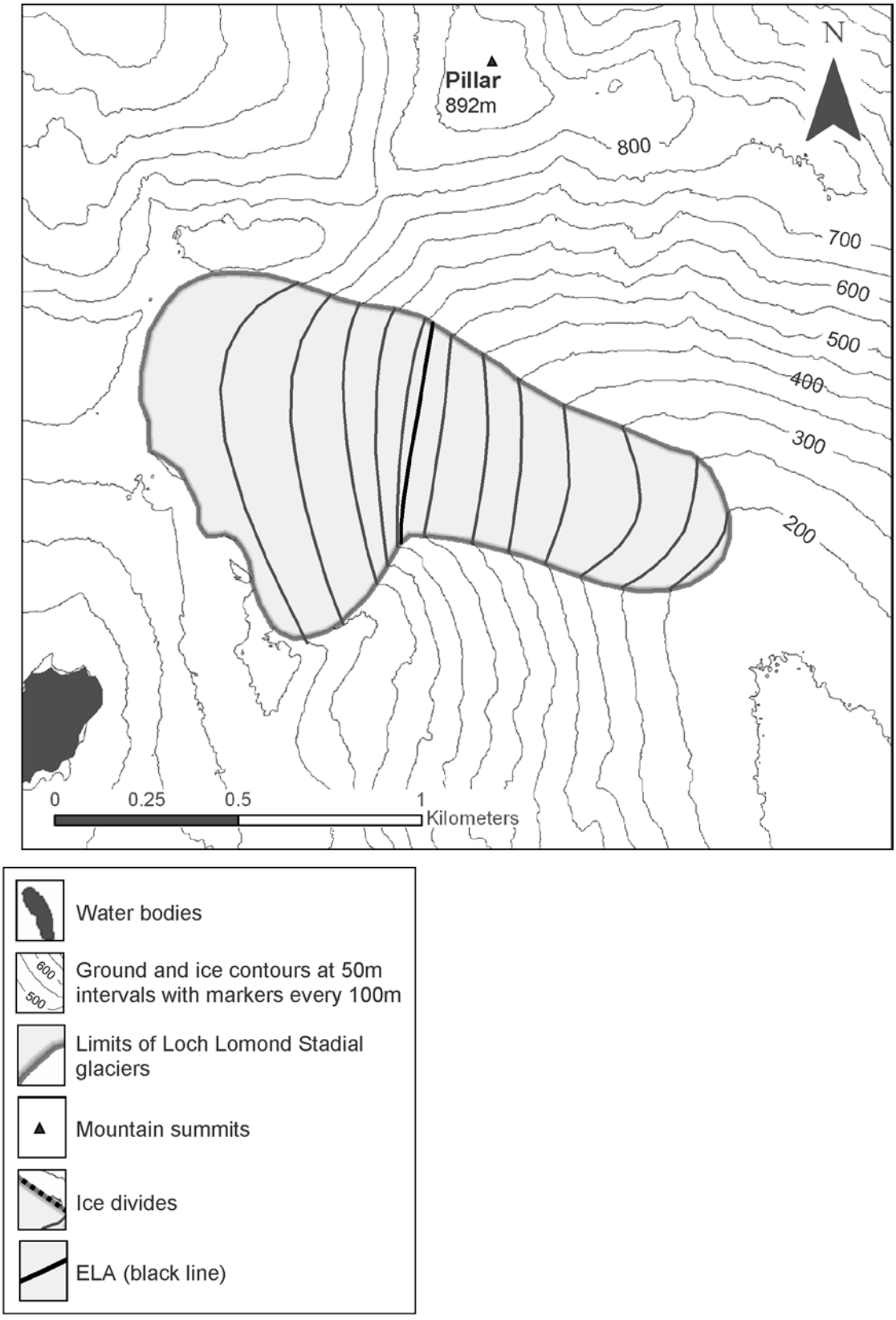


**Figure 5.11: A reconstruction of the glacier which occupied Black Comb at the north end of Mosedale during the Loch Lomond Stadial.**

As shown in figure 5.11 above, the glacier in Mosedale occupied the whole of the Black Comb cirque before narrowing to a thinner tongue in its ablation zone. The glacier had a surface area of 0.87 $km^2$ which is slightly larger than the area calculated by Sissons (1980) of 0.64 $km^2$. This increase is primarily due to the extension of the glacier along its northern margin and causes the glacier to be larger than 45 (compared to 43 glaciers based on the glacier area calculated by Sissons (1980)) of the 64 glaciers proposed by Sissons (1980). Further data relating to this glacier can be found below in table 5.1.

As previously stated, the calculation of a glacier's ELA has long been used as a basis for palaeoclimatic inferences and is the theoretical altitude on a glacier at which accumulation and ablation are exactly balanced over the period of one year (Mitchell, 1996: Benn and Lehmkuhl, 2000). Table 5.1 below shows the calculated ELAs for the Mosedale glacier using the various different methods reviewed in chapter 3. An altitude of 534 m OD has been used in subsequent calculations.

Mosedale is a good example of where lateral moraines are still present. As a result the use of lateral moraines to estimate the ELA of the Mosedale glacier appears to be reasonably successful as the maximum elevation of lateral moraines method provides a value which is just 11.3 m lower than the final ELA calculation taken as 534 m OD. Along with the lateral moraines and two arcuate moraine ridges, which are still present as a result of little post-glacial modification, there is no morainic evidence to suggest that readvance occurred during overall deglaciation. In contrast Upper Eskdale, a site that will be discussed in a subsequent chapter, has very few lateral moraines, which only occur very close the proposed glacier terminus. In settings such as this it is likely that the use of lateral moraines to estimate the ELA will seriously underestimate the ELA.

| | | Mosedale |
|---|---|---|
| Area ($km^2$) | | 0.87 |
| Long axis length (m) | | 1618.03 |
| Max altitude (m OD) | | 799.26 |
| Min altitude (m OD) | | 177.54 |
| Mid-altitude (m OD) | | 488.00 |
| Lowest cirque | | |
| Name | | 107. Black Comb or 90. Black Head, Mosedale |
| Altitude (m OD) | | 590 |
| Grade (according to Evans and Cox, 1995) | | 4 |
| Altitude of highest lateral moraine (m OD) | | 522.70 |
| Toe to head altitude ratio method (THAR) (m OD) | | |
| | 35% | 395.14 |
| | 40% | 426.23 |
| | 45% | 457.31 |
| | 50% | 488.50 |
| Accumulation area ratio method (AAR) (m OD) | | |
| | 70% | 498.00 |
| | 65% | 536.00 |
| | 60% | 555.00 |
| | 55% | 580.00 |
| | 50% | 630.00 |
| Area weighted mean altitude method (AWMA) (m OD) | | 565.41 |
| Balance ratio method (Benn and Gemmell, 1997) (m OD) | | |
| | BR=2.00 | 512.72 |
| | BR=1.81 | 520.78 |
| | BR=1.60 | 528.28 |
| | BR=1.54 | 531.34 |
| | BR=1.43 | 537.27 |
| Balance ratio method (Osmaston, 2005) (m OD) | | |
| | BR=2.00 | 507 |
| | BR=1.81 | 516 |
| | BR=1.60 | 526 |
| | BR=1.54 | 529 |
| | BR=1.43 | 535 |
| **Mean value of all of the above methods (m OD)** | | **518.94** |
| **Mean value of BR=1.54 (Benn and Gemmell,1997) and AAR 65%** | | **533.67** |
| **ELA used in subsequent calculations (m OD)** | | **534** |

**Table 5.1: ELA calculations and dimensions of the glacier occupying Mosedale during the Loch Lomond Stadial.**

- **Comparison to previous reconstructions**

As previously stated the south-west Lake District was not mapped by McDougall (1998) however earlier Loch Lomond Stadial reconstructions within Mosedale show considerable variation. Early work by Manley (1959) proposed a glacier which sat at the head of the valley below Pillar (892 m OD) but did not facilitate Black Comb as its primary accumulation area. Furthermore the maximum altitude of Manley's proposed glacier did not exceed 610 m OD which is surprising given the opportunity for a sheltered accumulation area within Black Comb.

Manley's proposed glacier does also not appear to terminate at the moraines proposed here as the down-slope limit of the Loch Lomond Stadial glacier although the coarse scale of the map produced by Manley (1959) makes it difficult to determine exactly where he intended his limit to be. Sissons (1980) also reconstructed the Loch Lomond Stadial glacier in Mosedale. Sissons' (1980) reconstruction agrees well with the reconstruction proposed here in terms of the down-slope limit of the glacier however some differences occur between the proposed lateral limits. The most notable difference between the reconstructions of Sissons (1980) and the current author occurs along the northern lateral limit where Sissons' limit is considered conservative. Here, an extension of the northern lateral limit of the glacier to coincide with the crest of a lateral moraine which runs up the northern side of the Black Comb valley is proposed (figure 5.11).

- **The contribution of snowblow**

The distribution of glaciers is often dictated by a number of regional and local climatic factors including temperature, precipitation and prevailing wind direction. These variables often give rise to local, regional and sometimes hemispherical trends in glacier aspect. During the Loch Lomond Stadial snowfall was largely associated with south to south-westerly winds. According to Sissons and Sutherland (1976), such winds were the result of cold polar water moving south to meet the relatively warm North Atlantic Drift waters around south-west Ireland (Ruddiman et al., 1977). This would have encouraged the vigorous interaction of air masses and produced stormy conditions with abundant precipitation. Consequently, snowfall was associated with depressions which followed more southerly tracks than those which prevail today (Sissons, 1980b).

During the Loch Lomond Stadial Sissons' (1980) glacier reconstruction suggests that the largest glaciers formed along the west-east mountain axis, especially in the Central Fells, with some of the smallest glaciers further to the north-west. Glaciers preferentially developed in areas which received low amounts of direct insolation and had large areas of adjacent higher ground which could provide input to the glacier through snowblow. The result of this was that many of the glaciers within the Lake District during the Loch Lomond Stadial had north to north-easterly aspects and were located on the north to north-eastern side of mountain ranges or ridges having a poleward aspect.

As noted by Evans (2006) regional variations in glaciation are largely a reflection of regional climate, however local variations are dictated by slope mesoclimate and topography. Furthermore, topography is influenced by bedrock geology, tectonics and climate (Evans,

2006). Topographically, the headwalls of cirques within the Lake District favour a north-easterly aspect with an average orientation of 049° ± 10° (Evans and Cox, 1995). This is a particularly significant finding when considering the reconstruction of Loch Lomond Stadial glaciers in the region provided by Sissons (1980a). Sissons (1980a) suggests that many of the glaciers present during the Loch Lomond Stadial had accumulation areas within cirques.

It is unlikely that the formation of large erosional landforms such as cirques relates to a single glacial episode. Cirques in the Lake District are likely to have been eroded by glaciers at valley-heads or on valley-sides. Since cirque initiation is therefore likely to pre-date the Loch Lomond Stadial: cirques in the Lake District are believed to have partially dictated the location of glaciers in the region during the Loch Lomond Stadial rather than vice versa (Evans, pers. com.: Evans, 2003).

In terms of climate, the persistence of snow on poleward slopes is favoured by two key factors: firstly, accumulation occurs in sheltered locations, and secondly, the reduction in air turbulence across the glacier surface on poleward slopes reduces the heat transfer from air to snow. The latter of these factors is particularly important when air temperatures exceed freezing point (Evans, 2006). A factor which has the opposite effect on glacier development is the angle at which precipitation input occurs. Precipitation rarely falls vertically and its incidence is frequently greater on windward slopes.

The long axis of the accumulation area of the Mosedale glacier (Black Comb) lies at 110° and the long axis of the main Mosedale valley lies at ~ 152°. Although Black Comb appears to have a relatively unfavourable and exposed aspect, the local topography outside the glacier limits counteracts this. To the south of the glacier is the summit of Red Pike (826 m OD) which forms the northernmost point of a ridge which extends south-eastwards parallel with the long axis of the main valley before curving slightly eastwards at the southern end of the valley. This ridge therefore provides shelter from winds associated with southerly air masses and also to a lesser degree from direct solar radiation.

In contrast, Black Sail Pass which is located on the opposite side of the valley to Black Comb is in a highly unfavourable location for glacier development. As shown in figure 5.1, glacial geomorphology in Black Sail Pass is sparse and fieldwork in the area brings the author to the conclusion that the area was not occupied by a glacier during the Loch Lomond Stadial. This agrees with the work of Manley (1959), Sissons (1980) and McDougall (1998). The primary reason for the lack of glaciation at this site during the Loch Lomond Stadial relates to the

aspect of the site (226°) relative to the prevailing wind direction (south-southwest). As a consequence, the site will have received little shading from direct insolation. Opportunities for snowblow also appear minimal due to a lack of suitable high ground to the south and south-west of the glacier. It is therefore unlikely that a glacier would have survived in Black Sail Pass.

### 5.1.4 The influence of snowblow on glacier development in Mosedale

Figures 5.12 and 5.13 below show the digitisation of the areas identified using the criteria above and a polar plot of snowblow area respectively for the glacier in Mosedale. As shown in figures 5.12 and 5.13 the glacier in Mosedale was surrounded by substantial amounts of terrain with the potential to contribute mass to the glacier through snowblow. Interestingly, a particularly large area with the potential for snowblow is found to the south of the glacier between 165° and 210°. Table 5.2 below shows the snowblow factors and snowblow areas calculated for the glacier in Mosedale.

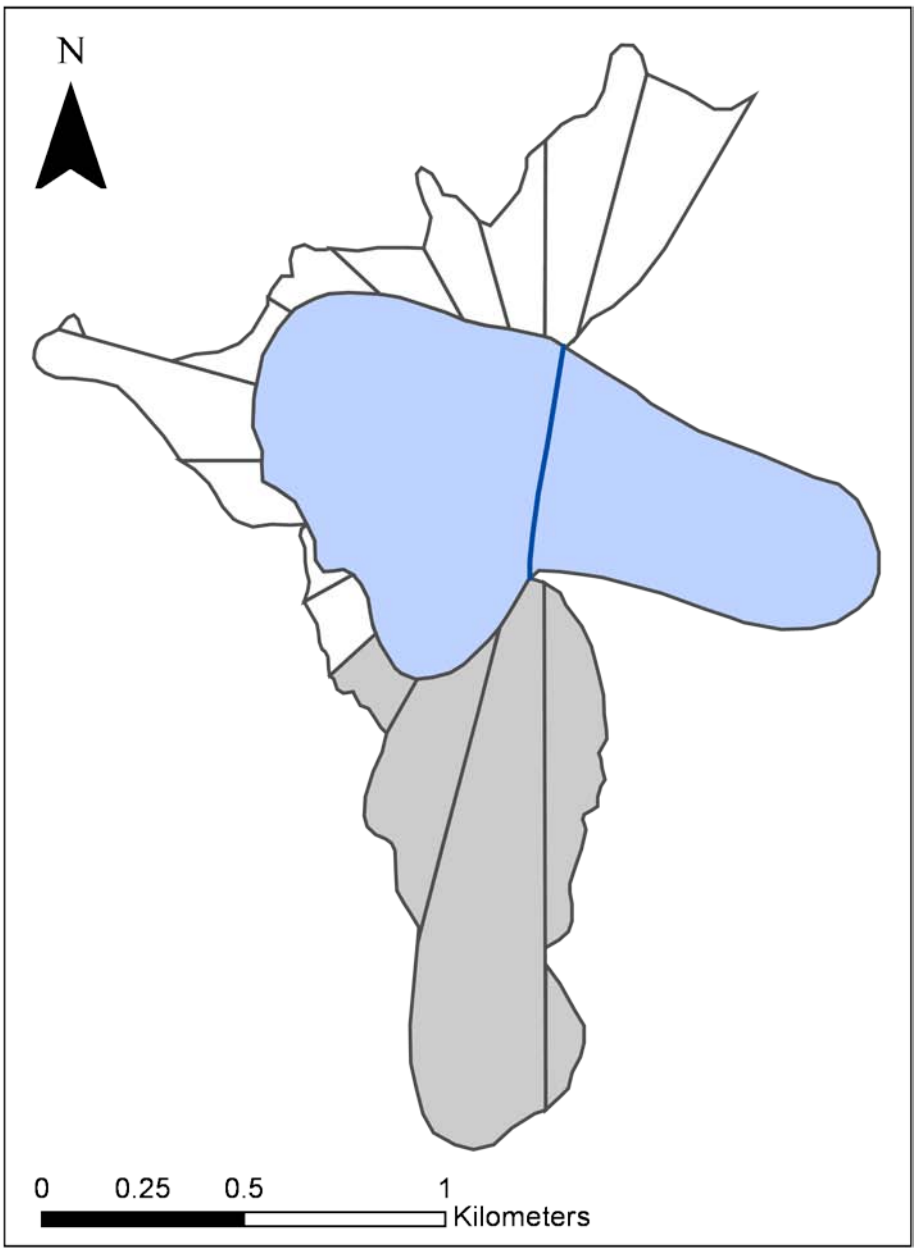


**Figure 5.12: The snowblow areas associated with the Mosedale glacier. The ELA of the glacier has been calculated at 534 m OD and is marked with a dark blue line above. The snowblow sectors shaded in grey indicate the snowblow area lying within the southern sector (135-225°).**

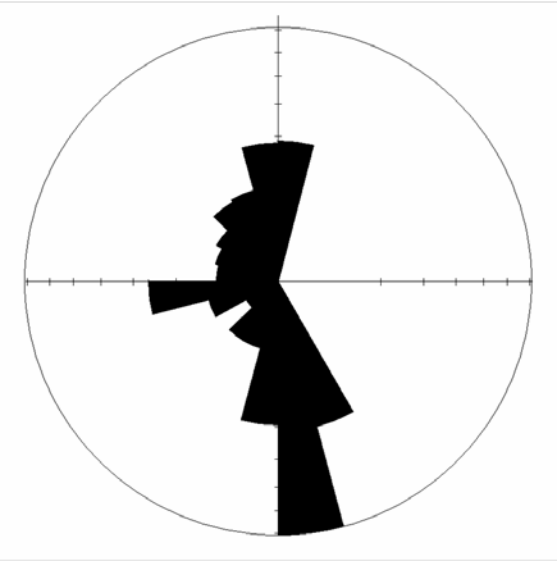

**Figure 5.13: Polar plot of snowblow area with area-weighted 15° sector lengths.**

| | |
|---|---|
| **Glacier name** | Mosedale |
| **Glacier area ($km^2$)** | 0.87 |
| **Total snowblow area ($km^2$)** | 1.08 |
| **Snowblow area by 90° quadrants expressed as a percentage of the total snowblow area (%)** | |
| **NE (0-90°)** | 18.49 |
| **SE (91-180°)** | 10.68 |
| **SW (181-270°)** | 48.07 |
| **NW (271-360°)** | 22.76 |
| **S (135-225°)** | 53.34 |
| **W (226-315°)** | 17.36 |
| **Snowblow factor by 90° quadrants** | |
| **NE (0-90°)** | 4.62 |
| **SE (91-180°)** | 3.51 |
| **SW (181-270°)** | 7.45 |
| **NW (271-360°)** | 5.13 |
| **S (135-225°)** | 7.85 |
| **W (226-315°)** | 4.48 |
| **Mean snowblow factor** | 5.51 |
| **Ratio of snowblow area to glacier area** | 1.24 |

**Table 5.2: Snowblow areas and snowblow factors identified around the Mosedale glacier using the criteria outlined in the text.**

The southern quadrant accounts for the highest percentage of snowblow area of out all the six quadrants. This is mirrored by the southern quadrant also having the highest snowblow factor of 7.85. This is closely followed by the southwest quadrant which has the second highest snowblow factor of 7.45. Since terrain within the southwest, southeast and southern quadrants may be considered windward of the glacier it may be significant that the largest areas with the potential for snowblow occur in these quadrants.

As a means of further refining the definition of snowblow areas outlined above it may be necessary to, in analysis, add in the following criteria to the above definition:

1. *surfaces which are windward of the glacier surface (i.e. in the south-east, south-west or southern quadrants in the case of the Loch Lomond Stadial in Britain).*

This addition refers more to the climatic setting of the glacier than the previous criteria which are more concerned with the topographic setting of the glacier. This particular criteria is separated from criteria 1 to 4 as it requires knowledge of the prevailing wind direction during a particular glacial episode and in a particular region. It is potentially therefore more effective to calculate the total snowblow area in all six quadrants before applying criteria 5 to the results. This will be particularly effective where prevailing wind directions are/were highly variable or where palaeoclimatic knowledge is lacking.

### 5.1.4 Glacier dynamics in Mosedale

Table 5.3 below displays the results of the above methodology when applied to the Mosedale glacier. A required basal motion of 0% indicates that the Mosedale glacier moved largely by internal ice deformation rather than basal slip. A cross sectional profile of the Mosedale glacier can be seen in figure 5.15 below. The glacier appears to maintain its thickness throughout its length with only minimal thinning in the ablation zone.

| | Mosedale |
|---|---|
| ELA (m) | 534 |
| Temperature proxy used | Coope and Joachim (1980) St Bees Head |
| Proxy site altitude (m OD) | 0.00 |
| $T_3$ at proxy site (°C) | 8.25 |
| Temp. at ELA (0.0065°C/m lapse rate) | 4.77 |
| Degrees surface slope at ELA | 18.22 |
| Max ice thickness at ELA (m) | 120.38 |
| Glacier shape factor | 0.54 |
| Normal stress at centre point of ELA (bars) | 10.50 |
| Ablation gradient at ELA (mm/m) | 6.05 |
| Mass loss at ELA (ma-1) | 2.26 |
| Net Ablation ($m^3$ w.e.) | 446,729 |
| Mass flux ($m^3$ ice) | 490,911 |
| Cross sectional area at ELA ($m^2$) | 40,774 |
| Perimeter of bed at ELA (m) | 635 |
| Mean balance velocity at ELA ($ma^{-1}$) | 12.04 |
| Basal shear stress at ELA (bars) | 2.06 |
| Max ice deformation velocity at ELA ($ma^{-1}$) | 368.82 |
| Average ice deformation velocity at ELA ($ma^{-1}$) | 130.28 |
| Required basal motion ($ma^{-1}$) | 0.00 |
| Required basal motion (%) | 0.00 |

**Table 5.3: Reconstructed steady-state dynamics and flow characteristics of the glacier occupying Mosedale during the Loch Lomond Stadial.**

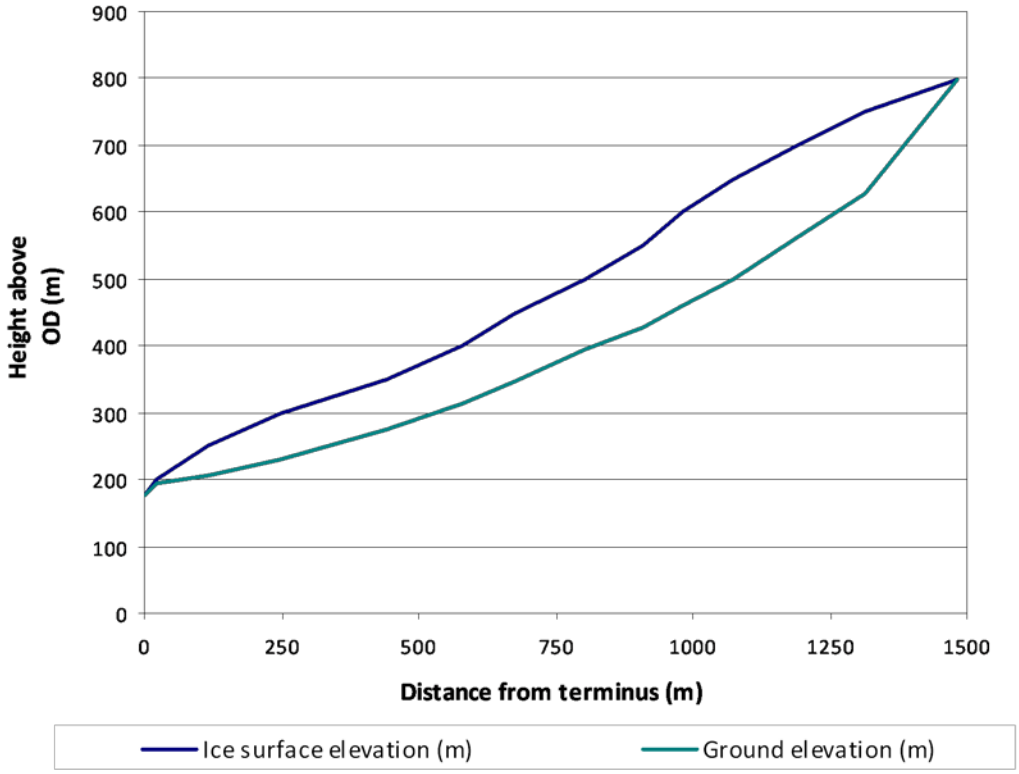


**Figure 5.15: A cross sectional profile along the long axis of the Mosedale glacier.**

Figure 5.16 below show the cross sectional profile from south to north across the ELA of the Mosedale glacier. The valley shows a surprisingly symmetrical profile which reaches its maximum depth slightly north of the centre point of the valley.

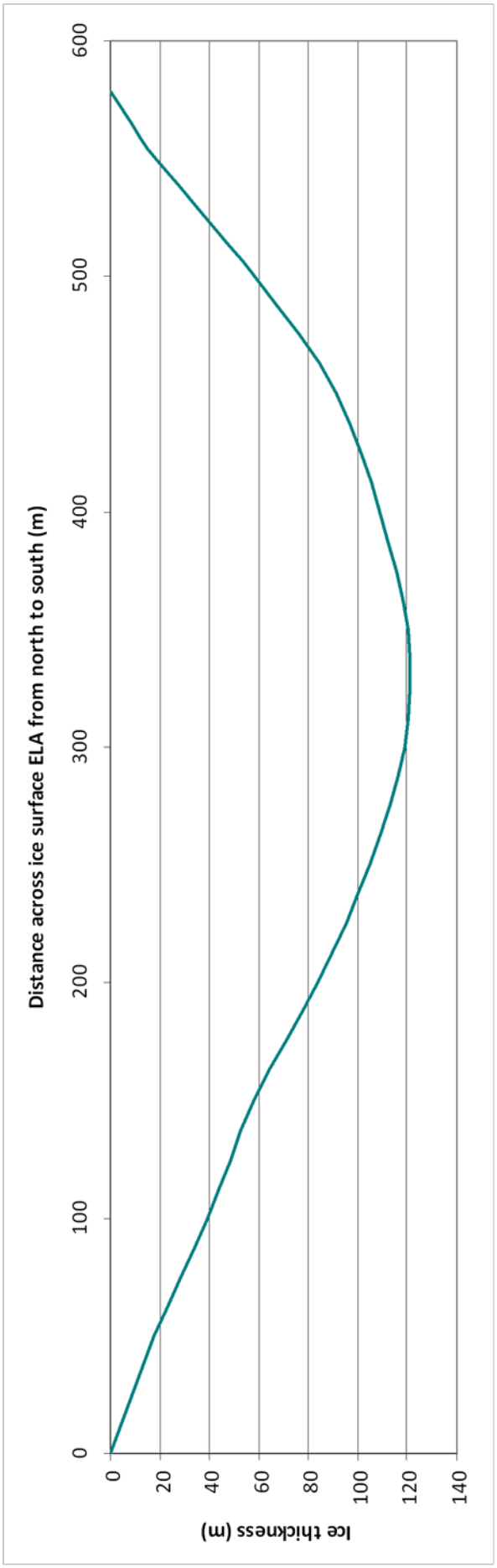


**Figure 5.16: A cross sectional profile south to north across the ELA of the Mosedale glacier. ELA = 534 m OD.**

The distribution of the glacier's surface area over altitude is graphically represented in figures 5.17 and 5.18 below. The largest surface area between any of the contours lies between the 751 and 800 m contour and has a total area of 0.167 $km^2$. The second largest area of 0.157 $km^2$ lies within the contour interval 701-750 m OD. This is primarily the result of the wide accumulation area of the Mosedale glacier. Overall the surface area between the 50 m contours of the Mosedale glacier increases from the 551-600 m contour interval to the maximum altitude of the glacier. Smaller surface areas are found between the lower contour intervals. This may be a reflection of the topographically induced narrow snout of the glacier.

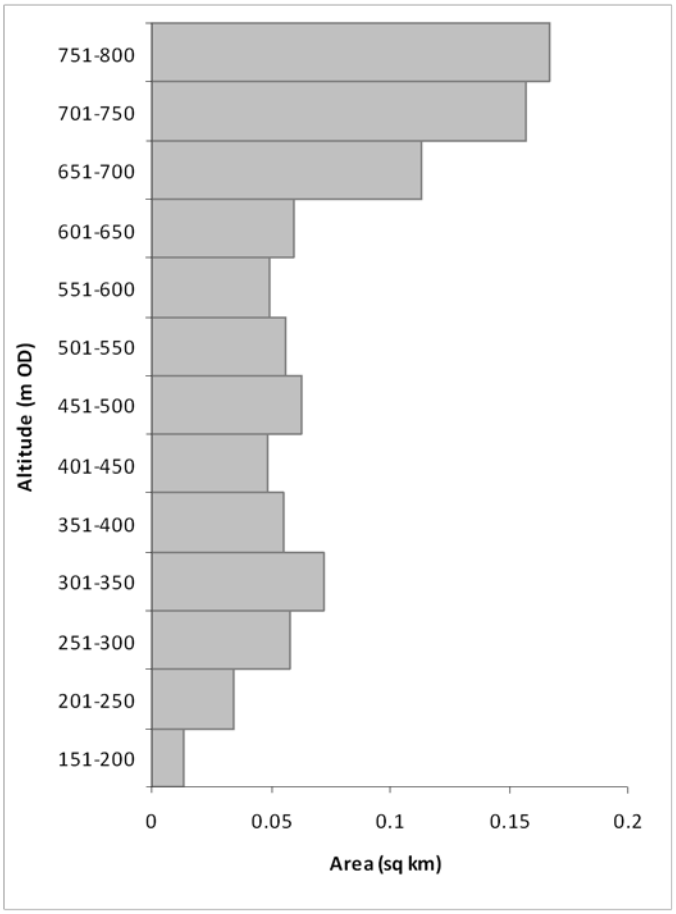


**Figure 5.17: The distribution of the glacier's surface area between the 50m ice surface contour intervals. ELA altitude = 534 m OD.**

Figure 5.19 below indicates the net balance profile of the glacier in Mosedale which indicates balanced accumulation and ablation as would be theoretically expected for a glacier under steady-state conditions.

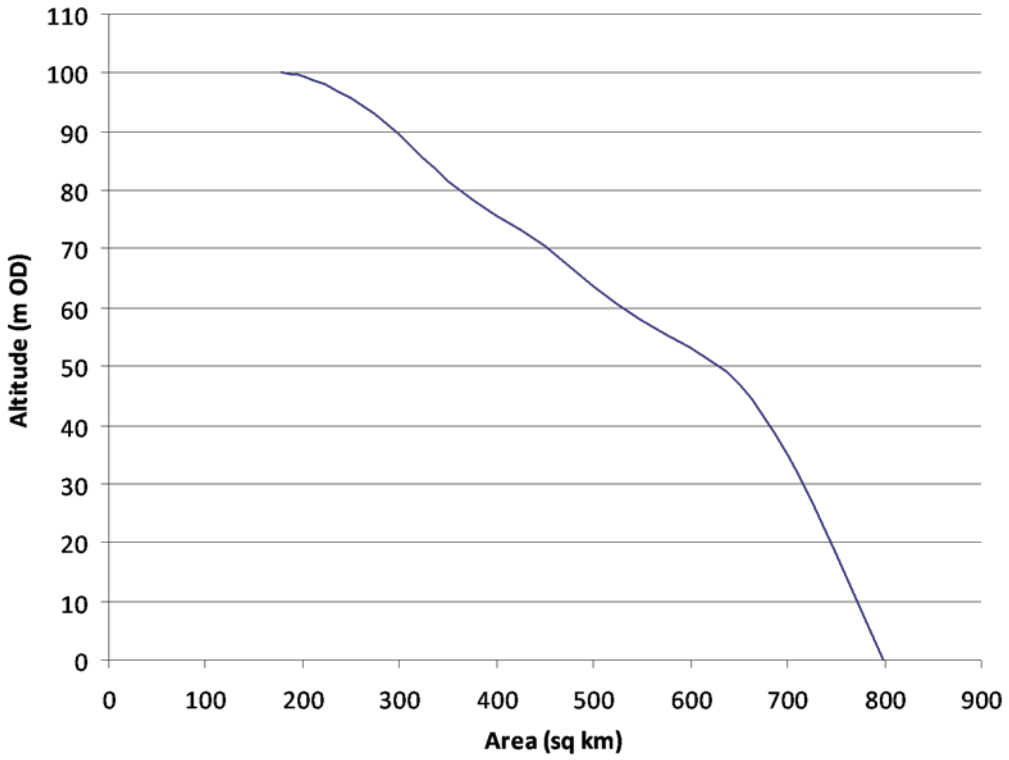


**Figure 5.18: Hypsometric curve for the Mosedale glacier.**

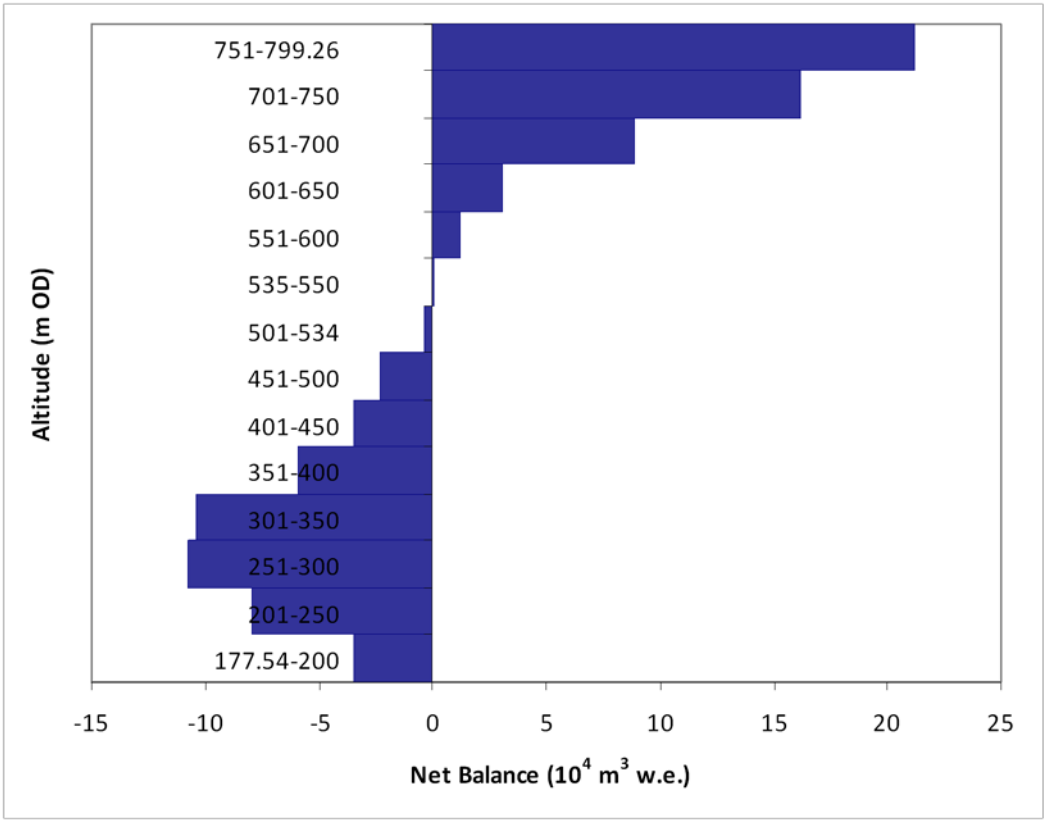


**Figure 5.19: The mass-balance profile of the Mosedale glacier.**

The viability of a glacier can be tested based on the contribution of basal sliding ($U_b$) to overall glacier motion ($U_s$). Carr (2001) suggested that where $U_b$ accounts for > 95 % of the total glacier flow velocity, $U_s$, the glacier exceeds the threshold for a glaciologically viable glacier under the environmental parameters used in the model. Carr and Coleman (2007) however suggest that this is a conservative suggestion. Based on observations of contemporary glaciers Andrews (1972) believe that 10 – 90 % basal motion through sliding at the ELA is more realistic. Consequently, Carr and Coleman (2007) suggest that the threshold for glacier viability should be reduced to a maximum of 90 % basal motion by basal sliding. Based on the above calculations, the Mosedale glacier can therefore be considered to have been viable under steady-state conditions and the temperature parameters on which the model is based. Since the mean rate of ice deformation at the ELA (m $a^{-1}$) exceeds the mean balance velocity at the ELA (m $a^{-1}$) the glacier is Mosedale believed to have moved purely by internal ice deformation with basal sliding.

## 5.2 Lingmell Beck

Lingmell Beck is a west/north-west facing valley in the south-west Lake District at the northern end of Wastwater. The valley is dominated by a river system which drains the north-western side of the Scafell Pike and Great End. At grid reference 213092 the main river of Lingmell Beck forms at the confluence of two tributaries; one which originates from the most easterly point of the valley and the other from below Scafell Pike (978 m OD). Below this point the lower section of the valley descends gently to the flat farmland around Wasdale Head. Moraines which appear to have undergone extensive fluvial dissection cover the valley walls along with large quantities of scree. On the northern side of the valley is the summit of Kirk Fell (802 m OD) which as previously mentioned, is suggested by McDougall (1997) to have supported a plateau icefield during the Loch Lomond Stadial. The upper section of the valley has a more north-westerly aspect and shows extensive evidence of fluvial incision in the form of Piers Gill; a deep zigzagging gill cut into the tuff bedrock. It is also surrounded by some of the highest ground in the British Isles with the summits of Scafell Pike (978 m OD) and Great End (910 m OD) directly to the east.

### 5.2.1 Geomorphology in the valley of Lingmell Beck

Extensive moraines cover the valley floor and walls up to an altitude of ~ 350 m OD. The river of Lingmell Beck shows clear evidence of having once supported a very high discharge. The river has thus deposited thick areas of fluvial gravels and cut through moraines which no longer form complete arcuate ridges across the valley. The majority of these moraines lie parallel to the long axis of the valley or trend slightly down slope towards the centre of the valley. This is particularly true of the moraines at lower elevations suggesting that these moraines formed at the snout of an ice mass topographically confined within the valley. Figure 5.20a below shows the geomorphology of Lingmell Beck.

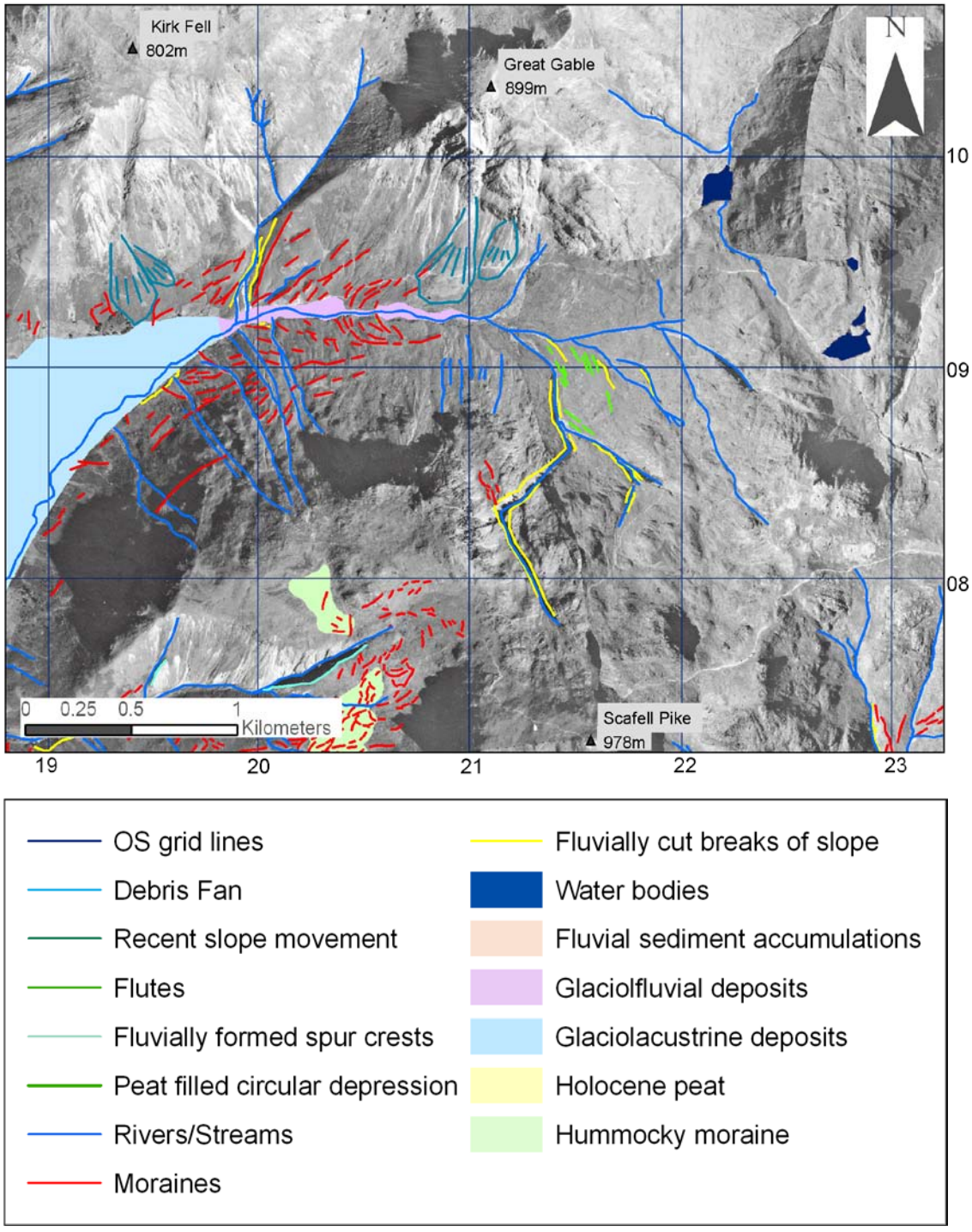


**Figure 5.20a: The geomorphology of Lingmell Beck**

A clear morphological change is seen between the moraines in the upper part of the valley and those further down the valley (see figure 5.20b below). The moraines shown in purple are much larger in both width and height than those marked in pink. As a consequence, the moraines in purple have been assigned a pre-Loch Lomond Stadial age in a similar way the moraines in Mosedale.

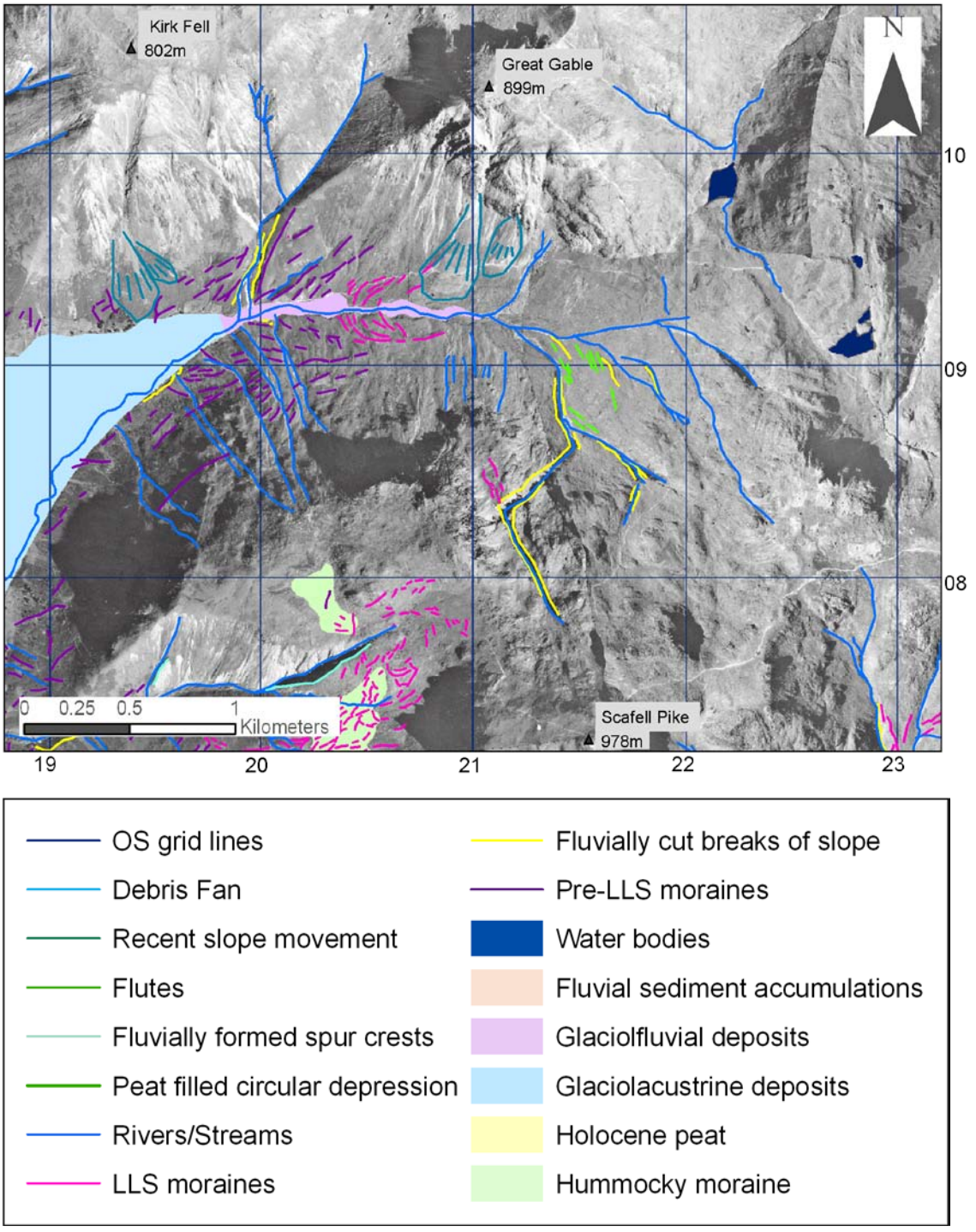


**Figure 5.20b: The geomorphology of the valley of Lingmell Beck including the distinction between Loch Lomond Stadial and pre-Loch Lomond Stadial moraines.**

Debris fans on the north side of the lower section of the valley support the suggestion that the morphological change seen between the moraines is a result of them being formed during different glacial episodes. It is suggested by Wilson and Smith (2006) that the Lateglacial Interstadial was a period of intense paraglacial slope activity. Since moraines directly below Great Gable are found to overrun the debris fans it can be suggested that these fans pre-date the Loch Lomond Stadial. It can then be assumed that the debris fans further to the west

below Kirk Fell, which have a similar morphology, are also of Lateglacial age. Given that moraines are only found around the edges of these debris fans but do not overrun the fans, it is likely that the moraines pre-date the formation of the debris fans and therefore also the pink moraines which are suggested to have formed during the Loch Lomond Stadial at the snout of a small valley glacier (see figure 5.20c below).

**Figure 5.20c: The moraines on the eastern side of the valley of Lingmell Beck which formed at the terminus of the Loch Lomond Stadial glacier**

A comparison with the moraines discussed in Mosedale also supports the above suggestion. The moraines believed to pre-date the Loch Lomond Stadial in Lingmell Beck show very similar morphological characteristics to those which can be more confidently assigned a pre-Loch Lomond Stadial age in Mosedale based on stratigraphic evidence (see section 5.1.2).

### 5.2.2 Loch Lomond Stadial glacier reconstruction in Lingmell Beck

It is concluded that the location of the snout of the Lingmell Beck glacier at its maximum extent during the Loch Lomond Stadial is marked by the pink moraines shown in figure 5.20b. These moraines are not only smaller in height and plan but also form more complete across valley arcuate ridges. The moraines marked in purple, therefore, are suggested to have

formed pre-Loch Lomond Stadial possibly during the Scottish Readvance or during deglaciation as ice became confined by topography to the valley. Evidence for varying rock mass strength along the length of the valley also confirms the smaller moraines as the limit of the Loch Lomond Stadial glacier. In order to confirm the upslope limit of the glacier near Styhead Tarn, the work of Pennington (1978) has been discussed and is considered sound evidence on which to base the glacier limit at this location. Negative evidence is provided by further coring by the author in Styhead Tarn which did not provide any reason to dispute the work of Pennington (1978). The glacier was therefore reconstructed based on this evidence, figure 5.21 below shows the glacier reconstruction.

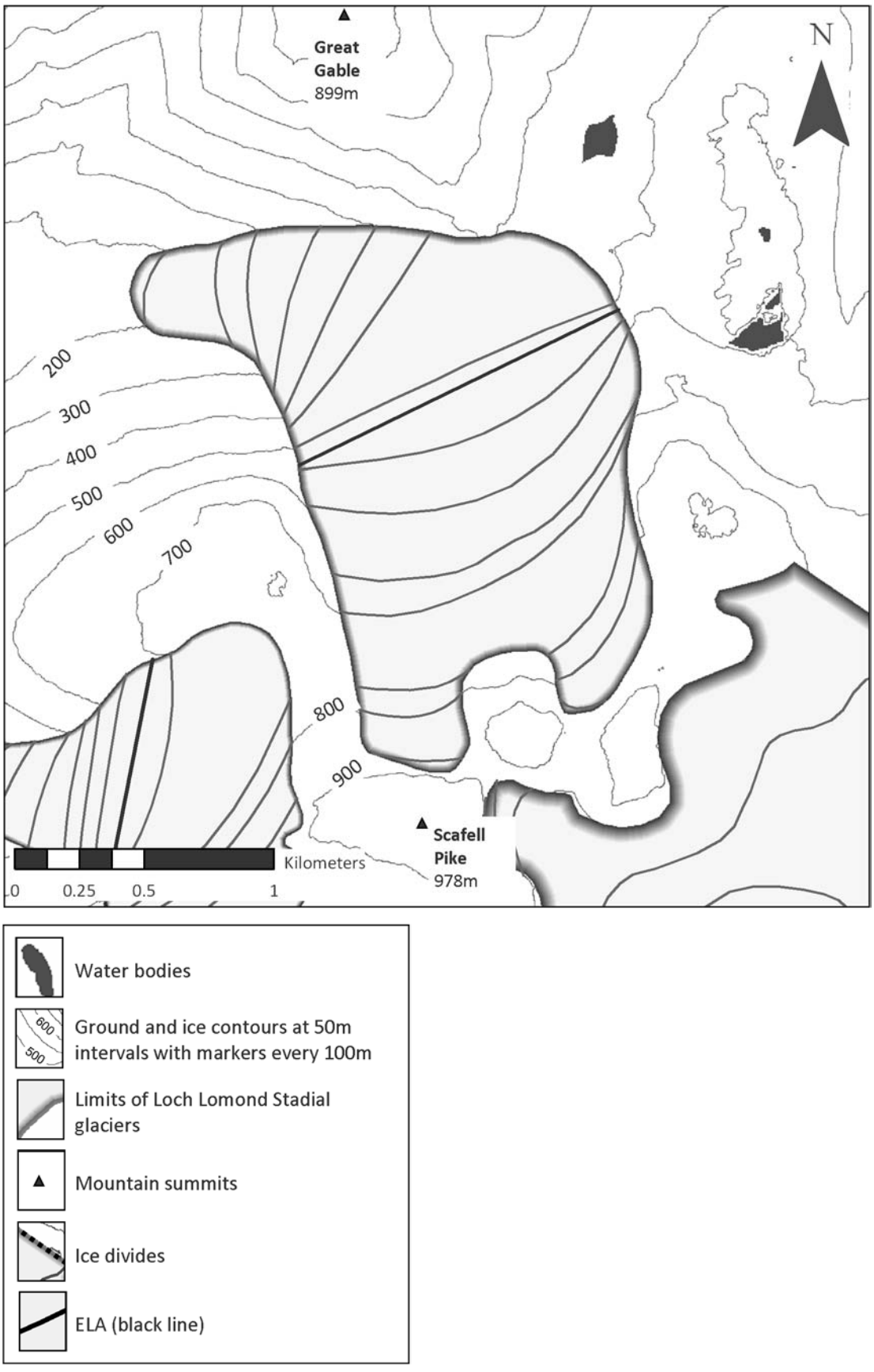


**Figure 5.21: A reconstruction of the glacier which occupied Lingmell Beck at the north end of Wastwater during the Loch Lomond Stadial.**

The glacier shown above had a surface area of 2.53 $km^2$ and although it is slightly larger than the reconstruction provided by Sissons (1980) for this valley, the reconstructions show glaciers of very similar shapes. Compared with the work of Sissons (1980), the glacier reconstructed here extends slightly higher up into the cirques located on the west side of the Scafell massif. Three cirques have been identified by Evans and Cox (1995) in this valley, all of which were occupied by the Lingmell Beck glacier during the Loch Lomond Stadial: Dropping Crag on Scafell Pike (grade 3), Broad Crag north-west (grade 3) and Broad Crag, Round Hollow (grade 4). It appears unlikely that these cirques were not occupied by ice during the Loch Lomond Stadial primarily due to their elevations of 305 m, 540 m and 445 m OD respectively on some of the highest ground in Britain. Although McDougall (1998) did not reconstruct the glaciers in the south-west Lake District in his plateau icefield model, he did show the tongue of the Lingmell Beck glacier in his regional plateau icefield reconstruction. It is suggested here that the reconstruction provided by McDougall (1998) is ambitious, with a tongue which extends beyond the moraines suggested here to mark the maximum extent of the Loch Lomond Stadial glacier.

Based on the reconstruction shown in figure 5.21, the ELA of the glacier was calculated using the methods previously described in section 5.1.3 and are shown in table 5.4 below. The Lingmell Beck glacier has a very similar ELA to the Mosedale glacier with just 4 m difference between them suggesting that these two glaciers have similar hypsometry. Both glaciers are also located in relatively sheltered locations. The lower valley of Lingmell Beck has a fairly unfavourable aspect with an orientation of 270°. If winds came often from the west, the ablation zone of the Lingmell Beck glacier in the main valley may often have faced windward. The accumulation zone of the glacier however had a much more favourable aspect with the upper portion of the valley facing 335° and surrounded by the highest ground in the region. Shelter is provided for the accumulation area of the Lingmell Beck glacier by Lingmell Crag to the west, Scafell Pike (978 m OD) and Ill Crag (935 m OD) to the south, and Great End (910 m OD) to the east.

| | | Lingmell Beck |
|---|---|---|
| Area ($km^2$) | | 2.53 |
| Long axis length (m) | | 2731.75 |
| Max altitude (m OD) | | 886.12 |
| Min altitude (m OD) | | 158.41 |
| Mid-altitude (m OD) | | 522.00 |
| Lowest cirque | | |
| Name | | 133. Broad Crag, Round How |
| Altitude (m OD) | | 720 |
| Grade (according to Evans and Cox, 1995) | | 4 |
| Altitude of highest lateral moraine (m OD) | | 612.06 |
| Toe to head altitude ratio method (THAR) (m OD) | | |
| | 35% | 413.11 |
| | 40% | 449.49 |
| | 45% | 485.88 |
| | 50% | 522.00 |
| Accumulation area ratio method (AAR) (m OD) | | |
| | 70% | 474.00 |
| | 65% | 482.00 |
| | 60% | 490.00 |
| | 55% | 505.00 |
| | 50% | 554.00 |
| Area weighted mean altitude method (AWMA) (m OD) | | 558.00 |
| Balance ratio method (Benn and Gemmell, 1997) (m OD) | | |
| | BR=2.00 | 536.68 |
| | BR=1.81 | 541.14 |
| | BR=1.60 | 546.76 |
| | BR=1.54 | 548.54 |
| | BR=1.43 | 551.86 |
| Balance ratio method (Osmaston, 2005) (m OD) | | |
| | BR=2.00 | 516 |
| | BR=1.81 | 522 |
| | BR=1.60 | 530 |
| | BR=1.54 | 535 |
| | BR=1.43 | 537 |
| **Mean value of all of the above methods (m OD)** | | **519.55** |
| **Mean value of BR=1.54 (Benn and Gemmell, 1997), AAR 65% and AWMA (m OD)** | | **529.51** |
| **ELA used in subsequent calculations (m OD)** | | **530** |

**Table 5.4: ELA calculations and dimensions of the glacier occupying Lingmell Beck during the Loch Lomond Stadial.**

### 5.2.3 The influence of snowblow on glacier development/maintenance

As previously noted, the topography which surrounds a valley can have a significant effect on the ability of a glacier to survive under a given set of environmental parameters. The morphology of the local topography dictates the areas which have the potential for snowblow. Ground surrounding the accumulation area of the Lingmell Beck glacier which had the potential to contribute mass to the glacier via snowblow has been identified using the criteria outlined in section 5.1.4 and is shown in figures 5.22 and 5.23 below.

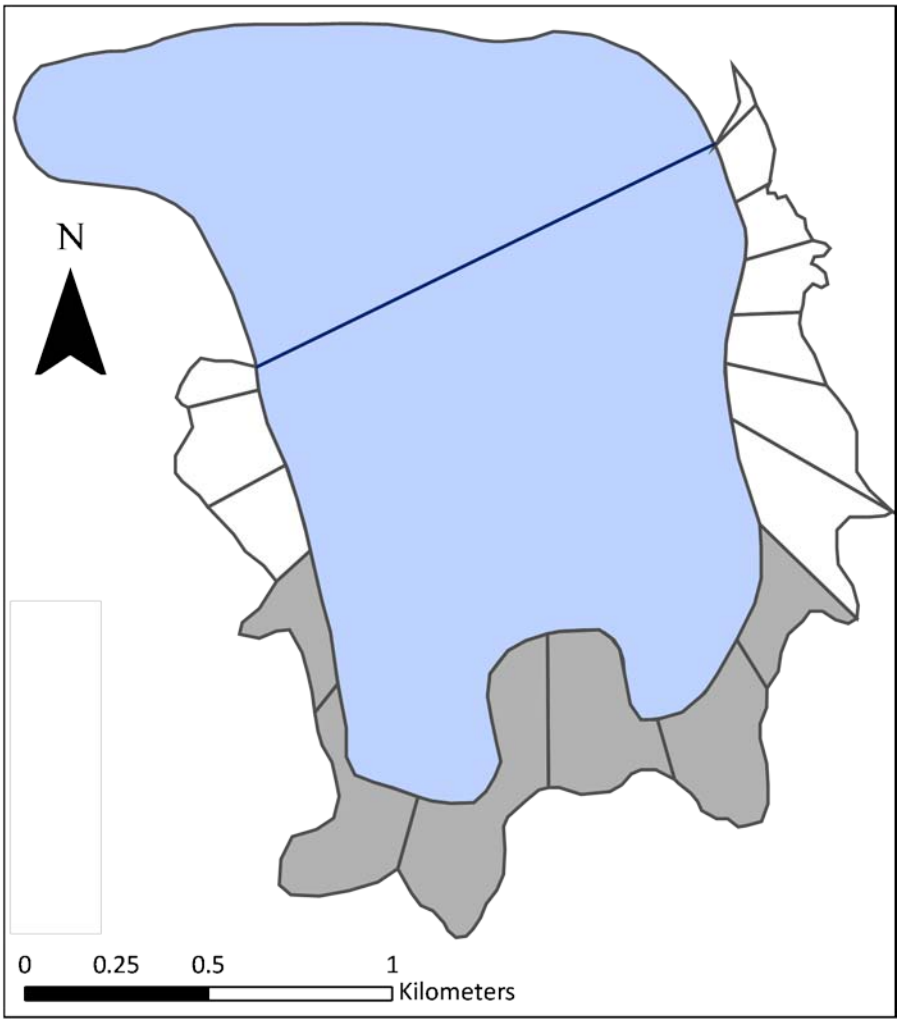


**Figure 5.22: The snowblow areas associated with the Lingmell Beck glacier. The ELA of the glacier has been calculated at 530 m OD and is marked with a dark blue line above. The snowblow sectors shaded in grey indicate the snowblow area lying within the southern sector (135-225°).**

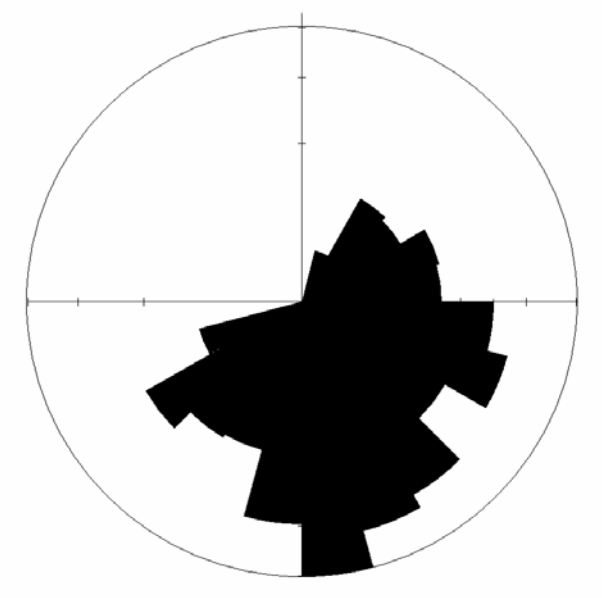

**Figure 5.23: Polar plot of snowblow area with area-weighted 15° sector lengths.**

Although no particular sector contains a significantly larger snowblow area, each of the SW, SE, S and W sectors contain ground with the potential to contribute mass to the glacier via snowblow. This is unusual amongst the glaciers considered in this project and is potentially significant since these quadrants are most likely to contain ground windward of the glacier.

Corresponding snowblow factors for each of the 90° quadrants: NW, SW, SE, NE, W and S, were then calculated and are shown in table 5.5 below. As expected the snowblow factors reflect the fact that potential snowblow area is located predominantly in the SW, S and SE quadrants. As with the Mosedale glacier, the highest snowblow factor is calculated for the S quadrant and the second highest factor for the SW quadrant.

| Glacier name | | Lingmell Beck |
|---|---|---|
| Glacier area ($km^2$) | | 2.53 |
| Total snowblow area ($km^2$) | | 0.93 |
| Snowblow area by 90° quadrants expressed as a percentage of the total snowblow area (%) | | |
| | NE (0-90°) | 9.97 |
| | SE (91-180°) | 46.72 |
| | SW (181-270°) | 43.32 |
| | NW (271-360°) | 0 |
| | S (135-225°) | 56.25 |
| | W (226-315°) | 13.65 |
| Snowblow factor by 90° quadrants | | |
| | NE (0-90°) | 1.99 |
| | SE (91-180°) | 4.3 |
| | SW (181-270°) | 4.14 |
| | NW (271-360°) | 2.61 |
| | S (135-225°) | 4.72 |
| | W (226-315°) | 2.32 |
| Mean snowblow factor | | 3.35 |
| Ratio of snowblow area to glacier area | | 0.37 |

**Table 5.5: Snowblow areas and snowblow factors identified around the Lingmell Beck glacier using the criteria outlined in section 3.1.4.**

### 5.2.4 Glacier dynamics in Lingmell Beck

The viability of the reconstructed glacier has again been assessed by applying the numerical model outlined above. The results of this model are shown below in table 5.6 and a cross sectional profile along the long axis of the glacier in figure 5.24. A required basal motion of 22.09 % suggests that the proposed Lingmell Beck glacier is glaciologically viable. Furthermore, a large proportion of glacier motion in Lingmell Beck occurred by internal ice deformation with a much smaller contribution from basal sliding.

| | Lingmell Beck |
|---|---|
| ELA (m) | 530.00 |
| Temperature proxy used | Coope and Joachim (1980) St Bees Head |
| Proxy site altitude (m OD) | 0.00 |
| $T_3$ at proxy site (°C) | 8.25 |
| Temp. at ELA (0.0065°C/m lapse rate) | 4.80 |
| Degrees surface slope at ELA | 21.60 |
| Max ice thickness at ELA (m) | 138.75 |
| Glacier shape factor | 0.86 |
| Normal stress at centre point of ELA (bars) | 5.11 |
| Ablation gradient at ELA (mm/m) | 6.08 |
| Mass loss at ELA (ma-1) | 2.27 |
| Net Ablation ($m^3$ w.e.) | 902,648.35 |
| Mass flux ($m^3$ ice) | 991,921.26 |
| Cross sectional area at ELA ($m^2$) | 71,110.14 |
| Perimeter of bed at ELA (m) | 1,474.59 |
| Mean balance velocity at ELA ($ma^{-1}$) | 12.69 |
| Basal shear stress at ELA (bars) | 0.89 |
| Max ice deformation velocity at ELA ($ma^{-1}$) | 39.90 |
| Average ice deformation velocity at ELA ($ma^{-1}$) | 9.92 |
| Required basal motion ($ma^{-1}$) | 2.77 |
| Required basal motion (%) | 21.83 |

**Table 5.6: Reconstructed steady-state dynamics and flow characteristics of the glacier occupying Lingmell Beck during the Loch Lomond Stadial.**

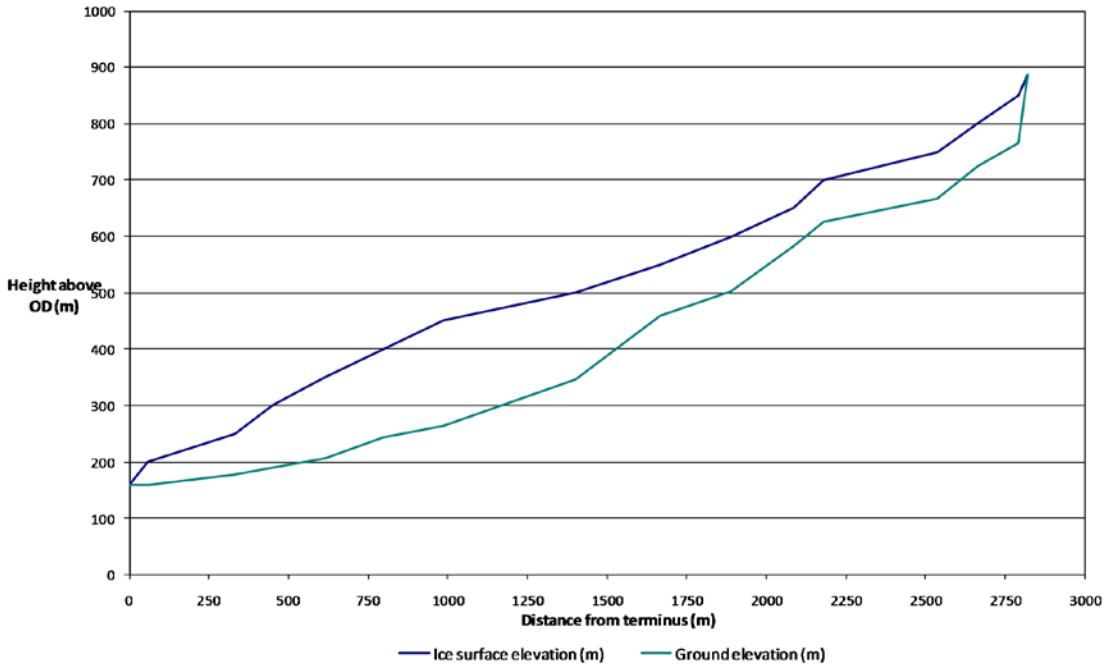


**Figure 5.24: A cross sectional profile along the long axis of the Lingmell Beck glacier.**

The cross sectional profile across the ELA of the Lingmell Beck glacier can be seen below in figure 5.25. The thickest ice at the ELA is 140.75 m near the centre of the glacier and, as expected, is associated with the highest basal shear stress of 2.55 bars at any point across the ELA and the highest basal velocity of 41.03 m $a^{-1}$.

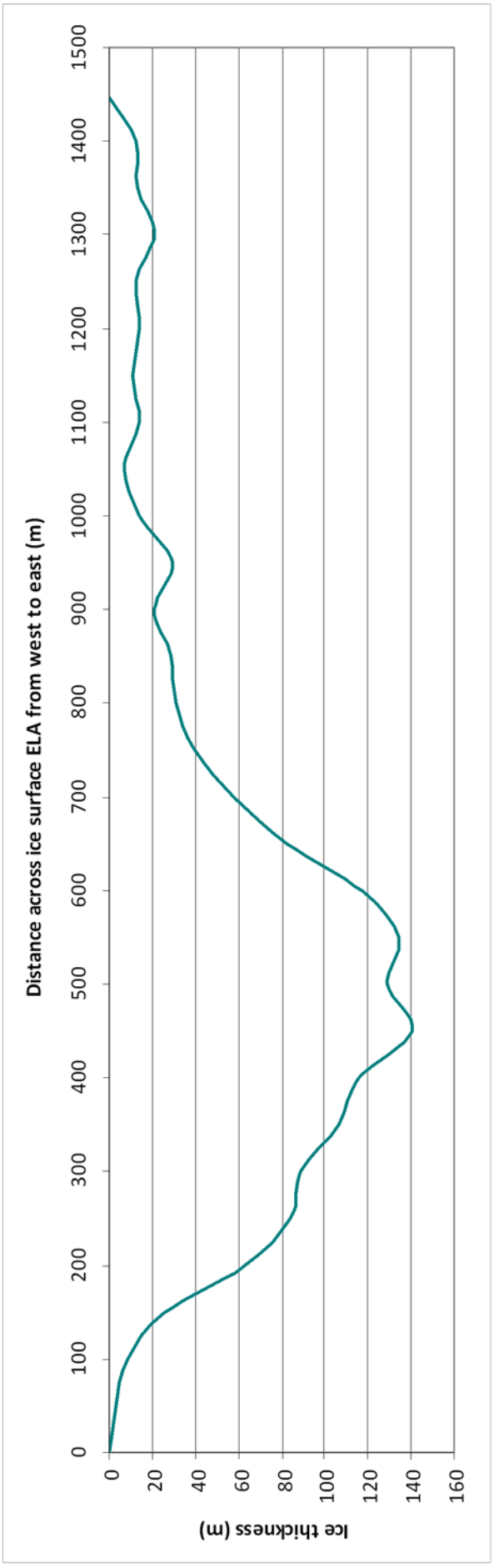


**Figure 5.25: A cross sectional profile west to east across the ELA of the Lingmell Beck glacier. ELA altitude = 530 m OD.**

Figure 5.26 below shows the distribution of the glacier's surface area over altitude. The largest surface between any of the contours lies between the 450 and 500 m contour and has an area of 0.609 $km^2$. This contrasts with the distribution of the surface area of the Mosedale glacier over altitude where the largest surface areas are found at higher altitudes within the accumulation area of the glacier. The reason for the large surface area near the altitude of the ELA is due to change in orientation of the valley topography. The distribution of the glacier's surface area over altitude is also illustrated in the hypsometric curve shown in figure 5.27 and the net balance profile in figure 5.28.

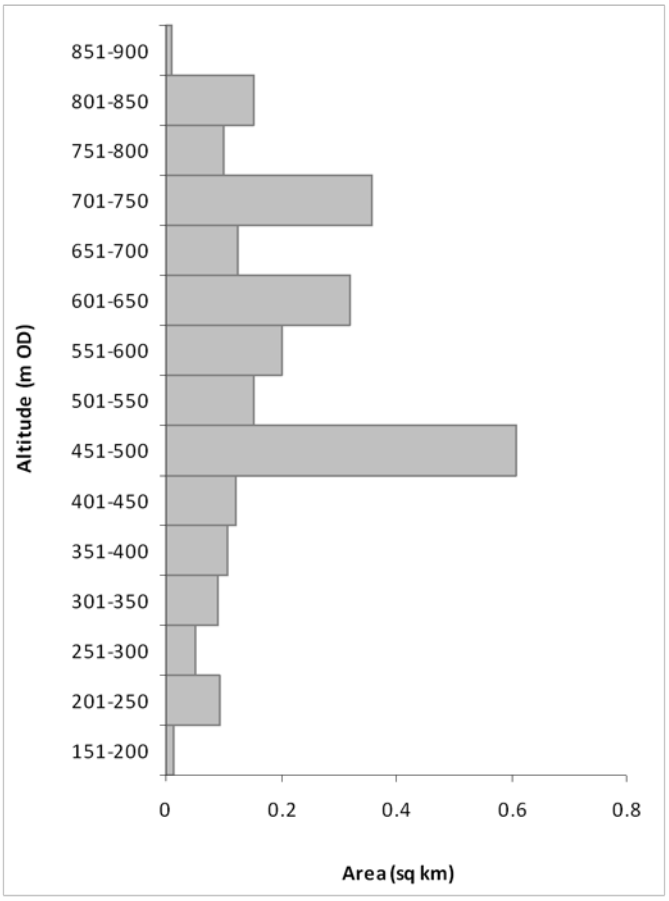


**Figure 5.26: The distribution of the glacier's surface area between the 50 m ice surface contour intervals. ELA = 530 m OD.**

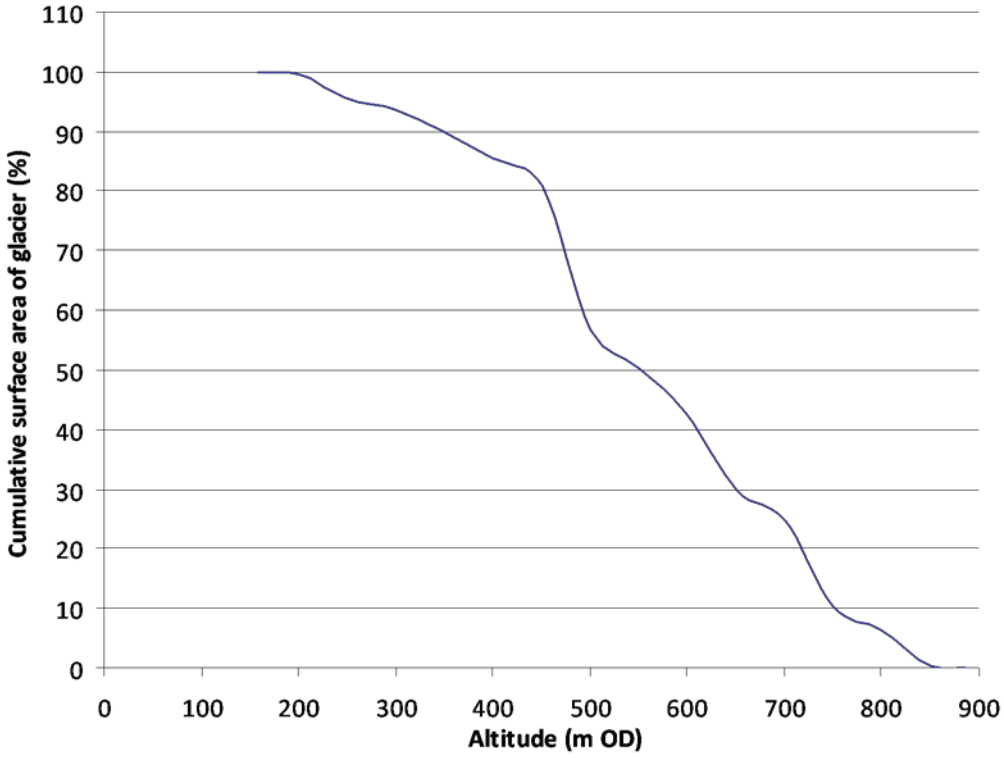


**Figure 5.27: Hypsometric curve for the Lingmell Beck glacier.**

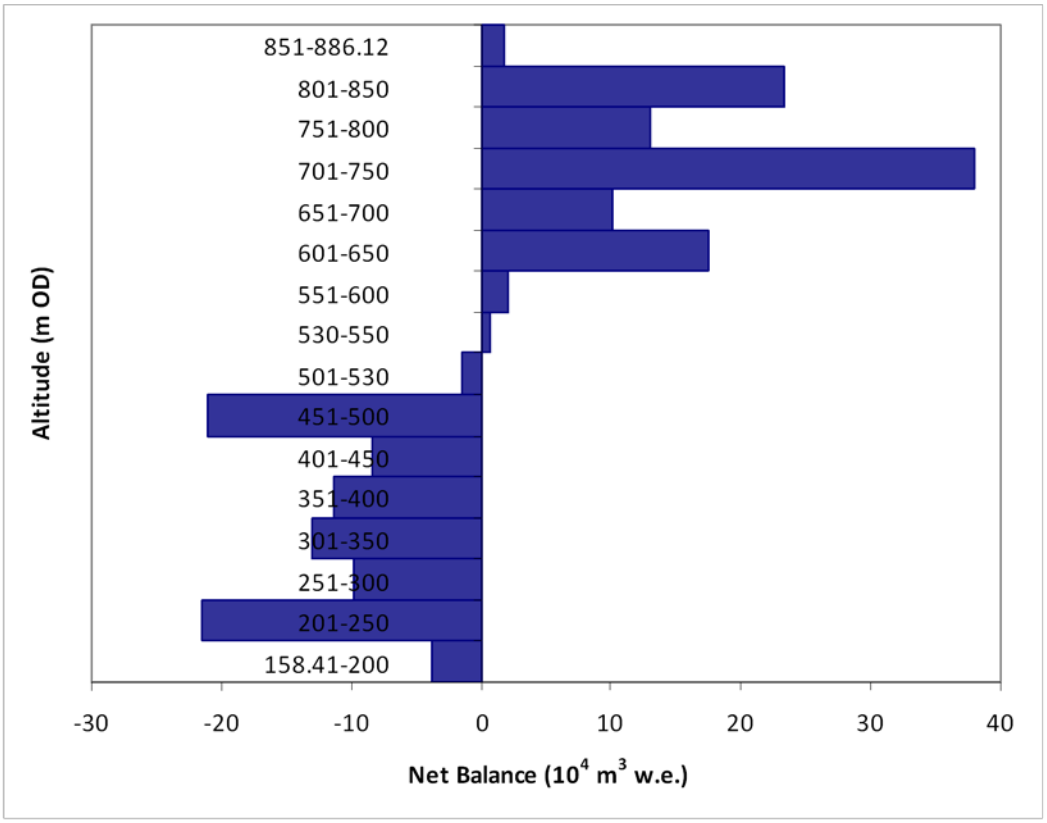


**Figure 5.28: The mass-balance profile of the Lingmell Beck glacier.**

## 5.3 Lingmell Gill

Lingmell Gill is located to the south of Lingmell Beck on the south side of Lingmell Crag. It is surrounded by Scafell Pike (978 m OD) to the west and Sca Fell (964 m OD) to the south. Steep crags are found along the southern edge of the valley facing north, and below Scafell Pike facing directly west. The valley is ~ 2.5 km long from the steep headwall to the point where it reaches the flat glaciolacustrine deposits at GR: 185074. The river of Lingmell Gill descends steeply from Lingmell Crag and Hollow Stones to form a confluence, below a large spur before eventually reaching Wastwater.

### 5.3.1 Geomorphology in the valley of Lingmell Gill

Although moraines are present throughout the whole length of the valley, moraines in the upper section of the valley are much more closely spaced. Moraines in the upper part of the valley also possess linearity in a variety of directions however they predominantly trend down valley rather than across valley. Moraines such as these which show variable orientations have been classified as 'hummocky' moraine in figure 5.29a. This classification reflects not only their orientations but also their subdued nature and apparent 'chaotic' arrangement when viewed from the ground.

Clear lateral moraines are visible on the south side of the valley below Lords Rake and Rakehead Crag. The lateral moraines follow the long axis of the valley and trend east to west before curving north towards the centre of the valley. In contrast the north side of the valley is virtually devoid of moraines and therefore provides little evidence as to the maximum extent of the Loch Lomond Stadial glacier in the valley. This can be explained by the large amount of fluvial incision that appear to have occurred post-glacially and thus destroyed any moraines that may have been present. The result of this incision is the large spur (crestline marked in light blue) which dominates the central upper section of the valley.

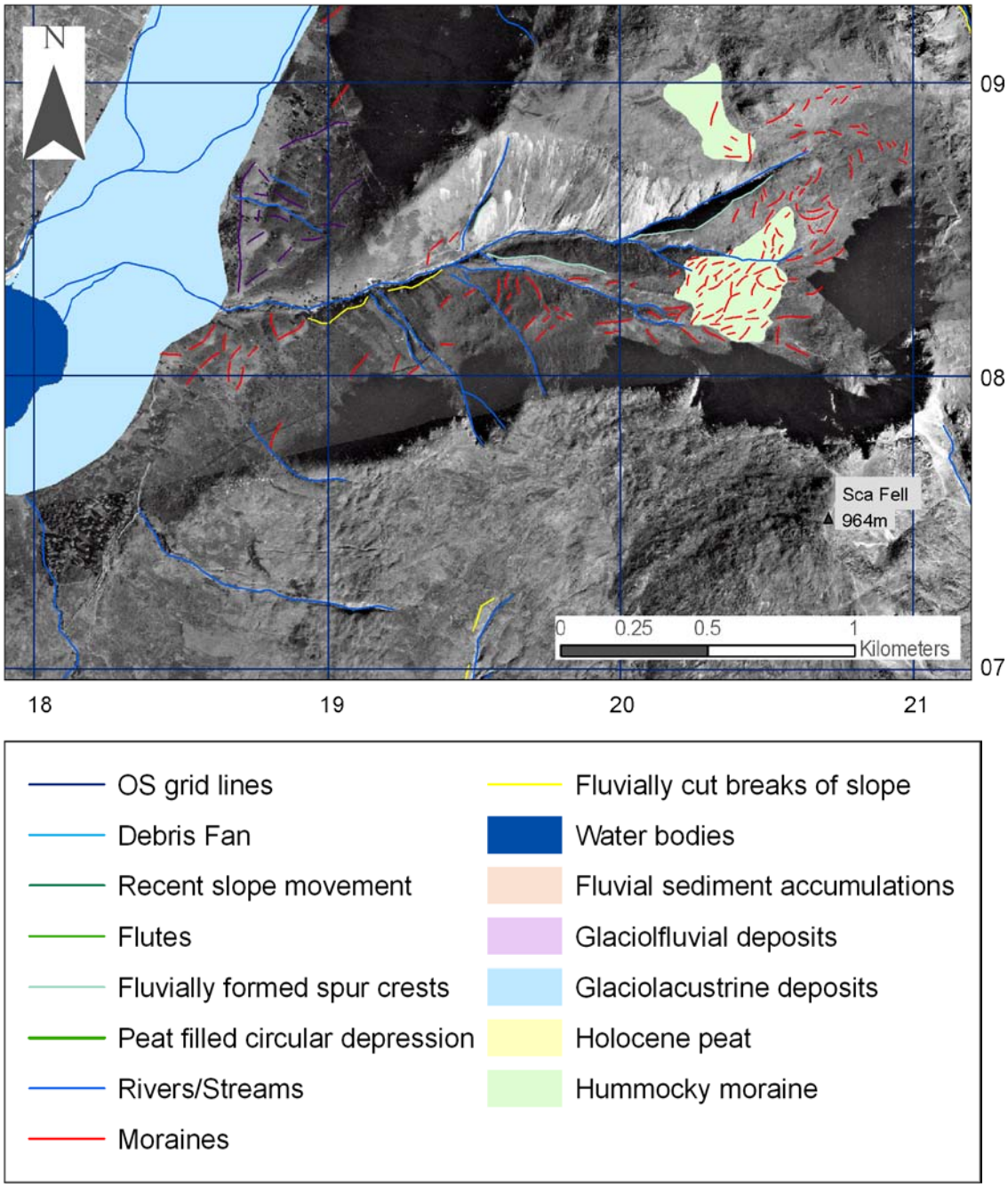


**Figure 5.29a: The geomorphology of Lingmell Gill.**

Moraines in the lower section of the valley show different morphological characteristics to those at higher elevations. The moraines shown in purple in figure 5.29b are much larger and sparser than those in the upper section of the valley and as a consequence these moraines are believed to represent glaciation during a different glacial episode to that represented by the moraines in the upper section of the valley. Sedimentological evidence in Mosedale and rock mass strength evidence in Lingmell Beck supports this assumption in nearby locations. Consequently, the similar morphological change seen in the moraines in Lingmell Gill is considered to represent the same phenomenon with the moraines in the upper section of the valley (shown in pink) formed during the Loch Lomond Stadial and those in the lower section

of the valley (shown in purple) formed during an earlier glacial phase, possibly the Scottish Readvance.

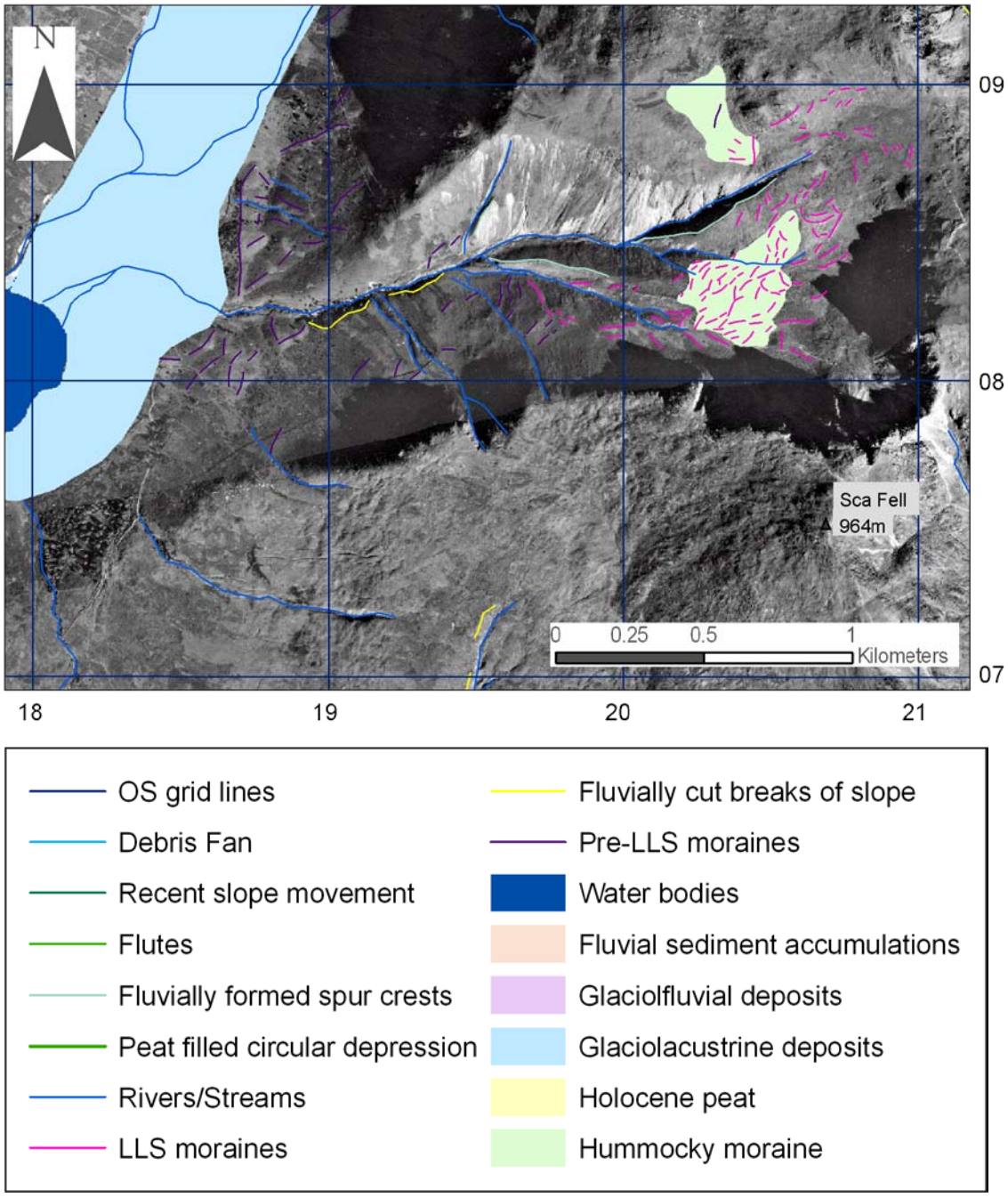


**Figure 5.29b: The geomorphology of the valley of Lingmell Gill including the distinction between Loch Lomond Stadial and pre-Loch Lomond Stadial moraines.**

### 5.3.2 Loch Lomond Stadial glacier reconstruction in Lingmell Beck

The maximum down-slope limit of the Loch Lomond Stadial glacier is therefore believed to have been located along the crest of the outermost pink moraine shown in figure 5.29. Based on the geomorphology shown in figure 5.29 the glacier was reconstructed and is shown below in figure 5.30.

The glacier shown in figure 5.30 had a surface area of 1.04 $km^2$ and occupied the grade 1 cirque of Hollow Stones near Scafell Crag. As with the Mosedale glacier, a broad accumulation area fed into a narrow ablation area as a result of the surrounding topography. The glacier reconstructed by Sissons (1980) in Lingmell Gill has a surface area of 0.30 $km^2$, 0.74 $km^2$ smaller than the reconstruction shown below. This increase in surface area is seen around the entire perimeter of the glacier reconstructed by Sissons (1980). The size increase means that the Lingmell Gill glacier was the 16th largest glacier in the Lake District during the Loch Lomond Stadial based on the size of the 64 glaciers reconstructed by Sissons (1980). This is an increase from the 43rd largest glacier based on the reconstruction provided by Sissons (1980) for the Lingmell Gill glacier. This area has not been mapped by any authors subsequent to Sissons (1980) including McDougall (1998).

Colalescent ice over Lingmell Coll may be assumed plausible give the local topography however, cosmic ray exposure dates from Lingmell Coll provided by Ballantyne (pers. comm.) indicate that the col was ice free during the Loch Lomond Stadial. Although these dates which are presented below are not conclusive, partially due to their wide error margins, they are consistent with the glacier reconstructions presented in the thesis for Lingmell Beck and Lingmell Gill which indicate that Lingmell Col was ice free during the Loch Lomond Stadial. All dated samples were obtained from lavas and were taken from the crests of outcrops or boulders in order to minimise the possibility of former sediment, peat or snow cover.

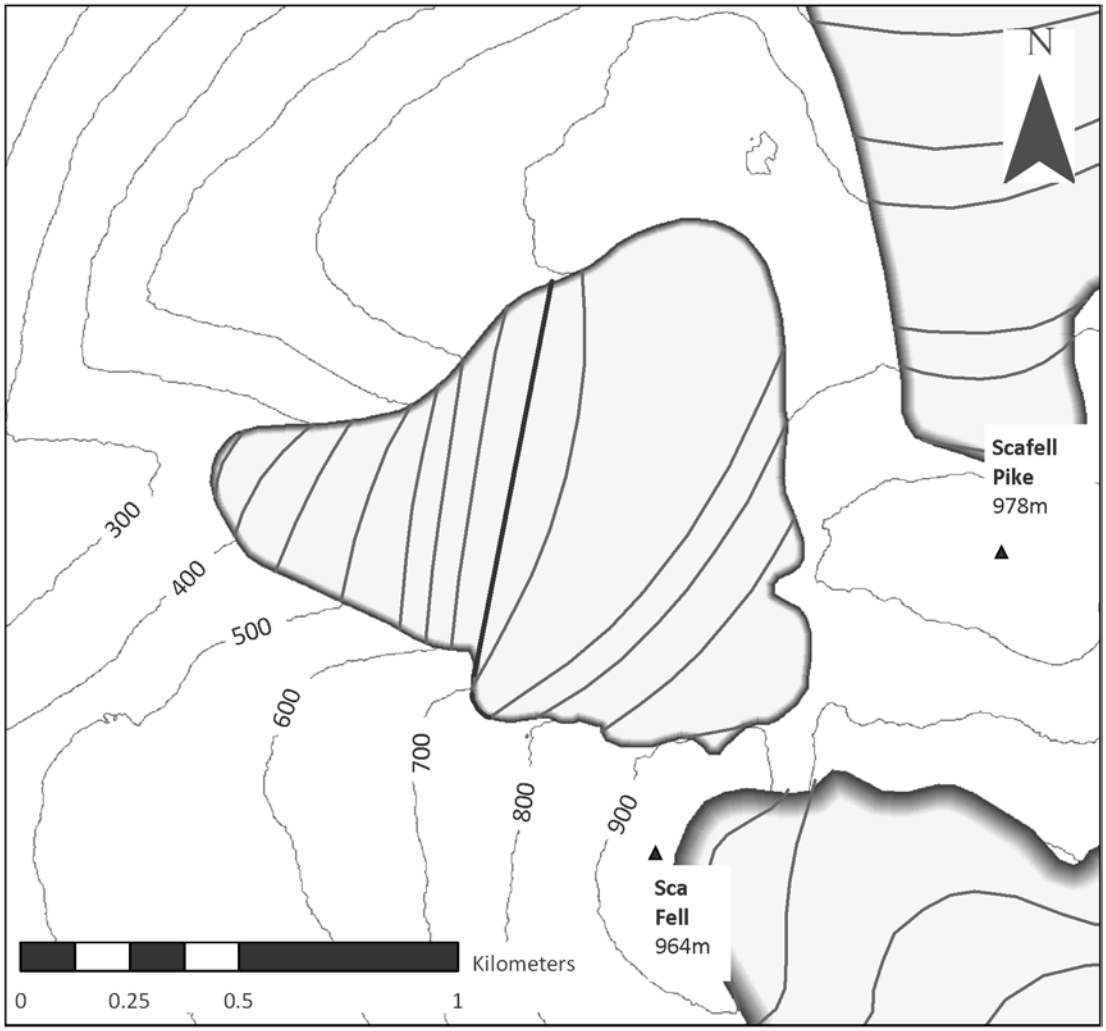


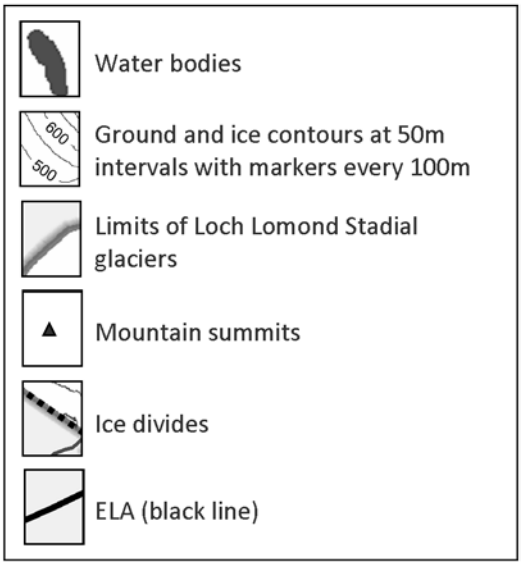


**Figure 5.30: A reconstruction of the glacier which occupied Lingmell Gill at the north end of Wastwater during the Loch Lomond Stadial.**

Widespread deglaciation of the Lake District occurred during the Windermere Interstadial of ~ 15.4-12.9 cal ka BP with the Wasdale trough being deglaciated ~ 20 ± 1.4 ka BP. Lamb and Ballantyne (1998) suggest that the summits of the Scafell range sat above the Late Devensian ice sheet at the Last Glacial Maximum as nunataks. These nunataks are also believed to have been located above the maximum altitude of the Loch Lomond Stadial cirque/valley glaciers in Lingmell Beck and Lingmell Gill. Exposure dates on the col between the glaciers in Lingmell Beck and Lingmell Gill of 13.2 ± 2 ka BP and 17.3 ± 1.1 ka BP are provided by Ballantyne (pers. comm.) (see locations 7 and 8 on figure 5.31 below). The samples from which these dates were obtained were collected from ice-abraded but pitted bedrock surfaces on Lingmell Col. The variation between these two dates can be explained by assuming that the site from which the younger age was obtained was covered with sediment until it was removed by erosion around 13.2 ± 2 ka BP. This suggestion is supported by a $^{14}C$ date from a lacustrine sequence at Blelham Bog 16 km south- east of Scafell Pike which indicates a rapid warming at the start of the Windermere Interstadial ~ 13.0 $^{14}C$ ka BP (~ 15.5 cal ka BP). Additionally, Brook and Birks (2000) indicate that a July temperature increase of 5.5°C occurred around 14.4 ka BP. It is therefore highly unlikely that ice persisted across the col until as late as 13.2 ± 2 ka BP in such conditions.

These dates therefore confirm that erosion by the Late Devensian ice sheet occurred up to an altitude of 765 m OD with the older of the two ages suggesting that Lingmell Col emerged from downwasting ice on the col between 18.4 and 16.2 ka BP (95 % confidence). This confirms that the col was not occupied by ice during the Loch Lomond Stadial. Furthermore, exposure dates within the limits of the Lingmell Gill glacier (locations 9 and 10 on figure 5.31 below) of 35.1 ± 2.3 ka BP and 12.5 ± 0.8 ka BP are provided by Ballantyne (pers. comm.). These dates were obtained from samples taken from the crests of large, angular boulders. The older of the two dates pre-dates the Last Glacial Maximum and is therefore invalid in the determination of the post-Last Glaciation Maximum ice occupation of the gill. The latter however is consistent with a Loch Lomond Stadial age for the last occupation of the gill by glacial ice. It is suggested therefore that the latter age indicates that the source rock was newly-exposed at the time of detachment and glacial transport. This evidence confirms that the glaciers in Lingmell Beck and Lingmell Gill remained independent of each other during the Loch Lomond Stadial and did not coalesce across Lingmell Col.

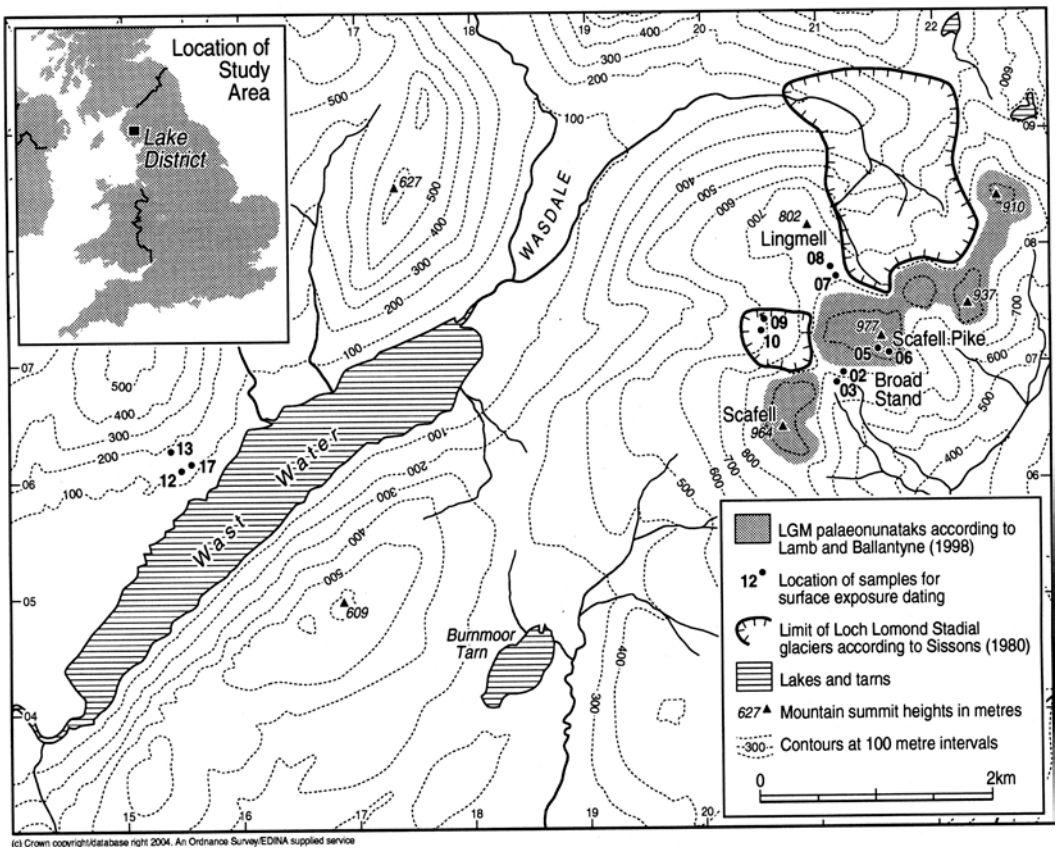


**Figure 5.31: The location of cosmic ray dating sites provided by Ballantyne (pers. comm.) for the south-west Lake District around the Scafell range.**

The ELA of the Lingmell Beck glacier was then calculated using the methods outlined in section 5.1.3 and the results of these calculations are shown below in table 5.7.

| | | Lingmell Gill |
|---|---|---|
| Area ($km^2$) | | 1.04 |
| Long axis length (m) | | 1393.39 |
| Max altitude (m OD) | | 943.72 |
| Min altitude (m OD) | | 338.99 |
| Mid-altitude (m OD) | | 641.00 |
| Lowest cirque | | |
| Name | | 131. Hollow Stones, Scafell Crag |
| Altitude (m OD) | | 580 |
| Grade (according to Evans and Cox, 1995) | | 1 |
| Altitude of highest lateral moraine (m OD) | | 491.01 |
| Toe to head altitude ratio method (THAR) (m OD) | | |
| | 35% | 550.65 |
| | 40% | 580.88 |
| | 45% | 611.12 |
| | 50% | 641.50 |
| Accumulation area ratio method (AAR) (m OD) | | |
| | 70% | 668.00 |
| | 65% | 692.00 |
| | 60% | 704.00 |
| | 55% | 710.00 |
| | 50% | 715.00 |
| Area weighted mean altitude method (AWMA) (m OD) | | 690.30 |
| Balance ratio method (Benn and Gemmell, 1997) (m OD) | | |
| | BR=2.00 | 593.59 |
| | BR=1.81 | 598.61 |
| | BR=1.60 | 604.65 |
| | BR=1.54 | 606.49 |
| | BR=1.43 | 610.02 |
| Balance ratio method (Osmaston, 2005) (m OD) | | |
| | BR=2.00 | 653 |
| | BR=1.81 | 659 |
| | BR=1.60 | 666 |
| | BR=1.54 | 668 |
| | BR=1.43 | 672 |
| **Mean value of all of the above methods (m OD)** | | **637.42** |
| **Mean value of BR=1.54 (Osmaston, 2005), AAR 65% and AWMA (m OD)** | | **662.93** |
| **ELA used in subsequent calculations (m OD)** | | **683** |

**Table 5.7: ELA calculations and dimensions of the glacier occupying Lingmell Gill during the Loch Lomond Stadial.**

The ELA of the proposed Lingmell Gill glacier is ~ 150 m higher than both the ELAs of the Mosedale and Lingmell Beck glaciers. This is a reflection of the higher altitudinal range over which this glacier is spread, for example, the minimum altitude of the Lingmell glacier is 389 m OD compared with 178 m OD for the Mosedale glacier and 158 m OD in Lingmell Beck. The minimum altitude of the glaciers can be related to the glacier aspect. The Lingmell Gill valley faces directly west and the occurrence of south to south-westerly winds during the Stadial makes this a relatively unfavourable aspect for glacier development. Furthermore, although

the highest ground in the Lake District lies to the east of the glacier, little shelter is provided by the surrounding topography to the south of the glacier. The result of this lack of shading is that the glacier was unable to extend to lower altitudes as this would have placed the glacier in negative mass balance where ablation is too great to maintain the glacier in steady-state conditions.

### 5.3.3 The influence of snowblow on glacier development/maintenance

It is possible for a glacier to be maintained in an unfavourable location e.g. on the windward side of a mountain range, by the input of snow from sources other than direct precipitation. One such source is snow which blows onto the accumulation area of a glacier from nearby unglaciated terrain. The areas surrounding the Lingmell Gill glacier with the potential to contribute mass to glacier through snowblow were identified using the criteria outlined in section 5.1.4 and are shown in figures 5.32 and 5.33 below.

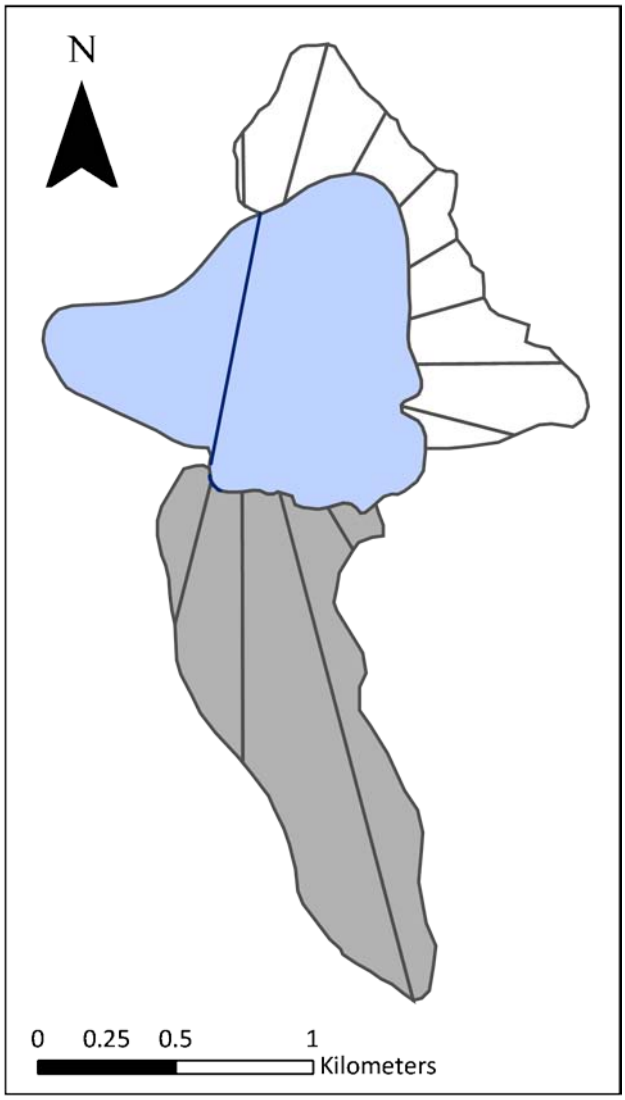


**Figure 5.32: The snowblow areas associated with the Lingmell Gill glacier. The ELA of the glacier has been calculated at 684 m OD and is marked with a dark blue line above. The snowblow sectors shaded in grey indicate the snowblow area lying within the southern sector (135-225°).**

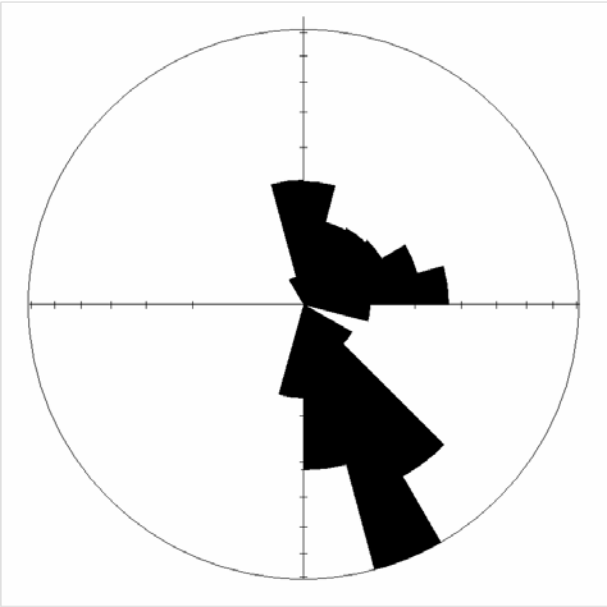

**Figure 5.33: Polar plot of snowblow area with area-weighted 15° sector lengths.**

The largest snowblow areas are found within the SE and S sectors. Crucially, the SW sector contains very little terrain with the potential for snowblow and may again be used to explain the high ELA of this glacier. Snowblow factors associated with these snowblow areas are shown below in table 5.8.

| Glacier name | Lingmell Gill |
|---|---|
| Glacier area ($km^2$) | 1.04 |
| Total snowblow area ($km^2$) | 1.55 |
| Snowblow area by 90° quadrants expressed as a percentage of the total snowblow area (%) | |
| NE (0-90°) | 27.31 |
| SE (91-180°) | 57.81 |
| SW (181-270°) | 14.55 |
| NW (271-360°) | 0.34 |
| S (135-225°) | 62.15 |
| W (226-315°) | 0 |
| Snowblow factor by 90° quadrants | |
| NE (0-90°) | 5.12 |
| SE (91-180°) | 7.46 |
| SW (181-270°) | 3.74 |
| NW (271-360°) | 0.57 |
| S (135-225°) | 7.73 |
| W (226-315°) | 0 |
| Mean snowblow factor | 4.10 |
| Ratio of snowblow area to glacier area | 1.49 |

**Table 5.8: Snowblow areas and snowblow factors identified around the Lingmell Gill glacier using the criteria outlined in the text.**

As with Mosedale and Lingmell Gill the largest snowblow factors are associated with the southern quadrant indicating that this quadrant had the greatest potential to contribute mass to the glacier through snowblow. This is interesting given the prevailing wind direction during the Stadial, and may suggest that snowblow played a crucial role in the maintenance of the Mosedale, Lingmell Beck and possibly Lingmell Gill glaciers presented in this chapter during the Loch Lomond Stadial.

The ratio of the snowblow area to glacier area should also be noted. Of the three glaciers in this chapter Lingmell Gill has the highest snowblow to glacier area ratio of 1.49. Mosedale then follows with a slightly lower ratio of 1.24; however, a substantially lower ratio of 0.37 was calculated for the Lingmell Beck glacier. This suggests that snowblow may have been a less

significant contributor of mass to the Lingmell Beck glacier than to the glaciers in Mosedale or Lingmell Gill.

### 5.3.4 Glacier dynamics in Lingmell Gill

The required basal motion for the Lingmell Gill glacier was calculated as 0 % thus implying that the glacier moved purely by internal ice deformation rather than basal motion (basal sliding or subglacial deformation). Despite this the glacier has been proven to be viable using the model outlined in section 5.1.4. Further results of this model are shown below in table 5.10 along with a cross sectional profile along the long axis of the glacier in figure 5.34.

The proposed Lingmell Gill glacier maintained a stable ice thickness throughout with just a small amount of thinning towards the snout. The bed of the glacier is smooth when compared with that of Lingmell Beck showing no evidence of rock steps or protruding bedrock. This can be compared to the cross sectional profile of the ELA shown in figure 5.35 below. Again the glacier bed across the ELA appears relative smooth forming a clear 'U' shape with just one significant step slightly north of the centre point of the ELA. A maximum ice thickness of 123 m is attained at the ELA, slightly south of the centre point of the ELA. This is very similar to the maximum ice thickness in Mosedale of 120 m, and just slightly less than that of the Lingmell Beck glacier (139 m). The result of this ice thickness is a basal shear stress (BSS) of 1.67 bars. This BSS is lower than that calculated in Mosedale (2.06 bars) where the ice surface slope is higher than Lingmell Gill and substantially higher than that of Lingmell Beck (0.89 bars), reflecting the lower ice surface slope (table 5.9 below).

| | Lingmell Gill |
|---|---|
| ELA (m) | 683.00 |
| Temperature proxy used | Coope and Joachim (1980) St Bees Head |
| Proxy site altitude (m OD) | 0.00 |
| $T_3$ at proxy site (°C) | 8.25 |
| Temp. at ELA (0.0065°C/m lapse rate) | 3.81 |
| Degrees surface slope at ELA | 19.62 |
| Max ice thickness at ELA (m) | 123.22 |
| Glacier shape factor | 0.63 |
| Normal stress at centre point of ELA (bars) | 10.72 |
| Ablation gradient at ELA (mm/m) | 5.08 |
| Mass loss at ELA (ma-1) | 1.90 |
| Net Ablation ($m^3$ w.e.) | 268,676.90 |
| Mass flux ($m^3$ ice) | 295,249.34 |
| Cross sectional area at ELA ($m^2$) | 75,472.62 |
| Perimeter of bed at ELA (m) | 996.92 |
| Mean balance velocity at ELA ($ma^{-1}$) | 3.56 |
| Basal shear stress at ELA (bars) | 1.67 |
| Max ice deformation velocity at ELA ($ma^{-1}$) | 34.98 |
| Average ice deformation velocity at ELA ($ma^{-1}$) | 19.57 |
| Required basal motion ($ma^{-1}$) | 0.00 |
| Required basal motion (%) | 0.00 |

**Table 5.9: Reconstructed steady-state dynamics and flow characteristics of the glacier occupying Lingmell Gill during the Loch Lomond Stadial.**

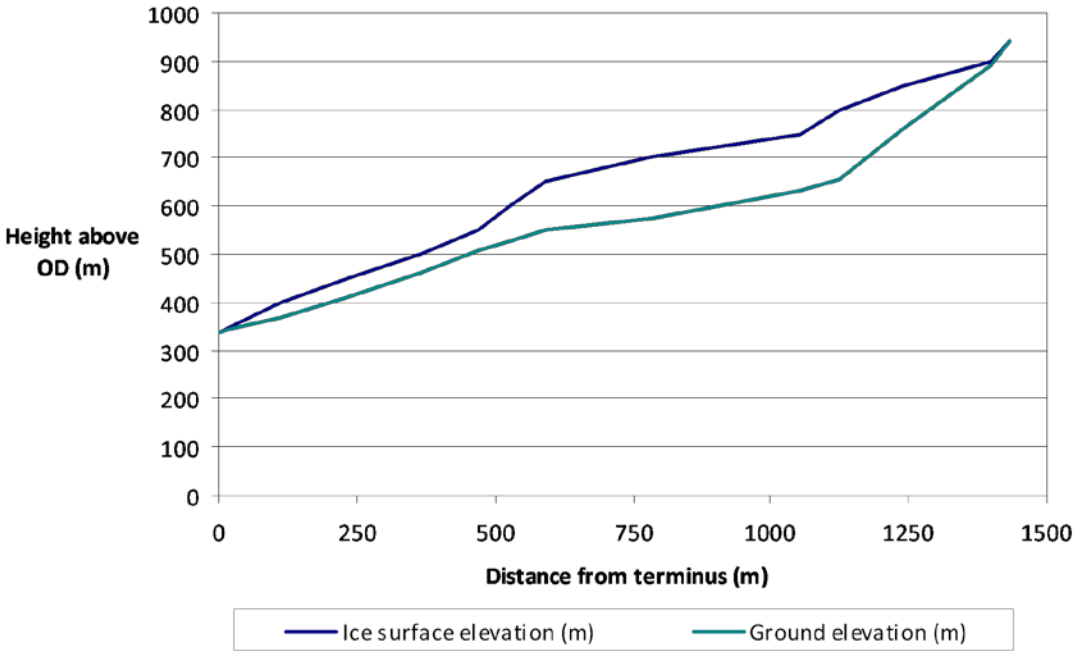


**Figure 5.34: A cross sectional profile along the long axis of the Lingmell Gill glacier.**

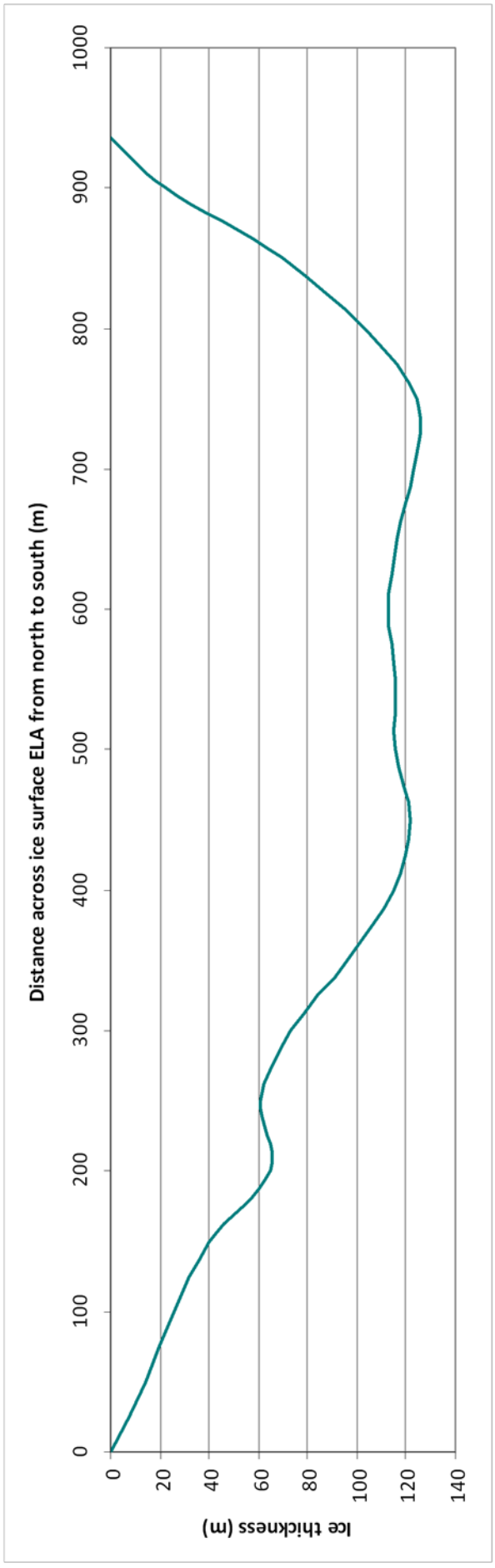


**Figure 5.35: A cross sectional profile north to south across the ELA of the Lingmell Gill glacier. ELA altitude = 683 m OD.**

The distribution of the glacier's surface area over altitude is shown below in figures 5.36 and 5.37 with the largest surface area of 0.39 $km^2$ found between 700 and 750 m OD. This is a reflection of the wide accumulation area of the glacier in this region. Furthermore, the reconstructed net accumulation/ablation values across the glacier are shown in figure 5.38 below and once again indicate balanced accumulation and ablation for the Lingmell Gill glacier when under steady-state conditions.

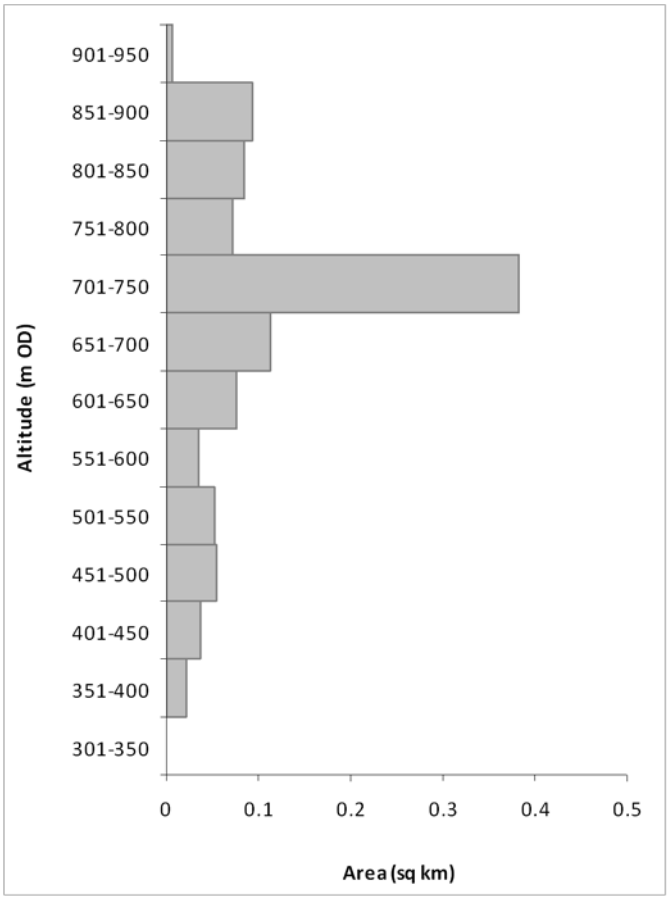


**Figure 5.36: The distribution of the glacier's surface area between the 50 m ice surface contour intervals. ELA = 683 m OD.**

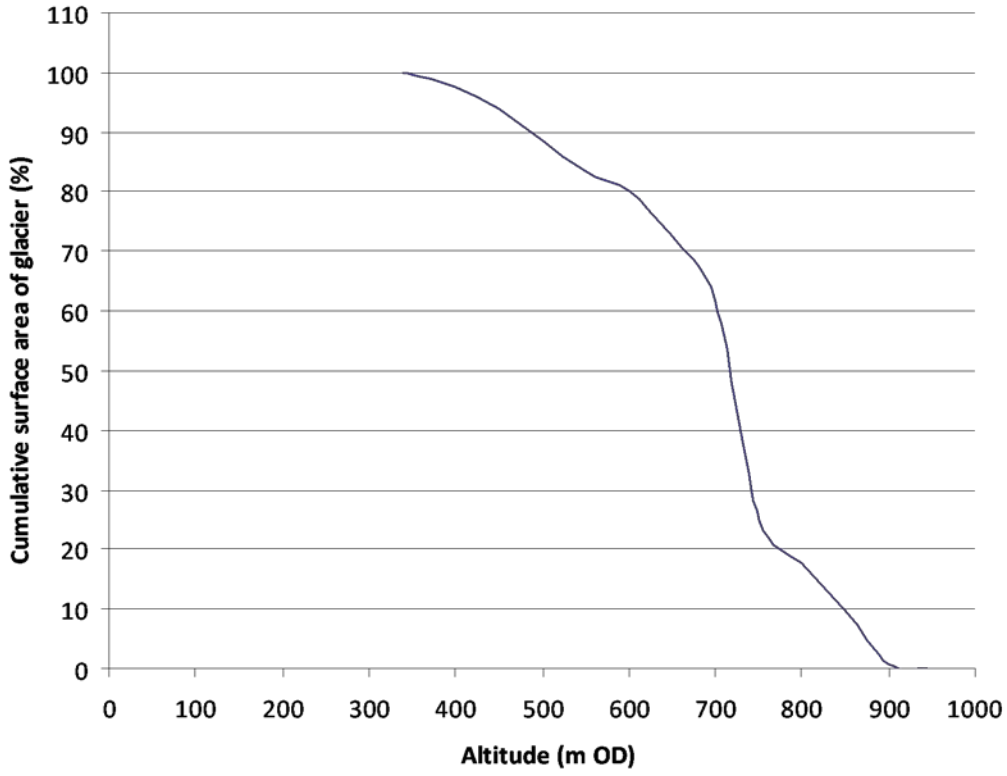


**Figure 5.37: Hypsometric curve for the Lingmell Gill glacier.**

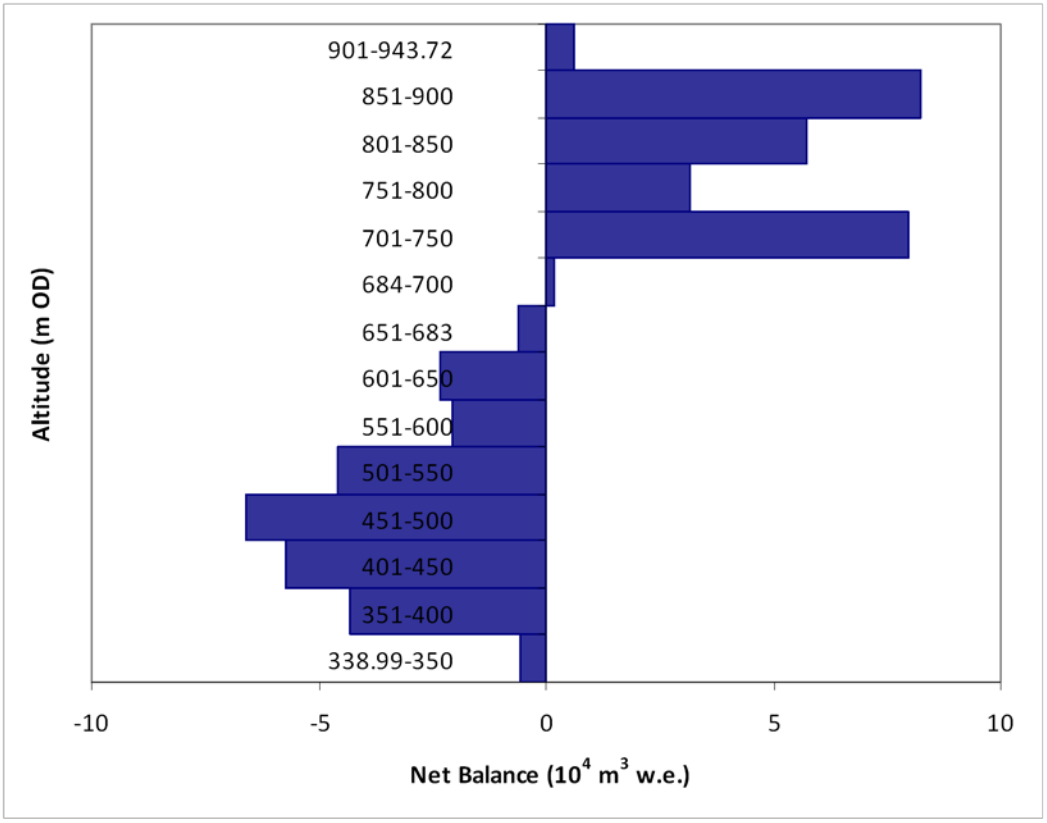


**Figure 5.38: The mass-balance profile of the Lingmell Gill glacier.**

## 5.4 Summary

- The geomorphology mapped has been used to identify the limits of LLS ice masses in Mosedale, Lingmell Beck and Lingmell Gill.
- The ELAs of the reconstructed ice masses have been used in the identification of potential snowblow areas and subsequent calculation of snowblow factors.
- The 2D mass balance model adapted from Carr and Coleman (2007) indicates that the reconstructed ice masses are glaciologically viable requiring 0%, 21.83% and 0% basal motion respectively.

## Chapter 6

# UPPER ESKDALE, RED TARN/WRYNOSE BOTTOM AND WIDDYGILL FOOT

# 6: UPPER ESKDALE, RED TARN AND WIDDYGILL FOOT

## 6.1 Upper Eskdale

Upper Eskdale is a large south facing valley in the south-west Lake District and at ~ 8 km long, is the largest valley to be considered in this study. The valley lies to the east of the Scafell massif and is surrounded by Scafell Pike (978 m OD), Great End (910 m OD) to the west and Bow Fell (902 m OD) and Crinkle Crags to the east. The upper section of the valley supports two rivers; the River Esk which drains the Scafell massif and Lingcove Beck which drains Bow Fell and Crinkle Crags to the east. These two rivers meet below Throstle Garth and continue flowing south-west as the River Esk.

### 6.1.1 Geomorphology in the valley of Upper Eskdale

Moraines are present throughout the entire length of Upper Eskdale from just below Esk Pike at the northern end of the valley to Dalegarth Station at the southern end of the valley and beyond. At the northern end of the valley two areas of thick drift have accumulated between the confluence of the streams. Fluvial incision has resulted in steepened riverside slopes however despite this prominent crest lines are present running principally north to south along the valley sides. This trend is continued further south where moraines with clear crest lines run parallel to the River Esk along the eastern edge of an area of more subdued moraine shown in green in figure 6.1a below. To the west of the River Esk, extensive talus covered slopes grade into a much flatter area of subdued 'hummocky' moraine and the peat bog of Great Moss. Moraines are more sparse to the west of the river with just a limited number of boulder covered moraines which, again, grade into the flat valley bottom. At the southern end of Great Moss linearity orientation in the moraines becomes more chaotic and hence the label 'hummocky' moraine. Moraines in this area lie on the northern side of a northward dipping slope where drift cover is believed to be locally variable based on the presence of several bedrock exposures. Drift also thins against the rising ground and consequently the southern ends of some of these moraines are poorly defined. To the south-west of Great Moss (GR: 218049), an area of moraines with a north-west to south-east orientation is found. These moraines, which were not mapped by Wilson (2004), possess distinct crest lines which can be seen from Great Moss and sharp basal breaks of slope. It is suggested that these moraines once marked the lateral margin of a glacier occupying Upper Eskdale.

**Figure 6.1a: The geomorphology of Upper Eskdale.**

**OVERSIZE FIGURE APPEARS AT END OF THESIS**

A small number of flutes are seen interspersed between these moraines and are suggested to represent the active removal of ice from the area following the Loch Lomond Stadial. The lateral margin of the ice on the eastern side of the valley is also marked by moraines which show considerable linearity in an east to west orientation in the vicinity of GR: 236040. An area of 'hummocky' moraine has also been identified in this area in order to acknowledge the presence of the randomly orientated moraines and moraine mounds with little or no linearity which cannot be satisfactorily shown using crestlines. As with the moraines along the River Esk below Scafell Pike, suites of moraines in Lingcove Beck also show linearity parallel to the stream and down-valley oblique to the valley's long axis.

South of the confluence of Lingcove Beck and the River Esk, no lateral moraines are seen. Heavily talus covered slopes fed by steep overlooking cliffs instead cover the slopes of the lower valley. At GR: 221028 however lateral moraines are once again present. To the south of this moraine a group of more arcuate moraines trending obliquely down-valley is present. Unlike the moraines further north, these moraines are largely devoid of surface boulders and display much sharper basal breaks of slope. Moraines in this area do not form complete across-valley ridges. It is suggested that this is the result of high post-glacial discharges in the River Esk which have cut through the moraines. Evidence for this is clear, firstly, a number of river terraces are found in the area which when correlated across the valley indicate that the river may have been significantly wider than at present. Secondly, coring amongst the moraines at the southern end of Upper Eskdale indicates that the current farmland is underlain by a substantial layer of gravel assumed to be of fluvial origin (figure 6.1).

Beyond the arcuate moraines in the vicinity of grid square (GS) 2102, moraine morphology becomes much more subdued with basal breaks of slope becoming much more gradual. Moraines are also seen to grade into the nearby hillside and are once again heavily boulder covered. A clear morphological change is therefore seen between the moraines in GS 2102 and those further to the south. It is therefore concluded that the two suites of moraines were formed under different environmental conditions. Wilson (2004) suggests that the moraines in GS 2102 and those further north are likely to have been formed during the Loch Lomond Stadial or during the latter stages of the Dimlington Stadial with the moraines further south being older.

Manley (1959) was the first to recognise that moraines were present in Upper Eskdale. Manley (1959) suggests that two independent ice masses were present in Upper Eskdale, one below Scafell Pike in Great Moss and the other slight smaller ice mass in Lingcove Beck below

Bow Fell. The ice mass in Great Moss was therefore believed to have been the second largest ice mass in the Lake District during the Loch Lomond Stadial and had an ELA of between 580 and 610 m OD (Manley, 1959). Neither Sissons (1980a) nor Pennington (1978) however included the south facing valley of Eskdale as a site that nourished a Loch Lomond Stadial glacier. It is important to note that the south facing aspect of this valley and the consequent unfavourable conditions that the valley is likely to have experienced during the Loch Lomond Stadial may be the reason why no further study of the valley was published until the work of Wilson (2004). Until recently therefore, it was believed that the debris accumulations found at the southern end of upper Eskdale were the products of pronival snowbed processes. Wilson (2004) however is able to rule this out by noting the presence of bedrock exposures on the west side of the river Esk. In the absence of absolute dates on the majority of moraines within the Lake District much of the work done in the region remains speculative and consequently the use modern dating techniques such as cosmogenic radionuclide dating is imperative. Wilson (2004) states that if dates were available to unquestionably link the moraines in Eskdale to the Loch Lomond Stadial then the glacier there would have been 6.7 km along its longest axis. Since five cirques have been identified on the eastern side of the Scafell massif by Evans and Cox (1995), two of which have the highest altitudes of any in the Lake District 'it is extremely unlikely that these remained empty during the Loch Lomond Stadial given their favourable aspects and proximity to the highest and wettest ground in the region' (Wilson, 2004, p. 59).

As a result of time constraints, it was not possible to obtain absolute dates on the moraines at the southern end of Upper Eskdale. Instead the model outlined in chapter 4 was applied to the reconstructed glacier that occupied Upper Eskdale to test its viability. In order to provide a reconstruction on which to base the model, the moraines in GS 2102 were assumed to be of Loch Lomond Stadial age. Figure 6.1b below indicates the respective glacial episodes to which the moraines are suggested to belong.

The nearby valley of Moasdale joins to the eastern side of the valley of Upper Eskdale across a saddle area. The moraines in this valley are shown in figure 6.1b below and show linearity at ~ 45° to the long axis of the valley. At the southern end of Moasdale a cluster of moraines is found with moraines showing linearity in varying directions. Throughout the valley the moraines appear relatively subdued with shallow basal breaks of slope as a result of post-glacial sediment accumulation. Similarly the crest lines of the moraines are much more rounded than those in nearby Upper Eskdale. The moraines in Moasdale are also much shorter and linear than those in Upper Eskdale.

The configuration of the Upper Eskdale glacier shown in figure 6.3 may suggest that meltwater would need to flow down Moasdale. There are two problems with this assumption. Firstly, the meltwater would need to flow slightly uphill in order to breach the saddle between Lingcove Beck and Moasdale and, secondly, there is no evidence of meltwater flow in Moasdale i.e. meltwater channels. If the first of these problems is assumed to have been overcome i.e. the ice margin was slightly higher up the saddle on the Lingcove Beck side or the saddle was slightly lower during the LLS as a result of Holocene peat accumulation, then the latter can be overcome by simply assuming that meltwater produced at this margin occupied the present day bedrock channel when flowing down Moasdale. As a consequence meltwater channels would not have formed in Moasdale.

In Upper Eskdale, south of Bow Fell, to the east of Lingcove Beck, moraines also run parallel to the long axis of the valley. They are therefore interpreted as lateral moraines formed at the eastern margin of the Loch Lomond Stadial glacier in Upper Eskdale. Given then these moraines mark the maximum extent of the Loch Lomond Stadial glacier, then the moraines in Moasdale must orginate from a pre-Loch Lomond Stadial glacial phase. The possibility of Moasdale supporting an independent ice mass during the Loch Lomond Stadial is also ruled out. There are two lines of evidence to support this. Firstly, the plan of the moraines at the southern end of the Moasdale valley, or indeed further north, does not indicate the present of a glacier terminus with across valley arcuate ridges. In order for a glacier in the valley to be a similar magnitude to those in the nearby valleys, a terminus within the valley or around its southern margin would be expected. Furthermore, the shallow topography at the upper end of Moasdale means that the valley does not have a suitable area for initial accumulation and glacier development. This is compounded by the southerly aspect of the valley.

**Figure 6.1b: The geomorphology of Upper Eskdale indicating the glacial episode during which moraine formation occurred.**

**OVERSIZE FIGURE APPEARS AT END OF THESIS**

### 6.1.2 Sedimentological evidence in Upper Eskdale

Coring in Great Moss at the northern end of Upper Eskdale reached a depth of 2.5 m. The location of the coring site is indicated on figures 6.1a and b. As shown in figure 6.2 below, the core collected contained peat to a depth of 2.4 m with the lower section found to contain 38 % sand and be classified as a very fine sand (20.4 %).

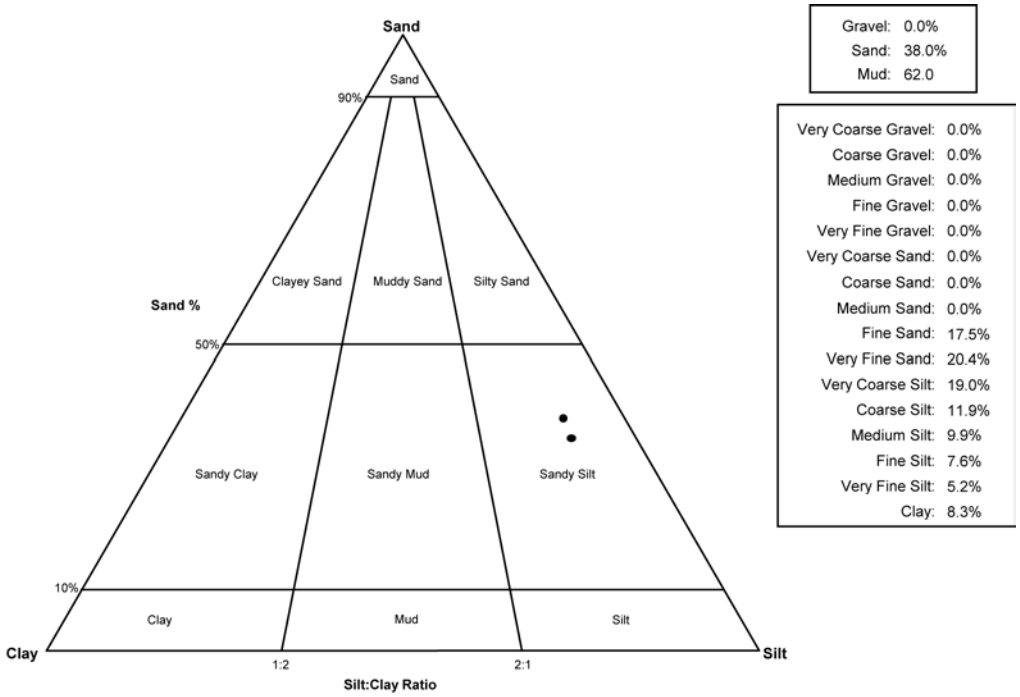


**Figure 6.2: Particle size analysis using a laser granulometer classifies 20.4 % of the samples taken from the base of the Great Moss core as a very fine sand.**

Based on particle size analysis, this sample can therefore be related to the base of unit 1 of the core obtained from Mosedale (see figure 6.3) which contains 23.7 % sand and is classified as a very coarse silt. Although this conclusion is tentative, it is unlikely that the sediment at the base of the Great Moss core correlates with any of the lower units in the Mosedale core (units 2 to 5). This is because the clay content of the core increases with depth and therefore increasing beyond the clay content of the sediment found in Great Moss. The sediment found at the base of the Great Moss core therefore probably accumulated during the early Holocene. Unfortunately it is not possible to establish whether a glacier did or did not occupy Great Moss during the Loch Lomond Stadial based on this evidence. Negative evidence, such as this, however, is taken to support the suggestion that Great Moss, and thus the rest of Upper Eskdale, was occupied during the Loch Lomond Stadial by a valley glacier. It should be noted that in terms of depth, the base of the Great Moss core at 2.5 m lies above the top of the Mosedale core. If the rate of peat formation in both valleys has been similar, the base of the Great Moss core is considered to represent only Holocene sedimentation with the base of the

core not extending further back in time than ~ 10ka BP. This may also indicate that peat in Great Moss has had a lesser amount of time to accumulate, thus supporting the suggestion that the valley was occupied by glacier ice during the Loch Lomond Stadial. In order to be more conclusive, absolute dates (e.g. $^{14}C$) and/or the use of more substantial coring equipment which could reach greater depths in the bog are needed.

### 6.1.3 Loch Lomond Stadial glacier reconstruction in Upper Eskdale

The glacier believed to have occupied Upper Eskdale during the Loch Lomond Stadial is shown below in figure 6.3. The proposed glacier has a surface area of 13.05 $km^2$ and is therefore significantly larger than any of the glaciers reconstructed by Sissons (1980) for the same period. The largest glacier reconstructed by Sissons (1980) is the Langstrath glacier which had a surface are of 5.36 $km^2$: less than half the size of the proposed Upper Eskdale glacier. In contrast, the plateau icefield reconstruction provided by McDougall (1998) covered an area of 79.79 $km^2$ including 55 $km^2$ of that forming the plateau icefield system around High Raise. A further 7 $km^2$, 3 $km^2$ and 1 $km^2$ then formed the plateau icefields on Grey Knotts/Brandreth, Dale Head and Kirk Fell respectively. A simple comparison of these areas suggests that should the occupation of Upper Eskdale by the glacier shown in figure 6.3 be proven it is likely that it coexisted alongside a regional glaciation of a magnitude closer to that of McDougall (1998) rather than that of Sissons (1980).

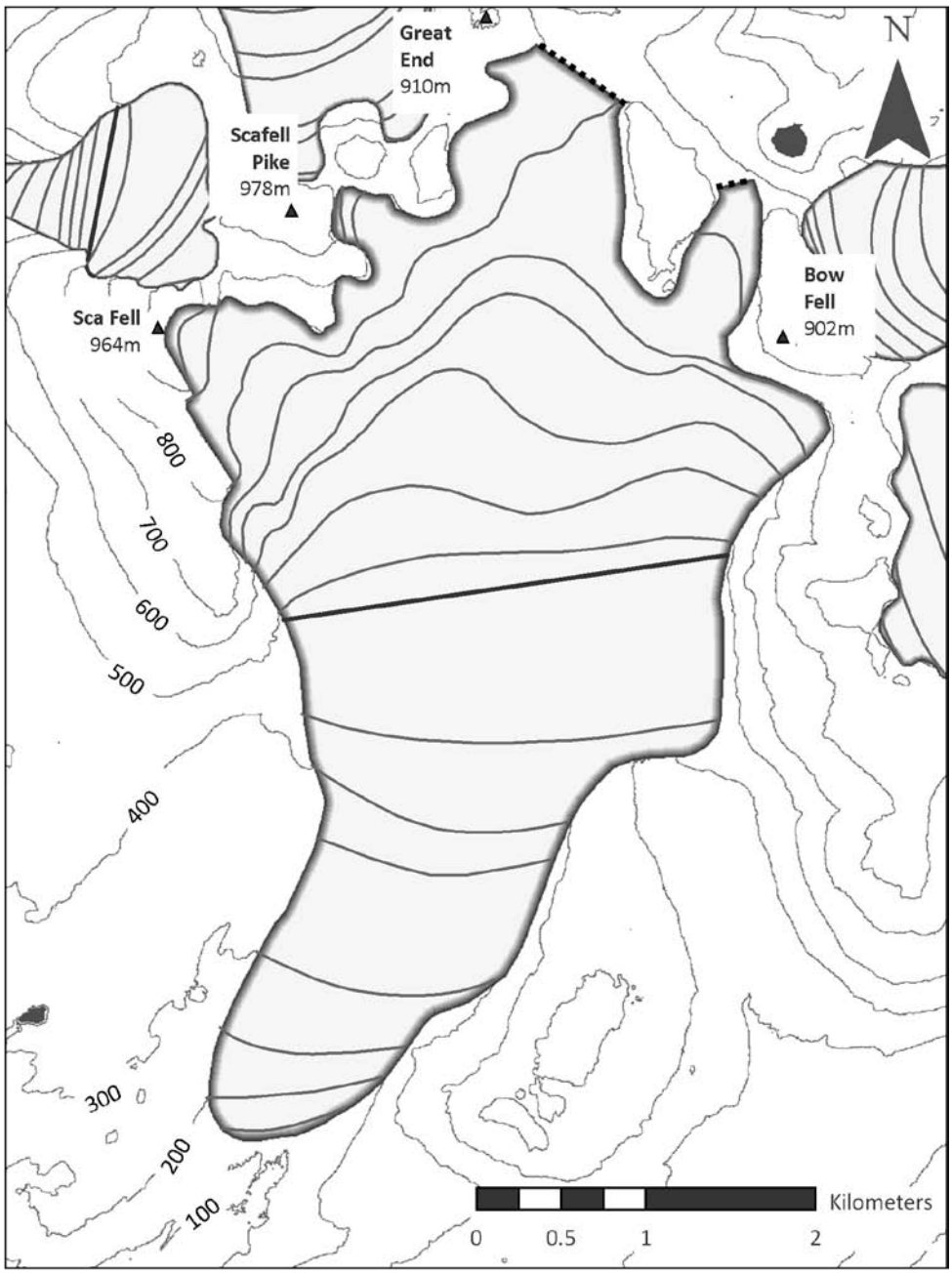


**Figure 6.3: A reconstruction of the glacier which occupied Upper Eskdale in the south-west Lake District during the Loch Lomond Stadial.**

The above reconstruction includes the occupation of five glacial cirques on the eastern side of the Scafell massif: Tom Fox's Crag, Slight Side (grade 3), Grencove Wyke, Scafell (grade 4), Foxes Tarn, Scafell (grade 4), How Beck, Scafell (grade 3) and Little Narrowcove, Scafell (grade 3). As noted by Wilson (2004) it is unlikely that these cirques, which lie on the highest ground in the Lake District, remained unoccupied during the Loch Lomond Stadial. Evans (pers. com.) notes that ice flowing out of these cirques into the floor of Eskdale, throughout much of the Loch Lomond Stadial, would explain the absence of terminal moraines in How Beck and Greencove Wyke.

It is also suggested that ice in Upper Eskdale coalesced with that in Langstrath and Grains Gill with ice divides situated over the saddle areas between Bow Fell and Esk Pike, and, Esk Pike and Great End. The terminus of the Upper Eskdale glacier shown above is situated alongside the moraines considered by Wilson (2004) and believed here to have been produced during the Loch Lomond Stadial. The ELA of the glacier shown in figure 6.3 was calculated using the methods outlined in chapter 3. An ELA of 484 m was calculated for the Upper Eskdale glacier (see table 6.1). This is the lowest ELA of the four glaciers considered thus far by a margin of over 50 m. This is a reflection of the high altitude attained in the accumulation area and the consequent low altitude of the terminus when compared to glaciers such as Mosedale or Lingmell Gill.

| | | Upper Eskdale |
|---|---|---|
| Area ($km^2$) | | 13.05 |
| Long axis length (m) | | 6611.44 |
| Max altitude (m OD) | | 948.53 |
| Min altitude (m OD) | | 113.29 |
| Mid-altitude (m OD) | | 531.00 |
| Lowest cirque | | |
| Name | | 129. How Beck, Sca Fell |
| Altitude (m OD) | | 540 |
| Grade (according to Evans and Cox, 1995) | | 3 |
| Altitude of highest lateral moraine (m OD) | | 723.97 |
| Toe to head altitude ratio method (THAR) (m OD) | | |
| | 35% | 405.62 |
| | 40% | 447.39 |
| | 45% | 489.15 |
| | 50% | 531.00 |
| Accumulation area ratio method (AAR) (m OD) | | |
| | 70% | 452.00 |
| | 65% | 469.00 |
| | 60% | 480.00 |
| | 55% | 497.00 |
| | 50% | 525.00 |
| Area weighted mean altitude method (AWMA) (m OD) | | 537.20 |
| Balance ratio method (Benn and Gemmell, 1997) (m OD) | | |
| | BR=2.00 | 459.58 |
| | BR=1.81 | 465.83 |
| | BR=1.60 | 473.72 |
| | BR=1.54 | 476.20 |
| | BR=1.43 | 481.06 |
| Balance ratio method (Osmaston, 2005) (m OD) | | |
| | BR=2.00 | 491 |
| | BR=1.81 | 497 |
| | BR=1.60 | 505 |
| | BR=1.54 | 508 |
| | BR=1.43 | 513 |
| **Mean value of all of the above methods (m OD)** | | **496.56** |
| **Mean value of BR=1.54 (Benn and Gemmell, 1997), AAR 65% and AWMA (m OD)** | | **494.13** |
| **ELA used in subsequent calculations (m OD)** | | **494** |

**Table 6.1: ELA calculations and dimensions of the glacier occupying Upper Eskdale during the Loch Lomond Stadial.**

### 6.1.4 The influence of snowblow on glacier development/maintenance

The long axis of the Upper Eskdale valley lies at ~ 198°, meaning that the valley faces almost directly south. This would have been a highly unfavourable aspect for glacier development during the Loch Lomond Stadial due to the proposed occurrence of south to south-westerly winds (Sissons, 1980) which cause the site to face a windward direction. The result of this will have been an increase in air turbulence across the glacier surface which will have increased the heat transfer from snow to the air and thus increased ablation when the temperature > 0°.

Accumulation may also have been inhibited in Upper Eskdale due to the unsheltered location. The angle of precipitation input may however have favoured glacier development in Upper Eskdale since the incidence of precipitation on windward slopes has been found to frequently be greater. The area surrounding the Upper Eskdale glacier with the potential to contribute mass to the glacier via snowblow was therefore calculated in order to determine whether or not snowblow could have been sufficient to provide accumulation which could sustain the glacier despite the unfavourable aspect. Using the method outlined in chapter 4 snowblow areas are identified and are illustrated in figure 6.4 and 6.5 below.

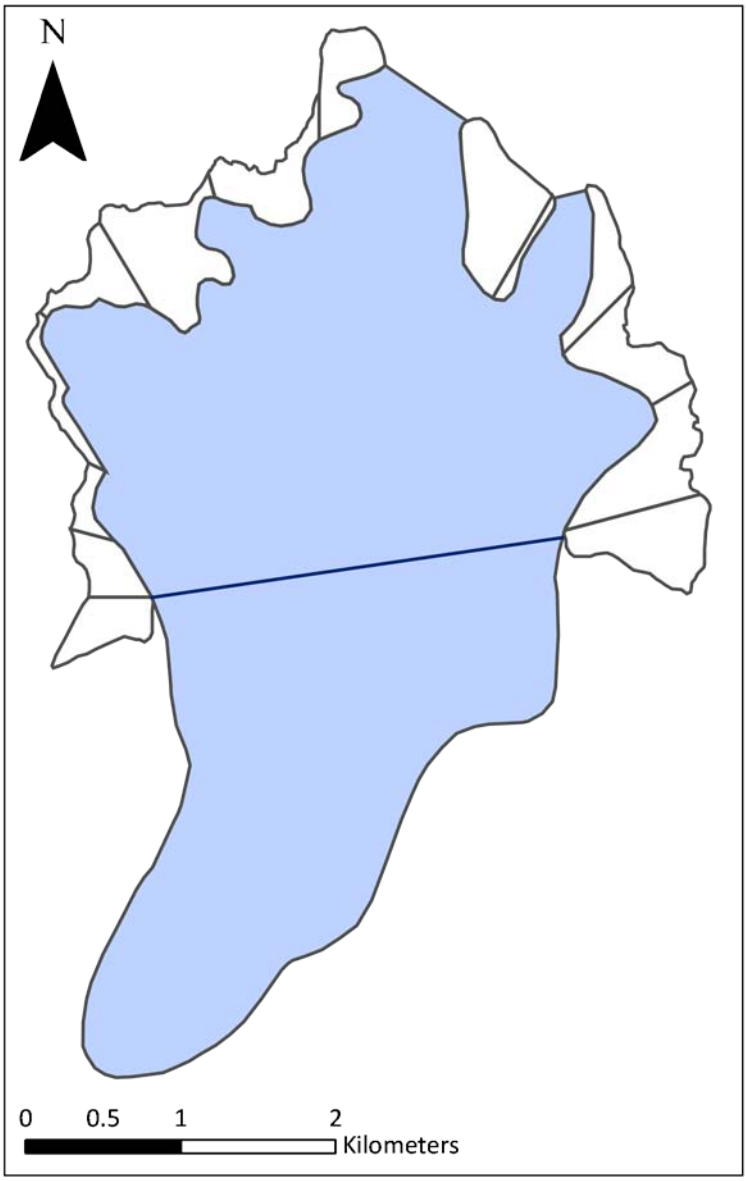


**Figure 6.4: The potential snowblow areas associated with the proposed Upper Eskdale glacier. The ELA of the glacier has been calculated at 494 m OD and is marked with a dark blue line above. It should be noted that no snowblow area is found within the southern quadrant (135-225°) for this glacier.**

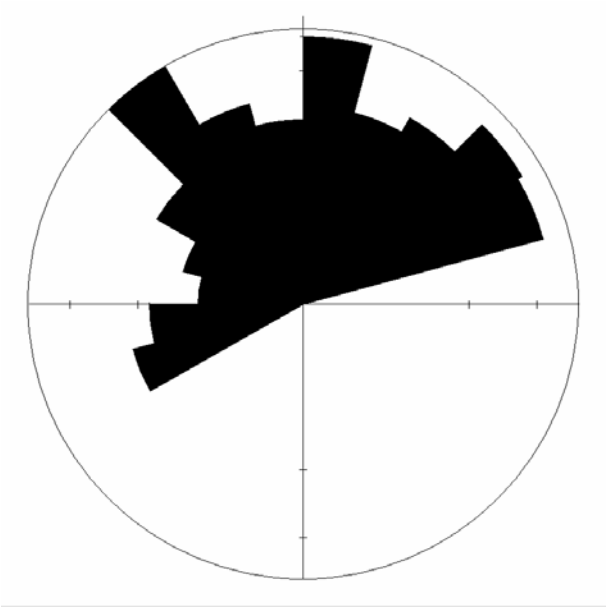

**Figure 6.5: Polar plot of snowblow area with area-weighted 15° sector lengths.**

Figure 6.4 and 6.5 above show that potential snowblow area associated with the Upper Eskdale glacier can be found principally in the north-east and north-west quadrants. In contrast, the south-east and southern quadrants do not contain any ground suitable for snowblow and the south-west sectors contains just a very small area. Snowblow factors associated with the above snowblow areas were calculated and are shown in table 6.2 below. The largest snowblow factor of 2.11 is associated with the north-east quadrant while the smallest snowblow factors of 0 relate to the south and south-eastern quadrants. Interestingly, all of the calculated snowblow factors are also much smaller than those calculated for the Mosedale, Lingmell Beck or Lingmell Gill glaciers. Referring back to section 3.1.4, the consideration of criteria 5 for the identification of potential snowblow areas requires that only windward slopes have the potential to contribute mass to a glacier via snowblow. On these grounds it appears that only the west and south-west quadrants which contain snowblow areas of 0.44 $km^2$ and 0.17 $km^2$ respectively had the potential for snowblow around the Upper Eskdale glacier. These two sectors provide a snowblow area of 0.61 $km^2$ and therefore a snowblow area to glacier area ratio of 0.05 which is clearly very low. It is therefore unlikely that snowblow played a significant role in mass accumulation on the Upper Eskdale glacier.

| Glacier name | | Upper Eskdale |
|---|---|---|
| Glacier area ($km^2$) | | 13.05 |
| Total snowblow area ($km^2$) | | 2.93 |
| Snowblow area by 90° quadrants expressed as a percentage of the total snowblow area (%) | | |
| | NE (0-90°) | 58.06 |
| | SE (91-180°) | 0 |
| | SW (181-270°) | 5.67 |
| | NW (271-360°) | 32.27 |
| | S (135-225°) | 0 |
| | W (226-315°) | 14.9 |
| Snowblow factor by 90° quadrants | | |
| | NE (0-90°) | 2.11 |
| | SE (91-180°) | 0 |
| | SW (181-270°) | 0.66 |
| | NW (271-360°) | 1.67 |
| | S (135-225°) | 0 |
| | W (226-315°) | 1.07 |
| Mean snowblow factor | | 0.92 |
| Ratio of snowblow area to glacier area | | 0.22 |

**Table 6.2: Snowblow areas and snowblow factors identified around the Upper Eskdale glacier using the criteria outlined in chapter 3.**

### 6.1.5 Glacier dynamics in Upper Eskdale

Dynamically, the Upper Eskdale glacier shown in figure 6.2 has been proven to be glaciologically viable using th60model outlined in section 5.1.5. Under steady-state conditions, the glacier required 11.12 m $a^{-1}$ basal motion which accounted for 62.25 % of the total glacier motion (table 6.3). According to Carr and Coleman (2007) and Andrews (1972), for a viable glacier, the percentage basal motion should not exceed 90 % of the total motion based on observations of contemporary alpine glaciers. The high mass flux of this glacier is a reflection of the size of the glacier surface and the size of the cross sectional area of the ELA. A shape factor of 0.61 theoretically reflects a near parabolic bed profile at the ELA of a glacier: however figure 6.6 below, a cross sectional profile across the ELA of the Upper Eskdale glacier, indicates that in practice this is not necessarily the case.

| | Upper Eskdale |
|---|---|
| ELA (m) | 494.00 |
| Temperature proxy used | Coope and Joachim (1980) St Bees Head |
| Proxy site altitude (m OD) | 0.00 |
| $T_3$ at proxy site (°C) | 8.25 |
| Temp. at ELA (0.0065°C/m lapse rate) | 5.03 |
| Degrees surface slope at ELA | 3.57 |
| Max ice thickness at ELA (m) | 144.55 |
| Glacier shape factor | 0.61 |
| Normal stress at centre point of ELA (bars) | 11.65 |
| Ablation gradient at ELA (mm/m) | 6.35 |
| Mass loss at ELA (ma-1) | 2.36 |
| Net Ablation ($m^3$ w.e.) | 4,341,667.06 |
| Mass flux ($m^3$ ice) | 4,771,062.70 |
| Cross sectional area at ELA ($m^2$) | 238,992.52 |
| Perimeter of bed at ELA (m) | 2,744.08 |
| Mean balance velocity at ELA ($ma^{-1}$) | 18.17 |
| Basal shear stress at ELA (bars) | 0.47 |
| Max ice deformation velocity at ELA ($ma^{-1}$) | 11.92 |
| Average ice deformation velocity at ELA ($ma^{-1}$) | 6.86 |
| Required basal motion ($ma^{-1}$) | 11.31 |
| Required basal motion (%) | 62.25 |

**Table 6.3: Reconstructed steady-state dynamics and flow characteristics of the glacier occupying Upper Eskdale during the Loch Lomond Stadial.**

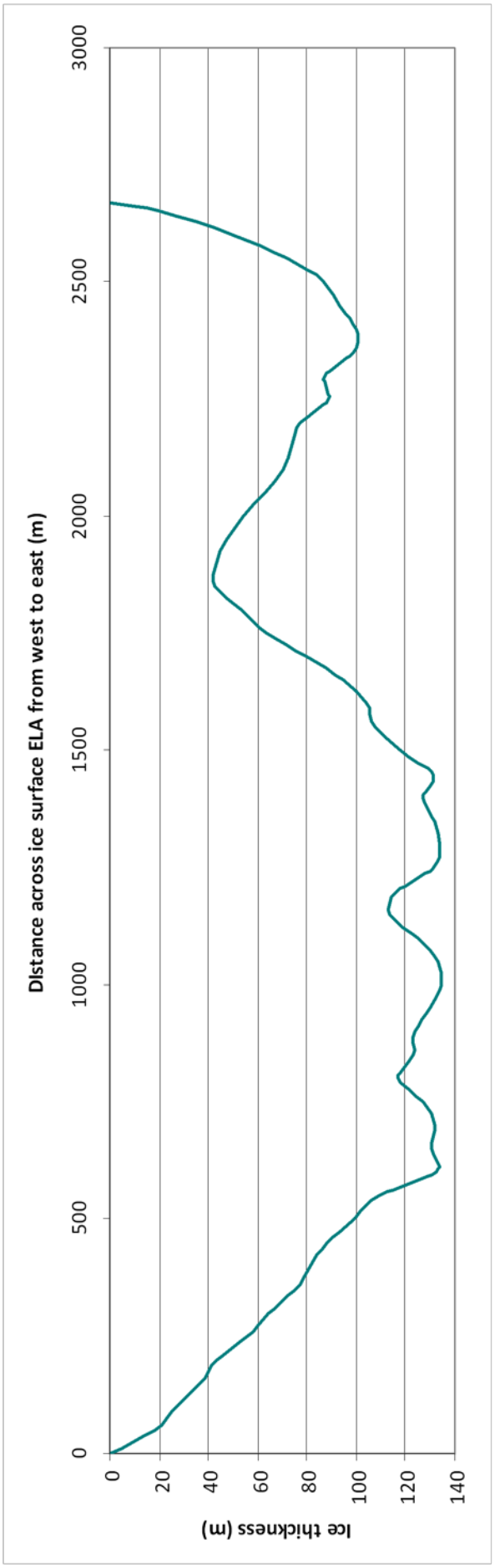


**Figure 6.6: A cross sectional profile west to east across the ELA of the Upper Eskdale glacier. ELA altitude = 483 m OD.**

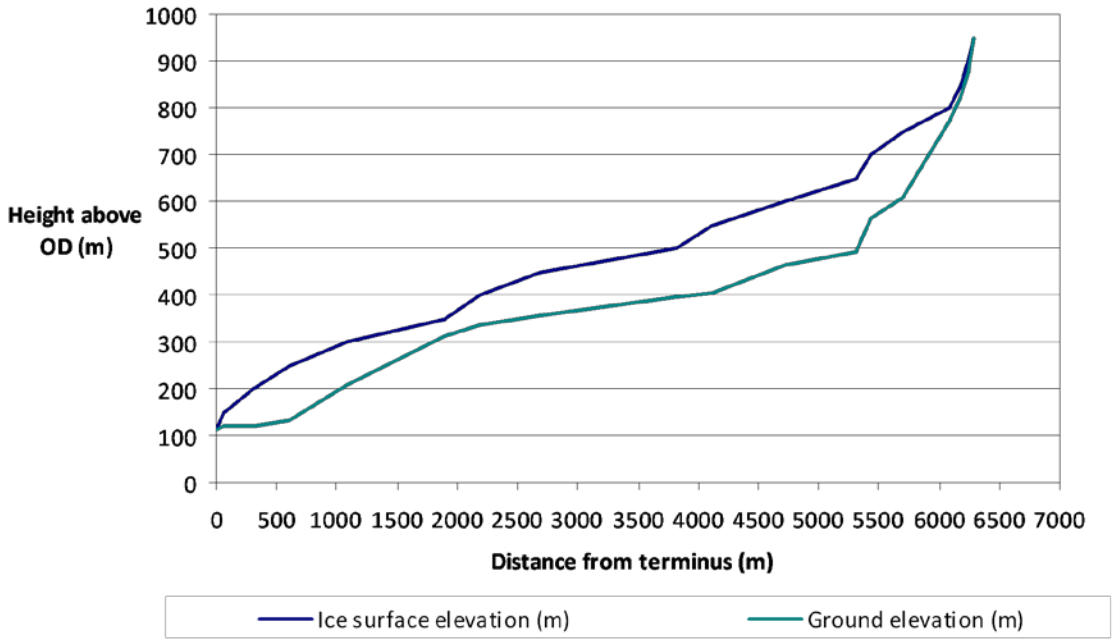


**Figure 6.7: A cross sectional profile along the long axis of the Upper Eskdale glacier.**

A maximum ice thickness at the ELA of 144.6 m is found west of the centre point of the ELA (see figure 6.6). This is greater than the maximum ice thickness at the ELA of all of the glaciers considered thus far. As shown in figure 6.7 above the Upper Eskdale glacier had a relatively constant thickness throughout except at the highest altitudes where ice appears to have been much thinner, probably as a result of the steep topographic gradient in such areas. Ice is also believed to have thinned ~ 2 km up-valley from the terminus.

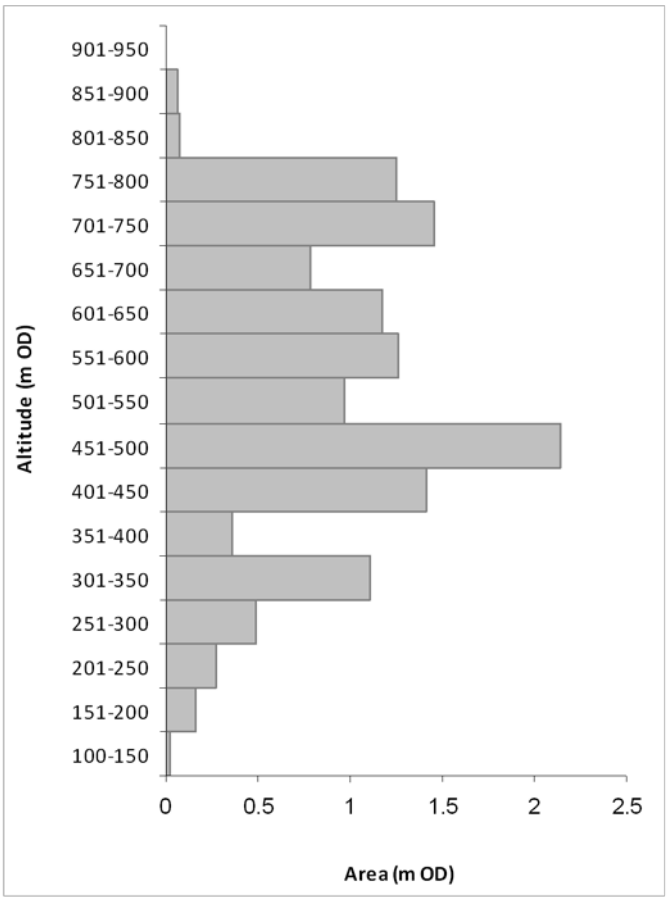


**Figure 6.8: The distribution of the glacier's surface area between the 50 m ice surface contour intervals. ELA = 483 m OD.**

Unlike the glaciers reconstructed in chapter 4, it is suggested that the largest areas of the glacier surface in Upper Eskdale were found in the middle altitudes of the glacier (figure 6.8). Notably, the largest surface areas are reconstructed between the 400 and 450 m and 450 and 500 m contours with areas of 1.41 $km^2$ and 2.15 $km^2$ respectively. This it the result of the very wide middle altitude region of the Upper Eskdale which at 2.5 km wide between the 450 and 500 m contours is equivalent to 19.2 % of the long axis of the glacier. The relationship between altitude and glacier surface area can be further demonstrated using a hypsometric curve as shown in figure 6.9 below. In accordance with the above inference, figure 6.9 shows the steepest increase in cumulative glacier surface area between 400 and 500 m OD. The net balance profile of the Upper Eskdale glacier is also consistent with equal accumulation and ablation during steady-state conditions (figure 6.10).

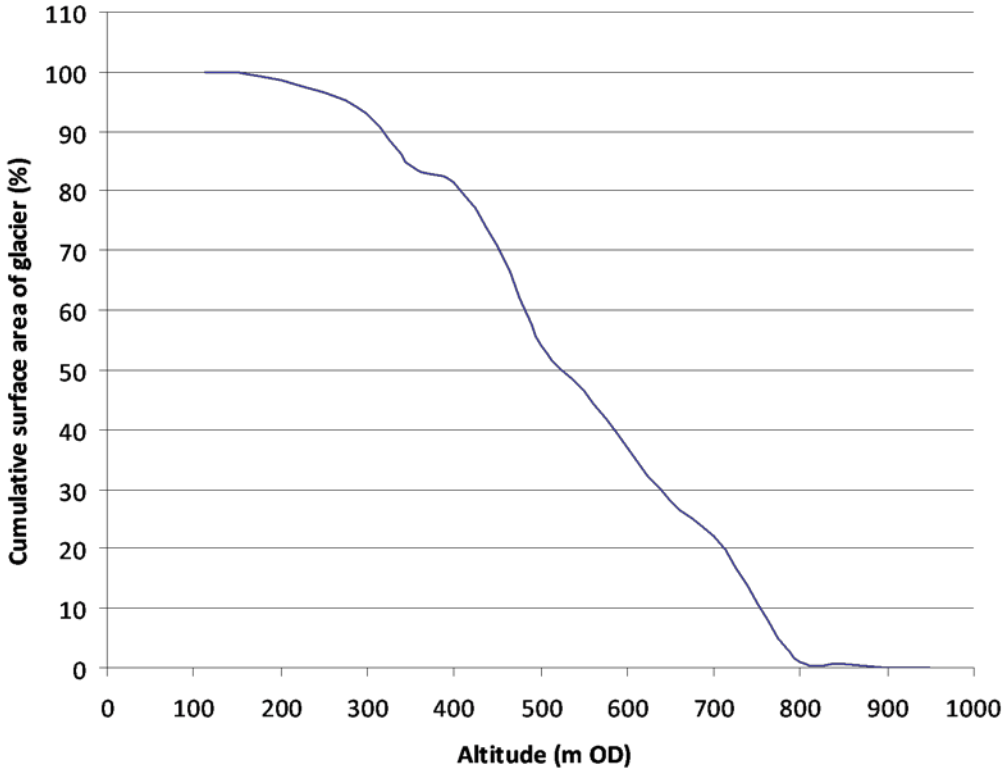


**Figure 6.9: Hypsometric curve for the Upper Eskdale glacier.**

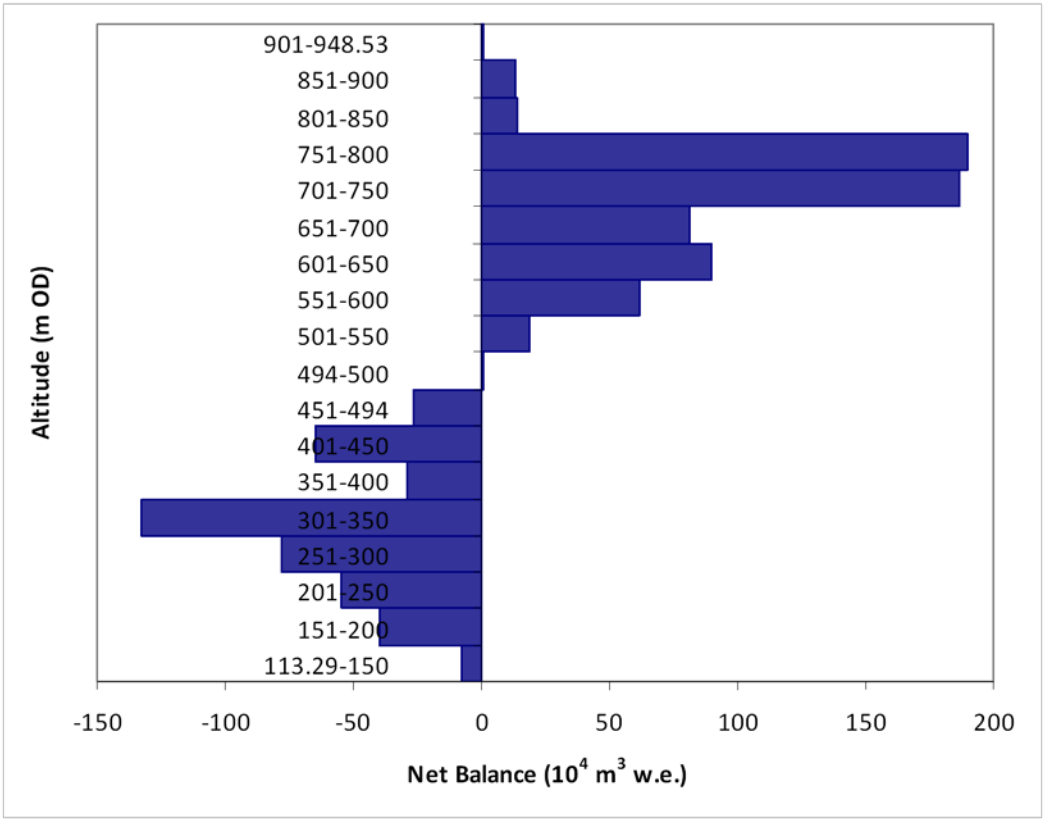


**Figure 6.10: The net balance profile of the Upper Eskdale glacier.**

## 6.2 Red Tarn, Wrynose Pass

Red Tarn is a small tarn of 0.0063 $km^2$ area located at 526 m OD just north of Wrynose Pass in the southern Lake District. The valley surrounding the tarn is overlooked by Cold Pike (701 m OD) to the west and Pike of Blisco (705 m OD) to the east. From the highest point of the valley, near Red Tarn, the valley descends to Wrynose Pass at 393 m OD before turning west and descending to Wrynose Bottom at 250 m OD. Three streams drain the area to the south of Red Tarn and converge on the western side of Wrynose Pass to form the River Duddon flowing west.

### 6.2.1 Geomorphology in the valley of Red Tarn

The area surrounding Red Tarn, Wrynose Pass and Wrynose Bottom has an abundance of moraines. The majority of these moraines, which are shown below in figure 6.11a, trend obliquely down valley or traverse the surrounding hillsides. The densest area of moraines lies just beyond the southern end of Red Tarn around GR 271033. These subtle moraines possess gradual basal breaks of slope as a result of peat accumulation between the moraines which often encroaches onto the slopes. The formation of many small drainage pathways beneath and within the peat has caused many of the moraines to have been dissected. This has caused some of the linearity between and within the moraines to have been lost. A large fluvially cut spur is also present south of Red Tarn and is testament to the high water content of the surrounding area which has resulted in river discharges suitably high as to incise deeply either side of the spur.

Further south, near the summit of Wrynose Pass moraine density reduces and moraine orientation change to run sub-parallel to the south-west facing valley leading the Wrynose Bottom (see figure 6.11a). It is here, near the summit of Wrynose Pass, that Sissons (1980) suggests the terminus of the Loch Lomond Stadial glacier was located. Following field investigation, it is suggested that this may be incorrect since the ridge proposed as the terminal moraine by Sissons (1980) has been found to be rock cored. The rock in this area appears to be responsible for a significant proportion of the feature's morphology with just a covering of till overlaying the bedrock ridge. It is thus suggested that the terminus of the Loch Lomond Stadial glacier was further down valley to the west of Wrynose Pass.

Peat cover reduces further down the valley and as a result moraines become less subdued and show more pronounced basal breaks of slope. Crestlines also become clearer and more inter- and intra-moraine linearity is shown.

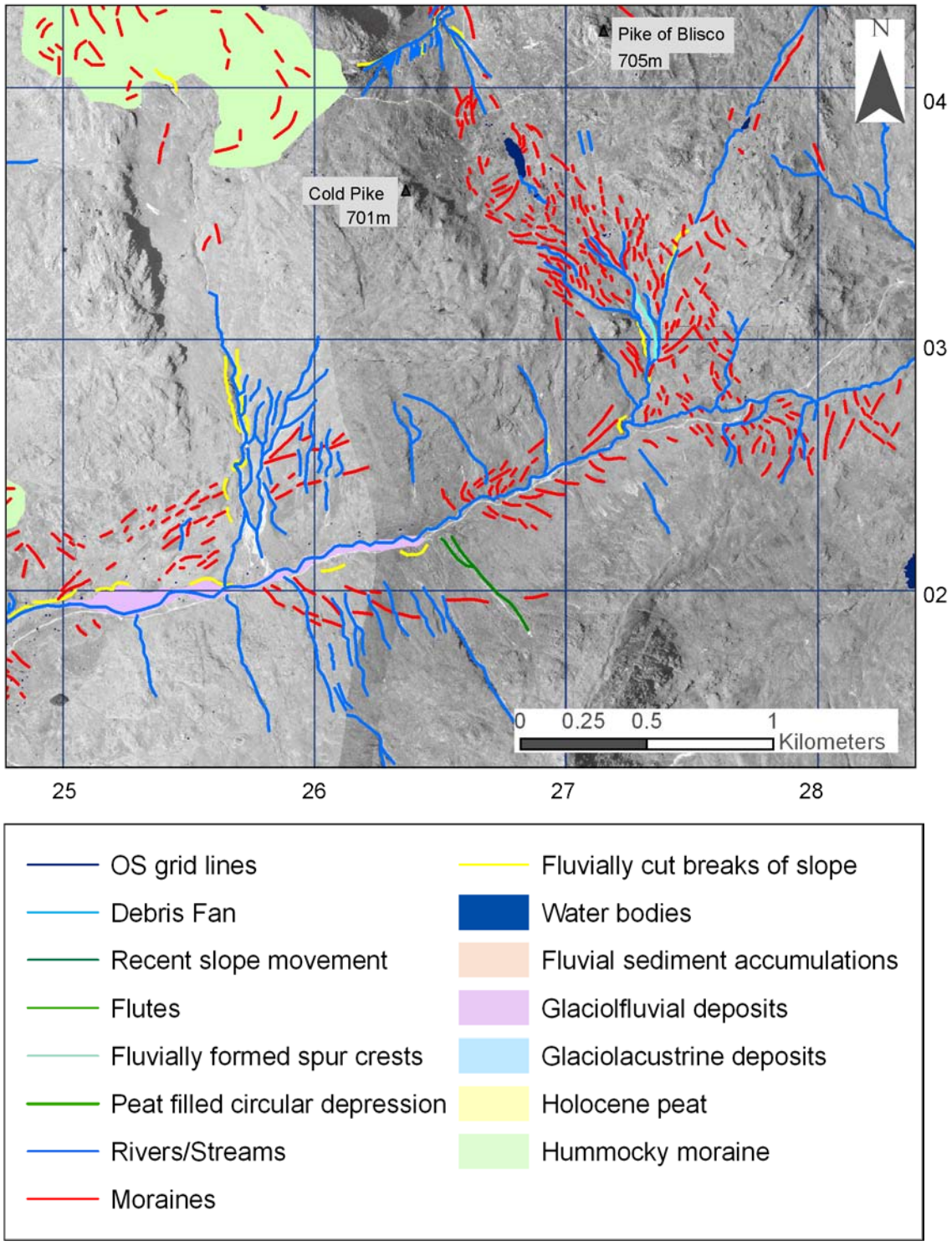


**Figure 6.11a: The geomorphology of Red Tarn and Wrynose Bottom.**

An area devoid of moraines then occurs to the west of GR 265024 before the occurrence of much larger moraines further to the west. These moraines are larger in both height and plan and show a greater degree of linearity despite areas of dissection. The moraines around GR 265024 also grade into the hillside more than the moraines further to the west. As shown in Figure 6.11a above, the larger moraines also show a greater degree of curvature than moraines further to the east. A smooth arc of moraines can therefore be traced across the

valley to form an arc which is ~ 700 m wide and believed to have formed at the front of a valley glacier. This is much wider than the maximum width of the moraines further east which at their maximum width spread only 250 m across the valley. These moraines are also believed to have formed at the front of a valley glacier. This morphological change is taken to represent formation under different environmental conditions at the front of valley glaciers of differing sizes. The morphological differences seen between the moraines can be compared to those seen in moraines in Mosedale and Lingmell Beck. Consequently, as shown in figure 6.11b below, the two groups of moraines have been assigned to different glacial episodes with those further to the east proposed as the terminal moraines of the Loch Lomond Stadial glacier which occupied Wrynose Bottom and Red Tarn. The pre-Loch Lomond Stadial moraines may relate to the Scottish Readvance or the Wester Ross Readvance.

Coring was also carried out in a peat bog on the summit of Wrynose Pass however this was unsuccessful due to the presence of an extensive layer of rocks and/or gravel at approximately 1.5 m below the surface.

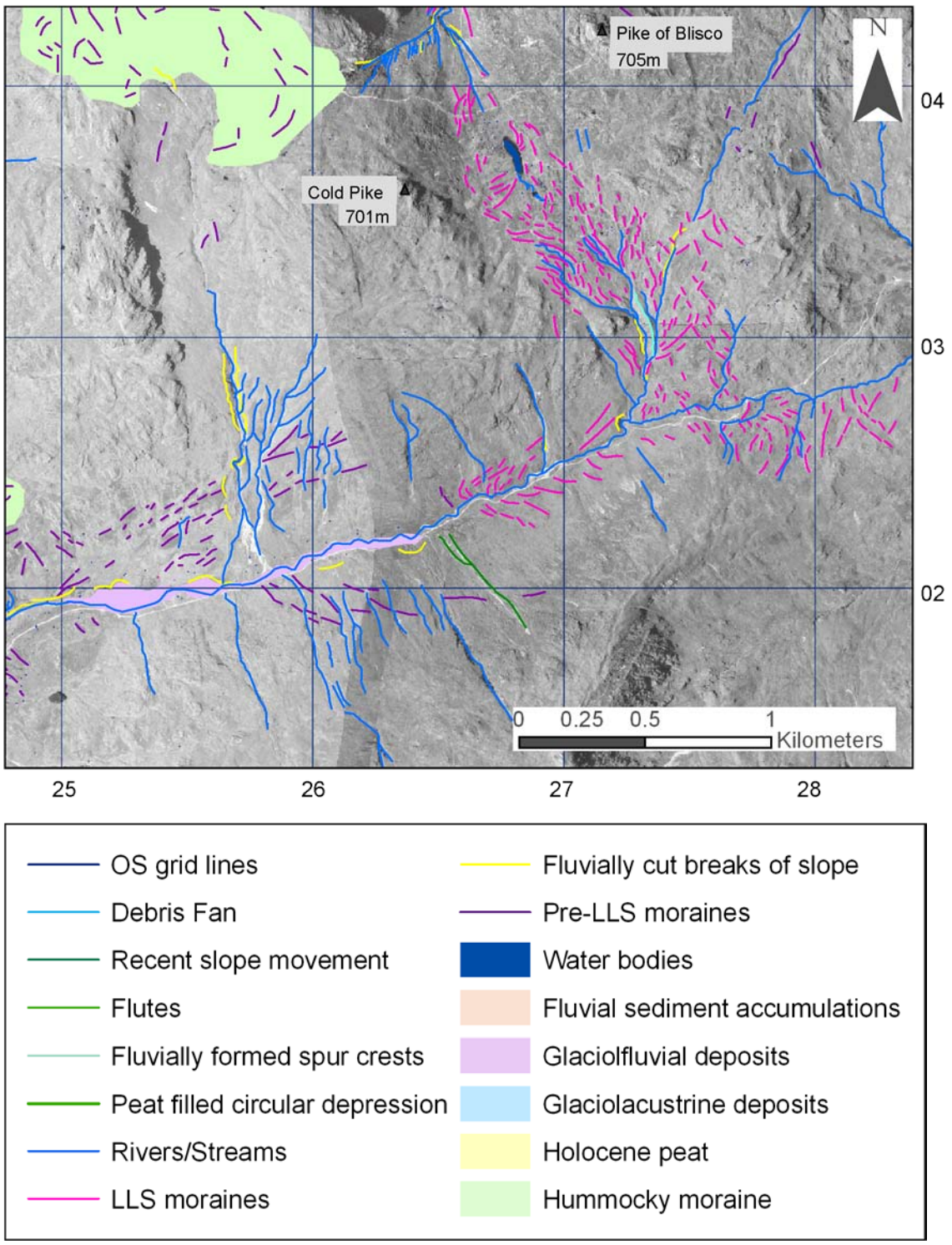


**Figure 6.11b: The geomorphology of Red Tarn and Wrynose Bottom proposing the glacial episode during which moraine formation occurred.**

### 6.2.2 Loch Lomond Stadial glacier reconstruction at Red Tarn

The proposed reconstruction of the glacier which occupied Red Tarn and Wrynose Bottom is shown below in figure 6.12. At its maximum extent the glacier had a surface area of 1.5 $km^2$ and an ELA of 494 m. Sissons (1980) and Manley (1959) also reconstructed glaciers in Red Tarn/ Wrynose Bottom. The reconstruction provided by Sissons (1980) indicates a glacier with

a surface area of just 0.62 $km^2$, which is less than half of the area of the glacier reconstructed here. Sissons' (1980) reconstruction of the glacier in Red Tarn is shown below in figure 6.13; however this is considered conservative since the moraine he took as the terminal moraine has since been found to be rock cored. Here, the terminus of the glacier has been extended further down the valley to coincide with a set of moraines in Wrynose Bottom (shown in figure 6.11b above). The result of this reconstruction which extends the ablation zone of the glacier to lower altitudes than suggested by Sissons (1980) is to lower the ELA of the glacier. Sissons (1980) suggests an ELA of 557 m OD for the glacier in Red Tarn (shown in figure 6.13), which is 45 m higher than the ELA calculated for the reconstruction shown in figure 6.12 below.

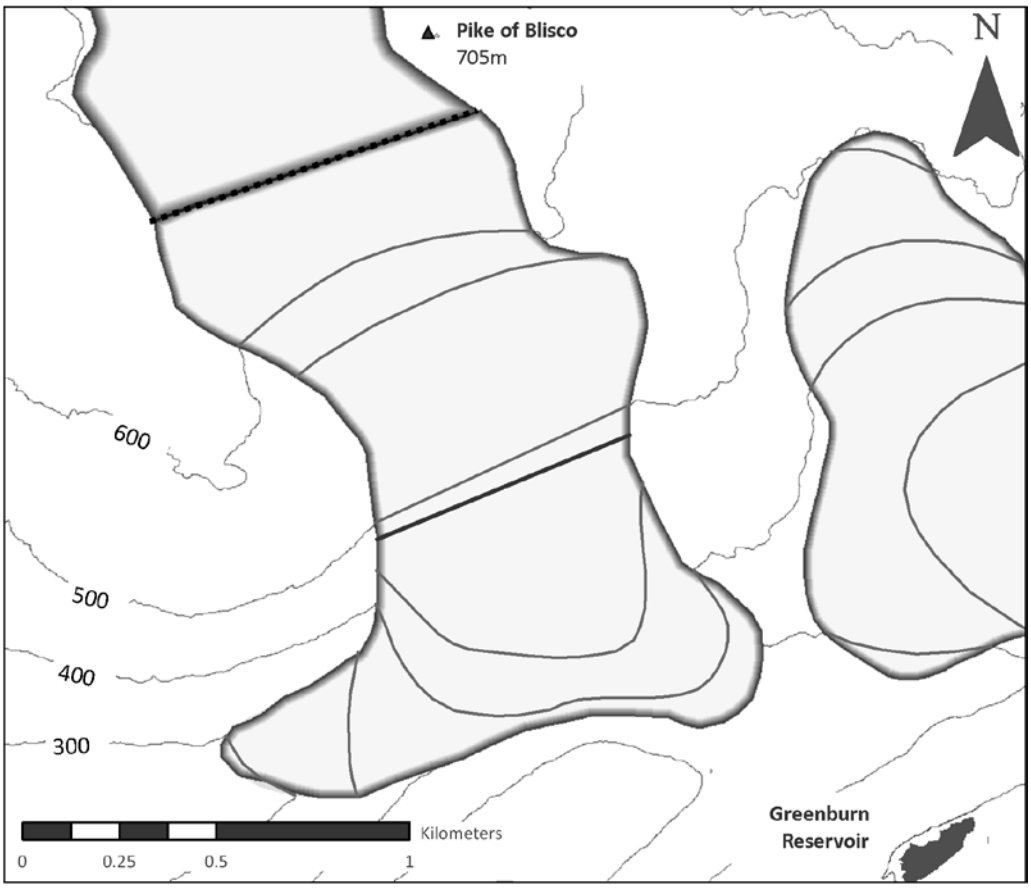


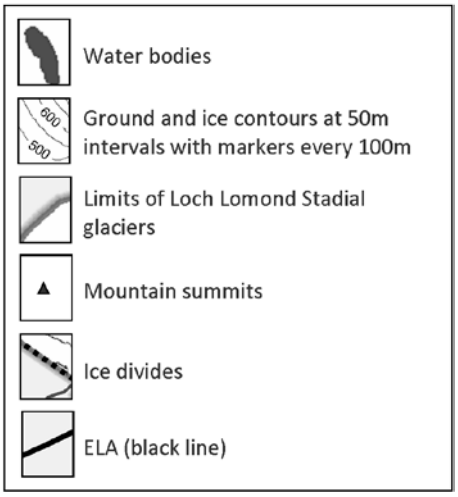


**Figure 6.12: A reconstruction of the glacier which occupied Red Tarn and Wrynose Bottom in the south-west Lake District during the Loch Lomond Stadial.**

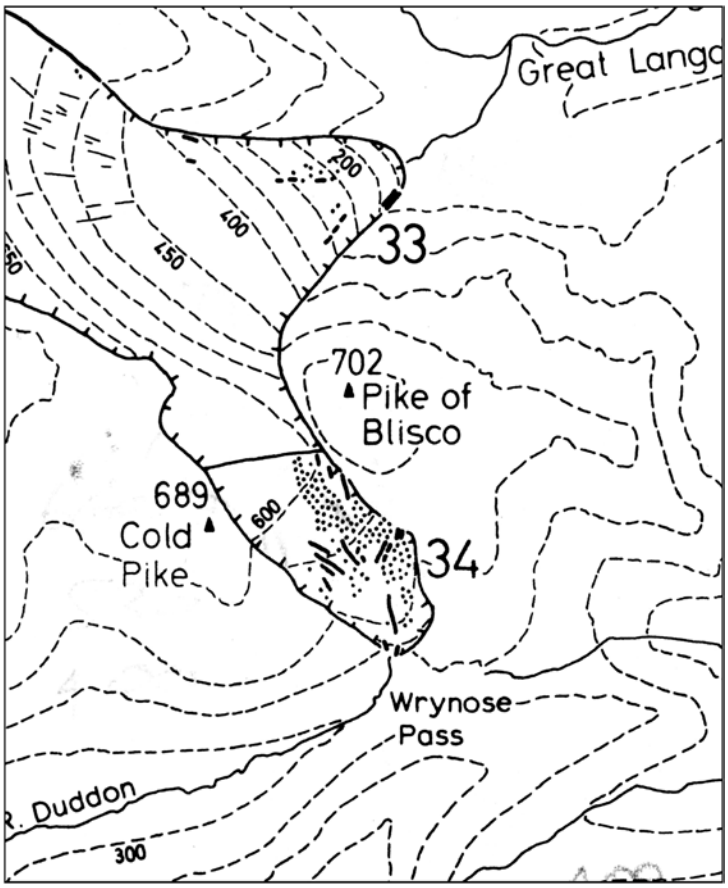


**Figure 6.13: The reconstruction of the Red Tarn/Wrynose Bottom glacier during the Loch Lomond Stadial according to Sissons (1980).**

Prior to Sissons (1980), Manley (1959) reconstructed the glacier occupying Red Tarn/ Wrynose Bottom during the Loch Lomond Stadial. This reconstruction was more extensive than that proposed by Sissons (1980) and not only involved ice being present in Widdygill Foot to the east but also required that the ice in Red Tarn and Widdygill Foot coalesced over Wrynose Pass. Furthermore although Manley (1959) extends ice to the east into Widdygill Foot, he does not extend ice down valley into Wrynose Bottom to the west. This seems an unlikely arrangement since it would be naturally easier for ice to extend to the west downslope than to the east over the pass. Although Wrynose Bottom has a more windward aspect than Widdygill Foot and could thus be considered to be in a less favourable location, Wrynose Bottom receives considerable shading from Cockley Beck Fell to the south. When compared with Widdygill Foot which is bounded to the south by Wet Side Edge, Wrynose Bottom can be considered to be relatively sheltered, particularly from southerly winds.

Morainic evidence of a glacier terminus around the location proposed by Manley (1959) on the western side of Wrynose Pass also appears tentative. Moraines are present in this area, as shown in figure 6.11b, but there is no clear arcuate downslope limit. Thus far, moraine

morphology has been used as a means of distinguishing between moraines which formed during different glacial episodes. In Wrynose Bottom just one clear morphological change is seen within the moraines and this is taken to represent the downslope limit of the Loch Lomond Stadial glacier in the valley as described above. Within this glacial limit moraines show consistent degrees of linearity, breaks of slope and size (both height and plan), and do not therefore support Manley's (1959) suggestion that the glacier terminus on the western side of Wrynose Pass lay up valley of the limit proposed in this study.

The upslope limit of the glacier proposed here also contests that of Manley (1959). Arcuate moraine ridges are seen across the pass (see figure 6.11b) lying transverse to the proposed ice flow eastward over the pass into Widdygill Foot. These moraines generally curve downslope and on the western side of the pass one such ridge is taken as the upslope limit of the Loch Lomond Stadial glacier proposed in this study. Evidence indicating the lateral margins of that ice flowed over the pass however is lacking, and it is thus suggested that ice did not coalesce between Red Tarn/Wrynose Bottom and Widdygill Foot.

The valley around Red Tarn itself over which ice is believed to have coalesced with that in Oxendale to the north has an unfavourable aspect facing almost directly south. The lower section of the valley in Wrynose Bottom has a more favourable aspect facing south-south-west and receives shelter from the high elevation topography to the south as previously discussed. The implications of this on mass accumulation in the accumulation zone of the glacier could be detrimental as a result of high amounts of direct solar radiation reaching the south facing parts of the glacier. This however, may have been counteracted by relatively low amounts of ablation as a consequence of the sheltered location of the ablation zone in Wrynose Bottom. It is therefore possible that the Red Tarn/Wrynose Pass glacier had a low mass turn over compared to a glacier such as Mosedale where the accumulation and ablation zones have a similar orientation.

The theoretical ELA of the Red Tarn/Wrynose Bottom glacier has been calculated via several methods, the results of which are shown below in table 6.4. Deviations from these theoretical results are however likely with a glacier such as that proposed for Red Tarn/Wrynose Bottom due to the variations in downslope flow direction.

| | | Red Tarn |
|---|---|---|
| Area ($km^2$) | | 1.45 |
| Long axis length (m) | | 2267.43 |
| Max altitude (m OD) | | 648.31 |
| Min altitude (m OD) | | 276.31 |
| Mid-altitude (m OD) | | 462.00 |
| Lowest cirque | | |
| Name | | - |
| Altitude (m OD) | | - |
| Grade (according to Evans and Cox, 1995) | | - |
| Altitude of highest lateral moraine (m OD) | | 530.53 |
| Toe to head altitude ratio method (THAR) (m OD) | | |
| | 35% | 406.51 |
| | 40% | 425.11 |
| | 45% | 443.71 |
| | 50% | 462.00 |
| Accumulation area ratio method (AAR) (m OD) | | |
| | 70% | 445.00 |
| | 65% | 457.00 |
| | 60% | 470.00 |
| | 55% | 480.00 |
| | 50% | 492.00 |
| Area weighted mean altitude method (AWMA) (m OD) | | 500.55 |
| Balance ratio method (Benn and Gemmell, 1997) (m OD) | | |
| | BR=2.00 | 492.81 |
| | BR=1.81 | 495.12 |
| | BR=1.60 | 497.99 |
| | BR=1.54 | 498.88 |
| | BR=1.43 | 500.60 |
| Balance ratio method (Osmaston, 2005) (m OD) | | |
| | BR=2.00 | 466 |
| | BR=1.81 | 464 |
| | BR=1.60 | 462 |
| | BR=1.54 | 461 |
| | BR=1.43 | 459 |
| **Mean value of all of the above methods (m OD)** | | **471.90** |
| **Mean value of BR=1.54 (Benn and Gemmell, 1997), AAR 65% and AWMA** | | **485.48** |
| **ELA used in subsequent calculations (m OD)** | | **485** |

**Table 6.4: ELA calculations and dimensions of the glacier occupying Red Tarn/Wrynose Bottom during the Loch Lomond Stadial.**

### 6.2.3 The influence of snowblow on glacier development/maintenance

Areas surrounding the reconstructed Red Tarn/Wrynose Bottom glacier with the potential to contribute mass to the glacier via snowblow were identified using the criteria outlined in chapter 4 and are shown in figures 6.14 and 6.15 below.

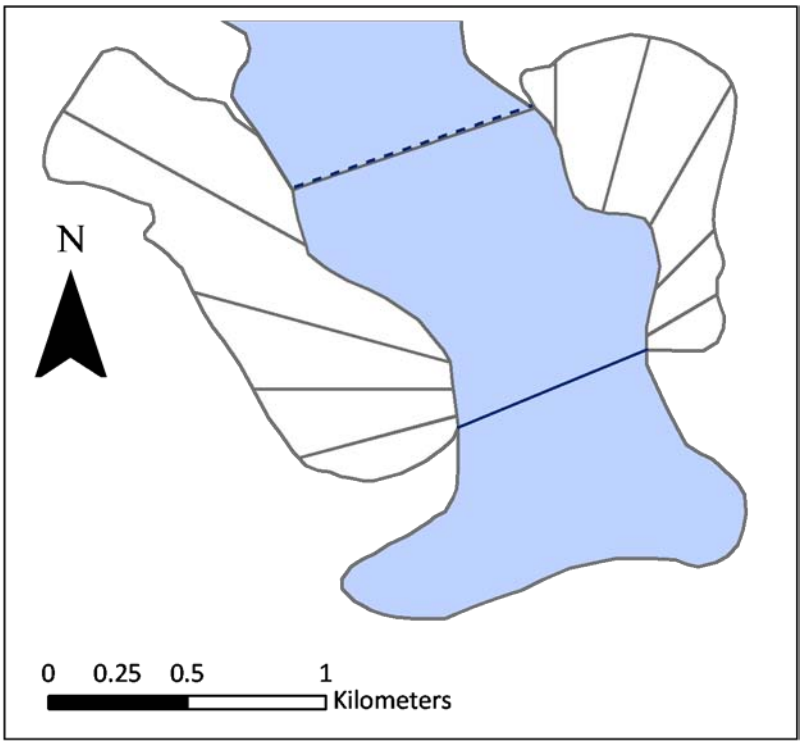


**Figure 6.14: The snowblow area associated with the Red Tarn/Wrynose Bottom glacier. The ELA of the glacier has been calculated at 485 m OD and is marked with a dark blue line above. The ice divide between the Red Tarn/Wrynose Bottom glacier and the Oxendale glacier to the north is marked with a dashed dark blue line. It should be noted that no snowblow area is found within the southern quadrant (135-225˚) for this glacier.**

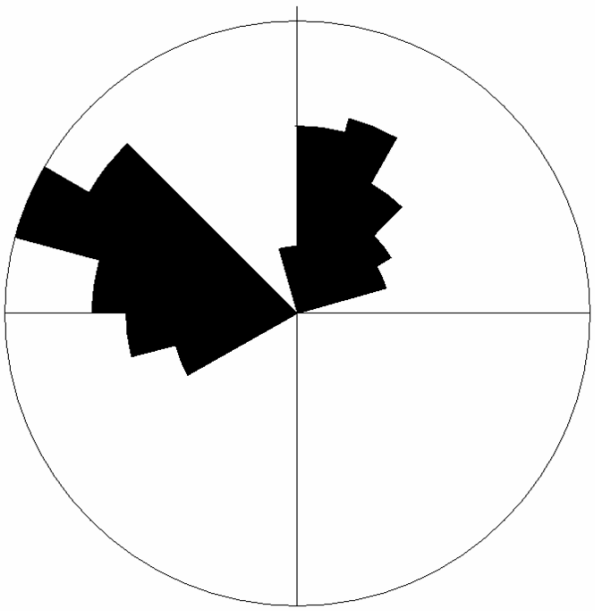

**Figure 6.15: Polar plot of snowblow area with area-weighted 15˚ sector lengths.**

The largest snowblow areas around the Red Tarn/Wrynose Bottom glacier are located in the north-east and north-west quadrants. Snowblow area is also found in the western quadrant

and a smaller amount is found in the south-western quadrant; however crucially no snowblow area is present in the southern sector. Table 6.5 below shows the snowblow areas found within each quadrant around the Red Tarn/Wrynose Bottom glacier. As expected from figures 6.14 and 6.15 above the highest snowblow factors are associated with the western and north-western quadrants. Since south to south-west winds were probably dominant during the Stadial, this arrangement of snowblow area around the glacier suggests that snowblow may have contributed only minimal quantities of mass to the glacier. This arrangement of potential snowblow area is however, more advantageous than the arrangement around the Upper Eskdale glacier. In Upper Eskdale, there is also an absence of potential snowblow area in both the south and south-east quadrants. However, a much lower proportion of the snowblow area is found within the western quadrant and thus a greater proportion of the snowblow area is likely to be windward of the glacier, thus favouring input via snowblow. It should also be considered that steeper ground surrounds Upper Eskdale so although snowblow contribution may have been limited, mass contribution through avalanching is likely.

| | Red Tarn |
|---|---|
| Glacier area ($km^2$) | 1.15 |
| Total snowblow area ($km^2$) | 1.32 |
| Snowblow area by 90° quadrants expressed as a percentage of the total snowblow area (%) | |
| NE (0-90°) | 33.41 |
| SE (91-180°) | 0.00 |
| SW (181-270°) | 12.79 |
| NW (271-360°) | 53.80 |
| S (135-225°) | 0.00 |
| W (226-315°) | 65.30 |
| Snowblow factor by 90° quadrants | |
| NE (0-90°) | 4.76 |
| SE (91-180°) | 0.00 |
| SW (181-270°) | 2.95 |
| NW (271-360°) | 6.04 |
| S (135-225°) | 0.00 |
| W (226-315°) | 6.66 |
| Mean snowblow factor | 3.40 |
| Ratio of snowblow area to glacier area | 1.15 |

**Table 6.5: Snowblow areas and snowblow factors identified around the Red Tarn/Wrynose Pass glacier using the criteria outlined in chapter 4.**

### 6.2.4 Glacier dynamics at Red Tarn

The proposed glacier occupying Red Tarn/Wrynose Bottom has been proven to be viable according to the method outlined by Carr and Coleman (2007). This glacier however requires the highest percentage of basal motion out of any of the glaciers studied here in order to remain in steady-state equilibrium. At 73.01 %, the required basal motion at Red Tarn is the

closest to the 90 % threshold of any of the glaciers studied here. This is the result of a shallow surface slope and relatively thin ice at the ELA of the glacier (see table 6.6 below).

| | Red Tarn |
|---|---|
| ELA (m) | 485.00 |
| Temperature proxy used | Coope and Joachim (1980) St Bees Head |
| Proxy site altitude (m OD) | 0.00 |
| $T_3$ at proxy site (°C) | 8.25 |
| Temp. at ELA (0.0065°C/m lapse rate) | 5.09 |
| Degrees surface slope at ELA | 7.28 |
| Max ice thickness at ELA (m) | 66.79 |
| Glacier shape factor | 1.00 |
| Normal stress at centre point of ELA (bars) | 5.27 |
| Ablation gradient at ELA (mm/m) | 6.42 |
| Mass loss at ELA (ma-1) | 2.39 |
| Net Ablation ($m^3$ w.e.) | 295,605.36 |
| Mass flux ($m^3$ ice) | 324,841.05 |
| Cross sectional area at ELA ($m^2$) | 38,006.11 |
| Perimeter of bed at ELA (m) | 724.67 |
| Mean balance velocity at ELA ($ma^{-1}$) | 7.78 |
| Basal shear stress at ELA (bars) | 0.27 |
| Max ice deformation velocity at ELA ($ma^{-1}$) | 5.52 |
| Average ice deformation velocity at ELA ($ma^{-1}$) | 2.10 |
| Required basal motion ($ma^{-1}$) | 5.68 |
| Required basal motion (%) | 73.01 |

**Table 6.6: Reconstructed steady-state dynamics and flow characteristics of the glacier occupying Red Tarn/Wrynose Pass during the Loch Lomond Stadial.**

Thin ice at the ELA of the Red Tarn/Wrynose Bottom glacier and a shallow surface slope also resulted in the lowest normal stress at the ELA of 5.27 bars, any of the glaciers studied. Variation in ice thickness along the long axis of the glacier is illustrated in figure 6.16 below along with the cross section at the ELA in figure 6.17. Ice thickness declines from the ELA down towards the glacier snout with a noticeable thinning occurring around 350 m from the terminus. At around 1.5 km from the terminus, just above the ELA, ice also becomes thinner

at the point where the ground begins to descend away from the relatively flat area around Red Tarn. This can be explained by the occurrence of extensional flow in this area.

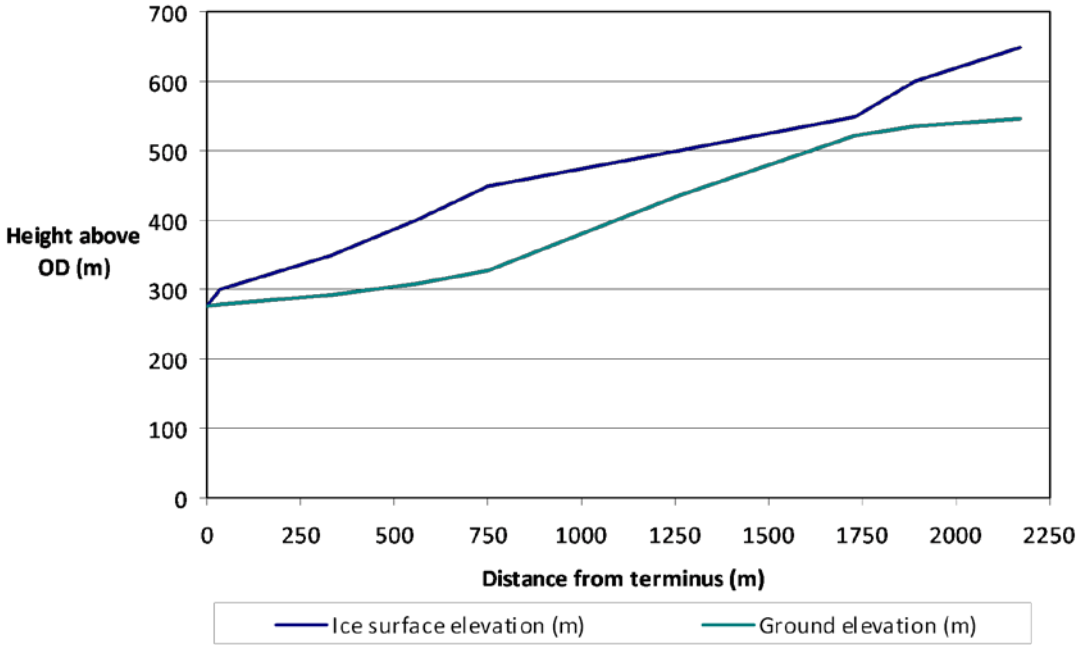


**Figure 6.16: Across sectional profile along the long axis of the Red Tarn/Wrynose Bottom glacier.**

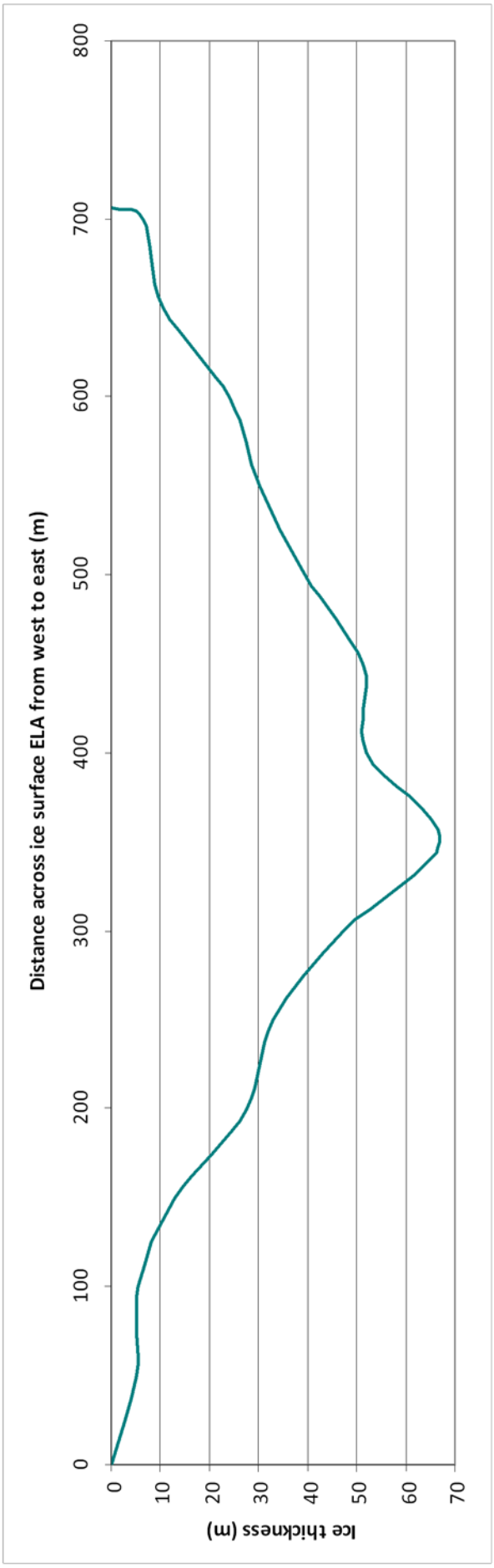


**Figure 6.17: A cross sectional profile west to east across the ELA of the Red Tarn/Wrynose Bottom glacier. ELA altitude = 485 m OD.**

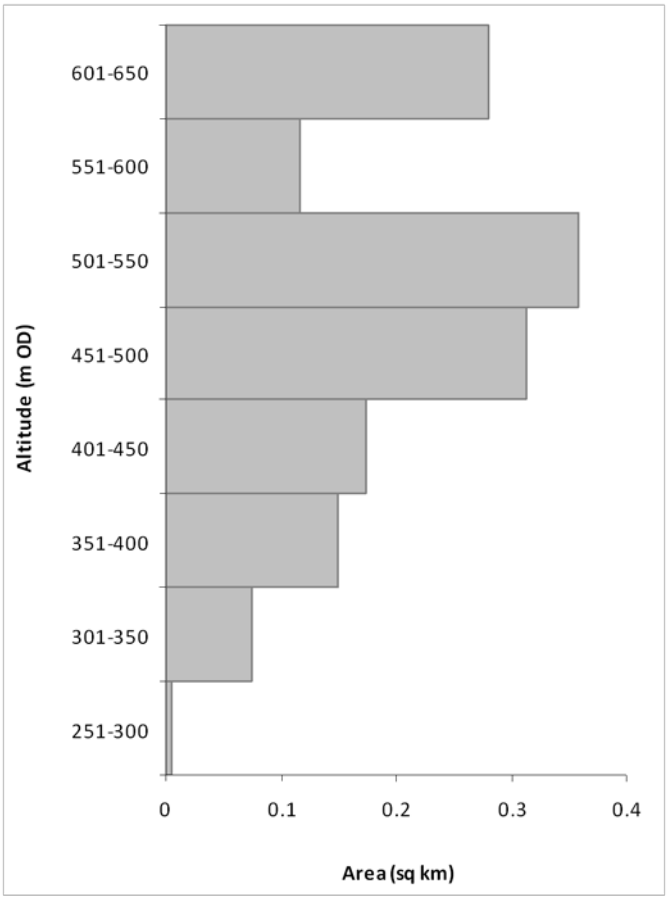


**Figure 6.18: The distribution of the glacier's surface area between the 50 m ice surface contour intervals. ELA = 485 m OD.**

As would be expected from an idealised glacier reconstruction, some of the largest surface areas of the glacier lie around the glacier's mid-altitudes between 400 and 550 m (see figure 6.18 above). However the single largest area between any of the contours lies within the 600-650 m contour interval. This is explained by the presence of the nearby ice divide with the Oxendale glacier to the north which means that the glacier does not become substantially narrower or thin towards its maximum altitude as is seen with an isolated glacier such as Mosedale for example. This is further illustrated by plotting cumulative surface area against altitude as shown figure 6.19 and also explains the slightly unbalanced net balance curve shown in figure 6.20 which illustrates calculations of net balance based on the surface area of the glacier.

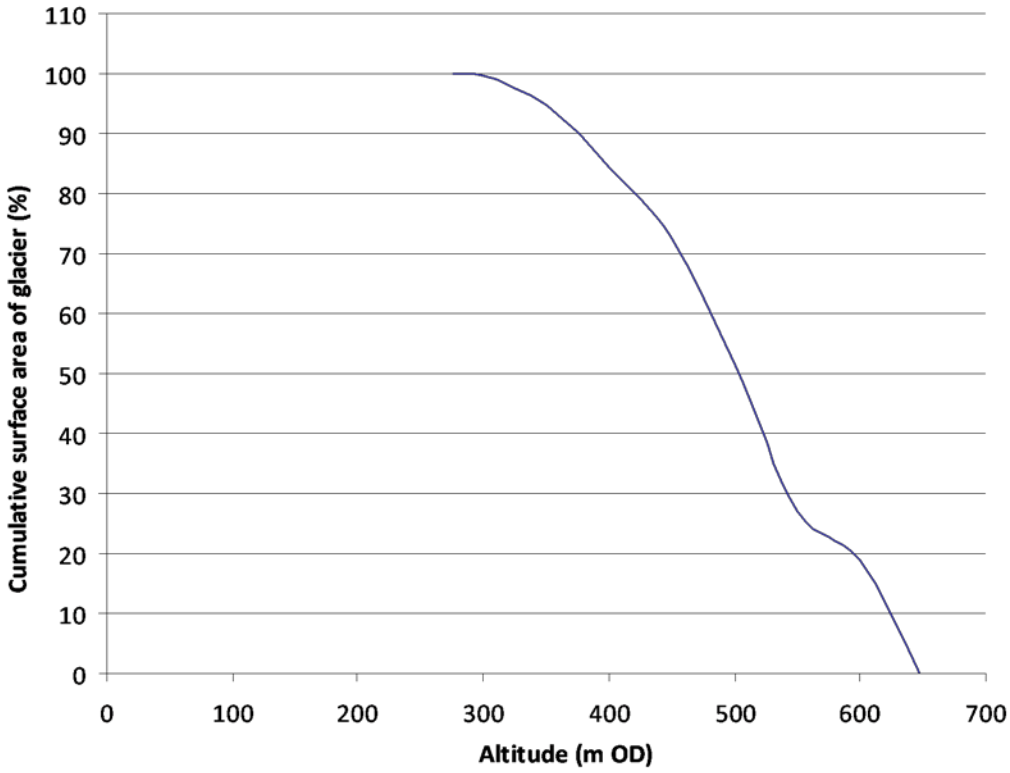


**Figure 6.19: Hypsometric curve for the Red Tarn/Wrynose Bottom glacier.**

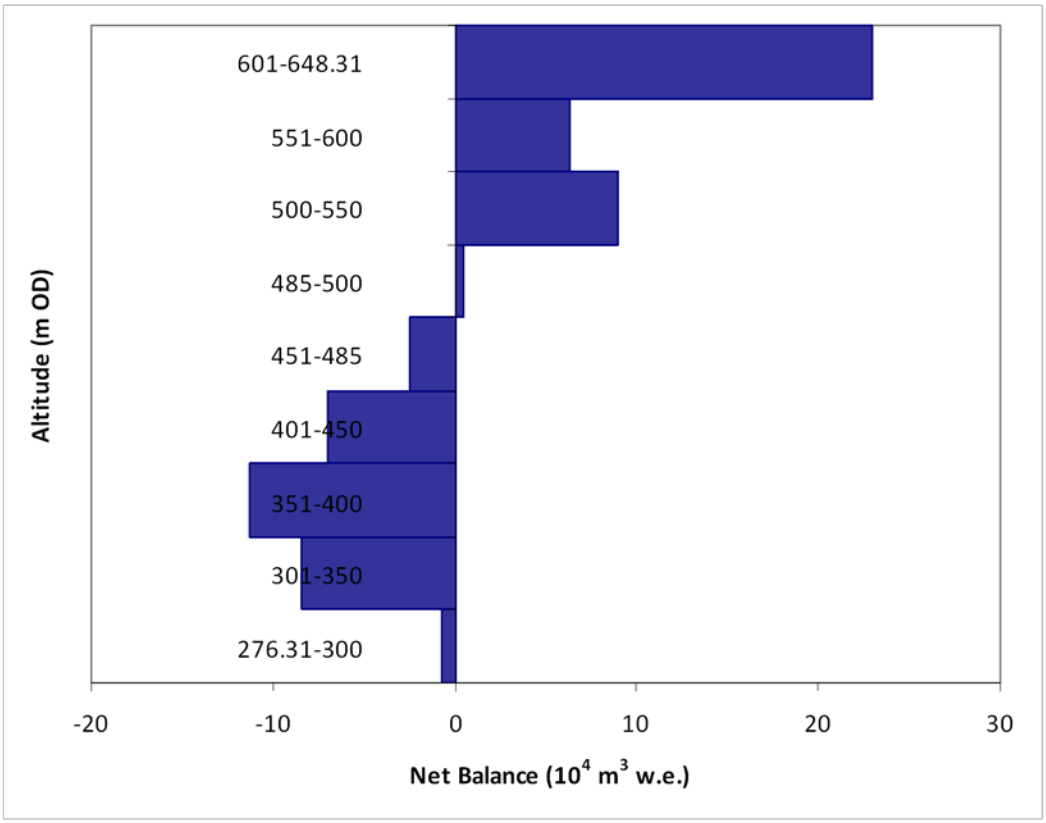


**Figure 6.20: The net balance profile of the Red Tarn/Wrynose Bottom glacier.**

## 6.3 Widdygill Foot

Widdygill Foot is a small east facing valley on the eastern wide of Wrynose Pass in the south central fells. The valley covers an area of ~ 3 $km^2$ and is occupied by the River Brathay which drains from Wrynose Pass, Pike of Blisco (705 m OD) and Wrynose Fell further north. Steep topography surrounds Widdygill Foot and forms an enclosed valley located directly beneath Wrynose Pass. To the south-west of the valley, Wet Side Edge separates Widdygill Foot from Greenburn Beck before the ground steeply ascents to Swirl How (805 m OD) ~ 2 km south of Wrynose Pass.

### 6.3.1 Geomorphology in the valley of Widdygill Foot

The floor of the Widdygill Foot valley is occupied by a series of moraine ridges and mounds extending ~ 1 km along either side of the River Brathay. Moraines on the northern side of the river are not only more extensive but also possess a much clearer morphology. Using Manley's idea of 'freshness of form', these moraines could be described as 'very fresh'. The moraines on the northern side of the valley trend obliquely down valley in a north-west to south-east orientation. Moraines initially grade out of the northern side of the valley although they are disrupted by the road which runs perpendicular to the moraine crest orientation. As the moraines progress southwards away from the northern side of the valley, crestlines and basal breaks of slope become much sharper. According to Wilson (2002), moraines are found between 130 and 220 m OD.

On the southern side of the valley, not all of the moraines were identified by Wilson (2002). Moraines on the southern side of the valley appear much more subdued than those identified by Wilson (2002) with less distinctive basal breaks of slope and crestlines. Their linearity is however still clearly visible from aerial photography and in some cases NextMap (see figure 6.21a below). They also appear to grade more smoothly into the southern side of the valley, probably as a result of their reduced height.

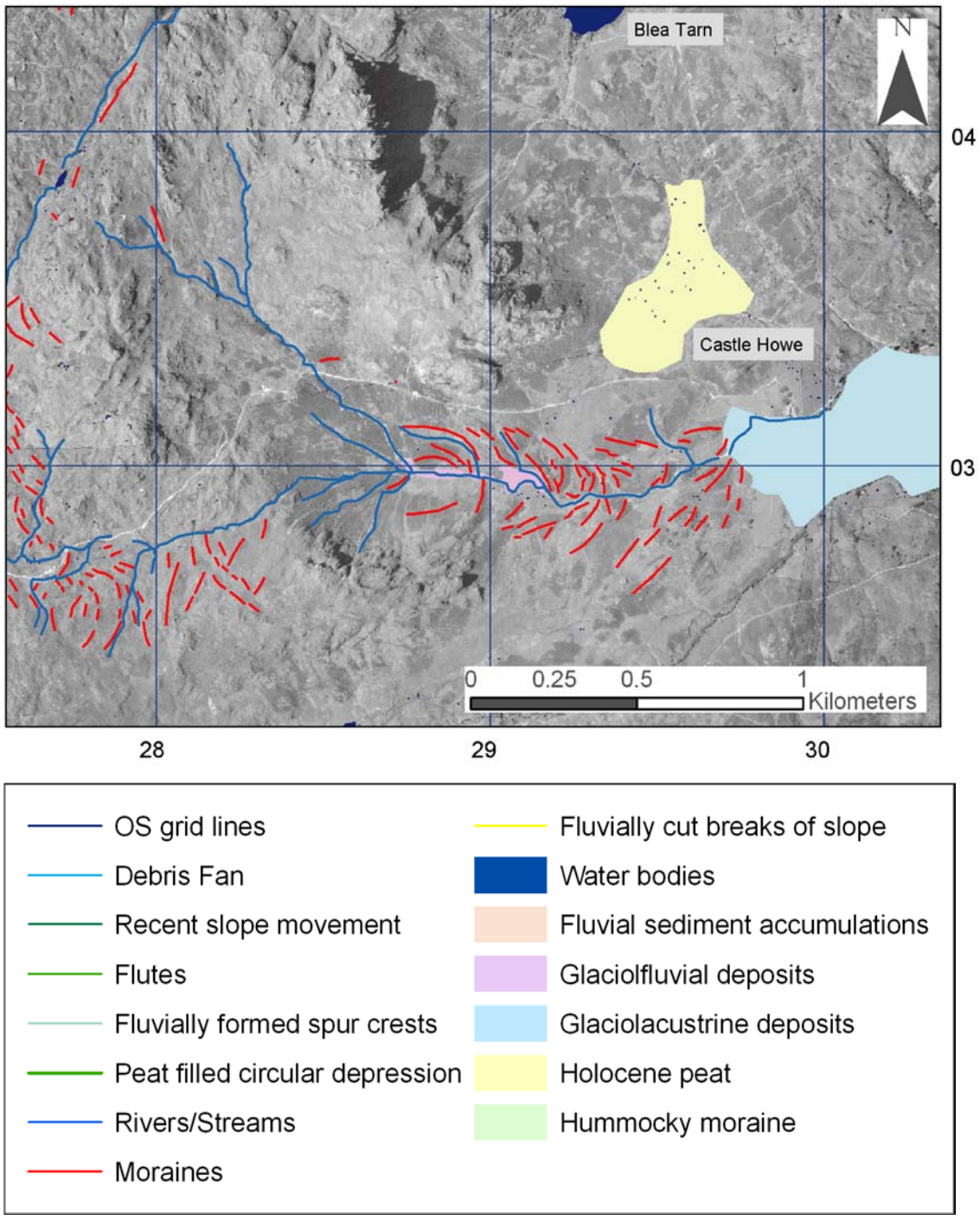


**Figure 6.21a: The geomorphology of Widdygill Foot.**

Between the larger moraines, particularly on the northern side of the valley, areas of peat infill are present. The very flat topography associated with these areas of infill may explain why such sharp breaks of slope are found around the nearby moraines. As noted by Wilson (2002), these areas of infill are found above the level of the present day river.

To the east of GR: 298030 moraines are not present. It is therefore not possible to assign these moraines to a particular glacial episode in the same way as the moraines discussed at the previous five sites based on morphology. Instead it is necessary to consider the moraines

at Widdygill Foot in the context of moraines elsewhere in the Lake District. Moraines at the southern ends of Coniston and Windermere are believed to have formed during the Gosforth Oscillation (Merritt and Auton, 2000). Comparatively, moraines formed during both the Gosforth Oscillation and the Scottish Readvance indicate a much more extensive glaciation than those at Widdygill Foot with ice extending out from the mountains to much lower altitudes. Consequently, the moraines in Widdygill Foot, and indeed each of the other areas considered in this study, were not formed during either of the above Dimlington Stadial readvances. Instead it is suggested that the moraines formed during a more recent glacial episode, based on their proximity to the mountain summits and well preserved morphology. The Loch Lomond Stadial, which is the most recent episode of mountain glaciation in the British Isles, therefore seems the most likely period for their formation. This is supported by the stratigraphy of the core taken from the kettle hole (feature A) in Mosedale (see chapter 4). Figure 6.21b below indicates the age that has been assigned to the moraines in and around Widdygill Foot. This figure indicates that the moraines above the main valley (shown in purple on figure 6.21b) are not of LLS age. Instead they are suggested to have formed during an earlier glacial episode on the basis of them being far more subdued and also much shorter than the moraines lower down in the Widdygill Foot valley bottom.

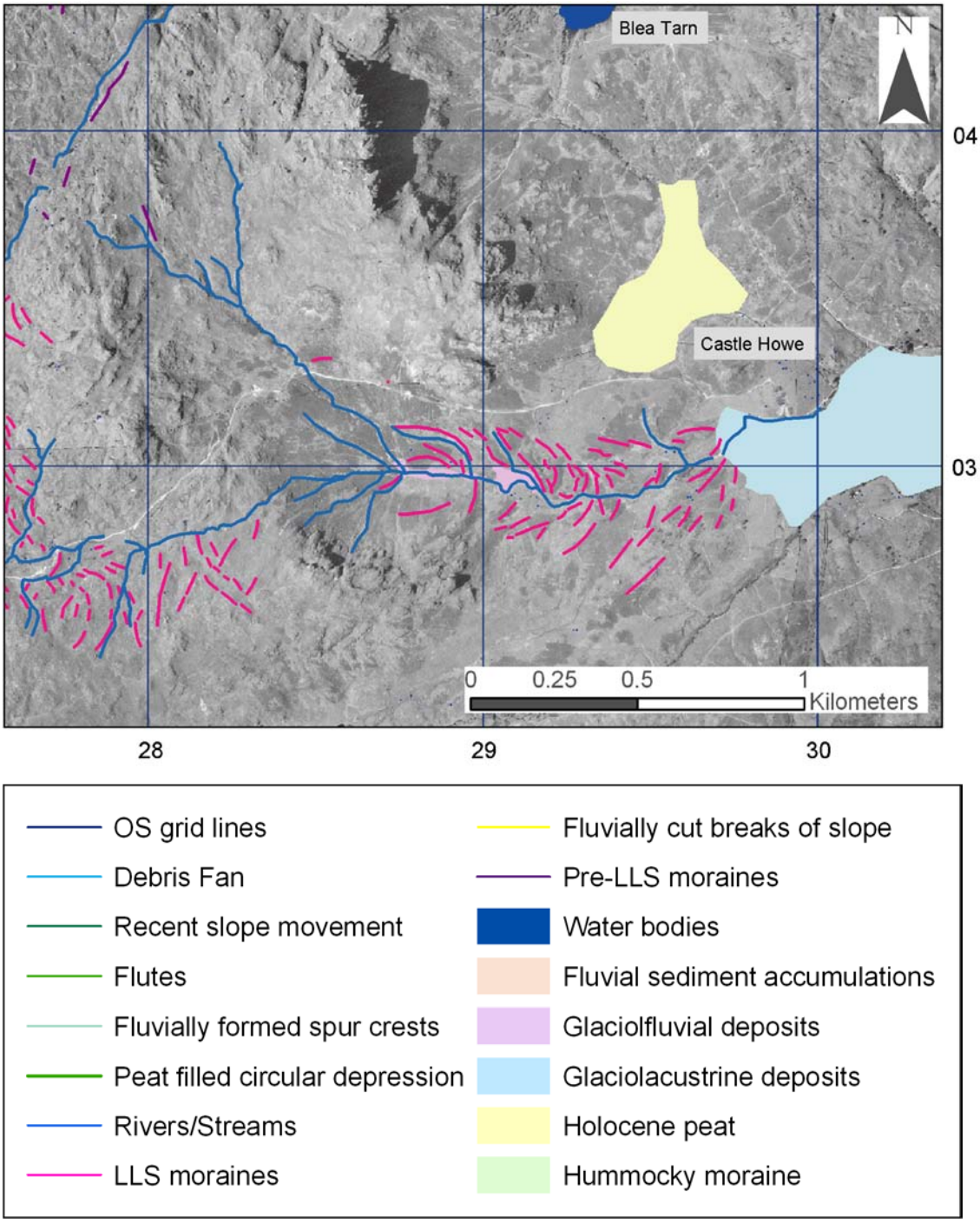


**Figure 6.21b: The geomorphology of Widdygill Foot indicating the glacial episode during which moraine formation occurred.**

Coring was also attempted in Widdygill Foot in order to relatively date the moraines (around GR: 278028). The presence of an extensive covering of fluvial gravels approximately 70 cm on average below the ground surface prevented any potentially valuable sediments being retrieved. Cores obtained from the area were devoid of minerogenic sediments and solely consisted of peat. $^{14}C$ dates on organic fragments in the base of the peat would establish a minimum age for the lower sediments and thus potentially confirm the above suggestion; however this was beyond the scope and time constraints of this project.

### 6.3.2 Loch Lomond Stadial glacier reconstruction in Widdygill Foot

The map of Manley (1959) was the first to indicate that a glacier occupied Widdygill Foot during the Loch Lomond Stadial. Although the coarse scale of this map makes it difficult to establish exactly where Manley (1959) intended his glacial limits to be, it is likely that he intended the terminus of the glacier to have been located in a similar place to that indicated below in figure 6.22. Pennington (1978) also suggests that a Loch Lomond Stadial glacier occupied the site: however, Sissons (1980) does not. More recently, Wilson (2002) has provides a more comprehensive geomorphological map of Widdygill Foot and convincingly argues that the moraines are of Loch Lomond Stadial age. Walker (1966) however identified the moraines in Widdygill Foot but was less confident in assigning them an age. Figure 6.22 shows the reconstructed glacier in Widdygill foot based on the geomorphological evidence presented in figure 6.21b above.

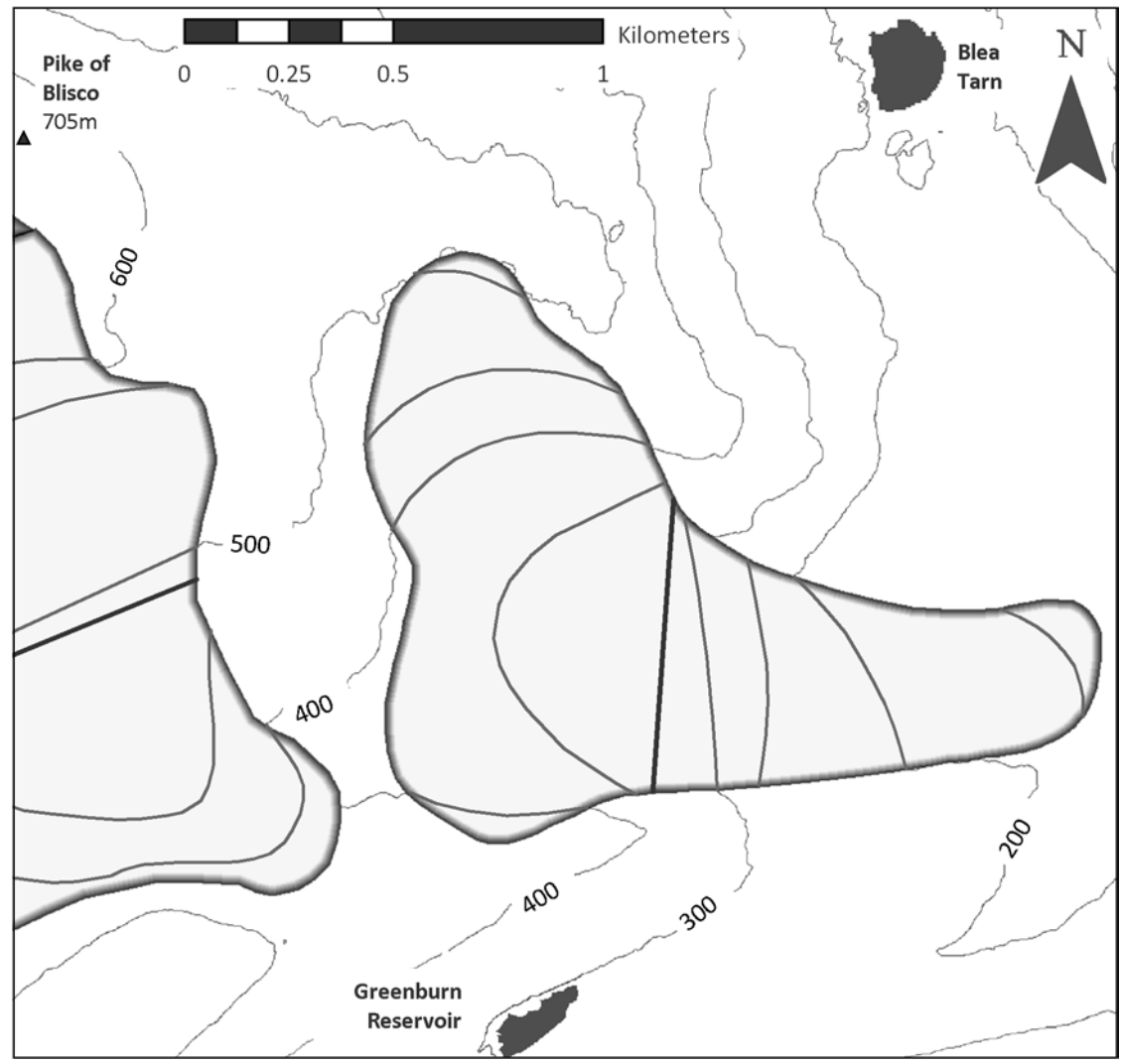


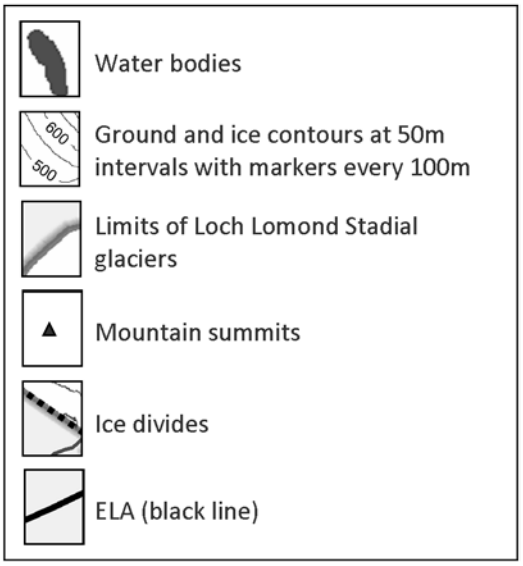


**Figure 6.22: A reconstruction of the glacier which occupied Widdygill Foot in the south central Lake District during the Loch Lomond Stadial.**

The reconstructed glacier shown above had a total area of 1.23 $km^2$ making it the fourth largest of the six glaciers reconstructed here. The ELA of the Widdygill Foot glacier was calculated following the methods outlines in chapter 4 and a final ELA of 323 m OD was used in subsequent calculations of glacier dynamics and flow characteristics. This is substantially lower than the ELAs of any of the other six glaciers presented by ~ 100 m and can be explained by the low altitudinal range of the glacier. At ~ 399 m the Widdygill Foot glacier has the second lowest altitudinal range of the six glaciers presented with a maximum altitude of 515 m and a minimum of 116 m OD. As shown in table 6.7 below, neither the Widdygill Foot glacier, nor the Red Tarn/Wrynose Bottom glacier, occupied a glacial cirque. In a situation where cirques formed during glacial episodes prior to the Loch Lomond Stadial, which is almost certainly the case in the Lake District, the occurrence of glacial cirques is likely to have facilitated glacier development. Conversely where cirques are not present, the development of Loch Lomond Stadial glaciers is suggested to have been more reliant on the wider valley topography and aspect rather than the specific environment conditions created within the cirque basin or hollow.

| | | Widdygill Foot |
|---|---|---|
| Area ($km^2$) | | 1.23 |
| Long axis length (m) | | 2292.25 |
| Max altitude (m OD) | | 515.00 |
| Min altitude (m OD) | | 116.33 |
| Mid-altitude (m OD) | | 315.00 |
| Lowest cirque | | |
| Name | | - |
| Altitude (m OD) | | - |
| Grade (according to Evans and Cox, 1995) | | - |
| Altitude of highest lateral moraine (m OD) | | 439.32 |
| Toe to head altitude ratio method (THAR) (m OD) | | |
| | 35% | 255.86 |
| | 40% | 275.80 |
| | 45% | 295.73 |
| | 50% | 315.50 |
| Accumulation area ratio method (AAR) (m OD) | | |
| | 70% | 294.00 |
| | 65% | 310.00 |
| | 60% | 321.00 |
| | 55% | 333.00 |
| | 50% | 343.00 |
| Area weighted mean altitude method (AWMA) (m OD) | | 325.50 |
| Balance ratio method (Benn and Gemmell, 1997) (m OD) | | |
| | BR=2.00 | 326.82 |
| | BR=1.81 | 329.29 |
| | BR=1.60 | 332.36 |
| | BR=1.54 | 333.31 |
| | BR=1.43 | 335.17 |
| Balance ratio method (Osmaston, 2005) (m OD) | | |
| | BR=2.00 | 485 |
| | BR=1.81 | 484 |
| | BR=1.60 | 482 |
| | BR=1.54 | 482 |
| | BR=1.43 | 481 |
| **Mean value of all of the above methods (m OD)** | | **360.94** |
| **Mean value of BR=1.54 (Benn and Gemmell,1997), AAR 65% and AWMA (m OD)** | | **322.94** |
| **ELA used in subsequent calculations (m OD)** | | **323** |

**Table 6.7: ELA calculations and dimensions of the glacier occupying Widdygill Foot during the Loch Lomond Stadial.**

The long axis of the Widdygill Foot valley has an easterly aspect. This is a relatively favourable aspect for glacier development as it means that the valley is located on the leeward side of Wet Side Edge and Wrynose Pass which both provide shelter from the south to south-westerly winds which occurred during the Stadial.

### 6.3.3 The influence of snowblow on glacier development/maintenance

Ground with the potential to contribute mass to the Widdygill Foot glacier via snowblow has been identified and is shown in figure 6.23 or 6.24 below. Snowblow area is found within all of the quadrants around the Widdygill Foot glacier with the largest areas in the NW and W quadrants, containing 52.49 % and 41.37 % of the total snowblow area respectively (table 6.8). Despite this, the Widdygill Foot glacier has the third smallest snowblow area to glacier area ratio meaning that mass contribution to glacier via snowblow may not be as significant as it may appear from initial inspection of figure 6.23, for example. The significance of snowblow around the Widdygill Foot glacier is further reduced by the implementation of criteria 5 for the identification of potential snowblow area as outlined in section 3.1.4. This criteria states that only surfaces which are windward of the glacier have the potential for snowblow. This reduces that total snowblow area from 0.81 $km^2$ to just 0.29 $km^2$ (just 36.25 % of the original calculated area) and the snowblow area to glacier area ratio from 0.65 to 0.23. It is therefore hypothesised that the sheltered location and aspect of the Widdygill Foot glacier played a significant role in glacier development by enabling mass input via direct precipitation and reducing ice melt. As a result the glacier was less reliant on inputs from snowblow than some of the other glaciers discussed previously.

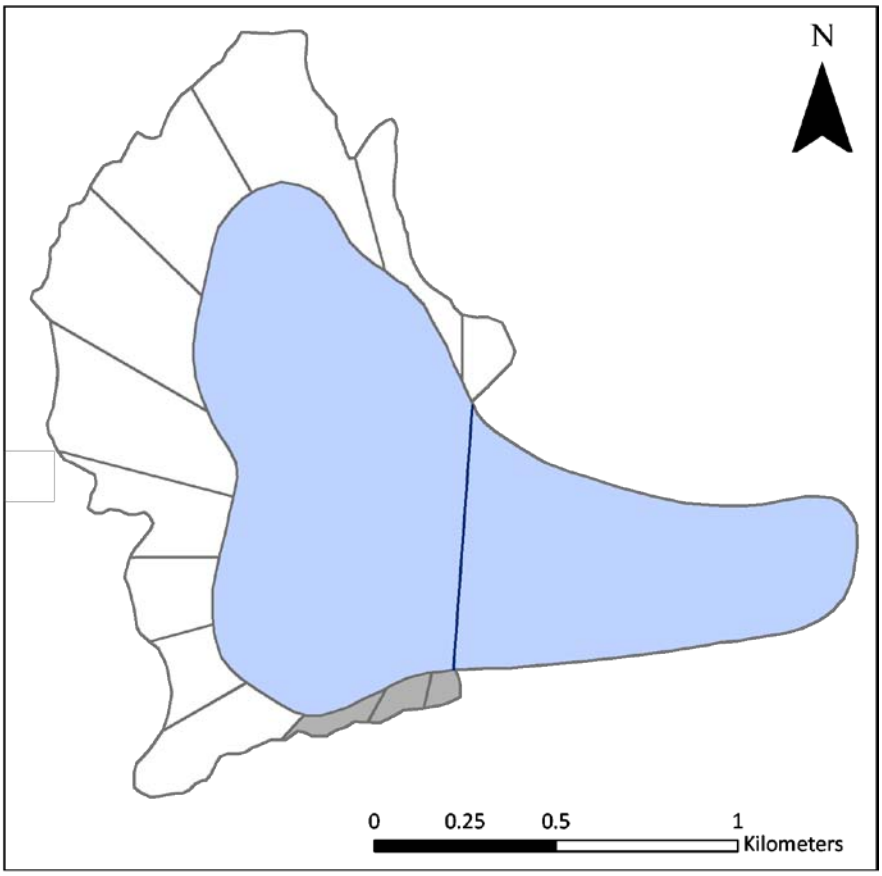


**Figure 6.23: The snowblow area associated with the Widdygill Foot glacier. The ELA of the glacier has been calculated at 323 m OD and is marked with a dark blue line above.**

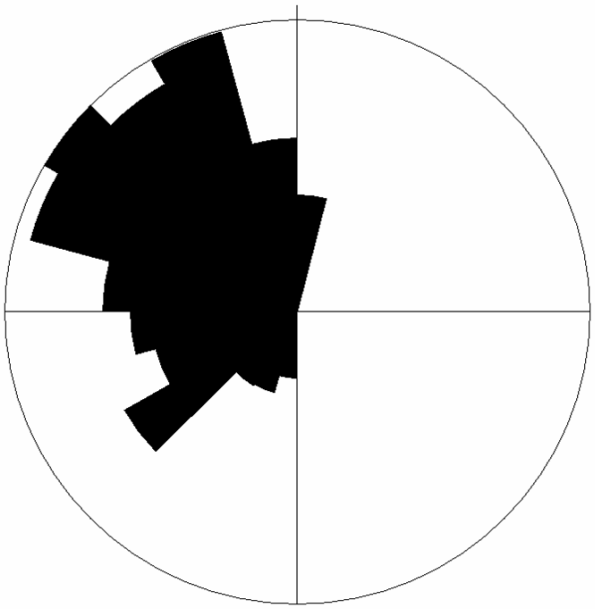

**Figure 6.24: Polar plot of snowblow are with area-weighted 15˚ sector lengths.**

| | Widdygill Foot |
|---|---|
| Glacier area ($km^2$) | 1.24 |
| Total snowblow area ($km^2$) | 0.81 |
| Snowblow area by 90° quadrants expressed as a percentage of the total snowblow area (%) | |
| NE (0-90°) | 2.73 |
| SE (91-180°) | 0.00 |
| SW (181-270°) | 21.28 |
| NW (271-360°) | 76.00 |
| S (135-225°) | 3.74 |
| W (226-315°) | 57.03 |
| Snowblow factor by 90° quadrants | |
| NE (0-90°) | 1.48 |
| SE (91-180°) | 0.00 |
| SW (181-270°) | 4.14 |
| NW (271-360°) | 7.83 |
| S (135-225°) | 1.74 |
| W (226-315°) | 6.79 |
| Mean snowblow factor | 3.66 |
| Ratio of snowblow area to glacier area | 0.65 |

**Table 6.8: Snowblow areas and snowblow factors identified around the Widdygill Foot glacier using the criteria outlined in chapter 3.**

### 6.3.4 Glacier dynamics in Widdygill Foot

Reconstructed steady state dynamics of the Widdygill Foot glacier indicate that the glacier is viable based on the methodology outlined in chapter 3. The glacier has a required basal motion of 0 % indicating that glacier motion was entirely by internal ice deformation or subglacial bed deformation (see table 6.9).

| | Widdygill Foot |
|---|---|
| ELA (m) | 323.00 |
| Temperature proxy used | Coope and Joachim (1980) St Bees Head |
| Proxy site altitude (m OD) | 0.00 |
| $T_3$ at proxy site (°C) | 8.25 |
| Temp. at ELA (0.0065°C/m lapse rate) | 6.15 |
| Degrees surface slope at ELA | 9.25 |
| Max ice thickness at ELA (m) | 148.36 |
| Glacier shape factor | 0.89 |
| Normal stress at centre point of ELA (bars) | 5.28 |
| Ablation gradient at ELA (mm/m) | 7.88 |
| Mass loss at ELA (ma-1) | 2.80 |
| Net Ablation ($m^3$ w.e.) | 382,966.76 |
| Mass flux ($m^3$ ice) | 420,842.59 |
| Cross sectional area at ELA ($m^2$) | 107,725.50 |
| Perimeter of bed at ELA (m) | 823.14 |
| Mean balance velocity at ELA ($ma^{-1}$) | 3.56 |
| Basal shear stress at ELA (bars) | 1.22 |
| Max ice deformation velocity at ELA ($ma^{-1}$) | 29.85 |
| Average ice deformation velocity at ELA ($ma^{-1}$) | 9.23 |
| Required basal motion ($ma^{-1}$) | 0.00 |
| Required basal motion (%) | 0.00 |

**Table 6.9: Reconstructed steady-state dynamics and flow characteristics of the glacier occupying Widdygill Foot during the Loch Lomond Stadial.**

The Widdygill Foot glacier also has the lowest ELA of the six glaciers considered thus far. Since temperature is a function of altitude, Widdygill Foot also has the highest 3-month summer temperature at the ELA of 6.15°C. Furthermore Widdygill Foot also has the highest ablation gradient, of 7.88 mm $m^{-1}$, which is again a function of the temperature at the ELA (see chapter 4 equations 8 and 9).

The shape factor of 0.89 associated with the Widdygill Foot glacier was calculated using equation 15 in chapter 4 and is a reflection of the across valley profile at the ELA of the glacier shown in figure 6.25 below. The across valley profile indicates a smooth sided valley with side

which slope at approximately the same angle. Unlike Mosedale however, the valley bottom contains a large undulation which accounts for the thinner ice seen in the centre of the channel while the maximum ice thickness is attained to the south of the valley centre point.

The ice surface of the proposed Widdygill Foot glacier displays a relatively smooth descent from ~ 1.8 km to the terminus. Above this point the ice becomes significantly thinner towards the glacier's maximum altitude and both the bed and ice surface slopes increase. The bed in the lower half of the glacier possesses a very shallow slope before an abrupt break of slope at ~ 1.25 km above which the valley floor ascends much more sharply. The result of this abrupt change in bed slope is a section of substantially thicker ice around the mid-altitude of the glacier (see figures 6.25 and 6.26 below).

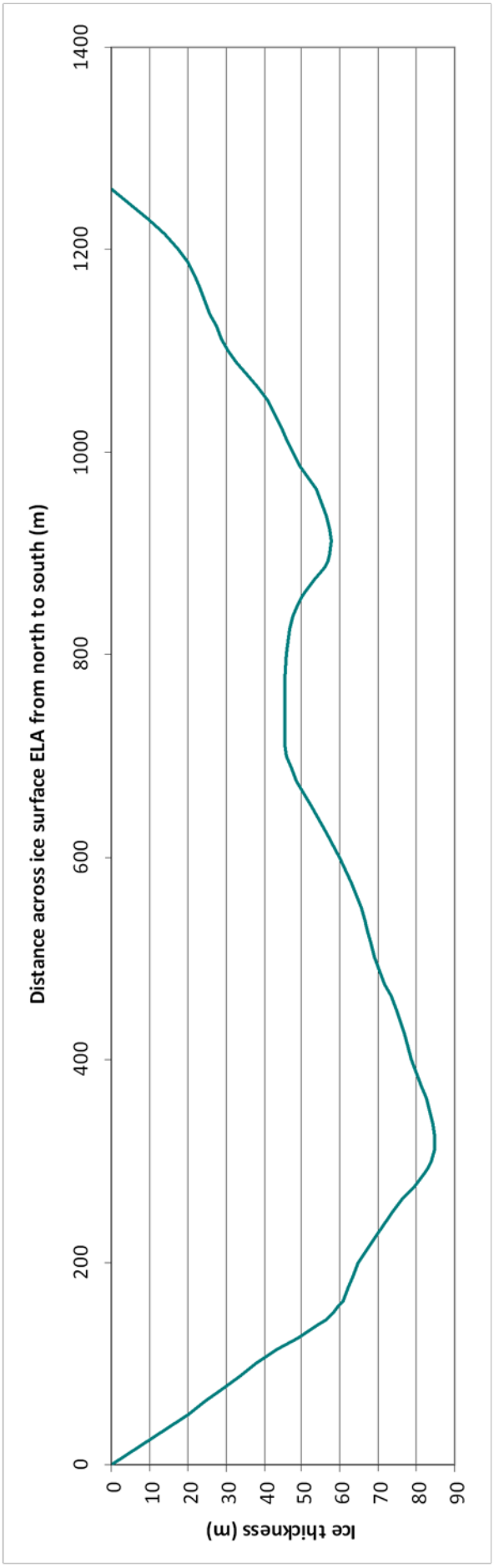


**Figure 6.25: A cross sectional profile south to north across the ELA of the Widdygill Foot glacier. ELA altitude = 323 m OD.**

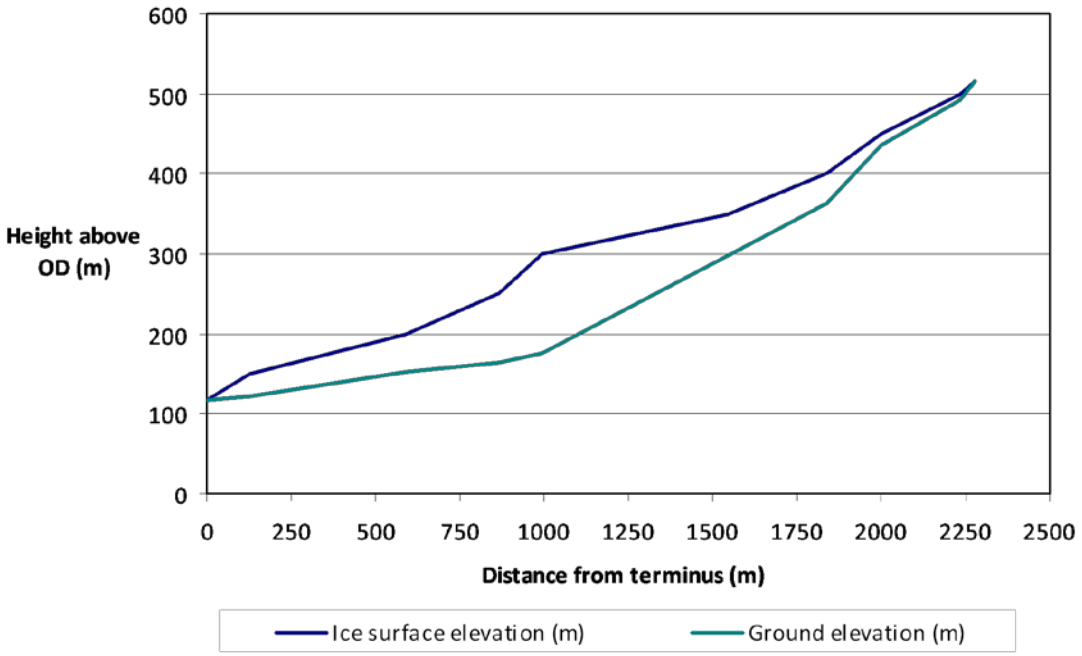


**Figure 6.26: A cross sectional profile along the long axis of the Widdygill Foot glacier.**

As would be expected from an idealised distribution of glacier surface area over altitude, the largest surfaces areas of the Widdygill Foot glacier are found in the mid-altitudes. Figure 6.27 below indicates that the largest surface area is found between 350 and 400 m OD with the smallest surfaces areas at the minimum and maximum altitudes. This is the result of the glacier occupying a 'bowl shaped' area at the head of the Widdygill Foot valley before the upper portion of the glacier curves around almost 90° up towards Pike of Blisco. This is further illustrated in the hypsometric curve of figure 6.28 and the net balance profile in figure 6.29, below which indicate a noticeably steeper increase in surface area at ~ 400 m OD.

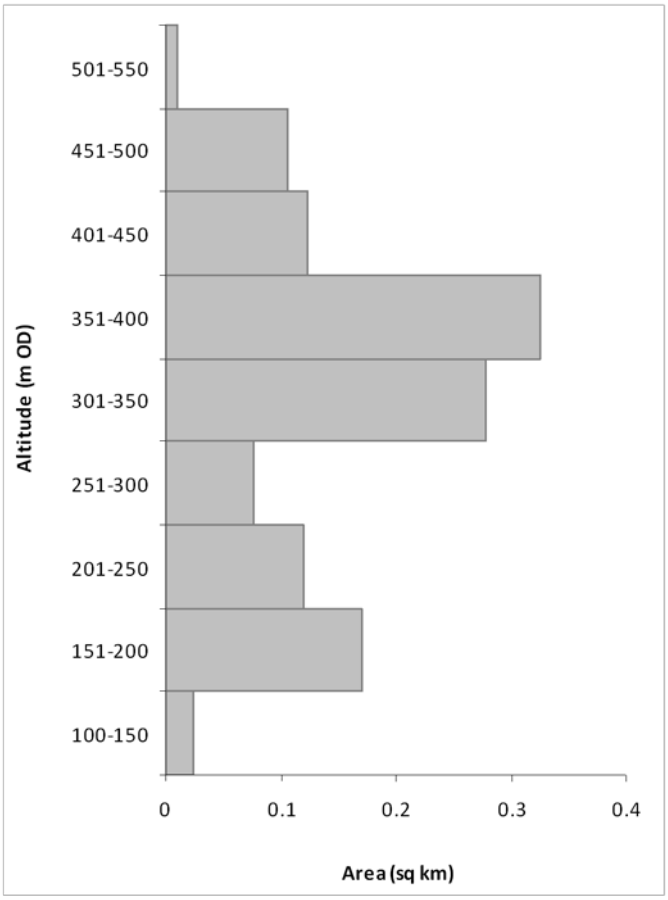


**Figure 6.27: The distribution of the glacier's surface area between the 50 m ice surface contour intervals. ELA = 323 m OD.**

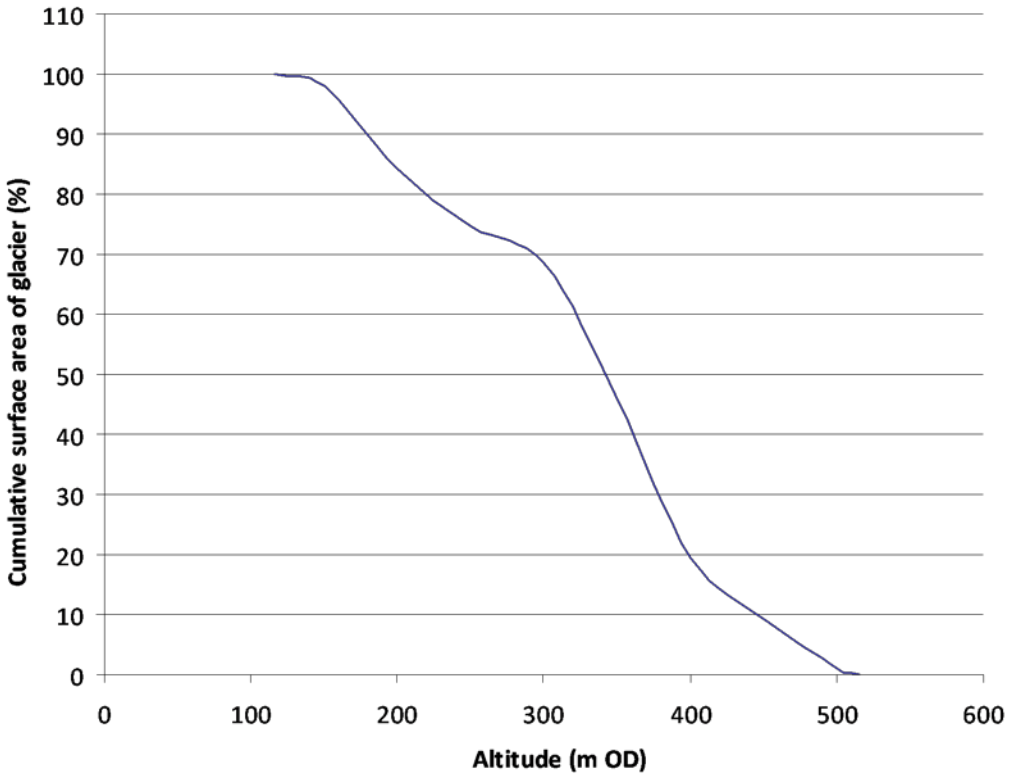


**Figure 6.28: Hypsometric curve for the Widdygill Foot glacier.**

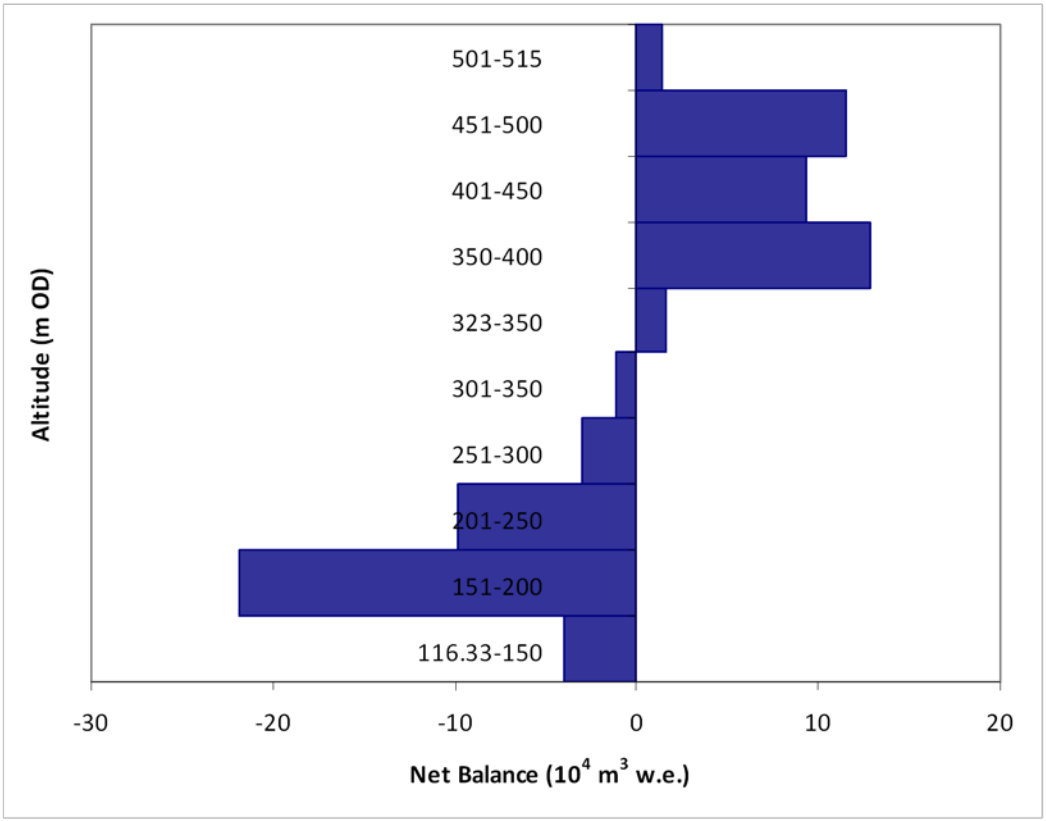


**Figure 6.29: The net balance profile of the Widdygill Foot glacier.**

## 6.4 Summary

- Six independent glaciers in the south-west Lake District have been proven to be glaciologically viable.
- The geomorphology associated with these glaciers in shown in a regional context below in figure .
- Throughout the south-west Lake District, moraines associated with the Loch Lomond Stadial trend down valley at approximately 45° to the long axis of the valley.
- The accumulation of post-glacial sediments has in some areas subdued the geomorphology however moraines of Loch Lomond Stadial origin generally have sharp basal breaks of slope and crestlines.
- They are also often present as arcuate ridges across the valley bottoms which formed around the snout of a Loch Lomond Stadial valley glacier.

**Figure 6.30: The geomorphology of the south-west Lake District from Kirk Fell in the north to Hardknott Pass in the south and from Pillar in the west to Langdale in the east.**

**OVERSIZE FIGURE APPEARS AT END OF THESIS**

# Chapter 7

# INTERPRETATION AND DISCUSSION

# 7: DISCUSSION

## 7.1 Previous work in the Lake District

### 7.1.1: The work of Manley (1955: 1959) and Sissons (1980)

It has long been recognised that glaciers occupied the valley-heads of the Lake District during the short lived climatic deterioration known as the Loch Lomond Stadial. Despite this the first attempt to map the extent of these glaciers was by Manley in 1959 (see figure 7.1). The small scale of this map however restricted the inclusion of detailed field data and impeded the precise identification of glacier limits. Consequently Sissons (1980a) (figure 7.2) later mapped the area at a scale of 1:10,000 and identified 64 independent alpine style glaciers in the Lake District during the Loch Lomond Stadial, many of which corresponded to the smaller glaciers initially mapped by Manley (1959).

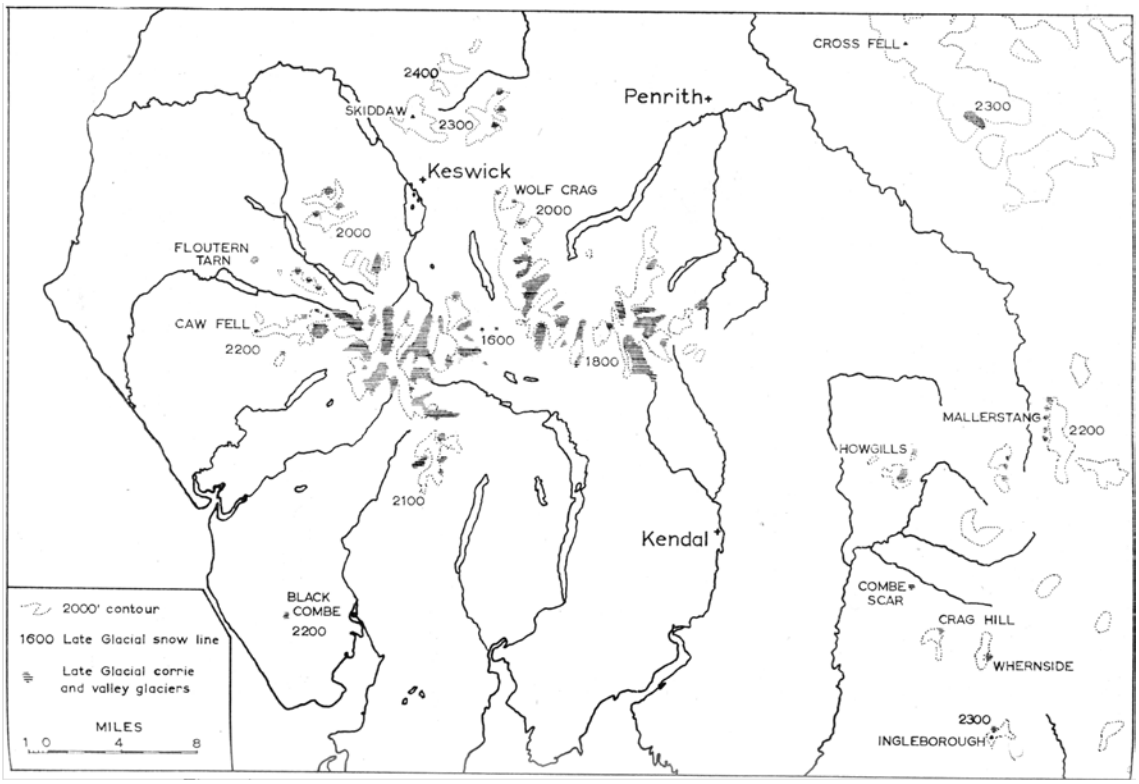


**Figure 7.1: Reconstructed Loch Lomond Stadial glaciers in the Lake District according to Manley (1959).**

In order to identify moraines pertaining to the Loch Lomond Stadial Manley (1955: 1959) used the idea of 'freshness' of form with respect to moraine morphology with the freshest moraines assigned to the most recent glaciation of the area, the Loch

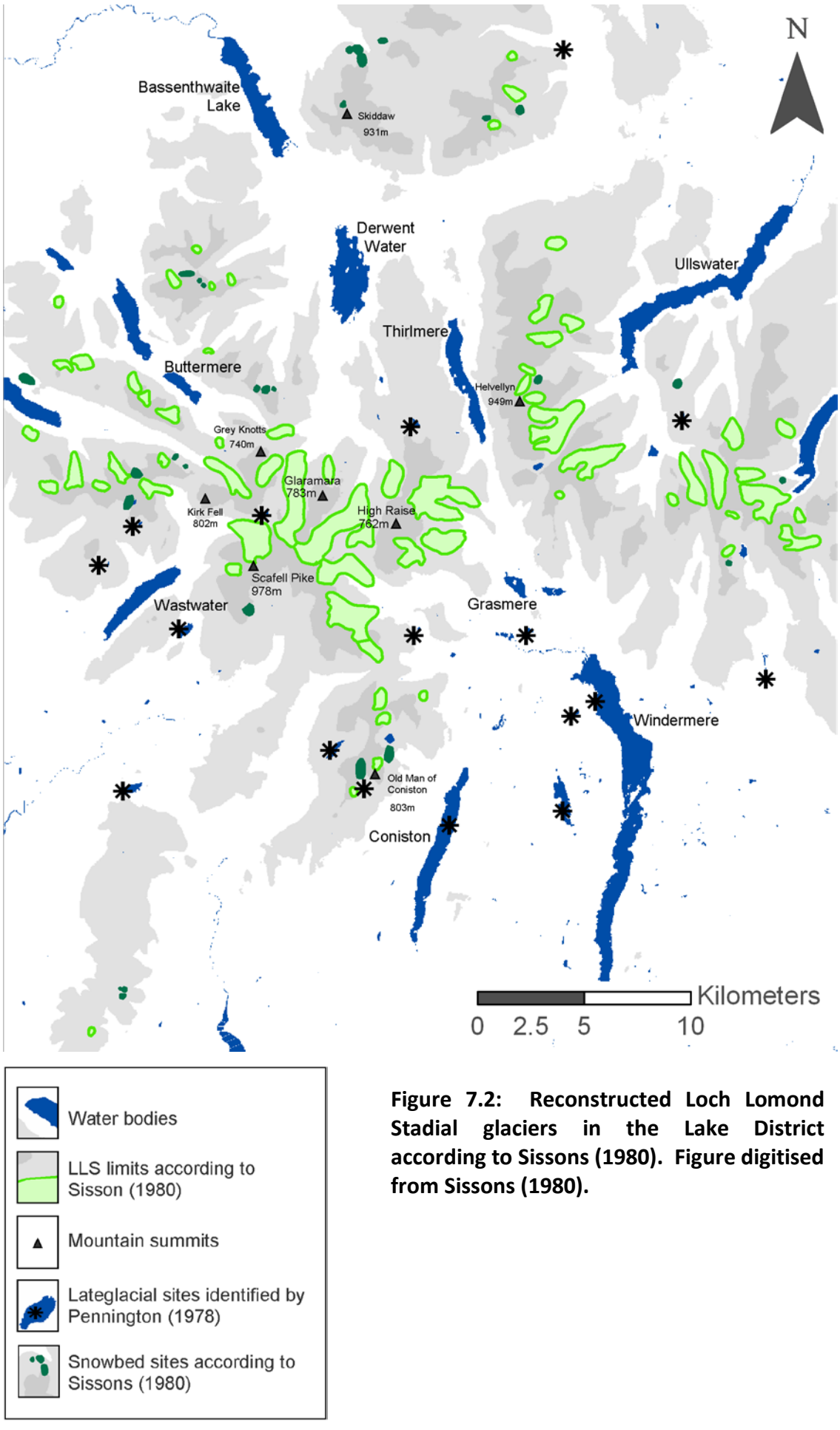


**Figure 7.2: Reconstructed Loch Lomond Stadial glaciers in the Lake District according to Sissons (1980). Figure digitised from Sissons (1980).**

Lomond Stadial. Sissons (1980) also adopted this approach. Wilson (2002) however notes that the differences found between the maps of glacier masses produced for the Loch Lomond Stadial in the Lake District by Manley (1959) and Sissons (1980) are substantial, with some glaciers identified by Manley (1959) and Pennington (1978) not included on Sissons (1980) map. This difference highlights the difficulty in using this method as a means of assigning landforms to a particular glacial phase (Wilson, 2002). More recent work has emphasised that moraine morphology is a reflection of a range of glaciological and sedimentological factors. Along with the impact of human occupation which may modify landforms from their original form, this suggests that the qualitative assessment of moraine morphology in terms of 'freshness' in order assign an age is tenuous (McDougall, 1997: Wilson, 2002).

On a smaller scale, the topography of the Lake District strongly influences precipitation distribution both at present and during the Loch Lomond Stadial (Sissons, 1980b). Of the 64 ice masses identified by Sissons (1980a), the largest ice masses were found along a west-east transect through the central fells, with the smallest glaciers in the north-west Lake District. Such small glaciers are likely to have been associated with a precipitation shadow in the north-west Lake District. This will have limited direct input of snow to the glacier surface so instead such glaciers were maintained as a result of local factors. These included high snow-blowing ratios in the south-east and south-west quadrants and low amounts of direct insolation (Sissons, 1980b). Also, Evans (1994) has calculated the mean aspect of the cirque median axes for the 158 cirques found within the Lake District as 048˚ which is coincident with the north-easterly aspect of glaciers proposed by Sissons (1980a).

### 7.1.2: Plateau Icefields: a more extensive glaciation in the Lake District

More recently however, McDougall (1997: 2001) has proposed a rather different style of glaciation during the Younger Dryas which involved the occurrence of plateau icefields centred principally on High Raise (55 $km^2$), with smaller icefields to the west centred on Grey Knotts/Brandreth (7 $km^2$) and Dale Head (3 $km^2$) (see figure 7.3). Gellatly et al. (1988), Rea et al. (1998) and Evans and Rea (2002) have studied modern plateau icefields in northern Norway, notably Troms-Finnmark, where receding icefields have revealed areas of little or no subglacial erosion. Such areas have been attributed to formation under the low basal shear stresses found beneath cold-based non-erosive ice. These conditions have been found to preferentially develop in association with slow-moving, relatively thin ice combined with low mean annual air temperatures found on plateau surfaces (McDougall, 2001). It must also be considered that the mass balance of the proposed outlet glaciers and thus their equilibrium line altitude (ELA) would largely have been dictated by the size of the plateau feeding it (Rea et

al., 1998). The presence of a plateau icefield would therefore imply a considerably higher ELA then for Sissons' proposed alpine-style glaciers: consequently, previous palaeoclimatic inferences based on those will require revision (McDougall, 2001).

The recession of plateau icefields in contemporary glacial environments during the 21st century has enabled researchers to gain a greater understanding of the geomorphology and ice dynamics associated with such areas. The geomorphic impact of the plateau icefields in the Lake District appears to have been minimal on the plateau summits. McDougall (2001) records the presence of blockfields and other frost-weathered debris (mostly peat-covered) which are taken as indicators of at least patchy cold-based ice occupation of the area during the Loch Lomond Stadial. The presence of ice moulded bedrock at the margins of the High Raise plateau indicates the transition from cold-based non-erosive ice on the plateau to warm, wet-based erosive ice in the valleys. The outlet glaciers of the plateau icefield proposed by McDougall (1998) are frequently delimited by extensive suites of moraines across the valley floors. The linearity within these moraines is taken, by McDougall (1998), as evidence of active ice retreat towards the plateau sources at the close of the Loch Lomond Stadial. The style of glaciation proposed by McDougall (1998) is clearly much more extensive than that proposed by Sissons (1980) and Manley (1959); however some similarities are present.

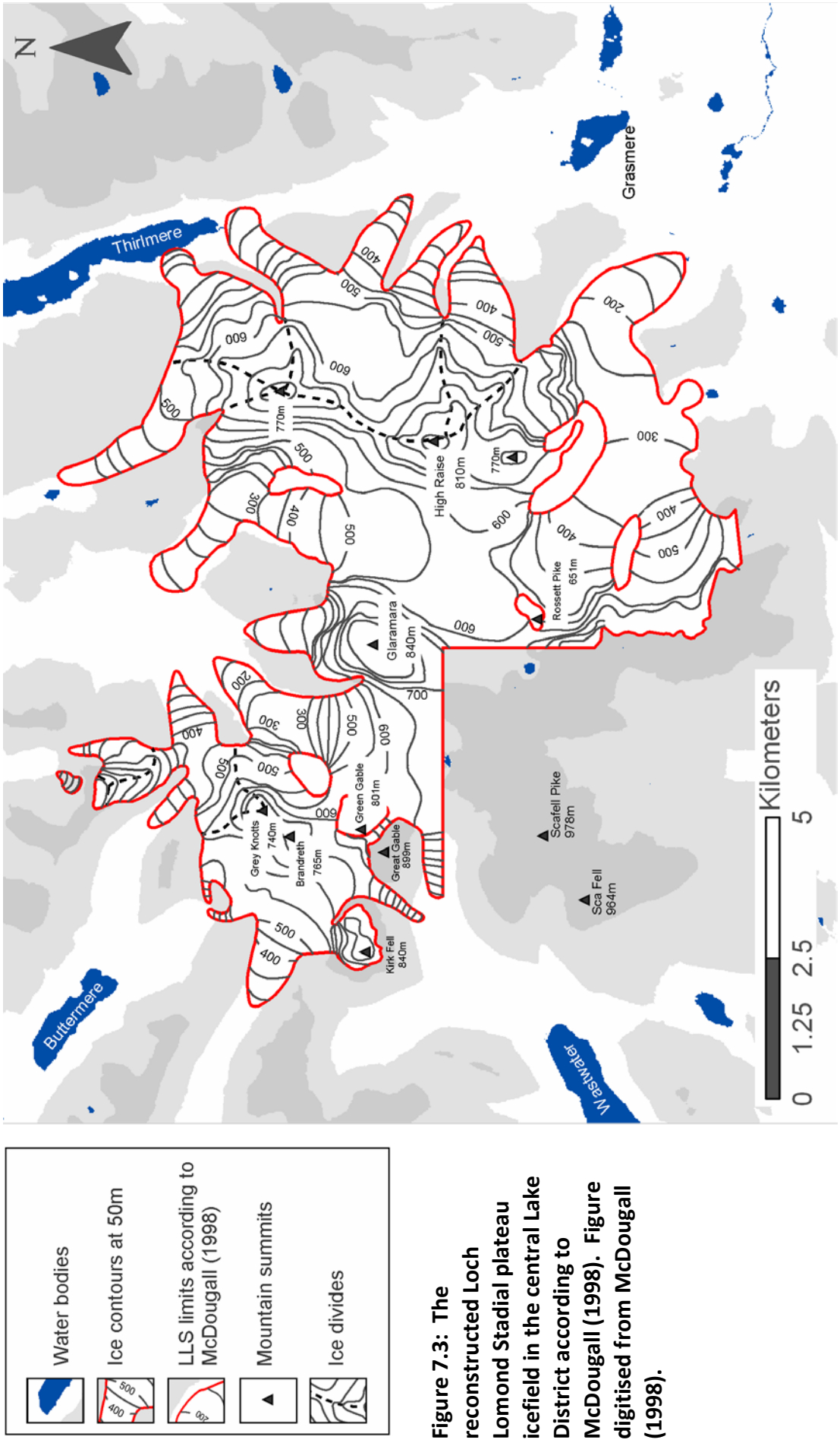


**Figure 7.3: The reconstructed Loch Lomond Stadial plateau icefield in the central Lake District according to McDougall (1998). Figure digitised from McDougall (1998).**

On the eastern side of the central fells, the termini of the Greenburn Beck and Easedale glaciers proposed by McDougall (1998) closely correspond with the limit of the alpine glaciers proposed by Sissons (1980). Similar correspondence occurs in Ennerdale and to the north of Glaramara. In other areas, McDougall (1998) interprets the moraines suggested by Sissons (1980) and Manley (1959) as the products of active ice retreat during deglaciation. The major difference however between the two styles of glaciation presented above relates to the upslope limit of glaciation. While Sissons (1980) interprets the transition from ice moulded topography below to frost shattered topography above as the upper limit of the ice, McDougall (1998) considers that this is merely a product of a thermal boundary within the ice. Unlike other areas of the British Isles the transition from ice moulded to frost shattered topography within the Lake District often appears as a continuum rather than a sudden change (a trimline). Ballantyne and McCarroll (1995) hypothesise that there are a number of explanations for these transitional zones.

Firstly, frost shattering on high ground may simply reflect more pronounced breakdown of rock at high altitudes. Secondly the weathering limit may be a high-level weathering limit, which developed during ice-sheet down wastage, possibly during the transition from Stadial to Interstadial, or may be the result of a readvance of ice during overall retreat (Ballantyne and McCarroll, 1995). Alternatively, it is proposed that the boundary is a weathering limit rather than a periglacial trimline representing a thermal boundary between the upper cold-based ice and the lower more erosive warm-based ice within the former ice sheet (Ballantyne, 1997: Ballantyne and McCarroll, 1995: Rae et al., 2004). Finally, Ballantyne (1997) notes that the weathering limit may be 'a 'true' periglacial trimline that marks the altitude of the surface of the last ice sheet at its maximum thickness` (Ballantyne, 1997, p. 128).

In the absence of reliable dates, it cannot be assumed that the geomorphology and the extent to which weathering has occurred can be used to distinguish between sites that remained uneroded because they were covered by cold based non-erosive ice and those that stood above the ice as nunataks in a periglacial environment (Nesje et al., 2007). The gradual nature of these transitions in the Lake District however allows the current author to agree with McDougall (1998) who believes that they are the products of a thermal boundary within the ice. This supports the conclusions that plateau icefields occupied the Lake District during the Loch Lomond Stadial.

### 7.1.3: Work more recent than Sissons (1980)

Work subsequent to that of Sissons (1980a) argues for a more extensive Loch Lomond Stadial glaciation. 13 further sites have been identified by Clark (1992), Evans (1994), Wilson and Clark (2002) and Wilson (1999: 2004) as hosts for Loch Lomond Stadial glaciers based on morphological evidence. Wilson (2002) has provided descriptions of moraines at three sites in the south-central Lake District: Widdygill Foot, Blindtarn Moss and Cotra.

Blindtarn Moss, a northeast facing cirque 2 km south-west of Grasmere, has been defined as a class 1 cirque by Clough (1977) who identified 198 possible cirques in the Lake District (72 of which were classified as 'dubious' or 'indistinct') (Evans and Cox, 1995). This number has since been reassessed by Evans and Cox (1995) who have identified a complete population of 158 cirques in the Lake District. Both Manley (1959) and Walker (1966) have identified moraine ridges and mounds within the Blindtarn Moss cirque however they disagree on their period of formation. Manley (1959) assigns the moraines, which he describes as 'crescentic and very fresh looking moraines' (Manley, 1959, p. 203), to the Loch Lomond Stadial, while Walker (1966) prefers an origin in an earlier glacial phase due to the more subdued topography found in the area.

Also not included as a site which nourished a Loch Lomond Stadial glacier by Sissons (1980a) was Cotra, a site on the steep eastern side of Steel Fell north of Grasmere. Several studies have identified moraines at this location: however most have suggested that this site pre-dates the Loch Lomond Stadial (Manley, 1959: Walker, 1966: Sissons, 1980a) with the exception of Pennington (1978). The dominant moraine at this site runs along the foot of the slope almost parallel to the A591 road for 1.5km and has a maximum width of 450 m. Its downslope limit is well defined (possibly with some steeping due to the influence of Raise Beck) however as a result of debris accumulation along its upslope margin the moraine's upper limit is somewhat obscured (Wilson, 2002). The reconstructed glacier at Cotra has however more recently been dismissed as 'glaciologically unviable' by Carr and Coleman (2007).

With respect to each of these sites, Wilson (2002) is able to convincingly argue that they nourished glaciers during the Loch Lomond Stadial by using three lines of evidence. Firstly, as outlined previously, in view of the work of Benn (1992) and McDougall (1997: 2001) the term 'freshness' with respect to moraine morphology in order to assign a date to its formation should be used with caution. Secondly, readvances of the Dimlington Stadial ice sheet in the Northern Irish Sea occurred between 17.6 and 16.8 cal. Ka BP as proposed by McCabe and Clark (1998) and McCabe et al. (1998) in response to Heinrich event 1 in the North Atlantic. Merritt and Auton (2000) have provided evidence of the 'Scottish Advance' into the Lake

District and have proposed substantial contemporaneous valley glaciers in both Ennerdale and Wasdale. However, the work of Pennington (1978) suggests that the Windermere basin was ice free between 17.6 and 16.8 cal. Ka BP and consequently correlative moraines in the southern Lake District have been assigned to an earlier glacial phase. Since the moraines discussed above lie well inside this glacial limit Wilson (2002) is able to propose that they date to a more recent glaciation. Based on biostratigraphy and geomorphology evidence, the most recent glaciation of the British uplands is confidently assigned to the Loch Lomond Stadial and consequently the absence of absolute dates for the moraines at Widdygill Foot, Blindtarn Moss and Cotra has led to the suggestion that these moraines also relate to that glacial phase (Wilson, 2002).

In the eastern fells the valleys of Fordingdale, Swindale and Wet Sleddale are considered to have nourished glacier ice during the Loch Lomond Stadial, again indicating that the Loch Lomond Stadial in the Lake District was far more widespread than initially indicated by Manley (1959) and Sissons (1980a). At these 3 locations Wilson and Clark (1998) note that despite the upslope limits of glaciation being unclear due to a lack of geomorphological evidence, the downslope limit provides sufficient evidence to propose glacier occupation of the 3 valleys.

Wilson and Clark (1999) have also investigated a further four sites in the northern Lake District where Loch Lomond Stadial glacial and periglacial debris accumulations are present. Three of these sites, Nine Gills Comb, Great Cockup and Dale Beck – Yard Steel, are considered to be the result of glacial deposition during the Loch Lomond Stadial. However, the deposits at Dale Beck – Clints Gill-Blea Gill are considered to be remnants of a protalus rampart due to their morphology, location and close proximity to the foot of the back slope (Wilson and Clark, 1999).

Further moraines are noted by Clark (1992) on the northern side of the Kirkstone Pass in the eastern Lake District however he did not reconstruct the associated Loch Lomond Stadial glaciers. Clark (1992) records the presence of moraines throughout Dovedale in Caudale Cove on Caudale Moor, around Brotherswater, below Black Crags and Dove Crag and around Hayswater. Extensive ground moraine is also present throughout Dovedale along with numerous moraine ridges which can be traced along the hillsides and are assumed to make the maximum extent of the Loch Lomond Stadial glaciers in the area. Figure 7.4 below provides a compilation of the Loch Lomond Stadial glacier reconstructions that have occurred in the Lake District and are believed to most accurately represent the maximum extent of the glacial occupation in the Lake District during the Stadial.

**Figure 7.4: The reconstructed Loch Lomond Stadial ice occupation of the Lake District according to McDougall (1998), Sissons (1980), Pennington (1978) and the current author. Figure digitised and modified from original sources.**

**OVERSIZE FIGURE APPEARS AT END OF THESIS**

### 7.2 Regional glaciation in the Lake District

Figures 7.4 and 7.5 provide compilations of the work of McDougall (1998), Sissons (1980), Wilson and Clark (1998: 1999), Pennington (1978) and the current author. The map assumes that the most recent interpretation of the ice in the Lake District during the Loch Lomond Stadial as a plateau icefield is correct. The plateau icefield replaces a series of alpine glaciers that were proposed by Sissons (1980) in the central fells. Away from the central fells, the maps indicate a more alpine style of glaciation where plateau summits are less extensive or are not present. These glaciers, which are shown in green, are digitisations of the glaciers proposed by Sissons (1980). In the far eastern fells near Haweswater, the glaciers reconstructed by Wilson and Clark (1998) in Fordingdale, Swindale and Wet Sleddale are also included. In the northern fells near Skiddaw, three glaciers reconstructed by Wilson and Clark (1999) occupy Nine Gills Comb, Great Cockup and Dale Head-Yard Steel.

In addition to this, the work of the current author has also been included to fill the area not covered by McDougall (1998) in the south-west Lake District. The glaciers in Mosedale, Lingmell Beck, Lingmell Gill and Widdygill Foot all remain independent of the central plateau icefield. The glaciers in Upper Eskdale and Red Tarn/Wrynose Bottom however are connected to the plateau icefield at ice divides to the east and west of Esk Pike and to the north of Red Tarn respectively. The glacier at Red Tarn joins onto the ice occupying Oxendale across an ice divide in a similar arrangement to that suggested by Sissons (1980) for the Oxendale/Red Tarn area. The glacier in Upper Eskdale has a northern margin around Esk Pike at two ice divides. On the northern side of the ice divides some modification of the reconstruction provided by McDougall (1998) was necessary in order to make it more compatible with the presence of a glacier in Upper Eskdale. Since fieldwork was not carried out around Allen Crags (785 m OD) the reconstruction in this area is based purely on that provide by Sissons (1980). This leaves Allen Crags as a nunatak and extends the southern margins of the Langstrath and Grains Gill glaciers further south to meet the Upper Eskdale glacier at the ice divides.

Further west around Lingmell Beck, the reconstruction provided by McDougall (1998), which shows ice covering Styhead Tarn, also required some modification. Pennington (1978) provides evidence for an ice free environment at Styhead Tarn during the Loch Lomond Stadial. This evidence was dismissed by McDougall (1998) as unsubstantive: however the current author disagrees.

Palynological analysis has been carried out at 35 sites in the Lake District by Pennington (1978: 1996). The sedimentology and associated pollen assemblages at each of these sites, all of

which are shown on figure 7.2, were used to establish the environmental conditions during the Loch Lomond Stadial, Lateglacial Interstadial and earlier. At Styhead Tarn, clay, believed to be of Loch Lomond Stadial age, overlies a slightly organic silt of Interstadial age, which overlies a series of pre-Interstadial clays. Styhead Tarn is the highest altitude tarn in the Lake District which does not show stratigraphic disturbance during the Interstadial but just slight disturbance in the uppermost section of the core which is believed to be associated with ice melt at the close of the Loch Lomond Stadial. The core taken from Styhead Tarn can essentially be split into 3 sections. The upper boundary of the pre-Interstadial clay lies at ~ 55 cm depth. Above this 18 cm of organic silt is represented in the pollen record by an increase in Betula, Cyperaceae, Juniperus and Emptrum during the Interstadial. At a depth of 37 cm an abrupt transition into the Loch Lomond Stadial clay is seen and is accompanied by a reduction in Betula, Cyperaceae, Juniperus and Emptrum and an increase in Artemsia. This core therefore provides a high resolution (1 cm sampling spacing) record of the pre-Interstadial to early Holocene environment around Styhead Tarn. Coring at Styhead Tarn by the current author unfortunately did not reveal a similar sedimentological record to that of Pennington (1996): however it did not provide any evidence upon which to question the findings of Pennington (1996). It is believed that the core retrieved from Styhead Tarn by the current author contained pre-Interstadial clay throughout its entire length. Further investigation would therefore have been preferable however a thick layer of gravel and lack of equipment by which to reach the centre of the lake made this unachievable. The grounds upon which McDougall (1998) therefore dismisses Styhead Tarn as an ice free site during the Loch Lomond Stadial can easily be questioned. It is therefore suggested that the record provided by Pennington (1996) is far more robust than an argument to the contrary.

The modified map therefore shows the glacier in Lingmell Beck as independent of the main plateau icefield with the area around Styhead Tarn as ice free during the Stadial (figure 7.5). In order to achieve this, ice descending from between Great Gable and Green Gable down Aaron Slack was shortened to form a tongue immediately to the west of Styhead Tarn. Ice to the north of the tarn was also modified to form a tongue of ice in Styhead Gill which leaves Seathwaite Fell (601 m OD) ice free. Neither of these modifications were based on geomorphological evidence collected by the current author, they are simply the most reasonable modifcations to the reconstruction provided by McDougall (1998) which allow an ice free environment at Styhead Tarn. By providing an ice free environment at Styhead Tarn, the work of Pennington (1976: 1996) noted above can be successfully incorporated into the regional LLS reconstruction for the whole Lake District. It is acknowledged that further investigation into the LLS conditions at Styhead Tarn is now necessary before further

refinement of the LLS ice margins in the area can be achieved. Further investigation should prioritize the need for a chronological control on the stratigraphy reported by Pennington (1976: 1996) at Styhead Tarn. Unfortunately, however, this was beyond the scope of this project.

A further much smaller addition to figure 7.4 occurs around Redacre Gill where inspection of the moraines around the ice margin proposed by McDougall (1998) reveals moraines further south than the proposed ice margin (see figure 7.4). These moraines show similar morphological characteristics and magnitude to the moraines deemed elsewhere in this study to be of Loch Lomond Stadial origin and thus the ice margin has been extended south. Due to time constraints, the limits of the plateau icefields proposed by McDougall (1998) have not all been reconsidered here. Further work would therefore be valuable on the ice margins, particularly around areas such as Blea Tarn where an unusually shaped ice lobe is shown.

**Figure 7.5: The reconstructed Loch Lomond Stadial ice occupation of the central Lake District according to McDougall (1998), Sissons (1980), Pennington (1978) and the current author. Figure digitised and modified from original sources.**

**OVERSIZE FIGURE APPEARS AT END OF THESIS**

Crucially, the core retrieved from Styhead Tarn by Pennington (1978) has no dated chronology. Although Pennington (1978) indicates the presence of a Lateglacial tripartite sequence in Styhead Tarn which suggests an ice free environment at the Tarn during the LLS, the local topographic and geomorphological context may be taken to suggest that the area was beneath ice during the this period. The work of Pennington (1978) cannot be rejected on the basis of a lack of chronological control as this work is the most detailed evidence to date pertaining to the environmental conditions around Styhead Tarn during the LLS, however, an alternative glaciological reconstruction in presented below which assumes that ice did occupy the tarn during the LLS (figure 7.5). In this scenario, ice would have developed over the summit Glaramara and flowed radially outwards including west towards Styhead Tarn before turning north due to the presence of an ice divide trending north-west to south-east from Green Gable to Allen crags. To the south of this ice divide, ice over Styhead coalesced with ice in Lingmell Beck thus implicating the Lingmell Beck glacier reconstruction presented in chapter 4 in the plateau icefield presented by McDougall (1998). The are around Styhead Tarn would therefore have acted as an ice source area.

Because of the uncertainty surrounding the stratigraphic record found in Styhead Tarn by Pennington (1978), further work is clarly required in the area in order to determine whether or not Styhead was ice free during the LLS. This information will then facilitate a more accurate and informed glaciological reconstruction in the vicinity of Styhead Tarn during the LLS i.e. which of the two reconstructions presented here (figure 7.4b or 7.5) is most appropriate.

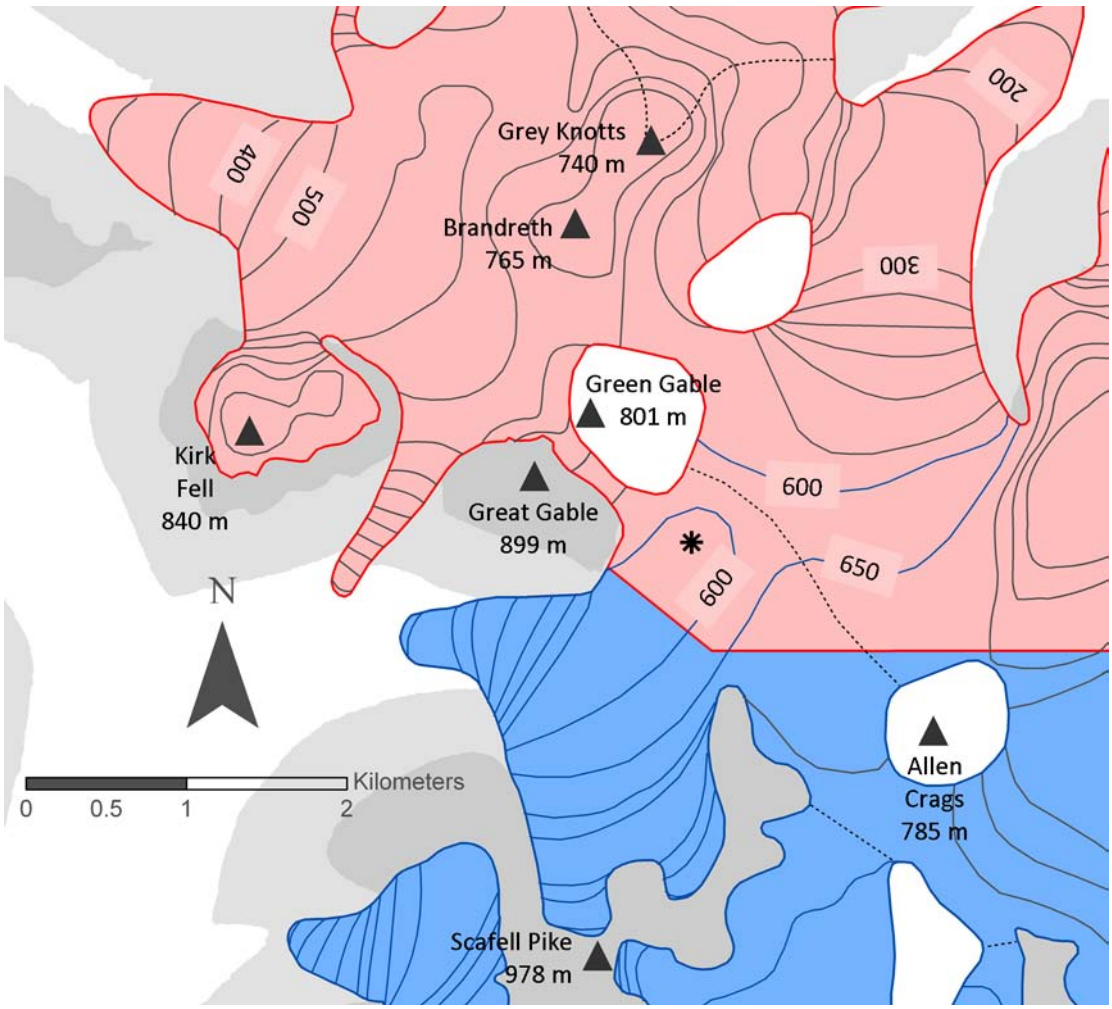


**Figure 7.5: An alternative LLS ice reconstruction for the area surrounding Styhead Tarn which involves the Lingmell Beck glacier presented in chapter 4 being connected to the plateau icefield proposed by McDougall (1998).**

## 7.3 Plateau icefields and palaeoclimate

### 7.3.1: Topoclimates and Plateau icefields

Manley (1955: 1959) demonstrated that a non-linear relationship exists between summit breadth and the altitude of the firn line on adjacent glaciers (figure 7.6). The impact of this on icefield formation is that as a summit becomes narrower, the altitude above the regional firn

line required in order to retain snow cover increases (Manley, 1955). The form of a summit will also strongly influence its ability to maintain permanent snow cover. Other factors controlling icefield formation relate to the climatic conditions. As discussed in an earlier chapter snowblow can often dictate the location of glacier formation however it should be remembered that snowblow also involves the removal of snow from adjacent ground. Manley (1955) notes that the proportion of snow removed by the wind can often result in snow/ice becoming too thin to withstand radiation and other losses and hence snow/ice is unable to persist in such areas to form an icefield. Interestingly Manley (1955) demonstrates this phenomenon with application to the rounded summit of Ben Nevis where it is roughly estimated that 'the winter's accumulation is of the order of one-half that which would prevail in shelter below the summit' (Manley, 1955, p. 453).

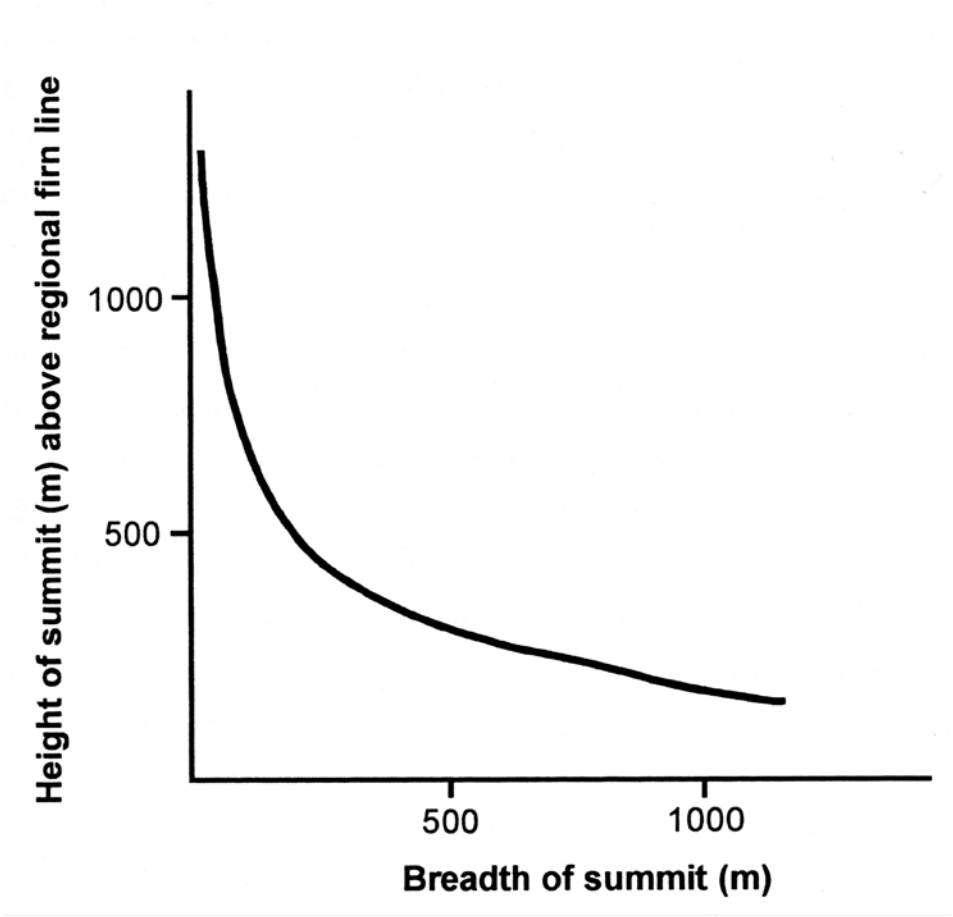


**Figure 7.6: As the breadth of a plateau summit decreases the height it must attain above the firn line in order for it to support a plateau icefield increases. Taken from McDougall (1998) originally adapted from Manley (1955).**

### 7.3.2: Plateau icefield landsystems.

As noted by Gellatly et al. (1988), in a study of Somerset Island Dyke (1983) suggested that Quaternary landform development can be associated with one of four zones: terrain covered by wet-based, highly erosive ice, terrain covered by dry-based, protective ice, nunataks that remained ice-free, and post-glacial marine sediments. Furthermore each zone is associated with distinctive geomorphology. Where wet based ice is found, ice-scoured bedrock and ice-sculpted forms with subglacial channels and ice-marginal channels in the till and bedrock are present. Contrastingly, where dry-based ice is found weathered bedrock and colluvium with an absence of glacial erosional features but with development of ice-marginal channels cut into weathered mantle is expected. Finally, weathered bedrock and colluvium with no ice-marginal channels can be associated with periglacial environments (Gellatly et al., 1988). It is therefore clear that temperature distributions have implication for glacial erosion and deposition and consequently for the formation of glacial landforms (Hooke, 2005). Via application of this theory, Rea et al. (1998) have derived a diagnostic landform assemblage associated with plateau icefields. Plateau icefield geomorphology can often be very subtle however if some parts of the plateau ice cover are above the pressure melting point and are therefore erosive, moraines may result. Such situations are largely associated with valley glaciers extending radially away from a central plateau region into lower altitude valleys. In these cases extensive suites of ice-marginal and ground moraine can be expected with variable inter- and intra-valley morphology. In the Lake District, 'ice-marginal moraines and drift limits have proved to be the single most important line of evidence in the search for palaeo-icefields' (Rea et al., 1998, p. 49).

Blockfields are landforms particularly associated with plateau icefields and commonly consist of '*in situ* angular boulders and stones up to several metres thick and formed through mechanical and chemical weathering of the local bedrock' (Nesje et al., 2007, p. 227). Rea et al. (1996) have considered the origin of blockfields associated with Øksfjordjøkulen, a plateau icefield in the Lyngen Alps Northern Norway where three hypotheses have been put forward regarding their formation. Firstly it is possible that they may be postglacial features which have evolved very quickly via a rapid freeze-thaw mechanism of bedrock exposed at the close of the last glaciation (the Loch Lomond Stadial). This theory can however be quickly dismissed as although a rapid freeze-thaw mechanism is plausible for softer carbonate rocks, this is not the case for much more resistant igneous or metamorphic rocks such as the Borrowdale volcanics in the Lake District. Similarly, the identification of many micro- and macro-scale erosional bedforms which remain preserved today in ancient glaciated landscapes such as the

British Isles make the suggestion of postglacial freeze-thaw action difficult to accept (Rea at al., 1996).

Secondly, blockfield formation during the various stages of deglaciation throughout the Pleistocene has been proposed notably by Nesje et al. (1988). This longer time period accounts for the occurrence of deep weathering profiles and rounded debris however it does not explain the relatively high abundance of clay minerals commonly found in blockfields which would require weathering rates to be fairly rapid rather than prolonged (Rea et al., 1996). Finally, a pre-pleistocene origin of blockfields has been proposed by various workers including Nesje et al. (1988), Rea et al. (1996), Fjellanger et al. (2006) and Nesje et al. (2007). This would involve blockfields first forming under temperate conditions followed by an exposure to periglacial conditions with clay-mineral assemblages being interpreted as the result of pre-glacial weathering. Rea et al. (1996) conclude by stating that blockfields are composite landforms resulting from a combination of deep weathering under temperate conditions and sorting by frost heaving processes, whereby corestones and coarser materials are moved vertically up, under periglacial conditions.

### 7.4 Oxendale and Mickleden: glaciologically viable glaciers

Before completely dismissing the alpine style of glaciation proposed by Sissons (1980) in the central fells, the glacier reconstructions should be tested. The glaciers proposed by Sissons (1980) in both Mickleden and Oxendale were digitised and slighted modified in line with the geomorphology (see figure 7.7 and 7.8). The valleys of Mickleden and Oxendale are large glacial troughs in the central fells of the Lake District. They lie at the head of the Langdale valley and both valley bottoms are occupied by extensive areas of linear moraines. Aerial photographs reveal moraines with distinct crests and clear basal breaks of slope. Such moraines are of a similar magnitude to those at the southern end of Upper Eskdale making the glacier margins relatively simple to reconstruct.

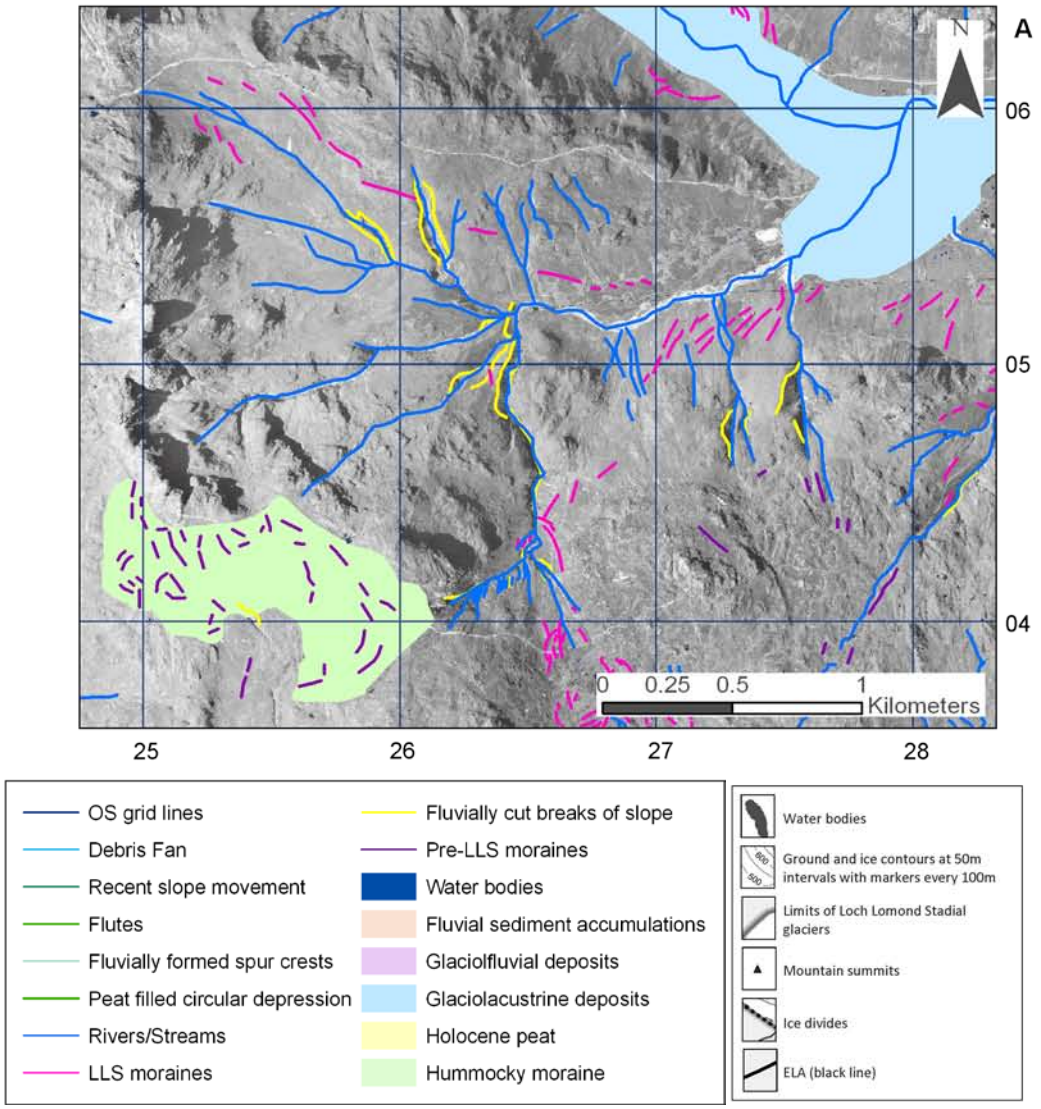


**Figure 7.7: The Loch Lomond Stadial in Oxendale according to Sissons (1980) and the current author. A: the geomorphology of the Oxendale valley. B: the reconstructed glacier in Oxendale.**

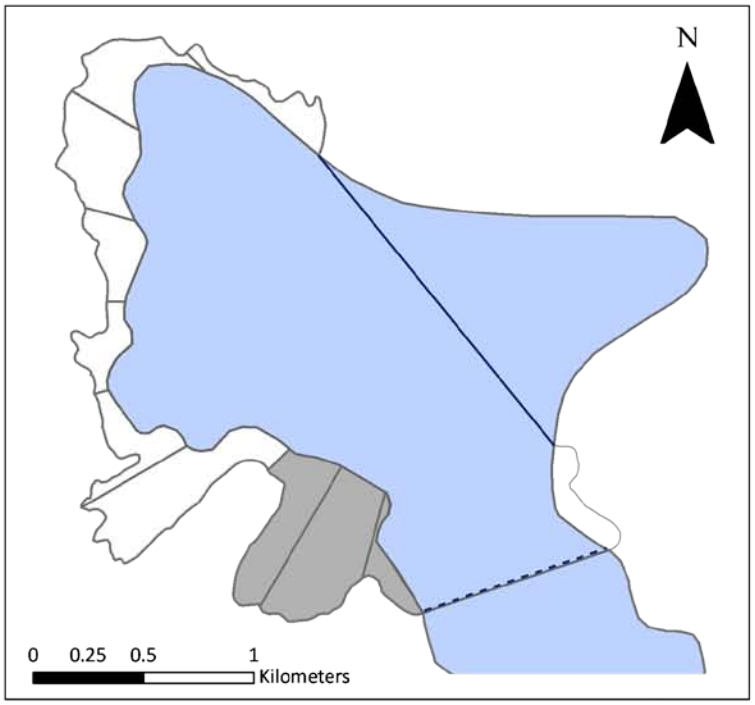


C

Figure 7.7: The Loch Lomond Stadial in Oxendale according to Sissons (1980) and the current author. C: the snowblow area associated with the Oxendale glacier. D: the hypsometric curve of the Oxendale glacier. E: the distribution of surface area over altitude of the Oxendale glacier. F: a cross sectional profile down the long axis of the Oxendale glacier

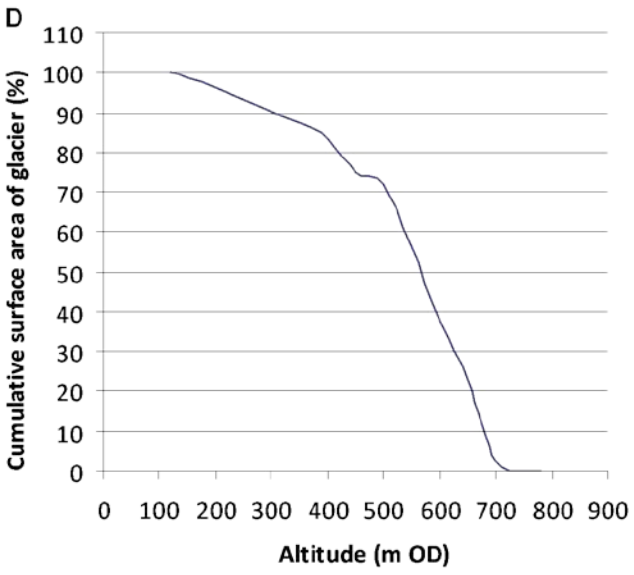


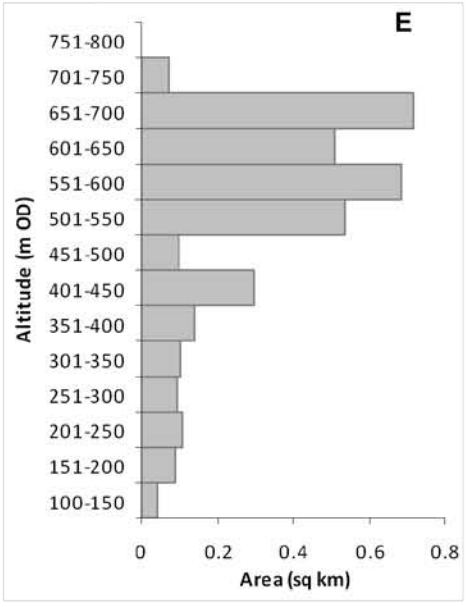


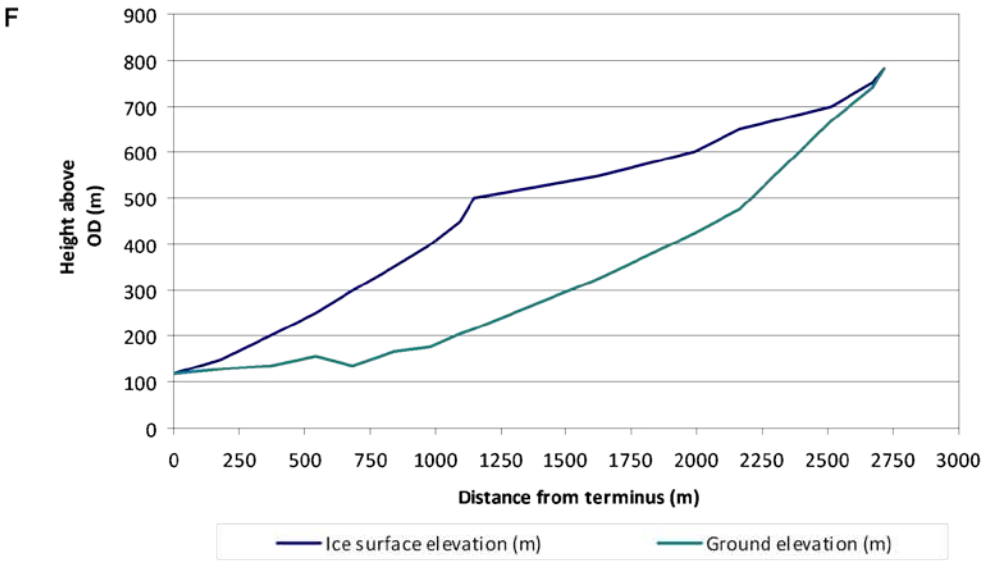

| TABLE A | | Oxendale |
|---|---|---|
| Area ($km^2$) | | 3.44 |
| Long axis length (m) | | 2756.35 |
| Max altitude (m OD) | | 781.45 |
| Min altitude (m OD) | | 117.55 |
| Mid-altitude (m OD) | | 449.00 |
| Lowest cirque | | |
| Name | | 127. Great Cove, Oxendale |
| Altitude (m OD) | | 635 |
| Grade (according to Evans and Cox, 1995) | | 2 |
| Altitude of highest lateral moraine (m OD) | | 599.97 |
| Toe to head altitude ratio method (THAR) (m OD) | | |
| | 35% | 349.92 |
| | 40% | 383.11 |
| | 45% | 416.31 |
| | 50% | 449.00 |
| Accumulation area ratio method (AAR) (m OD) | | |
| | 70% | 509.00 |
| | 65% | 526.00 |
| | 60% | 540.00 |
| | 55% | 555.00 |
| | 50% | 566.00 |
| Area weighted mean altitude method (AWMA) (m OD) | | 521.25 |
| Balance ratio method (Benn and Gemmell, 1997) (m OD) | | |
| | BR=2.00 | 512.17 |
| | BR=1.81 | 547.86 |
| | BR=1.60 | 551.83 |
| | BR=1.54 | 553.03 |
| | BR=1.43 | 555.38 |
| Balance ratio method (Osmaston, 2005) (m OD) | | |
| | BR=2.00 | 490.00 |
| | BR=1.81 | 497.00 |
| | BR=1.60 | 504.00 |
| | BR=1.54 | 507.00 |
| | BR=1.43 | 511.00 |
| | | 533.00 |
| Mean value of all of the above methods (m OD) | | 506.90 |
| Mean value of BR=1.54 (Osmaston, 2005), AAR 65% and AWMA (m OD) | | 518.08 |
| ELA used in subsequent calculations (m OD) | | 518 |

| TABLE B | Oxendale |
|---|---|
| ELA (m) | 518.00 |
| Temperature proxy used | Coope and Joachim (1980) St Bees Head |
| Proxy site altitude (m OD) | 0.00 |
| $T_3$ at proxy site (°C) | 8.25 |
| Temp. at ELA (0.0065°C/m lapse rate) | 4.88 |
| Degrees surface slope at ELA | 11.37 |
| Max ice thickness at ELA (m) | 302.20 |
| Glacier shape factor | 0.35 |
| Normal stress at centre point of ELA (bars) | 17.51 |
| Ablation gradient at ELA (mm/m) | 6.16 |
| Mass loss at ELA (ma-1) | 2.30 |
| Net Ablation ($m^3$ w.e.) | 1,253,364.85 |
| Mass flux ($m^3$ ice) | 1,377,324.01 |
| Cross sectional area at ELA ($m^2$) | 239,048.78 |
| Perimeter of bed at ELA (m) | 2,265.67 |
| Mean balance velocity at ELA ($ma^{-1}$) | 5.76 |
| Basal shear stress at ELA (bars) | 2.11 |
| Max ice deformation velocity at ELA ($ma^{-1}$) | 129.04 |
| Average ice deformation velocity at ELA ($ma^{-1}$) | 53.14 |
| Required basal motion ($ma^{-1}$) | 0.00 |
| Required basal motion (%) | 0.00 |

| TABLE C | Oxendale |
|---|---|
| Glacier area ($km^2$) | 3.44 |
| Total snowblow area ($km^2$) | 1.15 |
| Snowblow area by 90° quadrants expressed as a percentage of the total snowblow area (%) | |
| NE (0-90°) | 0.00 |
| SE (91-180°) | 5.10 |
| SW (181-270°) | 62.08 |
| NW (271-360°) | 32.82 |
| S (135-225°) | 33.03 |
| W (226-315°) | 56.33 |
| Snowblow factor by 90° quadrants | |
| NE (0-90°) | 0.00 |
| SE (91-180°) | 1.22 |
| SW (181-270°) | 4.25 |
| NW (271-360°) | 3.09 |
| S (135-225°) | 3.10 |
| W (226-315°) | 4.05 |
| Mean snowblow factor | 2.62 |
| Ratio of snowblow area to glacier area | 0.33 |

**Table 7.1: A: the reconstructed ELA of the Lomond Stadial in Oxendale using a variety of methods. B: the steady-state dynamics of the glacier in Oxendale. C: the snowblow area and factors associated with the Oxendale glacier.**

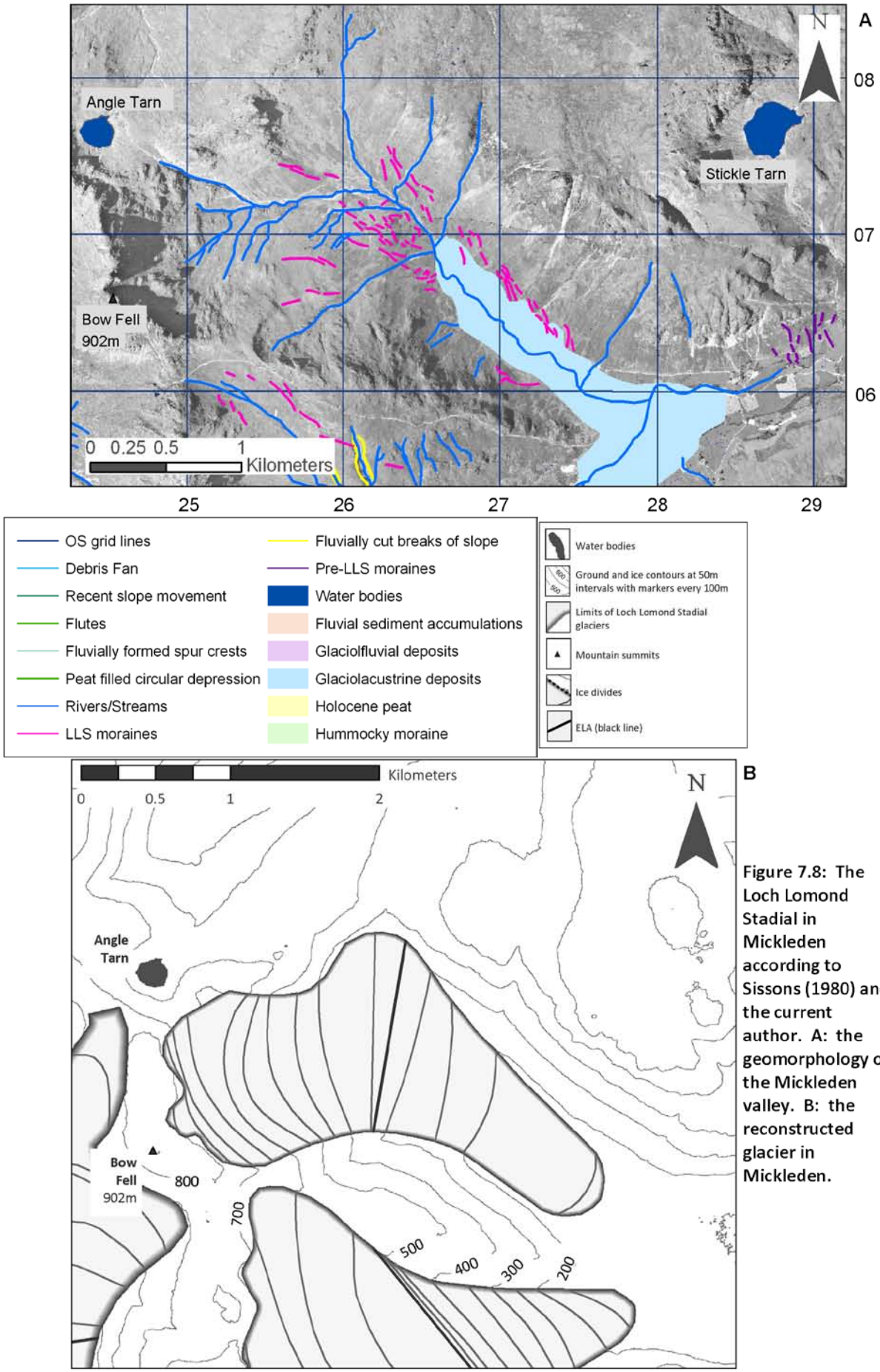


**Figure 7.8: The Loch Lomond Stadial in Mickleden according to Sissons (1980) and the current author. A: the geomorphology of the Mickleden valley. B: the reconstructed glacier in Mickleden.**

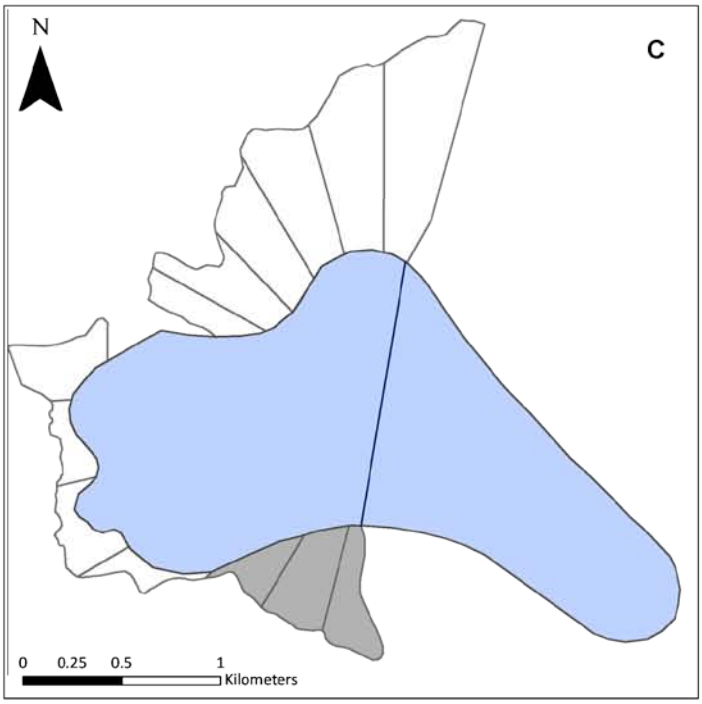


Figure 7.8: The Loch Lomond Stadial in Mickleden according to Sissons (1980) and the current author. C: the snowblow area associated with the Mickleden glacier. D: the hypsometric curve of the Mickleden glacier. E: the distribution of surface area over altitude of the Mickleden glacier. F: a cross sectional profile down the long axis of the Mickleden glacier.

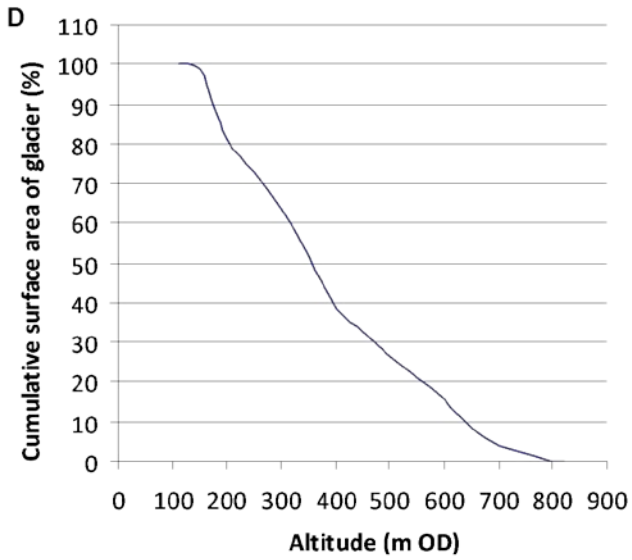


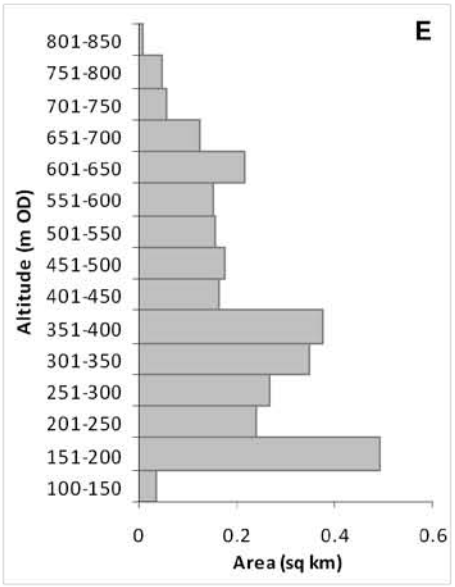


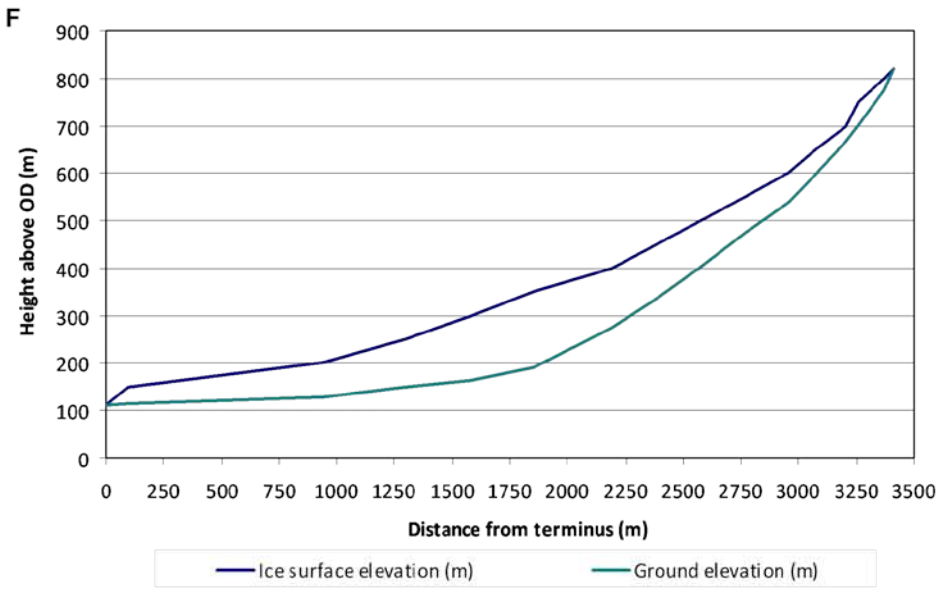

| TABLE A | Mickleden |
|---|---|
| Area ($km^2$) | 2.82 |
| Long axis length (m) | 1177.46 |
| Max altitude (m OD) | 820.96 |
| Min altitude (m OD) | 110.55 |
| Mid-altitude (m OD) | 466.00 |
| Lowest cirque | |
| Name | 124. Rossett Gill, Bowfell |
| Altitude (m OD) | 305 |
| Grade (according to Evans and Cox, 1995) | 5 |
| Altitude of highest lateral moraine (m OD) | 480.22 |
| Toe to head altitude ratio method (THAR) (m OD) | |
| 35% | 359.19 |
| 40% | 394.71 |
| 45% | 430.23 |
| 50% | 466.00 |
| Accumulation area ratio method (AAR) (m OD) | |
| 70% | 266.00 |
| 65% | 295.00 |
| 60% | 315.00 |
| 55% | 336.00 |
| 50% | 356.00 |
| Area weighted mean altitude method (AWMA) (m OD) | 383.82 |
| Balance ratio method (Benn and Gemmell, 1997) (m OD) | |
| BR=2.00 | 338.83 |
| BR=1.81 | 346.08 |
| BR=1.60 | 354.41 |
| BR=1.54 | 356.92 |
| BR=1.43 | 361.81 |
| Balance ratio method (Osmaston, 2005) (m OD) | |
| BR=2.00 | 459 |
| BR=1.81 | 453 |
| BR=1.60 | 446 |
| BR=1.54 | 444 |
| BR=1.43 | 439 |
| Mean value of all of the above methods (m OD) | 384.82 |
| Mean value of BR=1.54 (Benn and Gemmell,1997) and AAR 65% | 345.25 |
| ELA used in subsequent calculations (m OD) | 345 |

| TABLE B | Mickleden |
|---|---|
| ELA (m) | 345.00 |
| Temperature proxy used | Coope and Joachim (1980) St Bees Head |
| Proxy site altitude (m OD) | 0.00 |
| $T_s$ at proxy site (°C) | 8.25 |
| Temp. at ELA (0.0065°C/m lapse rate) | 6.00 |
| Degrees surface slope at ELA | 9.60 |
| Max ice thickness at ELA (m) | 204.61 |
| Glacier shape factor | 0.64 |
| Normal stress at centre point of ELA (bars) | 14.05 |
| Ablation gradient at ELA (mm/m) | 7.66 |
| Mass loss at ELA (ma-1) | 2.75 |
| Net Ablation ($m^3$ w.e.) | 1,227,021.51 |
| Mass flux ($m^3$ ice) | 1,348,375.28 |
| Cross sectional area at ELA ($m^2$) | 165,321.50 |
| Perimeter of bed at ELA (m) | 1,348.15 |
| Mean balance velocity at ELA ($ma^{-1}$) | 7.42 |
| Basal shear stress at ELA (bars) | 1.60 |
| Max ice deformation velocity at ELA ($ma^{-1}$) | 55.02 |
| Average ice deformation velocity at ELA ($ma^{-1}$) | 28.32 |
| Required basal motion ($ma^{-1}$) | 0.00 |
| Required basal motion (%) | 0.00 |

| TABLE C | Mickleden |
|---|---|
| Glacier area ($km^2$) | 2.82 |
| Total snowblow area ($km^2$) | 1.70 |
| Snowblow area by 90° quadrants expressed as a percentage of the total snowblow area (%) | |
| NE (0-90°) | 20.27 |
| SE (91-180°) | 0.00 |
| SW (181-270°) | 26.79 |
| NW (271-360°) | 52.94 |
| S (135-225°) | 16.56 |
| W (226-315°) | 27.83 |
| Snowblow factor by 90° quadrants | |
| NE (0-90°) | 2.68 |
| SE (91-180°) | 0.00 |
| SW (181-270°) | 3.08 |
| NW (271-360°) | 4.34 |
| S (135-225°) | 2.42 |
| W (226-315°) | 3.14 |
| Mean snowblow factor | 2.61 |
| Ratio of snowblow area to glacier area | 0.60 |

**Table 7.2: A: the reconstructed ELA of the Lomond Stadial in Mickleden using a variety of methods. B: the steady-state dynamics of the glacier in Mickleden. C: the snowblow area and factors associated with the Mickleden glacier.**

Suprisingly, the ELAs of the Mickleden and Oxendale glaciers (345 m OD and 518 m OD respectively) differ by 173 m; a significant difference given that they are of similar size (2.82 $km^2$ and 3.44 $km^2$) and aspect. The difference between the ELAs can therefore not be accounted for by local topographic factors. For comparison, Sissons (1980a) provides ELAs of 407 m OD and 511 m OD for the Mickleden and Oxendale glaciers respectively. Again these ELAs differ significantly (by 104 m) for glaciers for which the ELAs could be expected to show little variation.

The large difference between the ELAs calculated by the current author can be explained in two ways. Firstly, the larger difference in ELA could be associated with the slight changes made to the digitisations of Sissons (1980a) work in order for the glaciers to be coherent with the mapped geomorphology. Alternatively, the difference could relate to the difference in the ELA calculation methods used by the current author and Sissons (1980a). While Sissons (1980a) provides ELAs calculated solely using the AWMA method, the current author provides values which incorporate the more sophisticated balance ratio method.

As shown in table 7.2A the AWMA calculated by the current author for the slightly revised glacier reconstruction at Mickleden indicates an ELA of 383.8 m OD. This is just 23.2 m different from that calculated by Sissons (1980a) which suggests that the changes to the reconstruction provided by Sissons (1980a) have had minimal impact on the ELA and therefore the large difference in ELA seen between the Mickleden and Oxendale glaciers. Furthermore, it is likely that had Sissons (1980a) used the same method as the current author for the calculation of the ELA, a large difference between the ELA of the Mickleden and Oxendale glaciers would still have existed.

It is therefore concluded that the large, possibly unrealistic, variation in ELA seen between the Mickleden and Oxendale glaciers is infact a function of an 'unrealistic reconstruction'. However, according to the model produced by Carr and Coleman (2007), both of the glaciers in Mickleden and in Oxendale are glaciologically viable with both glaciers requiring 0 % basal motion suggesting that they were able to move entirely by internal ice deformation or through subglacial bed deformation. It would therefore seem that although the model of Carr and Coleman (2007) suggests that the glaciers are independantly viable, in the context of the regional glacial configuration, the reconstructions are not realistic.

With termini at least 4 km up valley of the nearest plateau icefield outlet terminus, both glaciers lie under an extensive area of ice in the plateau icefield model presented by

McDougall (1998). The reconstructions provided here may therefore be explained in a number of ways. Firstly, these glaciers can be interpreted as a model of the minimum plausible extent of the Loch Lomond Stadial glaciers in the Lake District e.g. Sissons (1980a), or alternatively, these glaciers may represent a retreat phase of the Loch Lomond Stadial ice occupation of the Lake District.

The first of these two options is highly unlikely since, as described above, the ELAs are rather too variable for the reconstructed glaciers to have co-existed in very similar neighbouring valleys. The latter of these two options is therefore favoured. This supports the suggestion that ice in the Lake District during the LLS was much more extensive than that suggested by Sissons (1980a) and is more likely to have followed a configuration similar to that indicated by McDougall (1998). Further investigation into the development of plateau icefields in the Lake District during the LLS is now required to confirm this. Most controversially however, these reconstructions arguably provide a basis upon which to question to usefulness of the model provided by Carr and Coleman (2007) in palaeo-glaciological reconstructions.

As previously stated, the ice surface contours were drawn perpendicular to the orientation of ice flow suggested by the geomorphology. Because of this, a rather large step occurs in the glacier long axis profile (figure 7.7F) at around 500 m which is perhaps not realistic. This further supports the above discussion which suggests that the reconstructions for the Mickleden and Oxendale glaciers may not be realistic based on their ELAs but also, as suggested by figure 7.7F in the case of their long profiles.

### 7.5 Further plateau icefields in the Lake District

As is also the case with alpine-style glaciers, it is likely that further Loch Lomond Stadial sites exist both in the Lake District and throughout the British Isles which simply remain undiscovered. This is primarily the result of a lack of research, particularly in the most inaccessible areas but in the case of plateau icefields is also compounded by the subtle nature of the evidence with which to identify them.

This research has identified two valley glaciers in the vicinity of Wrynose Pass: the Red Tarn/Wrynose Bottom glacier and the Widdygill Foot glacier. Both of these glaciers have been proven to be glaciologically viable using the methodology outlined in chapter 4, however, the location of moraines around these glaciers may suggest an alternative glacial arrangement. Slightly above the calculated ELA of the Widdygill Foot glacier and across Wrynose Pass, moraines are present. Since theoretically moraines cannot form in the accumulation zone of a

glacier, another explanation must exist which accounts for the location of these moraines. Firstly, the moraines may have formed during a deglacial phase. This idea does not in any way provide evidence against the presence of the previously reconstructed independent alpine-style glaciers in the area. Secondly, assuming that the moraines were formed at or close to the peak of the Loch Lomond Stadial, the location of the moraines, which suggests that the estimation of the ELA on the Widdygill Foot glacier is too low, may be a function of a methodological problem in the calculation of the ELA. Such methodological problems may include the location of ice surface contours or the lack of geomorpholgical evidence pertaining to the precise location of the ice margin, in particular the maximum altitude of the glacier. Further less substantial problems may be associated with the precise measurement of the glacier surface area between each of the contours for example.

Alternatively, under the same assumption, both the Red Tarn/Wrynose Bottom and Widdygill Foot glaciers may have been outlet glaciers of a plateau icefield rather than independent ice masses (figure 7.9). If this were the case then the ELA of the outlets would be raised, as previously discussed, and the moraines in question would then be located in the ablation zone of the outlet glaciers making their formation feasible.

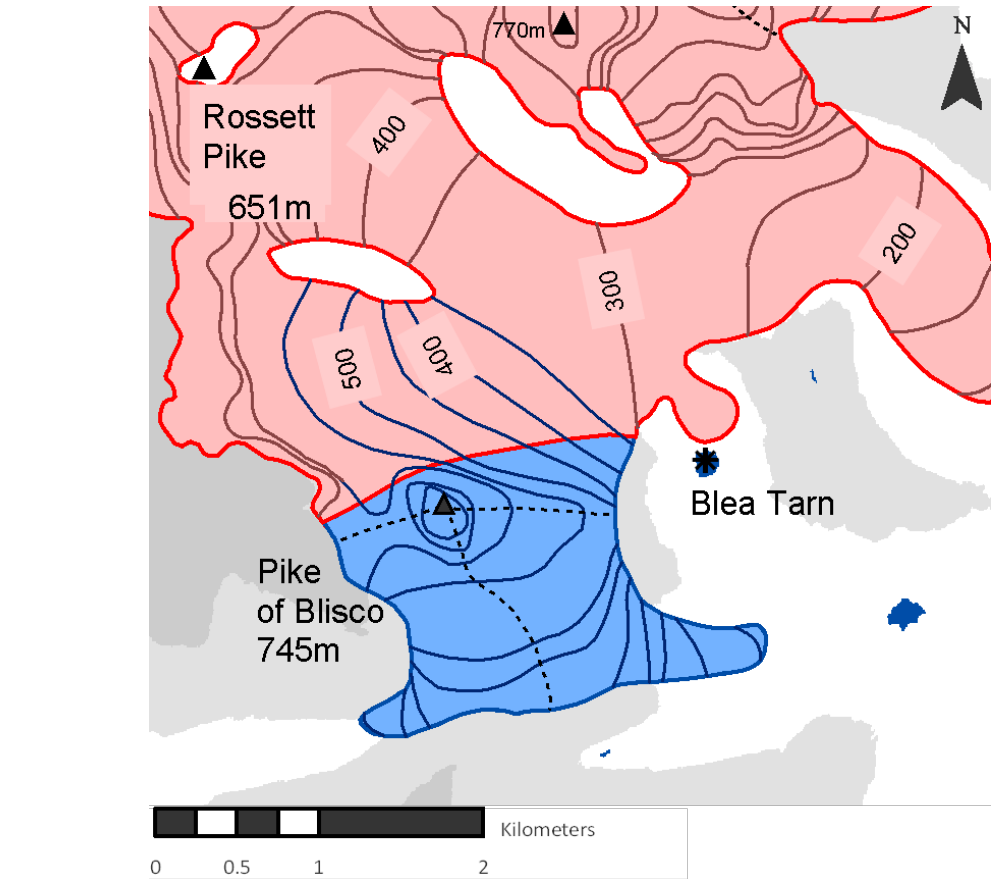


**Figure 7.9: A potential plateau icefield centred on Pike of Blisco in the south central fells of the Lake District. This contrasts with the ice arrangement shown in figure 7.5.**

Furthermore, the development of a plateau icefield also accounts for the altitude of the accumulation zone of the Widdygill Foot glacier which lies partially at the same altitude as the ablation zone of the Red Tarn glacier. The difference in ELA between the Widdygill Foot and the Red Tarn/Wrynose Bottom glaciers is ~ 150 m when they are reconstructed as independent ice masses. This could be accounted for by the contrasting aspects of the two glaciers however the presence of the terminus of the Widdygill Foot glacier at a particularly low altitude can be more simply accounted for by the presence of a plateau icefield centred on Pike of Blisco.

According to Manley (1959), the width of a summit can be defined as the distance across the peak from 30 m below either side of the summit in a windward direction. The summit of Pike of Blisco is therefore 130 m wide. Assuming a regional ELA of 500 m OD in line with that estimated by McDougall (1998), the summit of Pike of Blisco lies 205 m OD above the regional ELA. On Manley's curve (see figure 7.6), this sits below the suggested height and width at which a summit can support a plateau icefield. When compared with the summits on which McDougall (1998) proposes plateau icefields however, Pike of Blisco lies in a similar position on Manley's graph and thus it is considered that Pike of Blisco has the potential to support a plateau icefield.

In order to determine the thickness of the ice on the summit of Pike of Blisco, figure 10 below, taken from Rea et al. (1998), was used (figure 7.10). Using the minimum distance of Pike of Blisco from the ice margin, this method suggests an ice thickness of 95 m on the summit of Pike of Blisco which is almost double that proposed by McDougall (1998) on the much broader summit of High Raise in the central fells. A reduced ice thickness of 40 m was therefore assumed over the summit of Pike of Blisco which is more in line with that suggested by McDougall (1998) for High Raise, Dale Head/Grey Knotts and Brandreth. The relatively narrow summit of Pike of Blisco implies that ice could have been even thinner than this.

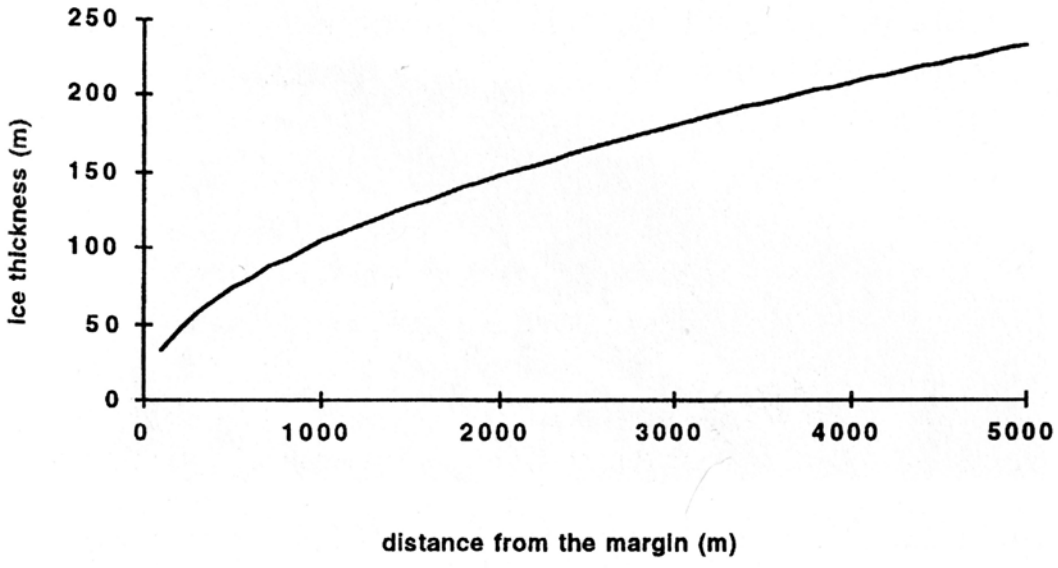


**Figure 7.10: A parabolic ice surface profile indicating the approximate ice thickness of a plateau icefield with the distance of the summit from the ice margin. Taken from Rea et al. (1998).**

Assuming 40 m of ice on the summit of Pike of Blisco, an ELA of 511 m OD and 431 m OD have been calculated as the mid-altitude ELAs of the Red Tarn/Wrynose Bottom and Widdygill Foot glaciers respectively. These conform well with the regional ELA of 500 m OD suggested by McDougall (1998).

The idea of a plateau icefield also still does not account for the moraines present above Widdygill Foot which are shown in purple on figure 6.21b since these moraines would still be located well above the ELA of the plateau icefield/outlet glaciers. This further supports the argument that these moraines were formed during an earlier glacial episode. However, if this is the case, then their survival below a plateau icefield seems ambitious despite the presence of cold based ice in the area. An ice free region around Pike of Blisco is therefore required in the LLS reconstruction in order to account for the presence of moraines above Widdygill Foot. This line of evidence therefore favours the reconstruction presented in chapter 6 which involves independent glaciers in Widdygill Foot and Red Tarn rather than a plateau icefield.

Aside from the ice over Pike of Blisco being implausibly thick according to figure 7.10 and the need to account for the moraines just below the summit, a number of other problems exist with the reconstruction shown in figure 7.9. Firstly, there is no field evidence to support the suggestion of a plateau icefield on the summit of Pike of Blisco and evidence from aerial photographs is very limited. Ideally, extensive field investigation involving the use of a reliable dating technique is now required to resolve the uncertainty surrounding the ice extent around Pike of Blisco during the LLS. Furthermore, the summit of Pike of Blisco is very narrow and the sides of the summit very steep. This contrasts with the summit of other proposed icefield supporting summits such as High Raise which has one of the broadest and flattest summits in the Lake District. Finally, the summit of Pike of Blisco is relatively exposed, particulary to the south-west; the direction from which winds were dominant during the LLS. This would have encouraged snowblow to the north and may have impeded the sustenance of the plateau icefield on the summit of Pike of Blisco. The morphology of the summit of Pike of Blisco may have compounded this problem as the chances of snow being removed from the summit rather than just relocated on it would have been much greater than on a much wider summit such as that of High Raise.

Problems therefore clearly exist with the suggestion of a plateau icefield centred on Pike of Blisco. Consequently, the above reconstruction shown in figure 7.9 should be taken as a first approximation of a potential plateau icefield in the area which requires further investigation. The above reconstruction is essentially based upon the location of the down-valley

geomorphology; also the basis for the reconstruction provided in chapter 6. It should be highlighted that the geomorphology associated with the upper limit of the ice particularly on the summit of Pike of Blisco has not been considered with respect to the presence of a plateau icefield in the field as a result of time constraints and thus there is an opportunity for further research here.

### 7.6 National and regional ELA trends

According to Manley (1959), climate during the Loch Lomond Stadial was often much more unsettled than today. Mean summer (June to September) air temperature during the Stadial is suggested to have been ~ 6.3°C, and ~ 7.5°C in July, along the shores of Windermere (Manley, 1959). This is substantially lower than the present day mean summer temperature of ~ 14.1°C. Since colder air is able to hold less moisture than warmer air, saturation of the air during the Stadial is likely to have occurred more regularly and thus, both the amount and frequency of precipitation was greater. A feature of this frequent precipitation would have been the occurrence of low cloud throughout the year. This is likely to have been the result of more vigorous atmospheric circulation than present, implying a more maritime influence, when the junction of polar water and relatively warm North Atlantic Drift water was in the vicinity of the British Isles around the latitude of south-west Ireland (Ruddiman et al., 1977). It is suggested by McDougall (2001) that a mean annual precipitation of 2000-2500 mm $yr^{-1}$ was feasible given the environmental parameters above. Furthermore, four fifths of this precipitation falling above or at the ELA fell as snow (Manley, 1959). This compares with a present day value of ~ 4000 mm $yr^{-1}$ of precipitation estimated by Sissons (1980a) around Scafell in the western Lake District. Manley (1959) suggests that the nearest present day climate analogy to the Loch Lomond Stadial is the very wet south-eastern fjords of Greenland.

Reconstructed ELAs from across Scotland, northern England and Snowdonia indicate a general eastward rise across the Western Highlands and Inner Hebrides (Sissons, 1980b). This can be attributed to the progressive eastward decline in precipitation across the area which is believed to have been associated with south to south-westerly winds during the Stadial (Ballantyne, 1989). A linear northward ELA decrease of 68.5 m/100 km is also observed along the western seaboard of Great Britain relating to a northward decrease in ablation-season temperatures (Manley, 1949). This trend is further identified by Ballantyne (2006) who, assuming an environmental lapse rate of 0.006°C $m^{-1}$, equates this to a southward ablation-season temperature rise of 0.42°C/100 km. Figure 7.11 below indicates the linear relationship between latitude and ELA when calculated using the AWMA method along the western coast of the British Isles. A favourable $r^2$ value of 0.906 indicates that 90.6 % of the total variance in

mean ELA across western Britain is attributable to the variation in latitude. Mean ablation-season temperature has therefore been inferred by Ballantyne (2006) as 1.2°C higher in Snowdonia than on Arran and 1.9°C higher than on the Isle of Skye during the Stadial.

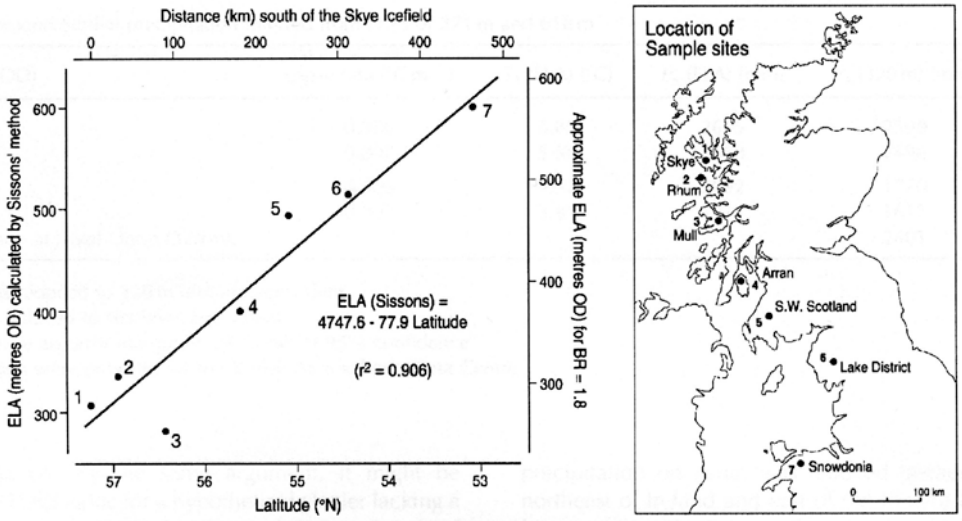


**Figure 7.11: The relationship between ELA and latitude using data from Skye (Ballantyne, 1989), Rhum (Ballantyne and Wain-Hobson, 1980), Mull (Ballantyne, 2002), Arran (Ballantyne, 2006), south-west Scotland (Cornish, 1981), the Lake District (Sissons, 1980a) and Snowdonia (Gray, 1982). Figure taken from Ballantyne (2006).**

Within-region ELA variation however is often more difficult to explain. Sissons (1980a) records no statistically significant ELA pattern within the Lake District and a similar problem is encountered on the Isle of Arran where, more recently, Ballantyne (2006) is unable to find any clear ELA trend across the island. Both of these regions cover relatively small areas and thus palaeotemperature and palaeoprecipitation variations are expected to have been minimal. Consequently, the largest ELA variations must reflect variation in local topographic characteristics. These characteristics influence two key aspects of glacier nourishment: snow accumulation (via snowblow or avalanching) and ablation (through shading from insolation) (Ballantyne, 2006).

In the Lake District, the insolation factors of the 64 glaciers reconstructed by Sissons (1980a) show a pronounced regional pattern. The insolation factor provides an indication of the favourability of the glacier's location with respect to its altitude, aspect, surface gradient and the proportion of direct solar radiation reflected from the glacier's surface. A high insolation factor indicates an adversely located glacier which received a large amount of insolation and vice versa (Sissons, 1979). In the Lake District the lowest insolation factors can be found in the north-west Lake District with the highest insolation factor being 10.9. Glaciers therefore

existed in areas of lowest insolation but, as a result of lower snowfall in the area, were also much smaller than glaciers elsewhere in the Lake District. These glaciers contrast with those in the central fells which, according to Sissons (1980a) reconstruction, were much larger than those in the south-west. Insolation factors were also much greater in the central fells, with the lowest insolation factor being 10.3 and several insolation factors > 14. In the southern Lake District small glaciers, similar in size to those in the north-west Lake District, are found but are associated with much greater insolation factors. In the central fells, the potential for a greater degree of cloudiness may explain the larger glaciers with lower insolation factors; however, over small distances this cannot solely explain the variation. Crucially, in the southern Lake District despite glaciers being of a similar size and ELAs of a similar altitude, insolation factors were much higher. This implies that another factor was compensating for the disadvantageous higher insolation factors (Sissons, 1980a).

Higher precipitation in the southern Lake District is the obvious explanation for this variation and is supported by the occurrence of a west-east mountain belt which will have induced orographic precipitation. However, variation in the central fells cannot be explained by this alone. Consequently, localised variation in the contribution of the various components of mass input to the glaciers, such as direct precipitation or snowblow, must occur.

### 7.7 The effect of snowblow on glacier development

Snowblow areas have been calculated for the six glaciers reconstructed here and for the 64 glaciers presented by Sissons (1980a). Mitchell (1996) notes that when there is a dominant wind direction such as during the Loch Lomond Stadial, snowblow may be critical in areas marginal to glaciation such as the Lake District. Of the six glaciers reconstructed Lingmell Beck had the highest snowblow area to glacier area ratio followed by the Mosedale glacier. It is important to consider however that large potential snowblow areas will not have had equal opportunity to contribute snow to the glacier throughout their area, with areas further away from the glacier less likely to add mass to the glacier (Mitchell, 1996). Sissons (1980a) therefore suggests that calculating the snowblow factor, i.e. the square root of the ratio, provides a solution to this problem. Furthermore, regression of snowblow factors against ELA reveals a series of interesting relationships (see figure 7.12i below).

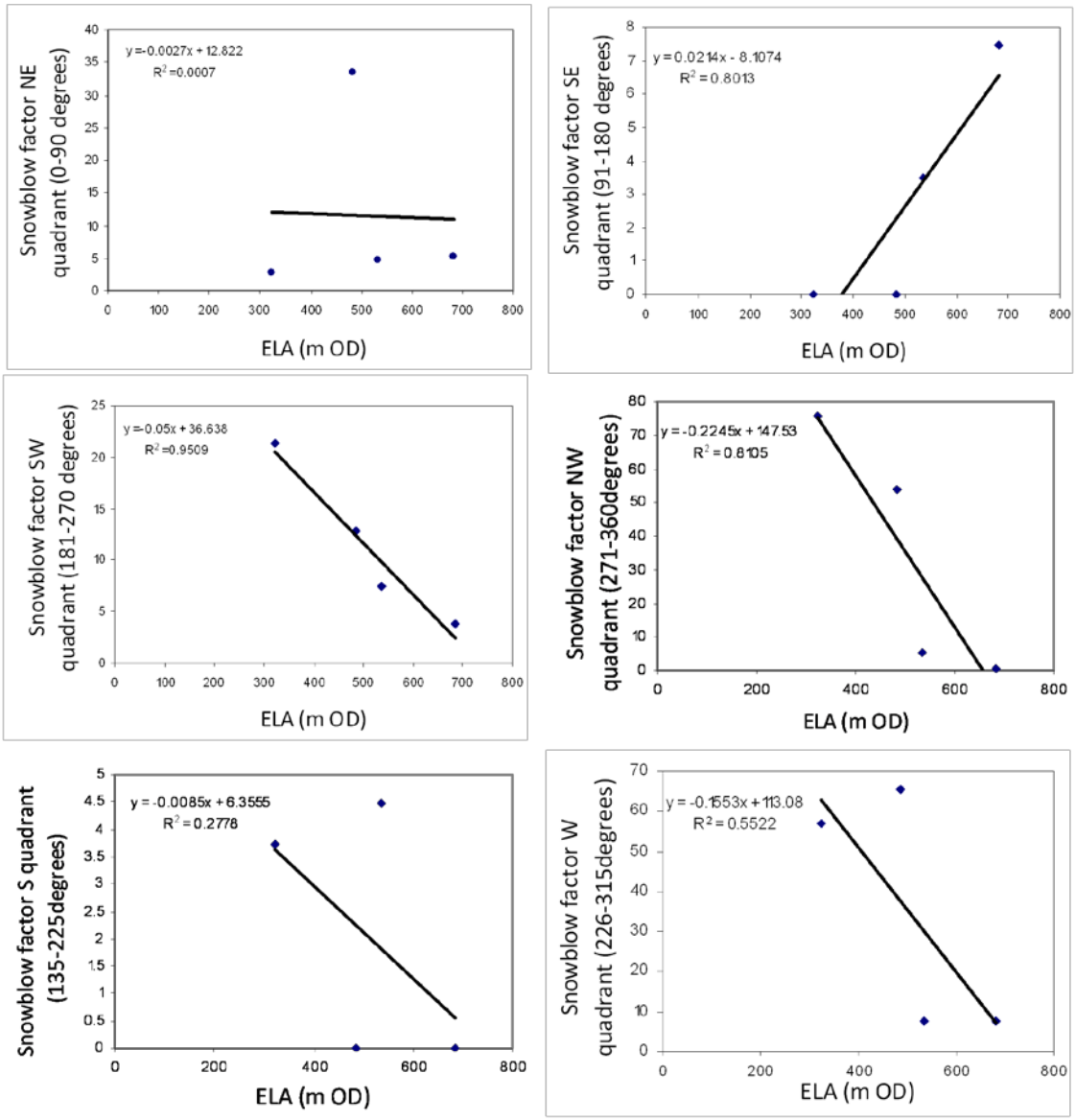


**Figure 7.12i: Bivariate plots showing the relationship between snowblow factor and ELA in the six quadrants for the Mosedale, Lingmell Gill, Widdygill Foot and Red Tarn glaciers.**

Figure 7.12i above shows the relationship between snowblow factor and ELA (m OD) for just four of the glaciers presented in chapters 5 and 6. The Upper Eskdale glacier has not been included in the above correlation since the accumulation area of the glacier faces almost directly south. This means that the glacier was vulnerable to high insolation factors and direct exposure to southerly winds. Furthermore criteria 5 in section 3.1.4 indicates that potential snowblow area can only include those areas which lie windward of the glacier surface i.e. in the south-east, south-west or southern quadrants. The Upper Eskdale glacier had potential snowblow area within these three quadrants and thus it is unlikely that it was aided by snowblow. The Lingmell Beck glacier is also omitted from the correlations since the snowblow factors associated with this glacier appear particularly anomalous amongst all of the snowblow factors of all the other glaciers.

Figure 7.12i indicates that the strongest correlation between snowblow factor and ELA (m OD) occurs in the south-west quadrant. An inverse relationship between snowblow factor and ELA provides and $r^2$ value of 0.95 which is statistically significant at the level of 0.05. This indicates that 95 % of the total variance seen in the ELA across the Lake District is attributable to the variation in the snowblow factor associated with the south-western quadrant. Hence, as the snowblow factor increases the ELA (m OD) decreases indicating that the ablation area of the glacier is able to descend to lower attitudes as a result of the extra mass accumulation.

In the north-western quadrant the relationship between the snowblow factor and the ELA provides an $r^2$ value of 0.81. Although this is not statistically significant at the level of 0.05, the large error margins associated with the reconstruction of palaeo-glaciers, the delimitation and calculation of snowblow area and the association of snowblow with a number of variables including local topography, leads the author to suggest that this is a pleasing correlation. The correlation in the north-western quadrant indicates that 86 % of the total variance seen in the ELA across western Britain is attributable to the variation in the snowblow factor associated with the north-western snowblow quadrant. Initially, it appears that although this is statistically a reasonable correlation, in practice winds from the north-west were rare during the Stadial. It is therefore concluded that as a result of the particularly steep topography in the Lake District this relationship may have been explained by avalanching rather than snowblow.

In the south-east quadrant a positive correlation is found between the snowblow factor and the ELA. An $r^2$ value of 0.80 indicates that 80 % of the variance of the ELA is attributable to variation in the snowblow factor for the south-east quadrant. Unlike the southern quadrant however, this positive correlation indicates that as the snowblow area increases the ELA also increases. This indicates that despite an increase in snowblow area, the mass of snow being input to the glacier is unaffected or potentially decreased, and is reflected by a coincident rise of the ELA. Firstly, assuming that an increase in snowblow area does not affect the ELA in the south-east quadrant, then it is likely that winds from the south-east were simply not involved in glacier development and sustenance during the Stadial. Alternatively, the effect of the local topography surrounding the Lingmell Beck, Lingmell Gill, Mosedale and Widdygill Foot glaciers may explain why such a strong positive correlation is found for the south-east quadrant.

Of particular note, with respect to local topography, is the apparent lack of plateau surfaces around the glaciers. This contrasts with glaciers such as those proposed by Sissons (1980a) near Dunmail Raise and Ullscarf which lie on the north to north-eastern side of the extensive

plateau area of High Raise in the central fells. Examples include the Lingmell Beck and Lingmell Gill glaciers which are surrounded by the steep, sharp peaks of the Scafell range. It is also possible that where such high, large mountain ranges occur that they act as barriers between the glacier and the oncoming wind/precipitation causing snow to accumulate on the windward side of the range. In this situation it would then be difficult for snow to move steeply uphill and settle on the leeward side of a range in order to be in a position favourable for snowblow. In such a situation where very steep ground surrounds a glacier it is also likely that avalanching as oppose snowblow may have occurred. It is suggested that this may have occurred along the Scafell range and thus, depending on wind direction, have favoured either the Upper Eskdale or the Lingmell Beck/Lingmell Gill glaciers. Another potential reason why the snowblow factors associated with the south-east quadrant of these glaciers may not be ideally representative of snowblow area within the south-east quadrant on a regional scale is that areas of very steep ground often reduce the distance away from the glacier from which snow can be blown and thus produces apparently anomalous results.

In the south and western quadrants very weak negative correlations are found (see figure 7.12i). $R^2$ values of 0.28 and 0.56 are recorded for the two quadrants respectively. These correlations are therefore inconclusive and do not indicate that snowblow during the Stadial was associated with either southerly or westerly air streams to any great degree. Evidence provided by Mitchell (1996) however statistically proves that snowblow in the North Pennines was associated with more westerly winds that is suggested by figure 7.12i. It is therefore inferred that local topographic factors combined with the regional precipitation pattern mean that the four glaciers tested here do not provide a sample representative of the effect of snowblow on ELA on a regional or national scale.

The assumption that the wind must come from the opposite orientation to aspect of the palaeoglacier however is inherently floored. This implies that glacier aspect is purely controlled by wind direction; however factors such as the degree of shading or continentality can also be influential. Of these, shading is the simplest to assess. Figure 7.12ii below indicates the combined effect of wind direction and shading on the resulting glacier aspect. In the northern hemisphere, in the absence of any wind, glacier aspect can be assumed to face directly north and hence shading is from the south. Where wind from the east of an equal influence on glacier aspect to the degree of shading occurs, the resulting glacier is expected to face north-east. Similarly, where a strong wind from the west-south-west occurs in a location of poor shading, the resulting glacier is assumed to have had an aspect facing approximately east-north-east. Such a wind direction is similar to what is expected to have occurred during

the Loch Lomond Stadial in Britain. It is also possible however that a north-westerly wind could have also resulted in a glacier with an aspect in the north eastern quadrant. For example, where a moderately strong north-westerly wind occurs over an area with a high degree of shading, the resulting glacier can be expected to face east-north-east.

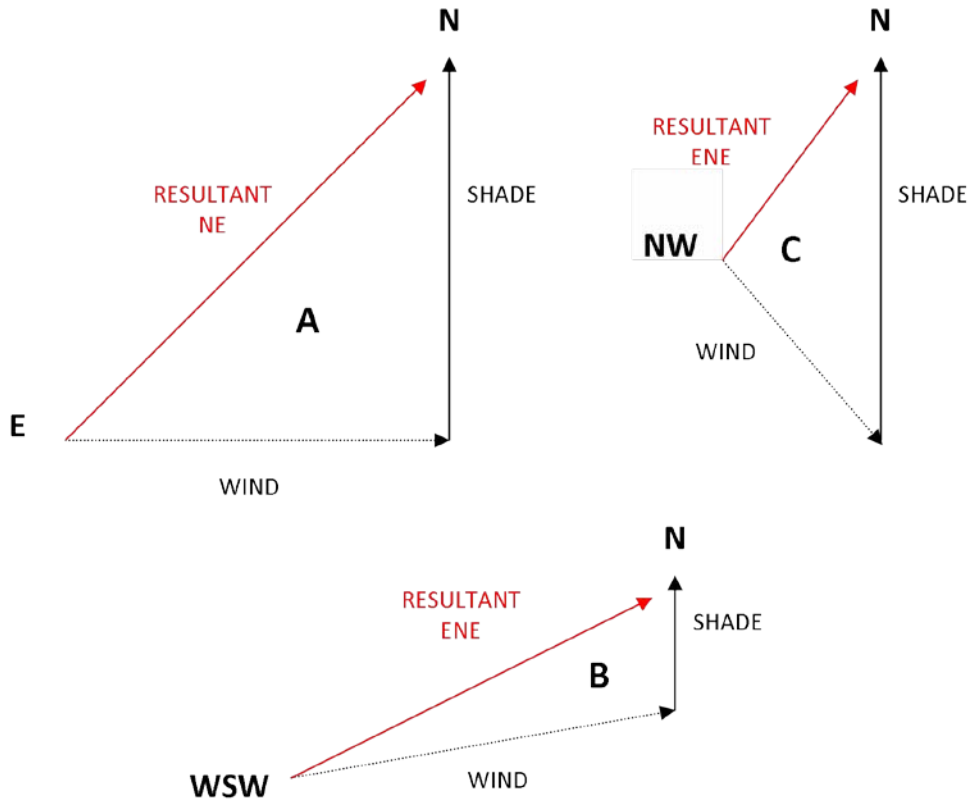


**Figure 7.12ii: The effect of shading and wind direction on glacier aspect. A: easterly wind with equally strong degree of shading, B: a moderate west-south-westerly wind with proportionally stronger shading, C: strong north-westerly wind with poor shading.**

In the Lake District, many of the glaciers reconstructed by Sissons (1980a) have aspects within the north-eastern quadrant (i.e. between 0 and 90°), particularly those in the eastern fells. Although wind from the north-west are less likely to have occurred during the Stadial than those form the south to south-west, short periods of north-westerly winds may have also contributed to the development of glaciers with north-easterly aspects. This lays into question criteria 5 in the definition of potential snowblow area, however, without a means by which to quantify the other contributing factors such as shading or continentality then this definition provides the most pleasing method by which to quantify the influence of snowblow on glacier development.

In conclusion, snowblow in the south-west Lake District is believed to have been associated with air streams slightly west of south based on the bivariance of snowblow factor with ELA (m OD). This corresponds well with work by various authors throughout the 20th century which suggests that winds during the Stadial were from the south or south-west. Sissons (1980b) notes that such snowblow is likely to have been most important during the time when snow was falling and for a time after snowfall had ceased. In an attempt to increase the sample size, data from Mitchell (1996) was added to figure 7.12i: however only a series of very weak correlations were produced with the highest $r^2$ of just 0.62 being associated again with the southern quadrant. Furthermore, the snowblow factors taken from Mitchell (1996) are consistently lower than those calculated by the current author but do show similar positive or negative relationships. This is assumed to be the result of variation in the methodology/criteria used to identify potential snowblow area and the more inland location of the glaciers considered by Mitchell (1996). As a result, the correlations produced are weakened, however, if the criteria outlined in chapter 3 for snowblow area identification were also applied to the North Pennines glaciers, it is hoped that the more consistent approach would provide more comparable and thus statistically significant results.

## 7.8 Problems associated with the Benn and Gemmell (1998) and Osmaston (2005) spreadsheets for the calculation of the ELA via the balance ratio method.

The spreadsheet provided by Benn and Gemmell (1997) is suggested by Osmaston (2005) to over estimate ELAs. It was found however, that to some extent, the spreadsheet which produced the highest values for the ELA was dictated by the hypsometry of the glacier in question. In general, the Benn and Gemmell (1997) spreadsheet produced lower ELA values than the Osmaston (2005) spreadsheet where the glacier's long axis was not linear. Examples of where this is the case include Lingmell Beck, Mickleden and Upper Eskdale. This suggests that rather than the Benn and Gemmell (1997) spreadsheet consistently overestimating the ELA, the two spreadsheets are simply better at coping with different hypsometric situations. Consequently, values from either the Osmaston (2005) spreadsheet or the Benn and Gemmell (1997) spreadsheet were used in the calculation of the final ELA, not both. The decision of which to use was dictated by the hypsometry of the glacier and the agreement of the values produced with those produced via the AAR and AWMA methods.

Unfortunately due to the Benn and Gemmell (1997) spreadsheet being written in Visual Basic embedded within MS Excel, the precise cause of the different outputs of the two spreadsheets are difficult to explain mathematically, however, two reasons aside from the glacier hypsometry (discussed above) will now be outlined qualitatively.

Firstly, the location of the snout and the upper end of the glacier might result in inaccuracies. The spreadsheet assumes that the glacier extends from the lowest contour down to an altitude infinitesimally close to the highest contour which does not cross glacier ice. There is thus no difference in the altitude range of a glacier which just gets below the 100 m contour on a map with a 20m contour interval for example, and a glacier which extends down to 81 m in terms of the methodology in the Benn and Gemmell (1997) spreadsheet. The converse applies at the upper end of the glacier, and the impact may be even more striking if the ice emanates from a plateau icefield, where there may be a very large area of ice between the highest contour to cross the glacier and the actual highest altitude of the ice-body. The larger the contour interval the greater the potential error in the ELA calculation (Gemmell, pers comm.). In the case of the Widdygill Foot glacier, the snout of the glacier is located on a rather flat area of land where the highest contour which does not cross glacier ice may be some distance from the snout: a potential source of error compared to the other reconstructed glaciers. This problem however does not address the reason why the Osmaston (2005) and Benn and Gemmell (1997) spreadsheets produce such different results for some of the glaciers reconstructed as both methods follow the above procedure.

The most likely source of variation in the output of the two spreadsheets is the methodological differences in the iterative technique used to solve the problem where the balance ratio is not equal to 1. Both spreadsheets calculate the ELA through a series of trial calculations, each time adjusting the results obtained until the balance sum comes to zero. This is a manually in-built function of the Osmaston (2005) spreadsheet however the Benn and Gemmell (1997) spreadsheet uses the Excel 'Goal Seek' tool to perform the successive approximations. 'Goal Seek' is a tool for solving equations iteratively where various inputs (the BR) are trialed until the desired output (the ELA) is reached. To calculate a single ELA, a first approximation for the ELA is fed into both of the spreadsheets and any adjustment to the approximated ELA is calculated. The adjusted value is then fed into the spreadsheet again repeatedly until two consecutive values are the same, i.e. the spreadsheet has converged upon the 'solution'. In the Osmaston (2005) spreadsheet this is done manually through a series of formulae written into the speadsheet by the author, however in the Benn and Gemmell (1997) spreadsheet this is process is carried out using 'Goal Seek'. It is possible that 'Goal Seek' allows error into the methodology if, for example, it takes the nearest integer at each iteration. This error would therefore be magnified with each further iteration and may account for the two spreadsheet producing rather different results.

### 7.9 Calculation of the ELA using multiple methods

As highlighted in the thesis, the methods of Osmaston (2005) and Benn and Gemmell (1997) can provide different ELAs for the same glacier. As shown in table 7.3 below, the two methods provide ELAs which differ by up to 149 m in the case of the Widdygill Foot glacier. With such large differences between the results of the two methods, it would not be appropriate to use both methods in the calculation of single glacier's ELA. Instead just one method has been used depending on the glacier hypsometry and then averaged with the AAR (65 %) and AWMA methods in order to smooth and allow comparison between the final results. This also allows the results to be comparable to those of the largest regional glacier reconstruction in the Lake District by Sissons (1980a).

| Glacier name | a. Benn and Gemmell (1997) (m) | b. Osmaston (2005) (m) | a - b (m) |
|---|---|---|---|
| Mosedale | 528.28 | 526 | 2.28 |
| Lingmell Beck | 546.76 | 530 | 16.76 |
| Lingmell Gill | 604.65 | 666 | -61.35 |
| Upper Eskdale | 473.72 | 505 | -31.28 |
| Widdygill Foot | 332.36 | 482 | -149.64 |
| Wrynose Pass | 497.99 | 462 | 35.99 |
| Oxendale | 551.83 | 504 | 47.83 |
| Mickleden | 354.41 | 446 | -91.59 |

**Table 7.3: The ELAs of glaciers in the South-West Lake District calculated using the methods of Benn and Gemmell (1997) and Osmaston (2005) with a BR of 1.6.**

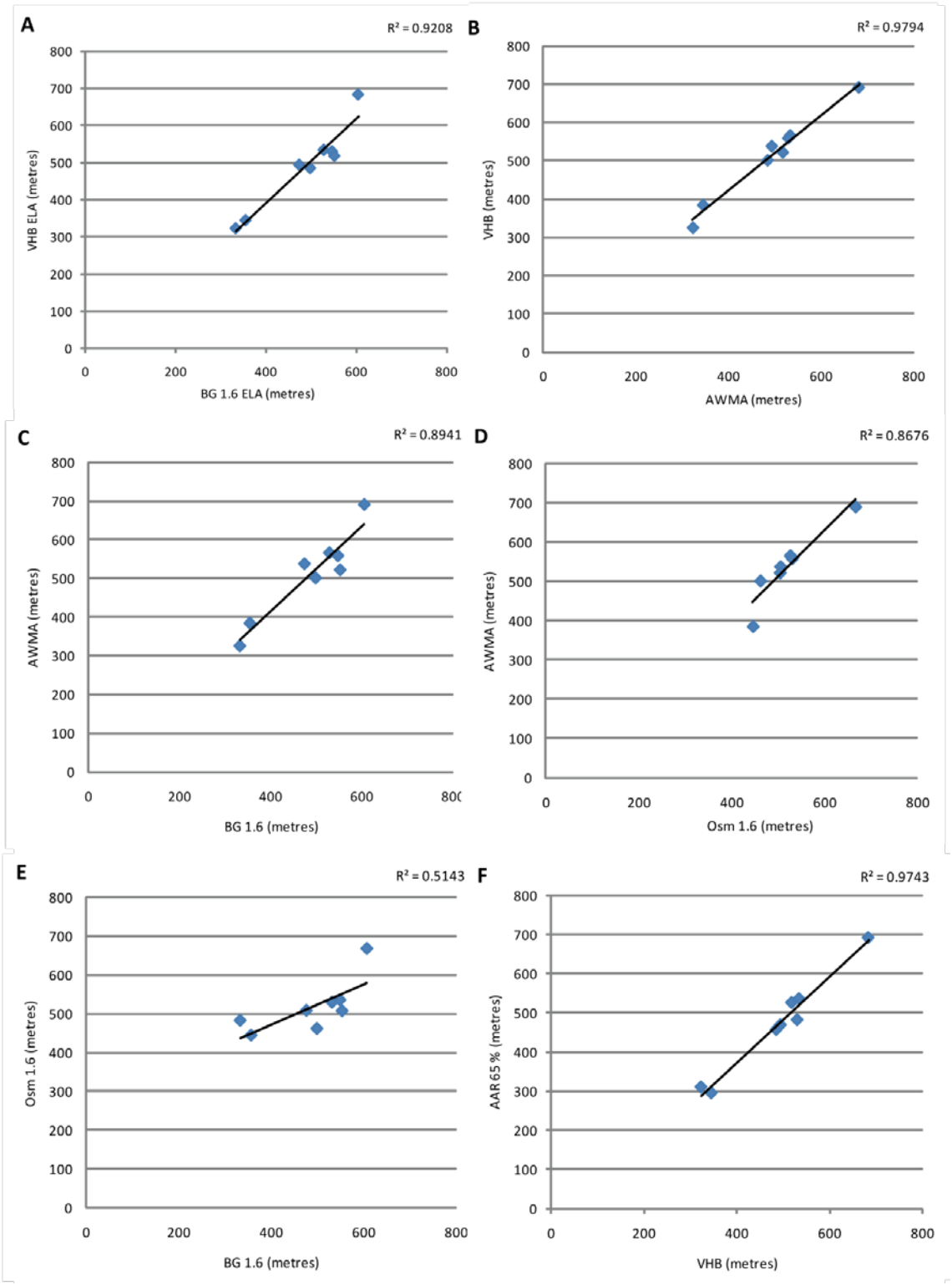


**Figure 7.13: Regression of the results provided by the Benn and Gemmell (1997), Osmaston (2005), the AWMA and AAR (65%) methods and the values used in the thesis. Note that figure 1D only has 7 data points due to the removal of Widdygill Foot (see below text for explanation).**

The relationship between the ELA used and the ELA provided by the spreadsheet of Benn and Gemmell (1997) is shown in figure 7.13. A favourable $r^2$ value of 0.92 suggests a close linear relationship between the two variables. Similarly, the slope of the trendline in figure 7.13 is 1.13 indicating that ratio between the two variables is close to 1:1; that is, the methods produce very similar values.

Further regression reveals similar favourable relationships between the AWMA and AAR (65%) methods, the ELA used in the thesis, and the AABR methods of Osmaston (2005) and Benn and Gemmell (1997). Of these correlations (shown in figure 7.12A, B, C, D and F above), $r^2$ values of 0.92, 0.98, 0.89, 0.87 and 0.97 (all taken to 2 decimal places) respectively indicate a very credible series of relationships. Most significantly, the regression of the results from the AABR method, where BR = 1.6, of Benn and Gemmell (1997) and Osmaston (2005), as shown in figure 1E, produces the least favourable $r^2$ value of all the relationships. In contrast to the above noted $r^2$ values, figure 7.13E produces an $r^2$ value of 0.51; a value from which a number of conclusions can be drawn.

Firstly, the weaker correlation may indicate that the sophisticated AABR method (which accounts for glacier hypsometry and variable mass balance gradients) is currently dependant on the particular methodology used for calculations, with different methodologies producing rather different ELAs for the same glacier. The trendline slope of figure 7.13E, which suggests that ***x*** increases as 0.51 times ***y***, is symptomatic of this issue.

Alternatively, as suggested above, this relationship may indicate that the speadsheets of Benn and Gemmell (1997) and Osmaston (2005) are simply better at coping with different hypsometric situations. For example, the thesis uses the Benn and Gemmell (1997) calculation of the AABR in the calculation of the mean ELA for the Widdygill Foot glacier. As shown in table 1 this glacier has the largest discrepancy between the two AABR methods. Regression of the Osmaston (2005) ELAs against the AWMA ELAs indicates a weak relationship between the two variables ($r^2$ = 0.66), however if the Widdygill Foot glacier is removed from the regression then figure 1D results and a much more favourable relationship is implied by the $r^2$ value of 0.87.

Aside from the above justification for the choice of a mean ELA in subsequent palaeoclimatic inferences in the thesis, a number of problems associated with glaciological reconstructions should also be highlighted as they potentially introduce much more significant error than that associated with the alternative method of ELA calculation suggested in the thesis corrections.

Firstly, problems associated with the misinterpretation of landforms which result in errors in ice margin positioning cause the input of the incorrect ice surface area into the glaciological model. The positioning of ice surface contours is unavoidably subjective, particularly in areas where geomorphological evidence of ice flow direction is sparse. In order to minimise the effect of subjective ice contour placement on glacier hypsometry (particularly important on small glaciers) an ice surface contour interval of 20 m was used. According to Rea (2009) the majority of the data derived from the WGMS database is reported in 50-100 m contour intervals.

Interestingly, Rea (2009) further states that 'using both AABRs the difference in ELA calculated using 20 m contour intervals is only 8 m [for Langfjordjokelen and Cascade Glacier] which can be deemed insignificant'. The question therefore arises: at what point does the difference between the two AABR methods become significant? In the context of a glacier which is ~ 7 km long with an altitudinal range of ~ 835 m, e.g. the Upper Eskdale glacier, an error of ± 20 m on the ELA is easily tolerated (see table 7.4). Mitchell (1996) stated errors of up to ± 32 m for glaciers with contours at 10 m intervals.

The horizontal resolution of the NextMap DEM (5 m) is also a key factor. In the case of the Mosedale glacier the difference between the ELA used in the thesis and that of the AABR method used to calculate that mean is only 5.72 m. In this context the difference between the two ELAs can be deemed insignificant when using a DEM with a resolution of 5 m.

| Glacier name | a. Benn and Gemmell (1997) (m) | b. Osmaston (2005) (m) | a - b (m) | c. ELA used in thesis (m) | c - (a or b)* (m) |
|---|---|---|---|---|---|
| Mosedale | 528.28 | 526 | 2.28 | 534 | 5.72 (a) |
| Lingmell Beck | 546.76 | 530 | 16.76 | 530 | -16.76 (a) |
| Lingmell Gill | 604.65 | 666 | -61.35 | 683 | 17 (b) |
| Upper Eskdale | 473.72 | 505 | -31.28 | 494 | 20.28 (a) |
| Widdygill Foot | 332.36 | 482 | -149.64 | 323 | -9.36 (a) |
| Wrynose Pass | 497.99 | 462 | 35.99 | 485 | -12.99 (a) |
| Oxendale | 551.83 | 504 | 47.83 | 518 | 14 (b) |
| Mickleden | 354.41 | 446 | -91.59 | 345 | -9.41 (a) |

**Table 7.4: The difference between the mean ELA used in the thesis and the AABR method used for each glacier in the mean value i.e. Benn and Gemmell (1997) or Osmaston (2005).**

### 7.10 Reconstruction of glacier mass balance and dynamics as suggested by Carr and Coleman (2007)

Application of the model outlined by Carr and Coleman (2007), which is based on a series of relationships earlier recorded by authors such as Paterson (1994), Oerlemans (2001) and Hooke (2005), concludes that all of the glaciers reconstructed here are 'glaciologically viable' under the temperature conditions used to drive the model. As stated by Hindmarsh et al. (1989), glacier flow is directly influenced by the mass-balance dynamics of a glacier, more than the reverse. The primary strength of this model is that it allows the reconstruction of steady-state balance dynamics using independently derived palaeo-temperature data. From this, glacier flow parameters can then be quantified making the model much more compatible with glaciological theory. The formulation of the relationship between the reconstructed palaeo-glaciers and climate in this way allows a comparison with contemporary glaciers and those in other parts of the world. Despite this, the model also has several weaknesses which cause the current author to question its reliability.

The reconstruction of former glaciers can be seen as highly subjective with ice margins often based on the presence of geomorphology; the genesis of which may be interpreted in various ways. Furthermore, the presence of complete cross-valley moraines which clearly indicate the location and morphology of a glacier terminus are rare within the Lake District, as indeed in many parts of the British Isles. This is often as a result of post-glacial fluvial dissection or in some cases human activity. The definition of the upper limits of a valley/cirque glacier are also difficult to identify. The presence of trimlines which are used to identify the upper limits of a glacier or ice sheet have several fundamental problems. Firstly, trimlines require a substantial period of time during which to form, with the Loch Lomond Stadial arguably being too short a period for trimline formation to occur on hard rocks. Secondly, the origin of trimlines is contentious, as described above, with four explanations for their formation, just one of which involves the trimline representing the maximum vertical limit of ice. Within the Lake District trimlines do not coincide with the upper limits of any of the glaciers considered in this study, making the identification of the upper ice limit difficult to accurately distinguish.

Such problems are recognised by Carr and Coleman (2007) however they do not recognise the sensitivity of the model to glacier extent, which makes the interpretation of geomorphology in order to delimit ice more crucial. The model provided by Carr and Coleman (2007) has been used here as a way of establishing the viability of the geomorphological interpretations since absolute dating was not possible given the time constraints. In light of the sensitivity of the model however, prior dating of the landforms used to delimit the ice would be preferable.

Cosmogenic radionuclide or radiocarbon dates would provide the most accurate results; in the absence of such resources relative age dating and/or sedimentological evidence would also be beneficial.

The reconstruction of ice surface contours is also highly subjective. Theoretically ice surface contours on valley glaciers display a distinctive pattern becoming more convex downstream closer to the snout and concave closer to the headwall. Contours therefore reflect the velocity field within the glacier indicating convergent flow in the accumulation area and divergent flow in the ablation area, with contours lying perpendicular to the slightly generalised direction of ice flow. The drawing of ice surface contours is therefore heavily dependant on the distribution and orientation of ice flow indicators such as moraines which as discussed above can often be interpreted incorrectly. However, despite this, ice surface contours unavoidably provide vital information about the distribution of ice surface area over altitude on palaeo-glaciers. This relationship is then used to derive the ELA, e.g. through the AAR method, which is further used extensively throughout the model, e.g. to calculate net ablation.

Ice surface contours also dictate the ice surface slope across the ELA. It is suggested here that the most satisfactory way to obtain the ice surface slope across the ELA is to use an area weighted mean whereby the surface slopes of the contour intervals one above the ELA, one below the ELA, and one across the ELA are calculated and weighted based on their proximity to the ELA. This limits the impact of potential anomalies in surface slope measurement resulting from an undulating reconstructed longitudinal topographical profile in the region of the ELA. Furthermore, it limits the impact of highly subjective contours lines on what appears to be a highly influential parameter of the model. Factors which dictate the surface slope of a glacier include the longitudinal topographical profile of the glacier bed. As previously noted, valleys such as Upper Eskdale contain rock steps of enough magnitude to form small ice falls however this model fails to take into account the presence of such features which can be high influential on ice surface, and basal, velocity. The model could therefore be refined by decreasing the contour interval on the ice surface or modelling the ice surface to establish the ice surface morphology not only at the contours but also between them.

Surface slope is primarily used to calculate basal shear stress which is then used to infer the maximum surface velocity of the ice in the centre of the channel. Accurate calculation of basal shear stress is therefore essential however the calculation appears to be highly sensitive to variations in surface slope. Ultimately the effect of this is to drastically affect the ice surface velocity and therefore the basal velocity. The result is that the percentage of basal velocity

required becomes inaccurate. If, for example, this exceeds the 90 % threshold required for a glaciologically viable glacier, then the glacier can appear unviable even if this is not the case. Carr and Coleman (2007) conclude that the reconstruction of the Loch Lomond Stadial glacier at Cotra, which lies of the eastern side of Steel Fells in the Central Lake District, does not constitute a glaciologically viable glacier. Irrespective of other evidence, this might be challenged given the above reasoning. A surface slope of 13.5° is provided by Carr and Coleman (2007). The current author suggests that the reconstructed glacier occupying Cotra could be classified as viable if subsequent calculations were carried out using a surface slope of just 1.5° lower than their value. The lower surface slope would increase the basal shear stress and thus increase the value for $V_c$ which when subtracted from $U_s$ would provide a lower value for the percentage required basal motion ($U_b$). The result would be a glaciologically viable glacier (according to the model of Carr and Coleman (2007)) which agrees with the work of Wilson (2002). Furthermore, Wilson (2002) suggests that ice at Cotra was much thicker (90 m) than that suggested by Carr and Coleman (2007): a problem which again highlights the subjectivity of ice surface contour location (Wilson, 2007). Such a significant thickness increase from that estimated by Carr and Coleman (2007) (three times the thickness) has major implications for the cross sectional area at the ELA, the mass flux and ultimately the balance velocity ($U_s$).

As previously stated in chapter 4, in order to derive the percentage basal motion required by a glacier, the following calculations are carried out:

*Mean balance velocity (m $a^{-1}$) – Mean rate of ice deformation (m $a^{-1}$) = Required basal motion (m $a^{-1}$)*

*Required basal motion (m $a^{-1}$) ÷ Mean balance velocity (m $a^{-1}$) = Percentage required basal motion (%)*

In circumstances however, where the mean rate of ice deformation at the ELA (m $a^{-1}$) exceeds the mean balance velocity (m $a^{-1}$) then Carr and Coleman (2007) assume that such a glacier requires 0 % basal motion. Firstly, not only is this a rather large assumption but it also, according to the model, implies that the glacier is glaciologically viable when the reality may be quite the opposite. A problem with this is that it is perhaps unrealistic to assume 0 % basal motion on a glacier with a steep surface slope or bed. In cases such as this it is unlikely that some basal sliding did not occur thus highlighting a floor in the model. Alternatively in cases where ice surface or topographic gradients are more reasonable, it is important that the lack

of basal motion can be accounted by other means e.g. through the presence of a deforming bed.

A further problem relating to the example of Cotra, and also of Fan Hir in South Wales, is that unlike many cirque glaciers, the glaciers are not laterally restricted by the topography but only by moraines which themselves are a product of the glacier's existence. This reduces the area of ice in contact with the bed/valley walls and thus also reduces the basal shear stress per unit volume of ice. This is a reflection of the shape of the channel and the surface area of ice in contact with the bed relative to the volume of the glacier. This highlights the necessity of the inclusion of an independently calculated shape factor in the calculation of basal shear stress. This was not achieved by Carr and Coleman (2007) but has been carried out on the glaciers reconstructed here. The inclusion of the shape factor can almost be seen as a token gesture however, as it does often not illustrate undulations in the valley bed satisfactorily. For example, in Upper Eskdale, a largely parabolic cross section at the ELA is interrupted by a bedrock spur coming down the centre of the valley from Esk Pike (885 m OD). This is emphasised by river development either side of the spur to form an almost 'double parabolic' profile consisting of two small valleys. This will have significantly increased the ice/bed interface relative to the ice volume and thus increased the friction at the bed around the ELA to lower the ice velocity at the surface and the bed. Conversely, a flatter bed lowers ice/bed interface relative to the ice volume and thus lowers the friction at the bed relative to the ice volume. Theoretically, a higher ice velocity would therefore be expected.

To further illustrate this point the ice surface velocity can be divided by the cross sectional area of the ice at the ELA to indicate the velocity per unit area of ice. The glaciers in Widdygill Foot (viable) and Cotra (not viable) were first compared due to the contrasting morphology of their underlying topography. As shown in table 7.5 below, Cotra is shown to have had a much greater velocity per unit area of ice than Widdygill Foot. Combined with the various other parameters of the glacier, this contributed to making Cotra 'not viable' as the motion cannot be accounted for by either basal slip or internal ice deformation. Widdygill Foot, in contrast, has a much lower velocity per unit area of ice at the ELA.

| | Widdygill Foot | Cotra |
|---|---|---|
| Ice thickness (m) | 83.69 | 26 |
| Surface velocity (m $a^{-1}$) | 12.39 | 8.61 |
| Cross sectional area at the ELA ($m^2$) | 64,165 | 14,950 |
| **Velocity per unit area of ice at the ELA ($a^{-1}$ $m^{-1}$)** | **1.93 x $10^{-4}$** | **5.76 x $10^{-4}$** |

**Table 7.5: A comparison between the velocity and ice/bed interface per unit area of ice for the glaciers occupying Widdygill Foot and Cotra during the Loch Lomond Stadial.**

Wilson (2002) however suggests that the ice at Cotra was 90 m thick at the ELA. By assuming a linear relationship between the cross sectional area of the ELA and the ice thickness, the cross sectional area of the channel for an ice thickness of 90 m rather than 26 m provides a cross sectional area at the ELA of 51,748 $m^2$. This is an area increase of 71.1 %. By assuming the same surface velocity of 8.61 m $a^{-1}$, this provides a velocity per unit area of ice at the ELA ($a^{-1}$ $m^{-1}$) of 1.66 x $10^{-4}$ $a^{-1}$ $m^{-1}$, a clear decrease from the 5.76 x $10^{-4}$ quoted in table 8.1 for an ice thickness of 26 m. These calculations are approximate however they may indicate that the reconstruction provided by Wilson (2002) is more realistic being more comparable with the velocity per unit area of ice at the ELA of the Widdygill Foot glacier

It is also possible to compare Fan Hir and Corrie of Balglass which are both glaciologically viable according to the model of Carr and Coleman (2007) but which have very different cross valley profiles. Qualitative assessment of the ice beds of the two glaciers suggests that Fan Hir had a much flatter bed than the Corrie of Balglass glacier which was located in a more classic U-shaped valley. The greater friction associated with the more rounded U-shaped valleys had the potential to reduce the basal motion. This is reflected in the generally lower values of reconstructed percentage required basal motion for the glaciers reconstructed in this study which have more classic U-shaped across valley profiles than those considered by Carr and Coleman (2007).

The flatter across valley profiles recorded by Carr and Coleman (2007) can also be questioned and potentially explained by the occurrence of sediment infill into such sites during the Holocene. This would not only alter the channel shape and therefore the perimeter of the bed at the ELA but also the ice thickness. This may be used to explain the rather low ice thickness at the ELA for the reconstructed Cotra glacier of just 26 m which also affects the final percentage of required basal motion. If an accumulation of 5 m of sediment such as peat is assumed to have occurred since the Loch Lomond Stadial during the Holocene then the ice

thickness stated by Carr and Coleman (2007) at a site such as Cotra is at least 5 m lower than the actual value. This value is also conservative as Barber and Charman (2005) state that raised mires of Europe are believed to accumulate at a rate of 1 cm per 10 years suggesting that 10 m of sediment has accumulated during the ~ 10 ka of the Holocene. It is also crucial to note that such ice thickness increases would also need to be applied to the ice thicknesses calculated by Wilson (2002) for glaciers such as Cotra. By increasing the ice thickness of the Cotra glacier from the 26 m suggested by Carr and Coleman (2007) to the 90 m suggested by Wilson (2002) it is possible to increase the basal shear stress ($\tau_b$) and consequently increase $V_c$ thus lowering $U_b$ relative to $U_s$. The result of this is that the glacier could then be classed as viable with $U_b$ not exceeding the 90 % threshold of $U_s$ for a glaciologically viable glacier. This may also be the case with glaciers other than Cotra.

Furthermore, the current author considers that the use of a 90 % basal motion threshold beyond which a glacier is considered to not be viable should be approached with caution. It has clearly been demonstrated that many parameters are involved in the formulation of surface and basal velocities and thus the classification of Corrie of Balglass as viable when the percentage basal motion of 89.46 % is so close to the threshold is highly tenuous.

Additionally, many of the glaciers to which the model has been applied (Carr and Coleman, 2007) occupy relatively flat topography which does not exhibit the classic valley 'U' shape. As a consequence, it is possible that the mean rate of ice deformation reflects a relatively uniform basal shear stress across the ELA as a function of reduced ice thinning towards the lateral margins. The difference between the mean and maximum rate of ice deformation will therefore be reduced, with the maximum rate of ice deformation not necessarily coinciding with the centre of the channel as occurs in a valley with a cross section similar to that of Mosedale. The result of this is that $V_m$ is raised relative to $V_c$ so that when $V_m$ is used to calculate the percentage of required basal motion, the result is lower than it would otherwise be. In such a situation glaciers may appear viable when in reality they are not. Conversely a lowering of $V_m$ produces a higher percentage basal motion. Of particular concern is the classification of the glacier at Corrie of Balglass as glaciologically viable. Carr and Coleman (2007) show that when $V_m$ = 0.16 m $a^{-1}$ for this glacier, $U_b$ (m $a^{-1}$) accounts for 89.46% of $U_s$ (2.169 m $a^{-1}$). However if $V_m$ is simply increased by 0.01 m $a^{-1}$ to 0.17 m $a^{-1}$ then $U_b$ = 1.999 m $a^{-1}$ and therefore accounts for 92.16 % of $U_s$ where $U_s$ = 2.169 m $a^{-1}$. This then takes the percentage of basal motion over the 90 % threshold stated by Andrews (1975) and employed by Carr and Coleman (2007) and thus the glacier is no longer glaciologically viable under the temperature parameters used to drive the model. It is concerning that such a small change in

$V_m$, which is highly possible given the large number of subjective variables involved in its calculation, can affect the distinction between a viable or unviable glacier.

Essentially, the reason for the high degree of sensitivity of the model when applied to the Corrie of Balglass glacier is that the values of $V_m$, $U_s$ and $U_b$ lie within a small range of just 2.009 m $a^{-1}$. This range is particularly small when considering the large error bars associated with the calculation of surface slope, basal shear stress, cross sectional area of the channel etc. Carr and Coleman (2007) do not provide details of the errors associated with their methodology: however, Murray and Locke (1989) suggest that the error associated with reconstructed ice velocity calculations can be as great as 40 %. Clearly, the specific errors associated with each stage of the model applied here would need to be calculated in order to refine this assumption, however, in order to be certain that reconstructed glaciers are glaciologically viable, this suggests that glaciers which have required basal velocities within 40 % of the 90% threshold should be approached with caution and another method of viability determination should be employed in such cases. This would mean that any glaciers with required basal velocities above 50 % require further assessment. Although the large errors associated with the various stages of the methodology outlined by Carr and Coleman (2007) are clearly a problem, the assumption of an across the board 40 % error bar seems precarious. The current author would therefore like to suggest that without calculation of such individual errors, a qualitative assumption of a 20 % error bar should be employed. This therefore questions the viability of glaciers which have required basal motion of greater that 70 %. This includes only the Red Tarn/Wrynose Bottom glacier from this research however it also suggests that the Corrie of Balglass glacier, Cotra glacier and the Fan Hir glacier may require further assessment.

This adjusted methodology accepts that dictating glacier viability based on such a narrow threshold is unrealistic and the following is proposed. Glaciers with required basal motion of ≤ 70 % require basal motion can be assumed to be glaciologically viable under the temperature parameters used to drive the model. Glaciers requiring a greater percentage of basal motion should, in the author's opinion, be validated as viable or not viable using other means. Ideally this would involve the dating of landforms using cosmogenic radionuclide or radiocarbon dating however this is beyond the scope of this project. Instead, in the cases of Mosedale and Lingmell Beck relative age dating of the outermost terminal or lateral moraines has been achieved sedimentologically through coring.

Finally, the implementation of Glen's flow law in the methodology of Carr and Coleman (2007) also introduces error. The maximum rate of ice deformation at the ELA (m $a^{-1}$) is calculated as

$$V_c = \frac{(2A\tau_b{}^n H)}{(n+1)}$$

Equation 7.1

where *A* is a temperature dependant constant of the flow law (assumed to be 0.167 $bar^{-3}$ $yr^{-1}$), $\tau_b$ is the basal shear stress, *n* is an exponential constant of the flow law (assumed to be 3) and *H* is the ice thickness. This is a well established general law for steady-state glacier ice deformation which has been shown be generally correct using laboratory tests and field investigations (Rea et al., 2000). It should be highlighted however that the above calculation assumes values for both *A* and *n* of 0.167 and 3 respectively. In this study, velocity calculations are focused on the surface and basal velocities of the glaciers. As a general rule, velocity decreases continuously with depth. Where $n \approx 3$ the majority of this decrease occurs relatively close to the bed (Paterson, 1994) as shown below in equation 7.2.

$$U_s - U(z) = \frac{2A}{n+1}(\rho g \sin\alpha)^n (h-z)^{n+1}$$

Equation 7.2

Here $U_s$ and $U_b$ are the velocities at the surface and the base of the glacier respectively, *U* is the velocity at the depth *(h – z),* A is a temperature dependant constant of the flow law (taken as 0.167 $bar^{-3}$ $yr^{-1}$), n is an exponential constant of the flow law (taken as 3), $\rho$ is the density of ice (910 $kg/m^3$), *g* is the acceleration due to gravity (9.81 $m/s^2$) and $\alpha$ is the ice surface slope at the ELA. According to Hooke (2005), the relationship between $U_b$ and $U_s$ is unaffected by variation in *n*, with variation in *n* only affecting internal ice velocity as shown in figure 7.14 below.

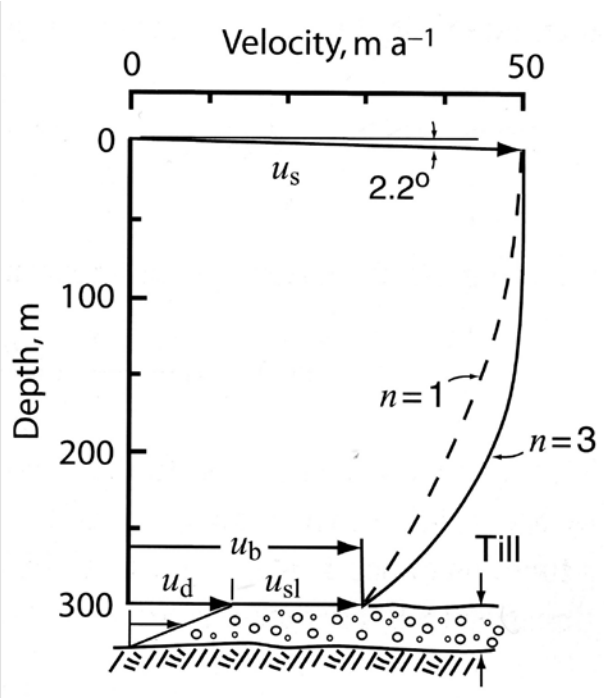


**Figure 7.14: The velocity profile of a glacier with a surface slope of 2.2° showing the effect of variation in *n* on the relationship between $U_s$ and $U_b$. Taken from Hooke (2005).**

In contrast, *A*, which is a measure of ice viscosity, is dependant on a number of factors including temperature, fabric and ice water content. Of these three, temperature is arguably the most important control on ice viscosity. Where the temperature of ice increases, the water content also increases and the ice becomes less viscous i.e. the value of *A* in equation 7.1 decreases. An assumed value for *A* of 0.167 $bar^{-3}$ $yr^{-1}$ is applied to Glen's flow law, however, in order to reduce the potential error associated with this assumption it may be more appropriate to assign a value for *A* on a case-by-case basis. This could be done using the calculated temperature at the ELA for the reconstructed glaciers and would require the development of a relationship between air temperature and ice temperature and therefore viscosity. Since this in itself is highly error-prone it is suggested that *A* would be most appropriately ascertained by measurement of ice viscosity on contemporary glaciers deemed appropriate to act as modern analogues. Ideally this would provide a value for *A* for a number of different environmental settings which would be primarily based on the glacier's degree of continentality (quantified as mass loss).

## 7.11 Summary

- Previous work in the Lake District by Sissons (1980) and Manley (1959) indicates an alpine style of glaciation however this was revised by McDougall (1998) who suggested a plateau icefield over the central fells.
- McDougall (1998) did not investigate the south-west Lake District where it is now suggested that a particularly large glacier occupied Upper Eskdale and coalesced with the plateau icefield. A smaller plateau icefield may also have existed over Pike of Blisco.
- Although the glaciers reconstructed in chapters 4 and 5 are glaciologically viable, ice occupation of Styhead Tarn remains problematic. Two different scenarios are presented here: one with ice over Styhead Tarn and one in which Styhead Tarn is ice free. This area requires further work.
- Problems exist with the methodology used to model mass balance which was originally adapted from Carr and Coleman (2007). Key sources of error in this methodology include the calculation of the surface slope of a glacier, the resolution of the data used to map the geomorphology i.e. NextMap, the drawing of the ice surface contours.

# Chapter 8

# CONCLUSIONS

# 8: CONCLUSIONS

## 8.1: A large valley glacier occupied Upper Eskdale during the Loch Lomond Stadial and was connected to a plateau icefield centred on High Raise, Grey Knotts, Dale Head and Kirk Fell.

The subtle geomorphology associated with plateau icefields is often overlooked or misinterpreted as being of para- or peri-glacial origin. In the Lake District, the summit of High Raise is occupied by shattered bedrock and blockfield. This is the result of inactive cold based ice covering the plateau during the Loch Lomond Stadial. In contrast warm based ice in the valleys has resulted in the formation of extensive latero-frontal moraines at the ice margins. The transition between warm and cold based ice in the valleys has produced a zone of transitional geomorphology. This contrasts with the sharp trimlines often associated with the upper limit of the ice occupation and is thus evidence for plateau icefield development. Plateau icefields were centred on High Raise (55 $km^2$), Grey Knotts (7 $km^2$), Dale Head (3 $km^2$) and Kirk Fell (1 $km^2$) in the Lake District and were connected to a series of valley glaciers including that in Upper Eskdale. Not interpreted by Sissons (1980) as of Loch Lomond Stadial origin, the moraines at the southern end of Upper Eskdale were later discussed by Wilson (2004) however a glacier was never reconstructed. It is suggested here that the moraines at the southern end of Upper Eskdale are of Loch Lomond Stadial rather than of Dimlington Stadial origin. This is largely based upon their comparative morphology to moraines elsewhere in the Lake District known to be of Loch Lomond Stadial age.

The reconstructed glacier in Upper Eskdale which assumes that these moraines mark the downslope limit of ice occupation is also 'glaciologically viable' according to the applied velocity model. With a surface area of 13.05 $km^2$, the Upper Eskdale glacier was therefore larger than any of the glaciers proposed by Sissons (1980). Addition of the areas of the Red Tarn and Upper Eskdale glaciers to the plateau icefields gives a total ice coverage of 79.05 $km^2$ of which the Upper Eskdale glacier accounted for 16.51 %. The plateau icefield proposed by McDougall (1998) replaces 14 of the cirque/valley glaciers proposed by Sissons (1980) in the central fells with an icefield which feeds 20 much larger outlet glaciers.

## 8.2: At least 58 ice masses occupied cirques/valleys independently of the central plateau icefield, these included glaciers in Mosedale, Lingmell Beck, Lingmell Gill and Widdygill Foot.

Away from the plateau icefield which covered the central fells, alpine style glaciers occupied cirques and valleys in a similar arrangement to that proposed by Sissons (1980). Such glaciers

were preferentially located on the more sheltered north or eastern side of mountain ranges as a result of the prevailing south to south-westerly winds. Plateau icefields were unable to develop in the far eastern and western fells due to the lack of plateau summits. Of the 58 glaciers away from the central plateau icefield, 47 were reconstructed by Sissons (1980), 3 by Wilson and Clark (1999), 3 by Wilson and Clark (1998) and 4 by the current author.

### 8.3: Glaciers were sustained not only by direct precipitation but also by wind blown snow associated with south to south-westerly winds during the Stadial.

The prevailing wind direction during the Stadial was from the south to south-west. The most favourable sites for glacier development were therefore located on the north or north-eastern side of mountain ranges. As a result many glaciers in the Lake District had a north to north-easterly aspect. Such glaciers were less affected by mass input from direct precipitation than those on the south or south-western side of mountain ranges. Indirect mass input via snowblow is therefore believed to have aided glacier sustenance. The need for a more transparent definition of what constitutes an area with snowblow potential was addressed and is outlined in chapter 4. This definition recognises that it is possible for snow to also move uphill and thus all ground sloping away from the glacier at an angle of≤ 5° was included in the snowblow area. Assuming the occurrence of south to south-westerly winds, no snowblow area was identified around the Upper Eskdale glacier and just a very small area was identified around the Red Tarn/Wrynose Bottom glacier. This is primarily the result of their southerly aspects. The other reconstructed glaciers all had significant potential snowblow areas in their southern, south-western or south-easterly quadrants. The largest snowblow are to glacier area ratios were associated with the Lingmell Gill and Mosedale glaciers.

The effect of an increased snowblow area is to lower the ELA of the glacier. A significant inverse relationship is therefore expected between the snowblow area and the ELA and is found for the south-west quadrant..

### 8.4: ELAs do not show any trends across the Lake District but do conform with a general southerly rise in ELA along the western seaboard of Great Britain.

The mean ELA of the six reconstructed glaciers was 508 m OD (range of 360 m). This is just 23 m lower than the average ELA of the 64 glaciers reconstructed by Sissons (1980). The ELAs of the reconstructed glaciers therefore conforms well with the rise in ELA with decreasing latitude seen along the western seaboard of Great Britain (see chapter 6 figure 6.2). The effect

of plateau icefields in the central fells however was to raise the ELA of the ice mass in the region. McDougall (1998) uses the example of the Honister Pass glacier which, according to Sissons (1980), had an ELA of 385 m OD. The addition of the plateau icefields however increases this value to 475 m OD (McDougall, 1998). Conversely however, the response of glaciers with accumulation areas at higher altitudes is to extend their ablation areas further downslope. If this was the case then the ELAs can expected to have been much the same as the mean value calculated by Sissons (1980) at 530.59 m OD. Outside of the central fells the remaining 50 glaciers reconstructed by Sissons (1980) have a mean ELA of 558.68 m OD which compares with 518 m OD for the glaciers reconstructed by the current author which are independent of the central plateau icefields.

### 8.5: All of the glaciers reconstructed are glaciologically viable under the assumption that $U_b$ cannot account for ≥ 90 % of $U_s$.

Andrews (1975) states that where the basal motion ($U_b$) of a glacier exceeds 95 % of the surface velocity ($U_s$) in the centre of a channel then a glacier is not glaciologically viable under the temperature parameters used to drive the calculations. Carr and Coleman (2007) further state that this value should be reduced to 90 % to be more in line with the velocity field of contemporary glaciers. The current author however suggests that as a result of the large errors associated with the model, the conclusion that a glacier is viable or not over such a narrow threshold is precarious. Furthermore, glaciers where $U_b \leq 70$ % of $U_s$ should be approached with caution and ideally another method by which to confirm the viability of the glacier such as absolute dating should be employed before conclusions are drawn.

Despite this, the model is a highly valuable tool by which to integrate independent palaeotemperature data to glacier reconstructions and reduces where possible the errors associated with speculative approaches to glaciological modelling. As such, all of the glaciers reconstructed here are 'glaciologically viable' with just the Red Tarn/Wrynose Bottom glacier exceeding the $U_b \leq 70$ % of $U_s$ threshold.

### 8.5: Limitations and recommendations for further research.

The Loch Lomond Stadial in the Lake District was clearly more extensive than first believed. In the Lake District, the proposal of a plateau icefield by McDougall (1998) and the identification of further Loch Lomond Stadial cirque/valley glaciers by authors such as Wilson and Clark (1998: 1999) have dramatically increased the volume of ice occupying the Lake District from

that suggested by Sissons (1980) and earlier by Manley (1959). It is therefore possible that further Loch Lomond Stadial sites simply remain undiscovered both in the Lake District and throughout the British Isles. The subtle evidence of plateau icefield existence compounds this possibility.

Sedimentological ice flow indicators would also be useful as a means of initially determining the origin of moraines in the Lake District and also mechanisms of landform genesis.

Of particular interest in the Lake District would be the development of a high resolution 3-dimensional glaciological model which could be applied to the plateau icefield. Ideally this would provide information about ice dynamics which would be comparable with morphologically similar contemporary ice masses. Critically, the errors associated with such a model would need to be reduced from those associated with the 2-dimensional model implemented here.

Finally, the absence of reliable absolute dating techniques such as cosmogenic radionuclide's or radiocarbon is a large inhibitor to Quaternary glacial research. A series of dates by which to confirm or reject the ideas presented in this thesis would therefore be the next obvious stage in developing an understanding of the Loch Lomond Stadial glaciation of the Lake District.

# BIBLIOGRAPHY

ALLEY, R. B. (1992) Flow law hypotheses for ice-sheet modelling. *Journal of Glaciology,* 38**,** 245-256.

ALLEY, R. B. & CLARK, P. U. (1999) The deglaciation of the Northern Hemisphere: a global perspective. *Annual Reviews of Earth and Planetary Science,* 27**,** 149-182.

ALLEY, R. B., MEESE, D. A., SHUMAN, C. A., GOW, A. J., TAYLOR, K. C., GROOTES, P. M., WHITE, J. W. C., RAM, M., WADDINGTON, E. D., MAYEWSKI, P. A. & ZEILINSKI, G. A. (1993) Abrupt increase in Greenland snow accumulation at the end of the Younger Dryas event. *Nature,* 362**,** 527-529.

ANDREWS, J. T. (1972) Glacier power, mass-balance, velocities and potential erosion. *Zeitschrift fur Geomorphologie. Supplementband,* 13**,** 1-17.

ANDREWS, J. T. (1975) *Glacial Systems and approach to glaciers and their environments,* North Scituate, Massachusetts, Duxbury Press.

AUTHORITY, L. D. N. P. (2003) Understanding the National Park: Factsheets. IN HTTP://WWW.LAKE-DISTRICT.GOV.UK (Ed.).

BALLANTYNE, C. K. (1986) Protalus rampart development and the limits of former glaciers in the vicinity of Baosbheinn, Wester Ross. *Scottish Journal of Geology,* 22**,** 13-25.

BALLANTYNE, C. K. (1988) Ice-sheet moraines in southern Skye. *Scottish Journals of Geology,* 24**,** 301-304.

BALLANTYNE, C. K. (1989) The Loch Lomond Readvance on the Isle of Skye, Scotland: glacier reconstruction and palaeoclimatic implications. *Journal of Quaternary Science,* 4**,** 95-108.

BALLANTYNE, C. K. (1997) Periglacial trimlines in the Scottish Highlands. *Quaternary International,* 38/39**,** 119 - 136.

BALLANTYNE, C. K. (1998) Age and significance of mountain-top detritus. *Permafrost and periglacial processes,* 9**,** 327-345.

BALLANTYNE, C. K. (2002) Paraglacial geomorphology. *Quaternary Science Reviews,* 18/19**,** 1935-2017.

BALLANTYNE, C. K. (2006) The Loch Lomond readvance on North Arran, Scotland: Glacier reconstruction and palaeoclimatic implications. *Journal of Quaternary Science,* 22**,** 343-359.

BALLANTYNE, C. K. (2007) Loch Lomond Stadial glaciers in North Harris, Outer Hebrides, North-West Scotland: glacier reconstruction and palaeoclimatic implications. *Quaternary Science Reviews,* 26**,** 3134-3149.

BALLANTYNE, C. K. & BENN, D. I. (1994) A Loch-Lomond Readvance Glacier in Duirinish, Nw Skye. *Scottish Journal of Geology,* 30**,** 183-186.

BALLANTYNE, C. K. & HALL, A. M. (2008) The altitude of the last ice sheet in Caithness and east Sutherland, northern Scotland. *Scottish Journal of Geology,* 44**,** 169-181.

BALLANTYNE, C. K. & MCCARROLL, D. (1995) The vertical dimensions of Late Devensian glaciation on the mountains of Harris and southeast Lewis, Outer Hebrides, Scotland. *Journal of Quaternary Science,* 10**,** 211 - 223.

BALLANTYNE, C. K., MCCARROLL, D., NESJE, A., DAHL, S. O. & STONE, J. O. (1998) The last ice-sheet in north-west Scotland. *Quaternary Science Reviews,* 17**,** 1149-1189.

BALLANTYNE, C. K., STONE, J. O. & FIFIELD, L. K. (2008) Glaciation and deglaciation of the SW Lake District, England: implications of cosmic ray exposure dating. St Andrews, Scotland.

BALLANTYNE, C. K. & WAIN-HOBSON, T. (1980) The Loch Lomond Advance on the Island of Rhum. *Scottish Journal of Geology,* 16**,** 1-10.

BARBER, K. & CHARMAN, D. (2005) Holocene palaeoclimate records from peatlands. IN MACKAY, A., BATTARBEE, R., BIRKS, J. & OLDFIELD, F. (Eds.) *Global Change in the Holocene.* London, Hodder Arnold.

BAUDER, A., FUNK, M. & HUSS, M. (2007) Ice-volume changes of selected glaciers in the Swiss Alps since the end of the 19th century. *Annals of Glaciology, Vol 46, 2007,* 46**,** 145-149.

BENN, D. I. (1992) The genesis and significance of 'hummocky moraine': evidence from the Isle of Skye, Scotland. *Quaternary Science Reviews,* 11**,** 781 - 799.

BENN, D. I. & BALLANTYNE, C. K. (2005) Palaeoclimatic reconstruction from Loch Lomond Readvance glaciers in the West Drumochter Hills, Scotland. *Journal of Quaternary Science,* 20**,** 577 - 592.

BENN, D. I. & EVANS, D. J. A. (1998) *Glaciers and Glaciation,* London, Arnold.

BENN, D. I. & GEMMELL, A. M. D. (1997) Calculating equilibrium line altitudes of former glaciers: a new computer spreadsheet. *Glacial Geology and Geomorphology*.

BENN, D. I. & LEHMKUHL, F. (2000) Mass balance and equilibrium-line altitudes of glaciers in high-mountain environments. *Quaternary International,* 65**,** 15-29.

BENN, D. I. & LUKAS, S. (2006) Younger Dryas glacial landsystems in North West Scotland: an assessment of modern analogues and palaeoclimatic implications. *Quaternary Science Reviews,* 25**,** 2390-2408.

BENN, D. I., OWEN, L. A., OSMASTON, H. A., SELTZER, G. O., PORTER, S. C. & MARK, B. (2005) Recontruction of equilibrium-line altitudes for tropical and sub-tropical glaciers. *Quaternary International,* 138-139**,** 8-21.

BENNETT, M. R. (1999) Paraglacial and periglacial slope adjustment of a degraded lateral moraine in Glen Torridon. *Scottish Journal of Geology,* 35**,** 79-83.

BOND, G., BROECKER, W., JOHNSEN, S., MCMANUS, J., LABEYRIE, L., JOUZEL, J. & BONANI, G. (1993) Correlations between climate records from North Atlantic sediments and Greenland ice. *Nature,* 365**,** 143-147.

BOULTON, G. S., JONES, A. S., CLAYTON, K. M. & KENNING, M. J. (1977) A British ice-sheet model and patterns of glacial erosion and deposition in Britain. IN SHOTTEN, F. W. (Ed.) *British Quaternary Studies: Recent Advances.* Oxford, Claredon Press.

BOYLE, E. A. & KEIGWIN, L. (1987) North Atlantic Thermohaline circulation during the past 20,000 years linked to high-latitude surface temperature. *Nature,* 330**,** 35-40.

BROECKER, W. S., ANDREE, M., WOLFLI, W., OESCHGER, H., BONANI, G., KENNETT, J. & PETEET, D. (1988) The chronology of the last deglaciation: Implications to the cause of the younger Dryas event. *Paleoceanography,* 3**,** 1-19.

BROECKER, W. S. & DENTON, G. H. (1990) The role of ocean-atmosphere reorganisations in glacial cycles. *Quaternary Science Reviews,* 9**,** 305-341.

BROEKE, M. R. V. D. (1997) Structure and diurnal variation of the atmospheric boundary layer over a mid-latitude glacier in summer. *Boundary-Layer Meteorology,* 83**,** 183-205.

BROOK, S. J. & BIRKS, H. J. B. (2000) Chironomid-inferred Late-glacial air temperatures at Whitrig Bog, southeast Scotland. *Journal of Quaternary Science,* 15**,** 759-764.

BUSBY, J. P. & MERRITT, J. W. (1999) Quaternary deformation mapping with ground penetrating radar. *Journal of Applied Geophysics,* 41**,** 75-91.

CARR, S. (2001) A glaciological approach for the discrimination of Loch Lomond Stadial glacial landforms in the Brecon Beacons, South Wales. *Proceedings of the Geologists Association,* 112**,** 253 - 262.

CARR, S. & COLEMAN, C. (2007) An improved technique for the reconstruction of former glacier mass-balance and dynamics. *Geomorphology,* 92.

CHIVERRELL, R. C., THOMAS, G. S. P. & FOSTER, G. C. (2008) Sediment–landform assemblages and digital elevation data: Testing an improved methodology for the assessment of sand and gravel aggregate resources in north-western Britain *Engineering Geology,* 99**,** 40-50.

CLARK, R. (1990) On the Last Glaciation of Cumbria. *Proceedings of the Cumberland Geological Society,* 5**,** 187 - 208.

CLARK, R. (1992) Quaternary Features north of the Kirkstone Pass. IN DODD, M. (Ed.) *Lakeland rocks and landscape.* Oxford, Cumberland Geological Society.

CLOUGH, R. M. (1977) Some aspects of corrie initiation and evolution in the English Lake District. *Proceedings of the Cumberland Geological Society,* 3**,** 209 - 232.

COLHOUN, E. A. (1988) Recent morphostratigraphic studies of the Australian Quaternary. *Progress in Physical Geography,* 12**,** 264-281.

COOPE, G. R. & JOACHIM, M. J. (1980) Lateglacial environmental changes interpreted from fossil Coleoptera from St. Bees, Cumbria, England. IN LOWE, J. J., GRAY, J. M. &

ROBINSON, J. E. (Eds.) *Studies in the Lateglacial of North-West Europe.* Oxford, Pergamon.

CORNISH, R. (1981) Glaciers of the Loch Lomond Stadial in the western Southern Uplands of Scotland *Proceedings of the Geologists Association,* 92.

DANSGAARD, W., WHITE, J. W. C. & JOHNSEN, S. J. (1989) The abrupt termination of the Younger Dryas climate event. *Nature,* 339**,** 532-534.

DELANEY, C. (2003) The Last Glacial Stage (the Devensian) in Northwest England. *North West Geography.*

DEMEK, J. & EMBLETON, C. (1978) *Guide to Medium-Scale Geomorphological Mapping,* Brno.

DOWMAN, I., BALAN, P., RENNER, K. & FISCHER, P. (2003) An Evaluation of Nextmap Terrain Data in the Context of UK National Datasets London, University College London.

DYKE, A. S. (1983) Quaternary geology of Somerset Island, District of Franklin. *Geological Survey of Canada Memoir,* 404**,** 32.

EVANS, D. J. A. (2003) Glaciers. *Progress in Physical Geography,* 27**,** 261-274.

EVANS, D. J. A. (2003) Glaciers. *Progress in Physical Geography,* 27**,** 261-274.

EVANS, D. J. A., LEMMEN, D. S. & REA, B. R. (1999) Glacial landsystems of the southwest Laurentide Ice Sheet: modern Icelandic analogues. *Journal of Quaternary Science,* 14**,** 673-679.

EVANS, D. J. A., REA, B. R., HANSOM, J. D. & WHALLEY, W. B. (2002) Geomorphology and style of plateau icefield deglaciation in fjord terrains: the example of Troms-Finnmark, north Norway. *Journal of Quaternary Science,* 17**,** 221-239.

EVANS, I. S. (1994) Cirques and Moraines of the Northern Fells, Cumbria: Bowscale and Bannerdale. IN BOARDMAN, J. & WALDEN, J. (Eds.) *Cumbria Field Guide.* Oxford, Quaternary Research Association.

EVANS, I. S. (2006) Local aspect asymmetry of mountain glaciation: A global survey of consistency of favoured directions for glacier numbers and altitudes. *Geomorphology,* 73**,** 166-184.

EVANS, I. S. (2008) Glacier aspect. IN BROWN, V. (Ed.). Durham.

EVANS, I. S. & COX, N. J. (1995) The form of glacial cirques in the English Lake District, Cumbria. *Zeitschrift fuer Geomorphologie,* 39**,** 175 - 202.

FAWCETT, P. J., AGUSTSDOTTIR, A. M., ALLEY, R. B. & SHUMAN, C. A. (1997) The Younger Dryas termination and North Atlantic Deep Water Formation: Insights from climate model simulations and Greenland ice cores. *Paleoceanography,* 12**,** 23-38.

FJELLANGER, J., SORBEL, L., LINGE, H., BROOK, E. J., RAISBECK, G. M. & YIOU, F. (2006) Glacial survival of blockfields on the Varanger Peninsula, northern Norway. *Geomorphology,* 82**,** 255-272.

FLORINSKY, I. V. (2002) Errors of signal processing in digital terrain modelling. *International Journal of Geographical Information Science,* 16**,** 475-501.

FURBISH, D. J. & ANDREWS, J. T. (1984) The use of hypsometry to indicate long-term stability and response of valley glaciers to changes in mass transfer. *Journal of Glaciology,* 30**,** 199-211.

GELLATLY, A. F., GORDON, J. E., WHALLEY, W. B. & HANSOM, J. D. (1988) Thermal Regime and Geomorphology of Plateau Ice Caps in Northern Norway - Observations and Implications. *Geology,* 16**,** 983-986.

GLEN, J. W. (1954) The creep of polycrystalline ice. *Proceedings of the Royal Society A,* 218**,** 519-538.

GLEN, J. W. (1958) The flow law for ice: a discussion of the assumptions made in glacier theory, their experimental foundations and consequences. *Association of Scientific Hydrology,* 47**,** 171-183.

GRAY, J. M. (1982) The last glaciers (Loch Lomond Advance) in Snowdonia, North Wales. *Geological Journal,* 17**,** 111-133.

GRAY, J. M. & BROOKS, C. L. (1972) The Loch Lomond Readvance on Mull and Menteith. *Scottish Journal of Geology,* 8**,** 95-103.

GRAY, J. M. & COXON, P. (1991) The Loch Lomond Stadial glaciation in Britain and Ireland. IN EHLERS, J., GIBBARD, P. L. & ROSE, J. (Eds.) *Glacial deposits in Great Britain and Ireland.* Brookfield, A A Balkema.

GROSVAL'D, M. G. & KOTLYAKOV, V. M. (1969) Present-day glaciers in the USSR and some data on their mass balance. *Journal of Glaciology,* 8**,** 9-22.

HAEBERLI, W., HOELZLE, M., PAUL, F. & ZEMP, M. (2007) Integrated monitoring of mountain glaciers as key indicators of global climate change: the European Alps. *Annals of Glaciology,* 46**,** 150-160.

HAWORTH, E., BOER, G. D., EVANS, I. S., OSMASTON, H., PENNINGTON, W., SMITH, A., STOREY, P. & WARE, B. (2003) *Tarns of the Central Lake District,* Ambleside, Cumbria, Brathay Exploration Group Trusy.

HILLER, J. K. & SMITH, M. (2008) Residual relief separation: digital elevation model enhancement for geomorphological mapping. *Earth Surface Processes and Landforms,* Technical Communication.

HINDMARSH, R. C. A., BOULTON, G. S. & HUTTER, K. (1989) Modes of operation of thermo-mechanically coupled ice sheets. *Annals of Glaciology,* 12**,** 57-69.

HOOKE, R. L. (2005) *Principles of Glacier Mechanics,* Cambridge, Cambridge University Press.

HUBBARD, B. & GLASSER, N. (2005) *Field techniques in glaciology and glacial geomorphology,* Chichester, Wiley.

LAMB, A. L. & BALLANTYNE, C. K. (1998) Palaeonunataks and the altitude of the last ice sheet in the SW Lake District, England. *Proceedings of the Geologists Association***,** 305 - 316.

LEHMKUHL, F. (1998) Quaternary glaciations in central and western Mongolia. *Quaternary Proceedings,* 6**,** 153-167.

LEMMEN, D. S. & ENGLAND, J. (1992) Multiple glaciations and sea level changes, northern Ellesmere Island, high arctic Canada. *Boreas,* 21**,** 137-152.

LEONARD, E. M. (1989) Climatic change in the Colorado Rocky mountains: estimates based on modern climate at Late Pleistocene equilibrium lines. *Arctic and Alpine Research,* 21.

LLIBOUTRY, L. (1957) Glacier mechanics in the perfect plasticity theory. *Journal of Glaciology,* 3**,** 162-169.

LUKAS, S. (2006) Morphostratigraphic principles in glacier reconstruction - a perspective from the British Younger Dryas. *Progress in Physical Geography,* 30**,** 719-736.

LUKAS, S. & BENN, D. I. (2007) Retreat dynamics of younger dryas glaciers in the far NW Scottish Highlands reconstructed from Moraine sequences. *Scottish Geographical Journal,* 122**,** 308-325.

MANLEY, G. (1949) The snowline in Britain. *Geografiska Annaler,* 31**,** 179-193.

MANLEY, G. (1955) On the occurence of ice domes and permanently snow-covered summits. *Journal of Glaciology,* 2**,** 453 - 456.

MANLEY, G. (1959) The late-glacial climate of north-west England. *Liverpool and Manchester Geological Journal,* 2**,** 188 - 215.

MCCABE, A. M. & CLARK, P. U. (1998) Ice-sheet variability around the North Atlantic Ocean during the last deglaciation. *Nature,* 392**,** 373-377.

MCCABE, M., KNIGHT, J. & MCCARRON, S. (1998) Evidence for Heinrich event 1 in the British Isles. *Journal of Quaternary Science,* 13**,** 549-568.

MCCARROLL, D. & BALLANTYNE, C. K. (2000) The last ice sheet in Snowdonia. *Journal of Quaternary Science,* 15**,** 765-778.

MCDOUGALL, D. A. (1997) Plateau icefield and the geomorphological record: an example from the central Lake District. IN J, B. (Ed.) *Geomorphology of the Lake District: a field guide.* Oxford, British Geomorphological Research Group.

MCDOUGALL, D. A. (1998) Loch Lomond Stadial plateau icefields in the Lake District, northwest England. *Department of Geography and Topographic Science.* Glasgow, University of Glasgow.

MCDOUGALL, D. A. (2001) The geomorphological impact of Loch Lomond (Younger Dryas) Stadial plateau icefields in the central Lake District, northwest England. *Journal of Quaternary Science,* 16**,** 531 - 543.

MEIERDING, T. C. (1982) Late Pleistocene glacial equilibrium line in the Colorado Front Range: a comparison of methods. *Quaternary Research,* 18.

MERRITT, J. W. & AUTON, C. A. (2000) An outline of the lithostratigraphy and depositional history of Quaternary deposits in the Sellafield District, west Cumbria. *Proceedings of the Yorkshire Geological Society,* 53**,** 129 - 154.

MITCHELL, W. A. (1991) Dimlington Stadial ice sheet in the western Pennines. IN MITCHELL, W. A. (Ed.) *Western Pennines: Field Guide.* London, Quaternary Research Association.

MITCHELL, W. A. (1994) Drumlins in ice sheet reconstructions, with reference to the western Pennines, northern England. *Sedimentary Geology,* 91**,** 313-331.

MITCHELL, W. A. (1996) Significance of snowblow in the generation of Loch Lomond Stadial (Younger Dryas) glaciers in the western Pennines, northern England. *Journal of Quaternary Science,* 11**,** 233 - 248.

MITCHELL, W. A. & CLARK, C. D. (1994) The Last Ice Sheet in Cumbria. IN BOARDMAN, J. & WALDEN, J. (Eds.) *Cumbria Field Guide.* Oxford, Quaternary Research Association.

MOORE, R. M. (1992) The Skiddaw group of Cumbria: Early Ordovcian turbidite sedimentation and provencance on an evolving microcontinental margin. Leeds, University of Leeds.

MOSELEY, F. (1978) *The Geology of the Lake District,* Leeds, The Yorkshire Geological Society.

MURRAY, D. R. & LOCKE, W. W. (1989) Dynamics of the late Pleistocene Big Timber glacier, Crazy mountains, Montana, USA. *Journal of Glaciology,* 35**,** 183-190.

NESJE, A., DAHL, S. O., ANDA, E. & RYE, N. (1988) Blockfields in southern Norway: significance for the Late Weichselian ice sheet. *Norsk Geologisk Tidsskrift,* 68**,** 149 - 169.

NESJE, A., DAHL, S. O., LINGE, H., BALLANTYNE, C. K., MCCARROLL, D., BROOK, E. J., RAISBECK, G. M. & YIOU, F. (2007) The surface geometry of the Last Glacial Maximum ice sheet in the Andoya-Skanland region, northern Norway, constrained by surface exposure dating and clay mineralogy. *Boreas,* 36**,** 227-239.

NYE, J. F. (1952) The mechanics of glacier flow. *Journal of Glaciology,* 2**,** 82 - 93.

OERLEMANS, J. (1997) A flowline model ofr Nigardsbreen, Norway: projection of future glacier length based on dynamic calibration with the historic record. *Annals of Glaciology,* 24**,** 382-389.

OERLEMANS, J. (2001) *Glaciers and Climate Change,* Lisse, A A Balkema.

OHMURA, A., KASSER, P. & FUNK, M. (1992) Climate at the equilibrium line of glaciers. *Journal of Glaciology,* 38**,** 397-410.

OSMASTON, H. (2005) Estimates of glacier equilibrium line altitudes by the Area x Altitude, the Area x Altitude Balance Ratio and the Area x Altitude Balance Index methods and their validation. *Quaternary International,* 138-139**,** 22-31.

PATTERSON, W. S. B. (1994) *The Physics of Glaciers,* Oxford, Butterworth-Heinemann.

PENNINGTON, W. (1996) Limnic sediments and the taphonomy of lateglacial pollen assemblages. *Quaternary Science Reviews,* 15**,** 501 - 520.

PENNINGTON, W. & MOSELEY, E. F. (1978) Quaternary Geology. *The Geology of the Lake District*.

PORTER, S. C. (1975) Equilibrium line altitudes of Late Quaternary glaciers in the Southern Alps, New Zealand. *Quaternary Research,* 5**,** 27-47.

PROSSER, R. (1977) *Geology explained in the Lake District*, Newton Abbot: David and Charles.

RAE, A. C., HARRISON, S., MIGHALL, T. & DAWSON, A. G. (2004) Periglacial trimlines and nunataks of the Last Glacial Maximum: the Gap of Dunloe, southwest Ireland. *Journal of Quaternary Science,* 19**,** 87-97.

RAHMSTORF, S. (2002) Ocean circulation and climate during the past 120,000 years. *Nature,* 419**,** 207-214.

REA, B. R., EVANS, D. J. A., DIXON, T. S. & WHALLEY, W. B. (2000) Contemporaneous, localized, basal ice-flow variations: implications for bedrock erosion and the origin of p-forms. *Journal of Glaciology,* 46**,** 470-476.

REA, B. R., IRVING, D. H. B., HUBBARD, B. & MCKINLEY, J. (2000) Preliminary investigations of centrifuge modelling of polycrystalline-ice deformation *Annals of Glaciology,* 31**,** 257-262.

REA, B. R., WHALLEY, B., DIXON, T. S. & GORDON, J. E. (1999) Plateau icefields as contributing areas to valley glaciers and the potential impact on reconstructed ELA's: a case study from the Lyngen Alps, North Norway. *Annals of Glaciology,* 28**,** 97 - 102.

REA, B. R., WHALLEY, W. B., EVENS, D. J. A., GORDON, J. E. & MCDOUGALL, D. A. (1998) Plateau icefields: Geomorphology and dynamics. *Journal of Quaternary Science,* 13**,** 35-54.

REA, B. R., WHALLEY, W. B. & MENEELY, J. (2004) Cation and sediment concentrations in basal ice from Oksfjordjokelen, North Norway. *Geografiska Annaler Series a-Physical Geography,* 86A**,** 91-105.

REA, B. R., WHALLEY, W. B., RAINEY, M. & GORDON, J. E. (1996) Blockfields: old or new? Evidence and implications from some plateau blockfields in northern Norway. *Geomorphology,* 15.

ROBERTSON, D. W. (1988) Aspects of the Lateglacial and Flandrian Environmental History of the Brecon Beacons, Fforest Fawr, Black Mountain and Abergavenny Black Mountains, South Wales (with emphasis on the Lateglacial and Early Flandrian Periods). University of Wales.

ROWAN, C. (2007) Out of the ice age, into the asteroid shower. IN HTTP://SCIENCEBLOGS.COM/HIGHLYALLOCHTHONOUS/2007/10/OUT_OF_THE_ICE_AGE_INTO_THE_AS.PHP (Ed.).

RUDDIMAN, W. F. & MCINTYRE, R. (1981) The North Atlantic Ocean during the last deglaciation. *Palaeogeography, Palaeoclimatology, Palaeoecology,* 35**,** 145-214.

RUDDIMAN, W. F., SANCETTA, C. D. & MCINTYRE, A. (1977) Glacial-interglacial response rate of subpolar north-atlantic waters to climatic change-record in oceanic sediments. *Philosophical Transactions of the Royal Society of London Series B-Biological Sciences,* 280**,** 119-142.

SCHYTT, V. (1967) A study of ablation gradient. *Geografiska Annaler,* 49**,** 327-332.

SHIPP, T. (1982) *The Lake District,* London, Unwin.

SIEGERT, M. J. (2001) *Ice Sheets and Late Quaternary Environmental Change,* Chichester, John Wiley and Sons Ltd.

SISSONS, J. B. (1974) A lateglacial ice cap in the central Grampians, Scotland. *Transactions of the Institute of British Geographers,* 62**,** 95-114.

SISSONS, J. B. (1976) *The Geomorphology of the British Isles,* London, Methuen.

SISSONS, J. B. (1979) The Loch Lomond advance in the Cairngorm Mountains. *Scottish Geographical Journal,* 95**,** 66-82.

SISSONS, J. B. (1980a) The Loch Lomond Advance in the Lake District, northern England. *Transactions of the Royal Society of Edinburgh: Earth Sciences,* 71**,** 13 - 27.

SISSONS, J. B. (1980b) Palaeoclimatic Inferences from Loch lomond Advance Glaciers. IN LOWE, J. J., GRAY, J. M. & ROBINSON, J. E. (Eds.) *Studies in the Lateglacial of North-West Europe.* Oxford, Pergamon Press.

SISSONS, J. B. & SUTHERLAND, D. G. (1976) Climatic Inferences from former glaciers in the South-East Grampian Highlands, Scotland. *Journal of Glaciology,* 17**,** 325 - 346.

SMITH, A. (1992) Geological Background. IN DODD, M. (Ed.) *Lakeland Rocks and Landscape.* Maryport, Ellenbank Press.

SMITH, M. J., ROSE, J. & BOOTH, S. (2006) Geomorphological mapping of glacial landforms from remotely sensed data: An evaluation of the principal data sources and an assessment of their quality. *Geomorphology,* 76**,** 148-165.

STOKES, C. R. (2000) The geomorphology of palaeo-ice streams: identification, characterisation and implications for ice stream functioning. *Department of Geography.* University of Sheffield.

STOKES, C. R., POPOVNIN, V., ALEYNIKOV, A., GURNEY, S. D. & SHAHGEDANOVA, M. (2007) Recent glacier retreat in the Caucasus Mountains, Russia, and associated increase in supraglacial debris cover and supra-/proglacial lake development. *Annals of Glaciology,* 46**,** 195-203.

SUGDEN, D. E. & JOHN, B. S. (1976) *Glaciers and Landscape,* London, Arnold.

SUTHERLAND, D. G. (1984) Modern glacier characteristics as a basis for inferring former climates with particular reference to the Loch Lomond Stadial. *Quaternary Science Reviews,* 3**,** 291-309.

THOMAS, G. S. P. (1985) The Late Devensian glaciation along the boarder of northeast Wales. *Geological Journal,* 20**,** 319-340.

THORP, P. W. (1986) A mountain icefield of Loch Lomond Stadial age, western Grampians, Scotland. *Boreas,* 15**,** 83-97.

WALKER, D. (1966) The Glaciation of the Langdale Fells. *Geological Journal,* 5**,** 208 - 215.

WEERTMAN, J. (1964) Theory of Glacier Sliding. *Journal of Glaciology,* 5**,** 287-303.

WILSON, P. (1977) The Rosthwaite Moraines. *Proceedings of the Cumberland Geological Society,* 3**,** 239 - 249.

WILSON, P. (2002) Morphology and significance of some Loch Lomond Stadial moraines in the south-central Lake District, England. *Proceedings of the Geologists Association,* 113**,** 9 - 21.

WILSON, P. (2004a) Description and implications of valley moraines in upper Eskdale, Lake District. *Proceedings of the Geologists Association,* 115**,** 55-61.

WILSON, P. (2004b) Implications of dissected drift at Stockdale Head, western Lake District, northern England. *Geological Journal,* 39**,** 111 - 115.

WILSON, P. (2005) Paraglacial rock-slope failures in Wasdale, western Lake District, England: morphology, styles and significance.

WILSON, P. (2007) Comment on Carr S and Coleman C (2007): 'An improved technique for the reconstruction of former glacier mass-balance and dynamics' Geomorphology 92, 76-90. *Geomorphology,* 99**,** 443-444.

WILSON, P. & CLARK, R. (1998) Characteristics and implications of some Loch Lomond Stadial moraine ridges and later landforms, eastern Lake District, northern England. *Geological Journal,* 33**,** 73 - 87.

WILSON, P. & CLARK, R. (1999) Further glacier and snowbed sites of inferred Loch Lomond Stadial age in the north Lake District. *Proceedings of the Geologists Association,* 110**,** 321 - 331.

WILSON, P., CLARK, R. & SMITH, A. (2004) Rock-slope failures in the Lake District: a preliminary report. *Proceedings of the Cumberland Geological Society,* 7.

WILSON, P. & SMITH, A. (2006) Geomorpholgical characteristics and significance of Late Quaternary Paraglacial rock-slope failures on Skiddaw Group Terrain, Lake DIstrict northwest England. *Geografiska Annaler: Series A, Physical Geography,* 88**,** 237-252.

WILSON, P. & SMITH, A. (2006) Geomorphological characteristics and significance of Late Quaternary paraglacial rock-slope failures on Skiddaw Group terrain, Lake District, northwest England. *Geografiska Annaler Series a-Physical Geography,* 88A**,** 237-252.

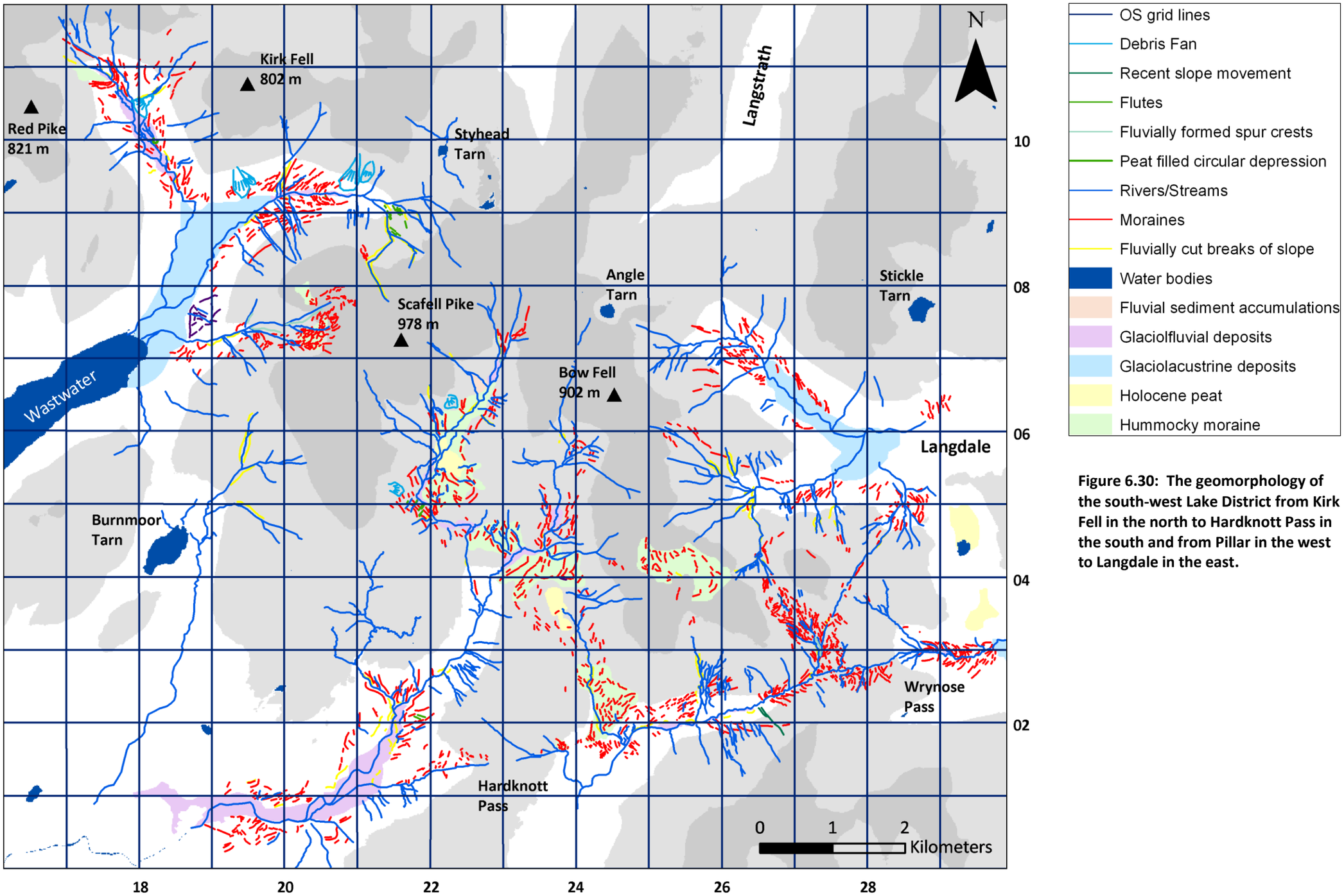


**Figure 6.30: The geomorphology of the south-west Lake District from Kirk Fell in the north to Hardknott Pass in the south and from Pillar in the west to Langdale in the east.**

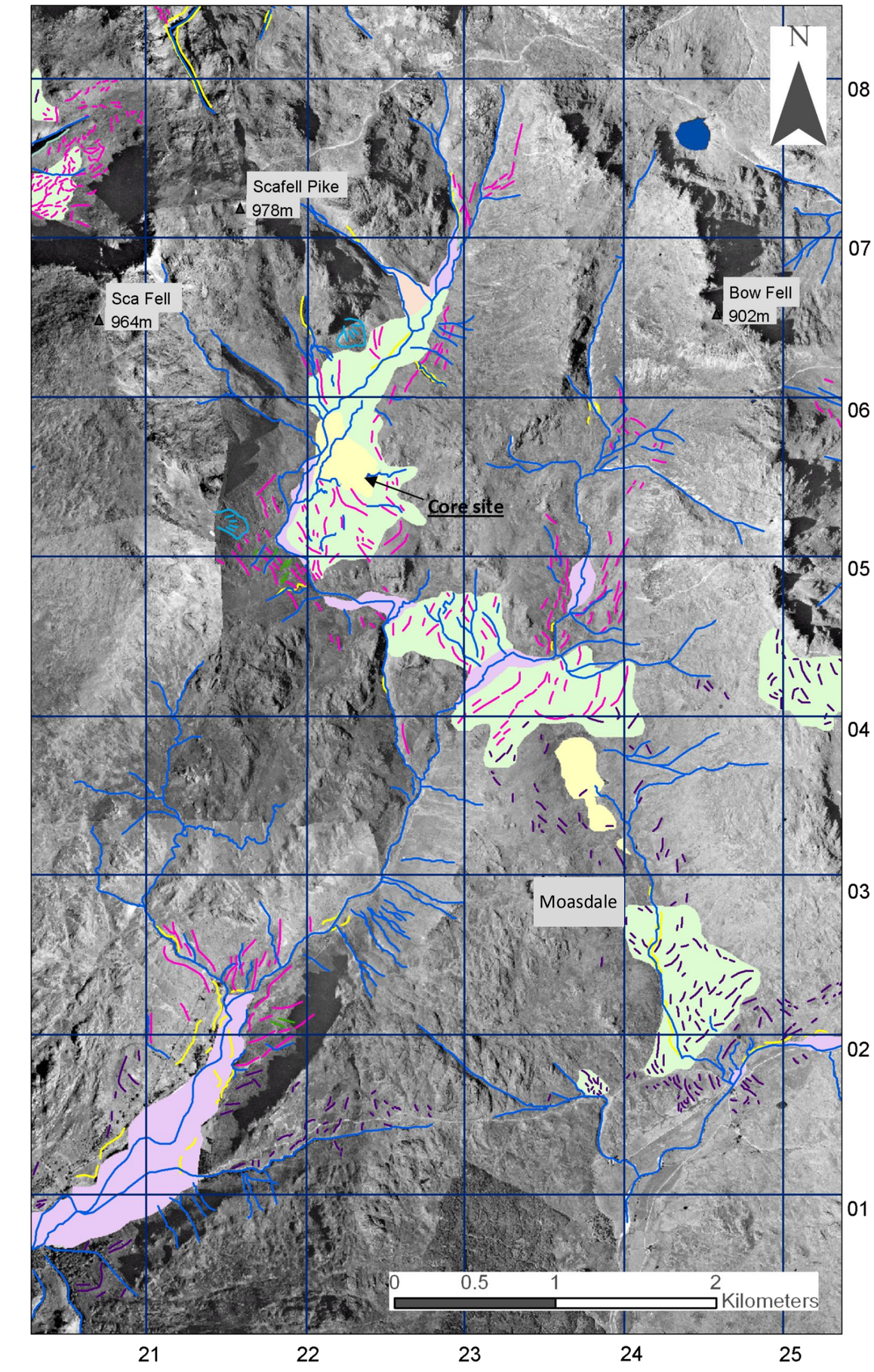


OS grid lines
Debris Fan
Recent slope movement
Flutes
Fluvially formed spur crests
Peat filled circular depression
Rivers/Streams
LLS moraines
Fluvially cut breaks of slope
Pre-LLS moraines
Water bodies
Fluvial sediment accumulations
Glaciolfluvial deposits
Glaciolacustrine deposits
Holocene peat
Hummocky moraine

**Figure 6.1b: The geomorphology of Upper Eskdale indicating the glacial episode during which moraine formation occurred.**

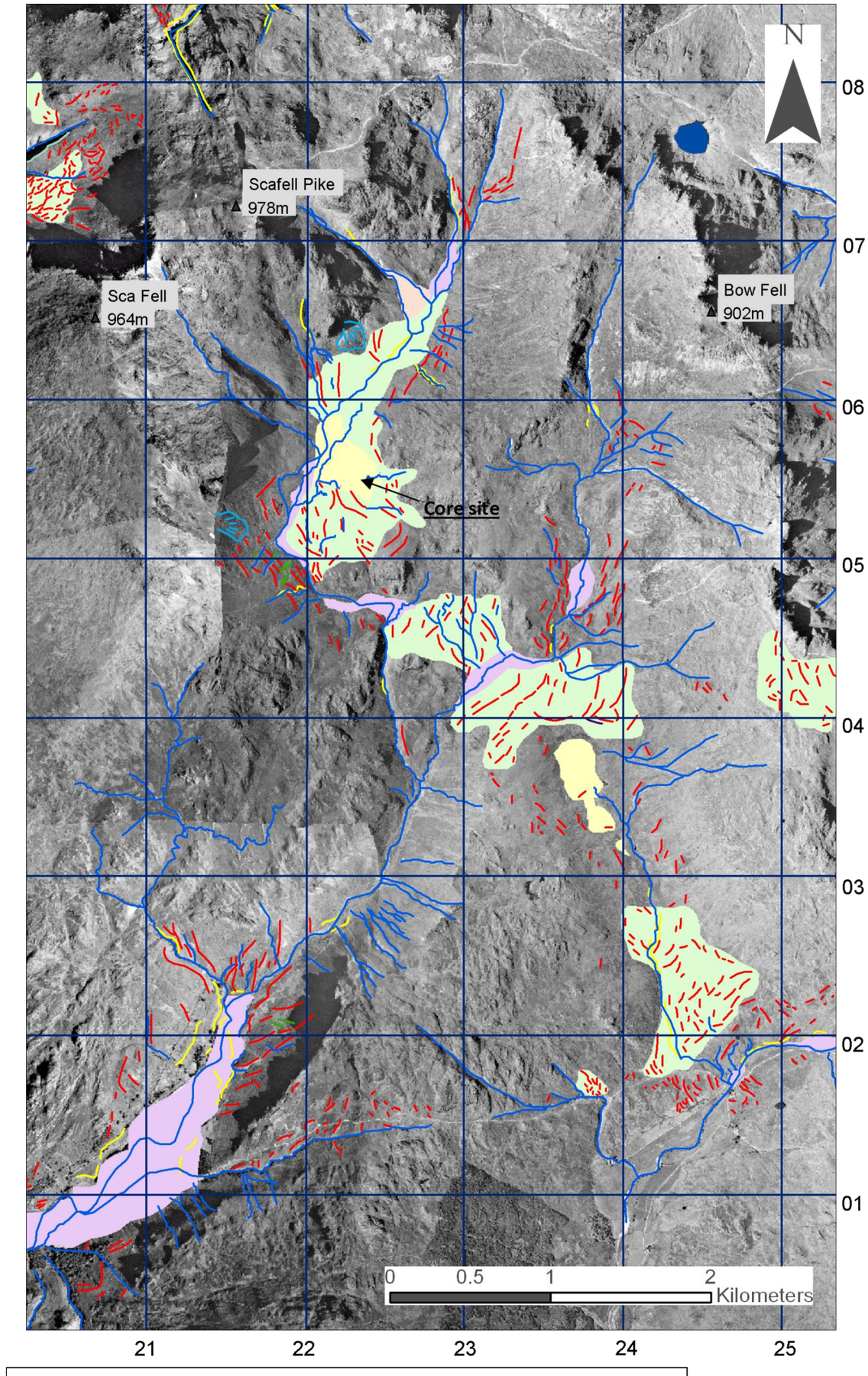


**Figure 6.1a: The geomorphology of Upper Eskdale.**


**Figure 4.14b: The orthorectified aerial photograph covering two of the selected field sites at the northern end of Wastwater: Mosedale and Lingmell Beck. This zoomed in image means that the edges of some photographs become visible. Photograph edges are, however, barely visible compared to the georeferencing done in ArcGIS (see figure 3.7) and consequently, due to the high degree of accuracy associated with this method, the mosaic shown in figure 3.14a was accepted as the final product of the orthorectification.**

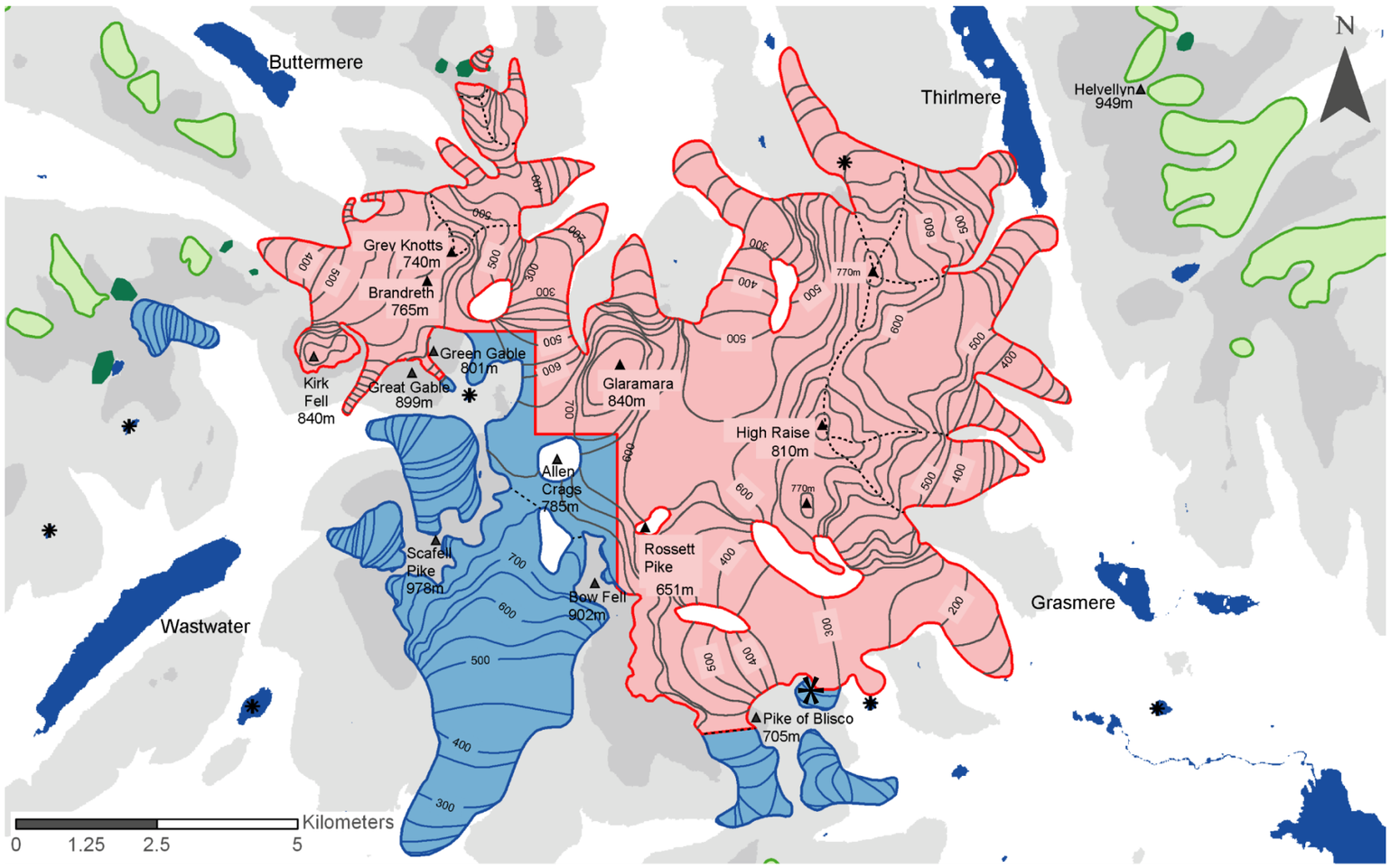


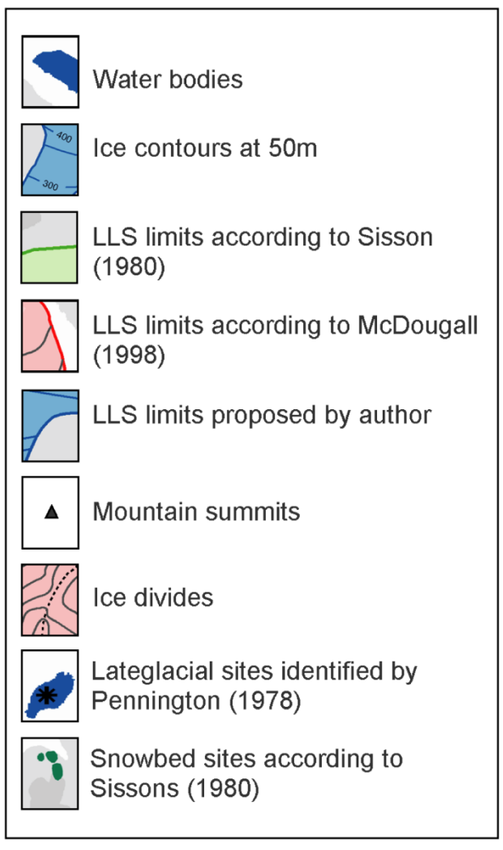


**Figure 7.5: The reconstructed Loch Lomond Stadial ice occupation of the central Lake District according to McDougall (1998), Sissons (1980), Pennington (1978) and the current author. Figure digitised and modified from original sources.**

**ELAs of glaciers reconstructed by current author.**

| Glacier | ELA (m) |
|---|---|
| Mosedale | 534 |
| Lingmell Beck | 530 |
| Lingmell Gill | 686 |
| Upper Eskdale | 494 |
| Red Tarn | 485 |
| Widdygill Foot | 323 |

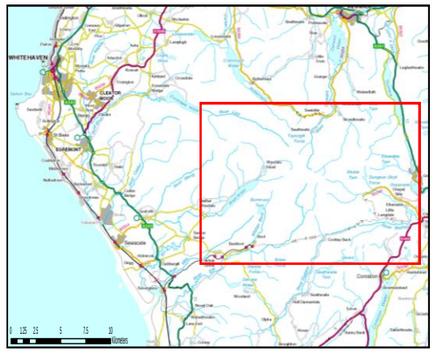


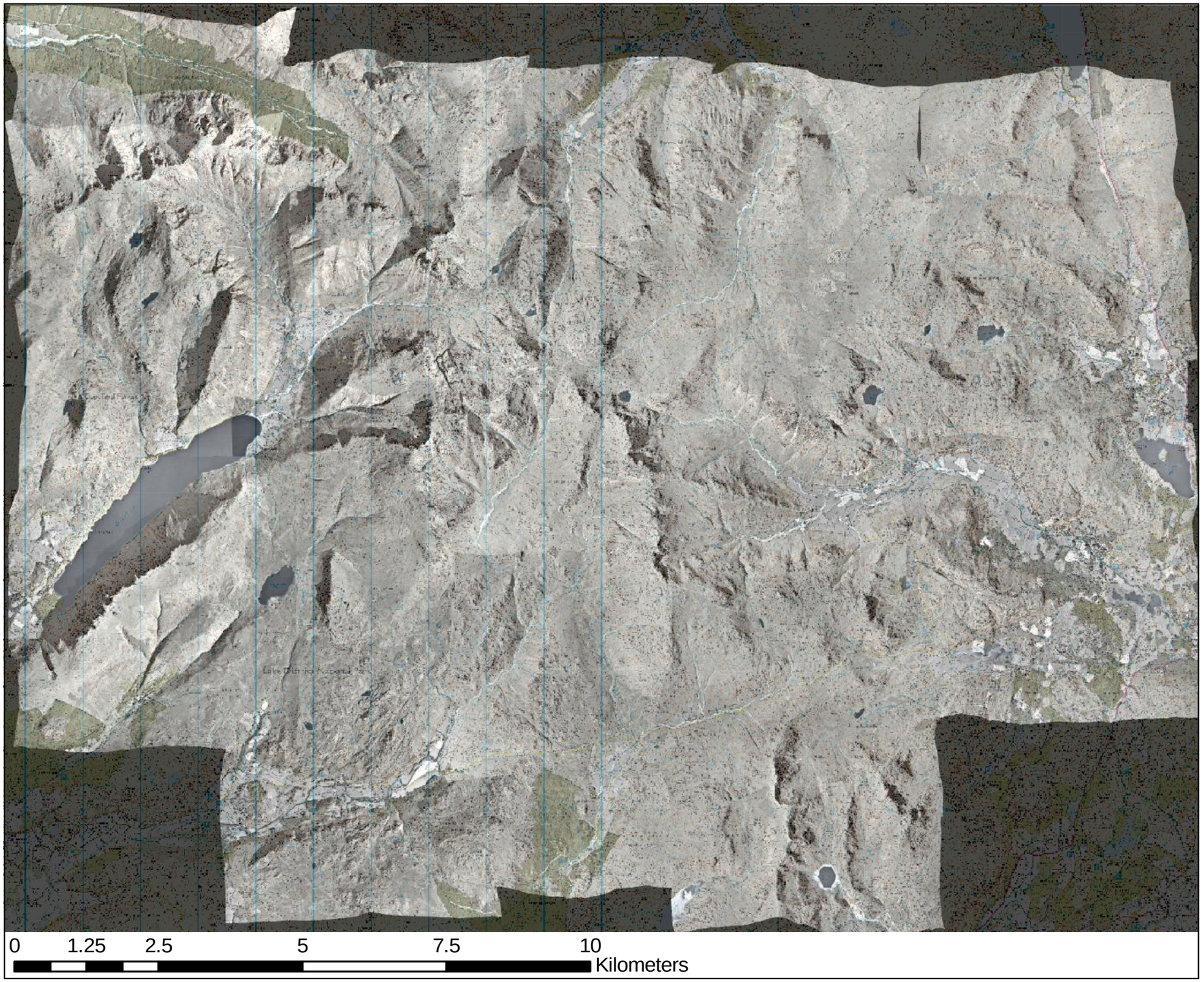


**Figure 4.14a:** The final mosaic of the orthorectified aerial photography covering the south-west Lake District. The area covered by the photography is indicated by the red box on map A. Photograph transparency = 40%.

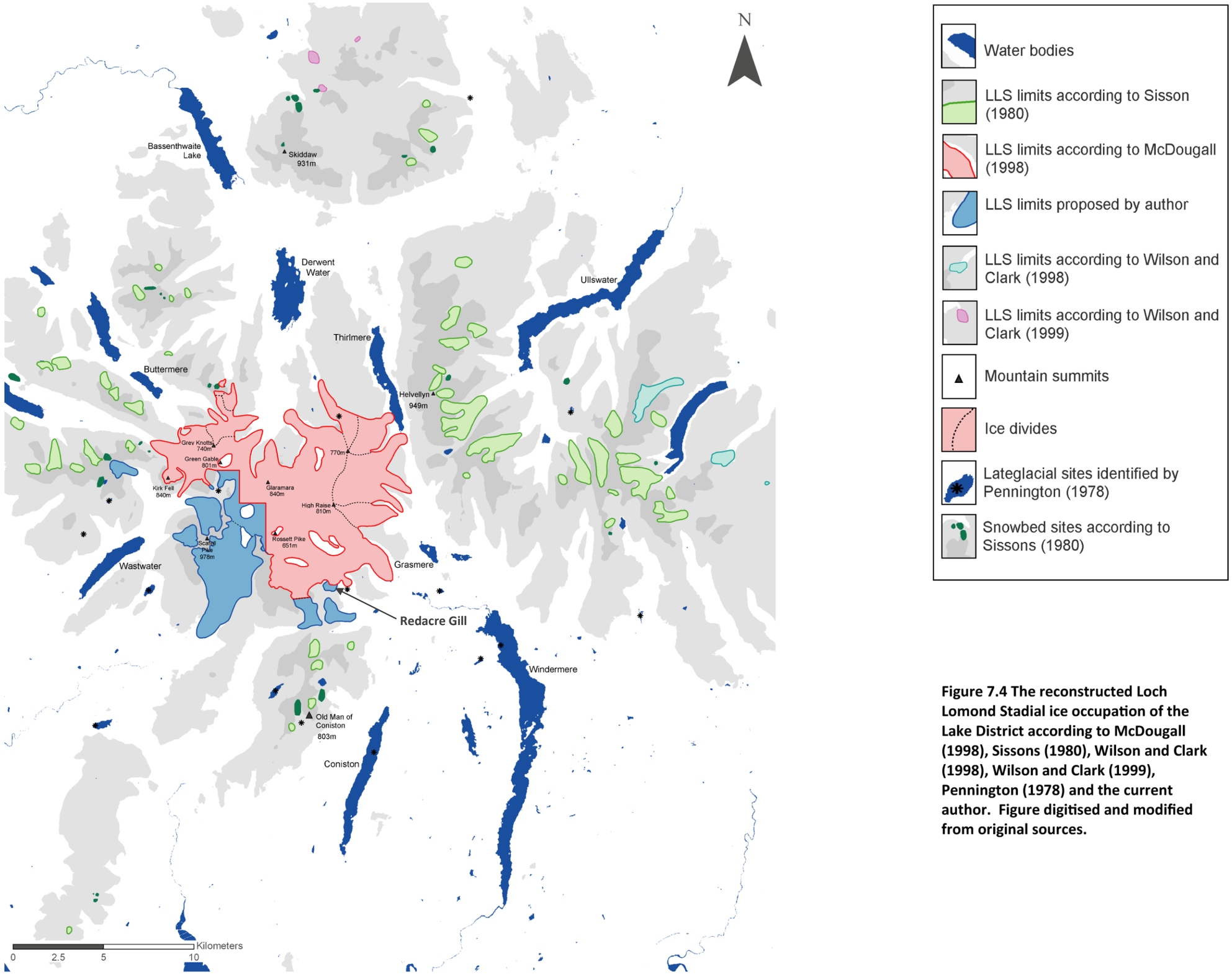


**Figure 7.4 The reconstructed Loch Lomond Stadial ice occupation of the Lake District according to McDougall (1998), Sissons (1980), Wilson and Clark (1998), Wilson and Clark (1999), Pennington (1978) and the current author. Figure digitised and modified from original sources.**